



Universiteit
Leiden
The Netherlands

Clinical glycomics of antibodies by mass spectrometry

Haan, N. de

Citation

Haan, N. de. (2019, February 14). *Clinical glycomics of antibodies by mass spectrometry*. Retrieved from <https://hdl.handle.net/1887/68328>

Version: Not Applicable (or Unknown)

License: [Licence agreement concerning inclusion of doctoral thesis in the Institutional Repository of the University of Leiden](#)

Downloaded from: <https://hdl.handle.net/1887/68328>

Note: To cite this publication please use the final published version (if applicable).

Cover Page



Universiteit Leiden



The following handle holds various files of this Leiden University dissertation:

<http://hdl.handle.net/1887/68328>

Author: Haan, N. de

Title: Clinical glycomics of antibodies by mass spectrometry

Issue Date: 2019-02-14

[illegible]



ISBN: 978-94-6375-236-7

© 2018 Noortje de Haan. All rights reserved. No part of this book may be reproduced, stored in a retrieval system, or transmitted in any form or by any means without permission of the author or the journals holding the copyrights of the published manuscripts. All published material was reprinted with permission.

The work presented in this thesis was performed at the Center for Proteomics and Metabolomics, Leiden University Medical Center, The Netherlands.

The work was supported by the European Union Seventh Framework Program IBD-BIOM, grant number: 305479

Design: Niko Spelbrink

Printing: Ridderprint BV, the Netherlands

Clinical

Glycomics of Antibodies

by Mass Spectrometry

Proefschrift

ter verkrijging van

de graad van Doctor aan de Universiteit Leiden,

op gezag van Rector Magnificus prof.mr. C.J.J.M. Stolker,

volgens besluit van het College voor Promoties

te verdedigen op donderdag 14 februari 2019

klokke 11:15 uur

door

Noortje de Haan

Geboren te Amsterdam

op 27 januari 1991



Promotor: Prof. dr. M. Wuhler

Co-promotor: Dr. D. Falck

Leden promotiecommissie: Prof. dr. A.C. Lankester

Prof. dr. C.M. Cobbaert

Prof. dr. G.-J. Boons, Department of Chemical
Biology and Drug Discovery, Utrecht University,
Utrecht, The Netherlands

Dr. G. Vidarsson, Department of Experimental
Immunohematology, Sanquin Research and
Landsteiner Laboratory, Amsterdam, The
Netherlands

To my family

Table of Contents

Chapter 1 - Introduction	9
Chapter 2 - Linkage-Specific Sialic Acid Derivatization for MALDI-TOF-MS Profiling of IgG Glycopeptides	31
Chapter 3 - Changes in Healthy Human IgG Fc Glycosylation after Birth and during Early Childhood	49
Chapter 4 - IgG Fc Glycosylation After Hematopoietic Stem Cell Transplantation is Dissimilar to Donor Profiles	67
Chapter 5 - Differences in IgG Fc Glycosylation are Associated with Outcome of Pediatric Meningococcal Sepsis	85
Chapter 6 - Glycosylation of Immunoglobulin G Associates With Clinical Features of Inflammatory Bowel Disease	105
Chapter 7 - The N-glycosylation of Mouse Immunoglobulin G (IgG) Fragment Crystallizable Differs Between IgG Subclasses and Strains	125
Chapter 8 - Comparative Glycomics of Immunoglobulin A and G from Saliva and Plasma Reveals Biomarker Potential	151
Chapter 9 - Discussion and Perspectives	171
Addendum	187
References	189
Nederlandse samenvatting	209
Acknowledgments	213
Curriculum Vitae	215
List of publications	217



Chapter 1

Introduction



A fascinating number of different components are continuously circulating in the human blood. While these components all have their own function, they largely play together in a complex arrangement to assure a - most of the time - healthy day-to-day life. The human circulation provides the infrastructure of the body, with the large arteries and veins serving as the highways, and the smaller, organ- and tissue-specific vessels facilitating the local transportation. It supplies the whole body with all necessities in the form of red blood cells, white blood cells, platelets, proteins, sugars, lipids, hormones, salts, vitamins and many other cells and substances. In addition to the nutrient-, defense-, and messenger-components that are constantly being distributed, the blood circulation ultimately picks up the waste created in the distant areas of the body, in order to remove it. Altogether, the specific composition of the human blood provides an extensive overview of a large part of the intriguing processes going on in the body. This can be sampled and studied with current medical and chemical technologies. In normal, healthy conditions, a blood sample represents the balanced processes of the body, homeostasis. Disruption of the homeostasis will result in the up- or down- regulation of one or more components. A minor, temporary imbalance might reflect the body restoring its own equilibrium. However, fierce or persisting disruptions of the normal situation might indicate the presence or emergence of a serious underlying pathology. Medical tests studying these processes are, for example, used for the diagnosis, prognosis or treatment monitoring of various diseases. Expanding and improving these tests will be beneficial for the early diagnosis of pathologies and personalized treatment of patients.

One of the most diverse groups of molecular species circulating in the blood is the group of the proteins, performing functions ranging from protection of the body and the coordination of biological processes, to aiding the synthesis, modification or transportation of other molecules. Fine-tuning the properties of the vast majority of these blood proteins happens by, so called, post-translational modifications of which phosphorylation, acetylation and *N*-linked glycosylation form the top three of most occurring modifications [1]. Of these three, *N*-linked glycosylation is by far the most diverse. This makes it highly challenging, and at the same time highly interesting, to investigate this protein modification for the identification of potential diagnostic and prognostic markers.

Antibodies are immune proteins that play an important role in the defense of the body against pathogenic substances, like viruses and bacteria. The working mechanism of antibodies is often highly dependent on their glycosylation, and the development of suitable analytical tools is crucial to map the glycans attached to these glycoproteins. The possibility to discriminate between differentially glycosylated antibodies has high potential in precision medicine by contributing to the sensitivity and specificity of medical

tests. Immunoglobulin G (IgG) is the major antibody in human plasma, plays an essential role in the humoral immunity and will be one of the key players in this thesis.

1.1 Protein glycosylation

Protein glycosylation describes the process of the co- or post-translational attachment of a combination of monosaccharides (also known as sugars or carbohydrates) to a protein [2]. *N*-glycosylation, comprising the addition of a glycan to the nitrogen atom of an asparagine residue, is one of the most occurring PTMs as well as the most occurring form of protein glycosylation. Another often occurring form of protein glycosylation involves the attachment of a glycan to the oxygen atom of serine or threonine residue (*O*-glycosylation) [1, 3]. As glycans often contribute to a large fraction of the total glycoprotein size and have distinct physicochemical properties, including a high hydrophilicity, one can imagine that the influence of a glycan on the structure and function of a protein is substantial [4]. The presence of a large hydrophilic structure indirectly alters the interaction possibilities of the glycoconjugate with other proteins by influencing its folding and/or stability [4]. In addition, specific monosaccharide residues can have a direct interaction with glycan recognizing proteins, like lectins [5-7].

1.1.1 *N*-glycan structure and biosynthesis

The biosynthetic coupling of an *N*-glycan to an asparagine almost exclusively occurs when the asparagine is present in the *N*-glycosylation consensus sequence, asparagine-x-serine/threonine, where “x” can be any amino acid except for proline [8]. Additionally, *N*-glycosylation is reported to take place, to a lower extent, in the asparagine-x-cysteine motive [9, 10]. During, or right after, the synthesis of the protein in the endoplasmic reticulum (ER), a precursor *N*-glycan structure, consisting of two *N*-acetylglucosamines (GlcNAc), nine mannoses (Man) and three glucoses (Glc; **Figure 1.1A**), is transferred in its entirety from a dolichol anchor to the asparagine in the consensus sequence [11]. During the folding of the protein, still in the ER, the terminal Glc residues are enzymatically removed, one-by-one, serving as a protein folding-quality control. Only after proper folding, the protein enters the Golgi apparatus, where the Man residues may be trimmed further, reaching a structure with two GlcNAcs and five Mans (Man5, a high-mannose glycan; **Figure 1.1B**). Later in the Golgi, the glycan is extended with a GlcNAc, forming a hybrid-type glycan (**Figure 1.1B**). The ongoing interplay between glycosidases and glycosyltransferases results in the formation of complex-type *N*-glycans, which can be extended by different GlcNAc branches (antennae), a bisecting GlcNAc, core and/or antennary fucoses (Fuc) and antennary galactoses (Gal), *N*-acetylgalactosamines (GalNAc), Gal-GlcNAc (LacNAc) repeats, GalNAc-GlcNAc (LacdiNAc) repeats and *N*-acetylneuraminic acids (Neu5Ac; in humans) or *N*-glycolylneuraminic acids (Neu5Gc; in

other mammals; **Figure 1.1**) [11]. The latter two monosaccharides belong to the group of sialic acids (Sia), a group of large monosaccharides containing a carboxylic acid functional group [12].

The aforementioned monosaccharides are the most common *N*-glycan building blocks in humans and other mammals. They usually form six-membered cyclic structures consisting of five carbons and one oxygen in the ring (**Figure 1.1A**) [13]. The five carbon atoms of the ring are all chiral (except from C-3 in sialic acids), resulting in the existence of multiple different monosaccharide stereoisomers. Monosaccharides that only differ from each other by the configuration of one of their chiral carbon atoms are known as epimers [14]. For example, Gal and Glc are epimers due to their different configurations at C-4. Additionally, exact mirror images, enantiomers, are denoted by the prefix L- or D-, based on the configuration at C-5. Most monosaccharides in humans are D-enantiomers, with the exception of L-fucose (**Figure 1.1A**) [14]. Finally, while the configurations at C-2 to C-5 are stable within a structure, the configuration of C-1 (or C-2 in sialic acids; the anomeric carbon) can be altered in solution, resulting in a mixture of α -anomers (when the configuration at C-1 and C-5 is the same) and β -anomers (when the configuration at C-1 and C-5 is different; **Figure 1.2A**) [14].

Two monosaccharides can be enzymatically linked by condensation between the hemiacetal group of one monosaccharide and one of the hydroxyl groups of the other monosaccharide [13]. Branched structures can be formed as multiple hydroxyl groups of one monosaccharide can form simultaneous glycosidic bonds [11]. This in contrast to, for example, the almost exclusively linear connection between amino acids to form a protein. The linkage between two monosaccharides can vary on the basis of the hydroxyl groups that are involved, resulting in different regioisomers. Additionally, the configuration around the involved anomeric center determines whether an α - or β -stereoisomer is formed (**Figure 1.2B**) [15]. The anomeric carbon not involved in a glycosidic bond is referred to as the reducing end of a glycan [13]. The formation of both regio- and stereoisomers is under specific enzymatic control and has a high influence on the 3D-structure of the resulting glycan, eventually influencing its function and activity [11].

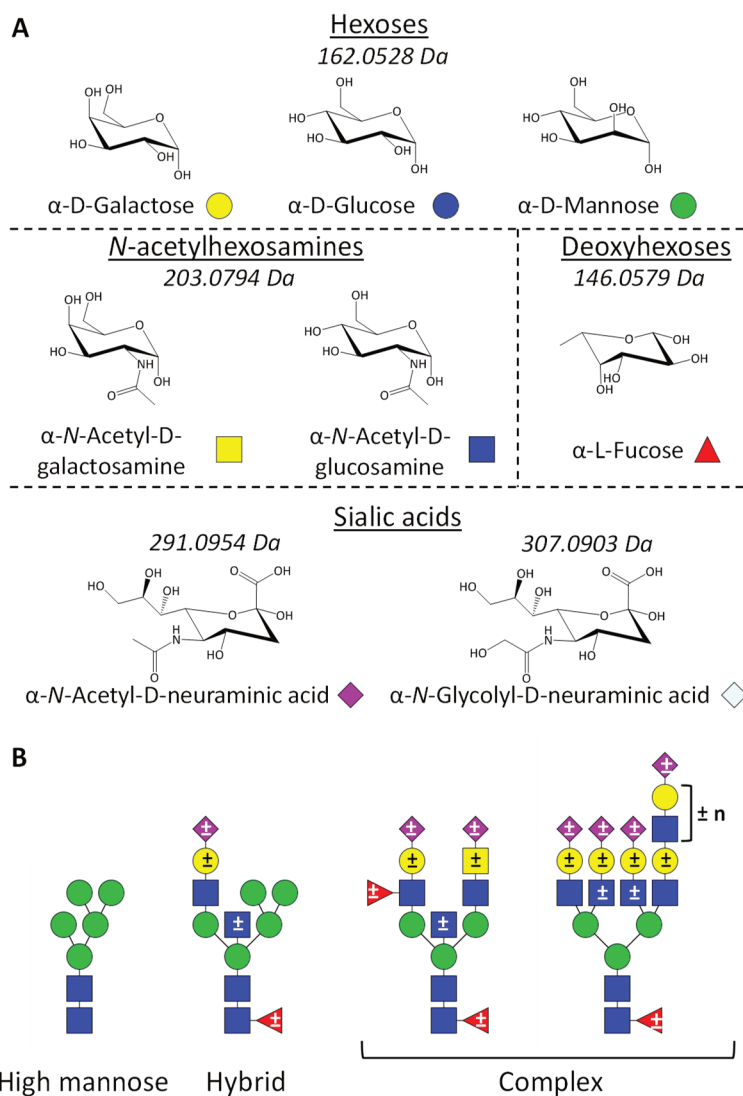


Figure 1.1 N- and O-glycan monosaccharides and the three common types of N-glycan structures. (A) The monosaccharides commonly found in mammalian N- and O-glycans and their representative symbols. While humans exclusively incorporate the sialic acid variant N-acetylneuraminic acid in their N- and O-glycans, other mammals additionally, or exclusively, feature N-glycolylneuraminic acids. The monosaccharide masses shown are the residue masses of the sugar units upon condensation with a glycan. (B) Symbolic representations of the three N-glycan types found on human proteins, including high mannose-, hybrid- and complex-type N-glycans. High mannose-type glycans carry five (as shown) to nine mannoses. Hybrid- and complex-type glycans carry optional core or antennary monosaccharide residues, indicated with a plus/minus sign (\pm).

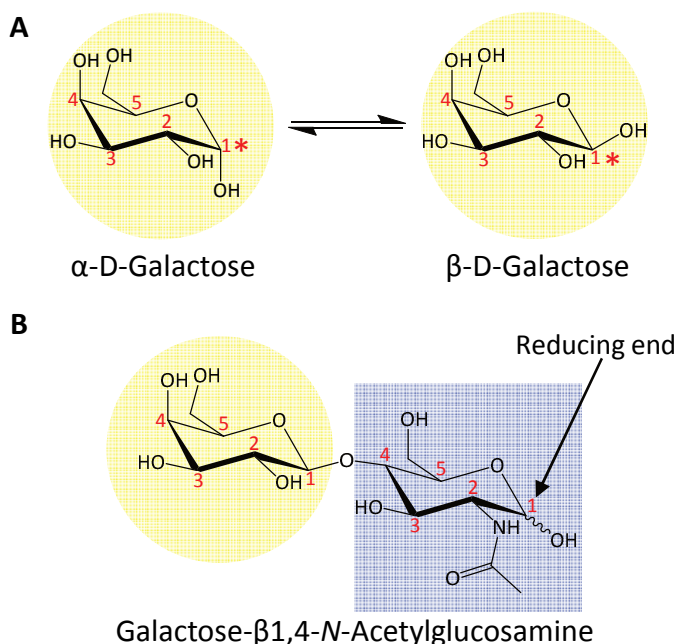


Figure 1.2 Monosaccharide anomers and linkages. (A) The α - and β -anomer of D-galactose. The anomeric center at C-1 is indicated by an asterisk (*). (B) A galactose linked to an *N*-acetylglucosamine via a β 1,4-linkage, the hydroxyl group at the anomeric center (reducing end) of the *N*-acetylglucosamine is connected with a wavy line, indicating the configuration is either α or β , alternatingly present in solution via an open ring intermediate.

1.1.2 O-glycan structure and biosynthesis

Different types of *O*-glycosylation exist, of which the *O*-GalNAc-type of glycosylation is most common (also known as mucin-type *O*-glycosylation). While the building blocks for the construction of a mucin-type *O*-glycan (further referred to as *O*-glycan) are matching the building blocks used for *N*-glycan synthesis (GalNAc, GlcNAc, Gal, Fuc and Sia; **Figure 1.1A**) and the glycosidic linkages formed are the same, the biosynthesis pathway is rather different between the two [16]. While *N*-glycosylation happens both co- and post-translationally and is initiated in the ER, *O*-glycosylation exclusively occurs post-translationally in the Golgi apparatus, starting with the enzymatic transfer of one GalNAc to a serine or threonine residue [16, 17]. Additionally, there is no known amino acid consensus sequence for the *O*-glycosylation to take place. A broad repertoire of enzymes can initiate the initial GalNAc transfer, which all have their own substrate specificity. Some of these enzymes prefer a serine as substrate and others a threonine. Additionally, it is known that a proline or another *O*-glycan in close proximity of the serine or threonine

facilitates *O*-glycosylation [17, 18]. After the attachment of the first GalNAc, the *O*-glycan can be extended by the interplay of a wide variety of glycosyltransferases, resulting in branched structures with one of the four common cores 1 to 4, consisting of GalGalNAc, GlcNAcGalGalNAc, GlcNAcGalNAc or GlcNAc₂GalNAc, respectively (**Figure 1.3**) [19].



Figure 1.3 Symbolic representations of the four common cores of mucin-type *O*-glycan structures. Yellow square: *N*-acetylgalactosamine (GalNAc); Yellow circle: galactose (Gal); Blue square: *N*-acetylglucosamine (GlcNAc). The linkages between monosaccharides are indicated at the connective lines.

1.2 IgG glycosylation

There are four human IgG subclasses, IgG1, 2, 3 and 4, all 150 kDa glycoproteins consisting of two heavy (H) and two light (L) chains, connected via disulfide bonds. The molecules consist of constant (C) domains (C_H1 to C_H3, and C_L) and variable (V), antigen binding domains (V_H and V_L; **Figure 1.4**), which together form the Fab (C_L, C_H1, V_L, V_H), and Fc (C_H2 and C_H3) region of the antibody. Fab and Fc are connected by the hinge region, which has a relatively flexible structure (**Figure 1.4**) [20]. All IgG subclasses can be subdivided into allotypes, based on the genetic variation between individuals in the heavy chain sequence of the antibody. With 19 different known allotypes, IgG3 is the subclass with the widest variety of constant domain sequence variants [21, 22].

Within the C_H2 domains of the IgG Fc regions an *N*-glycosylation consensus sequence can be found, carrying an *N*-glycan in over 99% of the IgG in the human circulation [23, 24]. IgG Fc *N*-glycosylation is rather special in its composition as compared to the glycosylation of other glycoproteins, as it shows predominantly diantennary complex-type glycans, and a minor fraction of hybrid-type glycans [25-27]. The complex-type IgG Fc glycans are mainly fucosylated (~93% in healthy adults) and may carry a bisecting GlcNAc (~12%). Furthermore, their composition varies from having zero to two antennary galactoses (~40% per antenna) and zero to two terminating *N*-acetylneuraminic acids (~4 % per antenna; further referred to as sialic acids when human glycosylation is concerned; **Figure 1.4**) [28, 29]. In addition to the aforementioned C_H2 *N*-glycosylation, that is conserved for

all IgG subclasses, IgG3 carries an *N*-glycosylation site in the C_H3 domain of most allotypes [23, 30] and three *O*-glycosylation sites in the hinge [31]. The occupancy of these additional sites was determined to be about 12% for the C_H3 *N*-glycosylation and about 10% for the *O*-glycosylation sites [23, 31]. Furthermore, 15 to 25% of the IgG Fab regions carry one or more occupied *N*-glycosylation consensus sequences. When present in the antigen-binding domain of the antibody, the glycans enhance the variability of these regions [32, 33]. Compared to Fc glycans, Fab glycans show higher levels of galactosylation, sialylation and bisecting GlcNAcs, while their fucosylation is lower [29].

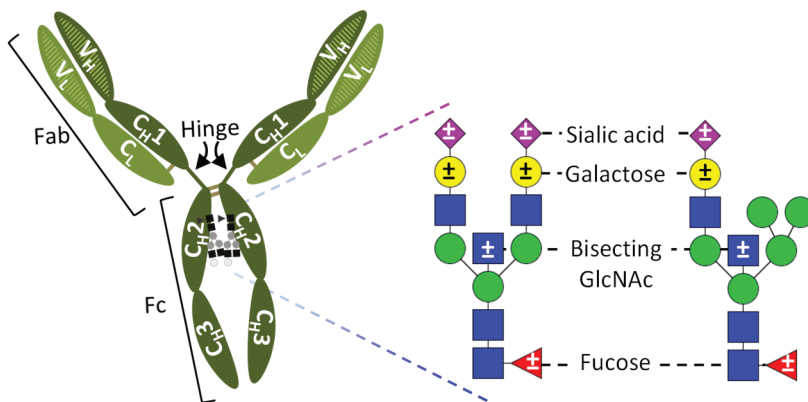


Figure 1.4 Schematic representation of IgG1 and its commonly found C_H2 glycan structures. IgG consists of two heavy chains (H; dark green) and two light chains (L; light green), connected via disulfide bridges (grey lines). Together, the heavy and light chain form the Fab and Fc portion, connected via the hinge region. The variable parts of the heavy and light chain (V) are both involved in the antigen binding sites (striped). On one of the constant domains (C), C_H2, a conserved *N*-glycosylation site is present. This site carries hybrid- and complex-type glycans with optional extra monosaccharide residues, like a core fucose, a bisecting *N*-acetylglucosamine (GlcNAc), galactoses and sialic acids, indicated with a plus/minus sign (±).

1.2.1 IgG Fc glycosylation effector mechanisms

IgG plays an important role in humoral immune responses, e.g. the immune events taking place in the extracellular space, by destroying microorganisms and foreign substances. IgG molecules bind antigens with their Fab regions and clear them via neutralization, opsonization by Fc receptor binding or activation of the complement system [34]. The latter two events involve the Fc region of the antibody and are highly influenced by both the presence [35, 36] and the structure [37] of the C_H2 *N*-glycan. Total absence of the Fc glycan minimizes the affinity between the IgG-Fc and most of its interaction partners by significantly changing the 3D-conformation of the Fc [38-40]. The presence or absence of

individual monosaccharides, on the other hand, modulates the binding affinity of the Fc for its interaction partners in a more subtle and specific way [41]. A large part of the studies into Fc glycan effector functions were performed in murine models, however murine glycosylation comprises some distinct glycosylation features as compared to human glycosylation. Most noticeable are the presence of different sialic acids, *N*-glycolylneuraminic acids, and the possibility to carry terminal α 1,3-linked galactoses attached to the β 1,4-linked antennary galactoses [42-44]. As it has been shown that functional results obtained from mouse experiments are not always straightforwardly translatable to the human situation [45, 46], in the following, only findings are presented obtained from human based *in vitro* studies, unless reported otherwise.

Fucosylation

The absence of a core fucose on complex-type IgG1 Fc glycans is known to enhance Fc γ receptor (Fc γ R)IIIa and b binding by 20- to 100-fold [37, 47], thereby strongly increasing the subsequent antibody-dependent cellular cytotoxicity (ADCC) [37, 48]. Both protein-glycan and glycan-glycan interactions between the uniquely glycosylated Fc γ RIIIa/b and the non-fucosylated Fc showed to play a key role in the increase in binding affinity [49].

Galactosylation

In contrast to the aforementioned core fucoses, terminal galactose residues are unlikely to be in close enough proximity to the Fc binding site to provide a direct interaction between the glycan and a receptor(-glycan) [50]. Still it has been shown that galactosylation slightly improves the binding of IgG1 to Fc γ RI, Fc γ RIIa/b/c and Fc γ RIIIa/b [51, 52], which might be due to an increase in Fc stability caused by glycan-protein and glycan-glycan interactions within the antibody [40, 50]. Although previous research indicated this galactosylation effect to be independent from the fucosylation effect [51], a more recent study showed the increased IgG1 affinity for Fc γ RIIIa/b upon galactosylation only to be present for afucosylated glycoforms [37]. In addition to the effect on Fc γ R binding, an increase in Fc galactosylation has been shown to improve complement activation via C1q binding and in consequence enhance complement-dependent cytotoxicity (CDC) [37, 53].

Sialylation

A lot of debate is going on about the effect of IgG Fc sialylation. Changes in sialylation often follow the effect of the galactosylation of the glycan, as the terminal galactose is a substrate for sialyltransferases [54, 55]. Therefore, the effects of sialylation and galactosylation in a biological system are often hard to distinguish. Whereas some report no effect of IgG1 sialylation on Fc γ R binding [52], others report a slight decrease in Fc γ RIIIa/b affinity for sialylated, afucosylated, bisected IgG1 as compared to its non-

sialylated, afucosylated, bisected form [37]. Furthermore, sialylation was both reported to increase [37] and to decrease [56] C1q binding. The latter discrepancy was suggested to be caused by the difference in monoclonal antibody studied, as the spatial distribution of the monoclonal antibodies on the cell surface might have a large influence on the activation of the complement [37]. In addition to FcγR and C1q binding, sialylation was reported to exert its effect via binding to the cell surface receptor DC-SIGN and its murine orthologue SIGN-R1, which results in the upregulation of anti-inflammatory components [57, 58]. However, also this is under debate as others reported the affinity of IgG to DC-SIGN to be independent of Fc glycosylation, but rather influenced by Fab glycosylation [59]. The potential cause of this confusion is the large difference between humans and mice in DC-SIGN and SIGN-R1 cellular and tissue distribution and the different sialic acid variants found in both species [45, 60].

Bisection

Although the presence or absence of a bisecting GlcNAc has a large effect on the overall Fc *N*-glycan structure [61], it did not seem to directly influence C1q or FcγR binding in any way [37]. Little is known about the biological relevance of Fc bisection, although presence of a bisecting GlcNAc was reported to inhibit the subsequent fucosylation of *N*-glycans [62]. Additionally, when bisection happens early in the biosynthesis pathway, that is, prior to full mannose trimming in the Golgi apparatus, the conversion from hybrid- to complex-type glycan is blocked, resulting in the propagation of bisected hybrid-type glycoforms [62, 63]. Together, this suggests that the presence of a bisecting GlcNAc might rather play a role as regulatory tool early in the glycan biosynthesis pathway, instead of having a direct effect on Fc interactions.

Hybrid-type glycans

Hybrid-type glycans occur on IgG in minor amounts [26, 27] and are present when the protein leaves the biosynthesis process before the formation of complex-type glycans was initiated. Although very little is known about the biological relevance of hybrid-type glycans on IgG, one study showed the negative effect of afucosylated, bisected, hybrid-type glycans on complement activation, as compared to afucosylated, bisected complex-type glycans [62].

Alternative mechanisms influenced by Fc glycosylation

The effect of Fc glycosylation on immunological responses is best studied for FcγR binding and complement activation via C1q protein. However, IgG has additional interaction partners that might influence an immunological response. The dependence on specific Fc glycosylation of these interaction partners is less well studied. One example is the DC-SIGN

receptor, briefly mentioned above [57, 59]. Others include the family of Fc receptor-like proteins (FcRL1 to 6), the neonatal Fc receptor (FcRn) and various lectins [64-66]. FcRL4 and 5 are expressed on B cells and have been shown to bind IgG. Furthermore, FcRL5 is reported to bind IgG in a glycan-specific manner, although it is unknown whether this is based on Fc or Fab glycosylation [65]. The FcRn binds IgG-Fc in the placenta thereby mediating the transport of IgG molecules from the mother to the fetus. Additionally, FcRn present on epithelial cells helps to recycle IgG, resulting in its relatively long half-life of about three weeks [67]. Differences – albeit not striking – in binding affinity for FcRn were found between differently glycosylated Fc regions [64]. Additionally, the IgG Fc glycosylation between mothers and their newborns was reported to be slightly different [68]. Although there is no consensus about the biological relevance of Fc glycosylation for FcRn binding, large effects can rather safely be ruled out [69, 70]. Furthermore, while for other glycoproteins, and also for Fab glycosylation, the asialoglycoprotein receptor expressed in the liver binds asialylated glycoforms and in that way reduces the half-life of the proteins, for IgG-Fc this receptor plays no role, likely due to restricted accessibility of the glycans [71, 72]. For IgG based biopharmaceuticals it is known that the presences of high mannose-type glycans of the Fc region does play a role in reducing its half-life, possibly caused by the involvement of specific lectins such as the mannose receptor [73]. This might be a reason why this glycoform is hardly found on endogenous IgG in the circulation.

1.2.2 IgG Fc glycosylation in health and disease

Fc glycosylation plays an important role in modulating IgG effector functions, as described above. IgG glycosylation is partly genetically regulated [74, 75], but also highly influenced by environmental factors [76-78]. The biological relevance of Fc glycosylation is supported by its associations found with altered physiological states, both in health and disease. First, Fc glycosylation associates with basic descriptors of the human population, like age and sex [28, 79-81]. Most pronounced is the lower galactosylation observed with older age [28, 79-81]. Notably, while women have higher galactosylation in early adulthood than men, this changes around female menopause, and results in similar galactosylation for women and men in late adulthood [28]. Fc sialylation follows this trend in the adult population, while bisection increases in early adulthood and fucosylation stays relatively constant [28, 79, 82]. For children, especially of the youngest age category, less is known about their Fc glycosylation differences connected to age and sex. The studies done until now only describe IgG glycosylation on the level of released glycans [83, 84], which ignore the effects of potential Fab glycosylation or differences in IgG subclass distributions. This issue will be assessed later in this thesis (Chapter 3). However, what is known until now is that in children agalactosylated species on IgG are lower with higher age and monogalactosylated species stay relatively constant [83]. Additionally, for children

between 6 and 18 years of age, it was found that bisection increases for boys and fucosylation decreases for girls [84]. Furthermore, it was proposed that most of the sex-related Fc glycosylation differences are introduced during puberty, under the influence of sex-related hormones [79, 84].

Moreover, Fc glycosylation is well characterized in healthy pregnant women [29, 85] and their newborns [86, 87], showing a substantial increase in galactosylation with pregnancy, which normalizes after delivery [29, 85]. Newborns exhibit similarly high galactosylation levels, as their IgG is completely mother-derived [86, 87]. Furthermore, pregnant women have high levels of IgG sialylation, while the levels of bisection and fucosylation are lower during pregnancy than after delivery [29, 85].

While age, sex and pregnancy are natural descriptors of the population, there are indications that also lifestyle influences IgG glycosylation. For example, smoking results in a slightly higher level of bisection [77, 88], and the level of Fc galactosylation is correlated to living area (e.g. rural or urban) [76]. Additionally, the food substance all-trans retinoic acid, when directly applied on cultured B cells, has shown to influence the galactosylation profiles of the IgGs produced in these cells [78].

All described genetic, environmental and physiological influencers of the Fc glycosylation suggest large inter-individual differences in this IgG feature, which were indeed observed in numerous IgG Fc glycosylation studies [28, 74, 89]. Although this might complicate the discovery of disease-related markers, intra-individual glycosylation changes are in general quite minor over restricted periods of time [90, 91] and common disease-related changes in IgG Fc glycosylation have previously been identified in the adult population. For example, patients suffering from various autoimmune diseases like rheumatoid arthritis [92-94], inflammatory bowel diseases [95] and lupus [96] have shown to carry a low Fc galactosylation on their total pool of IgG as compared to healthy controls. For ANCA-associated vasculitis, IgG Fc galactosylation and sialylation levels have shown to be able to predict a relapse of the disease [97]. Additionally, other inflammatory conditions, like HIV [98], alloimmune cytopenias [99, 100], and active tuberculosis infections [101], and also cancers such as ovarian cancer [102] and colorectal cancer [103] did show to associate with specific features of the total Fc glycosylation. Interestingly, antigen-specific subsets of IgG showed distinct glycosylation profiles from the total IgG. For example, HIV gp120-, HPA-1a- and RhD-specific IgGs all carry relatively high levels of afucosylated glycan structures, as compared to the total pool of IgG [98-100]. For the RhD-specific IgGs in hemolytic disease of the fetus and newborn it was shown that this low fucosylation was correlated to their ability to induce FcγRIIIa mediated ADCC of the red blood cells, and in that way likely influences the severity of the disease [99].

Both the innate and adaptive immune system of the human child are relatively immature at birth and their maturation process continues until early adulthood [104]. Therefore, one can imagine that the IgG glycosylation effects found in children might be different from the ones observed in adults, both in healthy and diseased conditions. In general, information on IgG Fc glycosylation in children is scarce, especially when compared to the numerous studies performed in human adults. A recent study showed juvenile idiopathic arthritis to be associated with a lowered galactosylation and sialylation on the total IgG pool [66]. Furthermore, studies into pediatric patients with allergic diseases and asthma showed no disease-specific IgG glycosylation effects [76, 105]. Evaluating the similarities and differences between IgG glycosylation responses in children and adults might contribute to the better understanding of the immune system as a whole and the humoral immune responses in children, specifically.

1.3 Mass spectrometric glycosylation analysis

In order to unravel the exact glycosidic profile of any glycoprotein in a certain sample taken from a biological system, analytical methods are required that can assess protein glycosylation in a precise, accurate, and preferably protein- and glycosylation site-specific manner. Not one method exists that can easily perform the complete characterization of the glycoproteome of a complex sample, however various complementary separation and detection methods are around that can together give an in-depth overview. One important branch of glycosylation analysis methods makes use of mass spectrometry (MS) to separate and detect glycans or glycoconjugates based on their mass-to-charge ratio (m/z). Using MS, one can have roughly three different approaches studying the glycoproteome: 1) By the chemical or enzymatic release of glycans from proteins, resulting in a mixture of all glycan structures present in the sample, irrespective from which protein they were derived. This provides the opportunity to perform an in-depth characterization of the exact chemical structure of all glycans, however this approach fails to provide protein- or site-specific information. 2) By the enzymatic digestion of the glycoprotein backbone into smaller protein fragments or peptides, resulting in a mixture of glycosylated and glycan-free protein fragments. In this way, protein-specificity is maintained, as well as site-specificity, if only one glycosylation site is present per created fragment. As a downside, this approach will lead to a rapid increase of sample complexity when more than one kind of protein is present, making detailed structural glycan analysis laborious and the generation of protein- and site-specific glycopeptides challenging. 3) By the analysis of intact glycoproteins, often preceded by their specific isolation. Besides protein-specific data, this approach also provides the opportunity to assess the combination of different glycan structures and other post-translational modifications

present at one protein at the same time, however losing knowledge on site-specificity. For this approach high-resolution instruments are required.

The current work will focus on approach number 2, making use of a protease to create (glyco)peptides, which subsequently can be characterized by MS. Using MS, the glycan composition of a glycopeptide can be determined based on the theoretical mass of the peptide and the individual monosaccharides. However, stereoisomers cannot be distinguished, neither those arising from isomeric monosaccharides nor those arising from linkage isomerism, as they all result in identical m/z values (**Figure 1**). Additional information on the structure of specific glycan compositions and on the sequence of the peptide moiety can be obtained by applying tandem mass spectrometry (MS/MS) on selected ions, creating fragmentation spectra of the analytes of interest. Depending on the fragmentation mode used, either the glycan or the peptide portion of the glycopeptide is fragmented. Lower energy collision-induced dissociation (CID) results in glycan fragments, while higher energy CID, electron-transfer dissociation or electron-capture dissociation provide information about the peptide sequence [106]. A combination of high and low energy CID or post-source decay fragmentation results in the fragmentation of both portions of the glycopeptide [106, 107].

1.3.1 Mass spectrometers

Two important parts of a mass spectrometer are its ion source and mass analyzer, which both exist in different flavors and can be used in various combinations, all providing their own advantages in particular situations [108]. One frequently, yet not exclusively, used mass analyzer for glycopeptides is the reflectron time-of-flight (TOF) analyzer, which is able to separate analytes in a broad m/z range in a relatively short period of time [109]. This analyzer initially exposes all ions to an electrical field causing their acceleration while obtaining the same kinetic energy per charge. After their acceleration, the ions enter the flight tube of the TOF analyzer, where they travel with a constant velocity. Under these conditions, their velocity (and thus the flight time) is proportional to the m/z of the ions, with low mass or highly charged analytes traveling faster than high mass or lowly charged analytes [108]. Prior to entering the acceleration field of the TOF, during their ionization, the ions did acquire an initial velocity, which is not necessarily the same for all of them. This results in a dispersion of the final velocity (the sum of the initial velocity and the velocity acquired during acceleration) of identical species, which hampers the resolving power of TOF instrumentation. However, this is largely overcome by the implementation of delayed extraction of the ions during their acceleration [110] and the reflectron in the flight tube [111], both correcting for the spread in kinetic energy between ions with the same m/z .

As (glyco)peptides are not volatile and are preferably analyzed in their intact form, soft ionization technologies are required that allow ionization of the analytes from a liquid or solid sample. Next to obtaining a charge during the ionization, the molecules need to be brought into the gas phase, either via their own sublimation or desorption, or via the evaporation of their solvent or of a matrix. While some ionization techniques cause the molecules to fragment during ionization, soft ionization techniques will leave them largely intact. Two suitable approaches, often used in combination with a reflectron TOF analyzer, are matrix assisted laser desorption/ionization (MALDI) and electrospray ionization (ESI) [108], both discussed in detail in the following sections.

1.3.2 MALDI-TOF-MS of glycopeptides

Ionization with MALDI takes place by the irradiation with a laser of a solid sample in vacuum. For this procedure the analyte molecules need to be embedded in a matrix, consisting of small organic compounds that absorb the light of the laser, which has a wavelength in either the UV or IR range, and are easy to sublime [108, 112]. The exact mechanism behind MALDI is not completely understood as of yet, but ionization likely happens either via reactions in the gas phase after matrix ablation, or via the desorption and desolvation of ions formed in the solid sample [108, 113]. For the ionization of glycopeptides using MALDI with an UV-laser, examples of suitable matrices are α -cyano-4-hydroxycinnamic acid (CHCA), 4-chloro- α -cyanocinnamic acid (Cl-CCA) and 2,5-dihydroxybenzoic acid (DHB) [108, 114]. These matrices are soluble in diluted organic solvents that are compatible with the glycopeptides and carry an acidic group that stimulates the protonation of the analytes.

MALDI-TOF-MS is a widely recognized approach for the analysis of glycopeptides as the technique allows rapid acquisition of data, which are, in addition, relatively straightforward to interpret as the ions are usually singly charged [115, 116]. A typical MALDI glycopeptide workflow includes the enzymatic digestion of the (isolated) glycoproteins, enrichment of the glycopeptides, and co-application of the sample and matrix on the MALDI target [117]. Glycosylation profiles obtained by MALDI-TOF-MS of glycopeptides have shown to correlate well with the profiles obtained by other techniques, based on the high-performance liquid chromatography (HPLC)-fluorescence detection of released glycans [117]. However, this is only valid for the non-sialylated subset of the glycoproteome, as sialic acids are highly labile during MALDI-TOF-MS [117, 118]. In addition to the loss of sialic acids due to in-source or metastable decay, the negative charge of these sugar residues results in ionization biases for sialylated species, both in negative and positive ion mode, and in salt formation. The labile nature of the sialylated glycopeptides is especially problematic when they are analyzed in reflectron mode TOF-MS, as metastable fragments travel together in the field free region and are only separated after passing through the reflectron. Therefore, sialylated glycoconjugates

are often analyzed in linear mode TOF-MS, highly compromising the resolving power of the measurements. Other means for improving the detection of sialylated glycopeptides are the use of cold matrices like DHB or Cl-CCA and/or performing the analyses in negative ion mode [114]. However, none of these approaches fully prevent the loss of sialylated species, their ionization biases and salt formation.

In recent years, the neutralization and stabilization of sialylated glycans and glycoconjugates has appeared as an attractive approach for their MALDI-TOF-MS analysis. One method for this is the permethylation of released glycans or glycopeptides, resulting in the methylation of all hydroxyl, amine and carboxyl moieties in the molecules [119, 120]. Other approaches are sialic acid-specific and include the esterification or amidation of the sialic acid carboxyl groups [115]. This involves, on the one hand, the uniform modification of all sialic acids, for example by their amidation with the nucleophiles acetohydrazide [121] or methylamine [122]. On the other hand, linkage-specific sialic acid modifications have been reported, allowing the differentiation between α 2,3- and α 2,6-linked sialic acids based on their analysis by MALDI-TOF-MS. For example, α 2,6-linked sialic acids can be methylesterified [123], ethylesterified [124, 125] or isopropylamidated [126], while α 2,3-linked sialic acids are simultaneously lactonized [123, 124] or methylamidated [125, 126]. Specifically for glycopeptides, the application of a sialic acid linkage-specific derivatization method is more complicated than for released glycans, as the peptide moieties also carry carboxylic acids (at least one at their C-terminus and additionally one at every aspartic acid and glutamic acid residue). Based on the local environment of these peptide carboxylic acids, they might either react with the added nucleophile or create by-products by forming lactones or lactams with neighboring hydroxyl or amine groups, respectively. This was shown for glycopeptides derived from IgG that were subjected to the ethylesterification reaction proven to be suitable for released glycans [124], resulting in three modification variants of the peptide moiety [127]. On the other hand, the uniform derivatization of glycopeptide sialic acids by methylamidation resulted in consistent peptide modifications for glycopeptides derived from both IgG and fetuin [128].

1.3.3 ESI-TOF-MS of glycopeptides

In contrast to MALDI, ESI requires a liquid sample that is passed through a capillary and which creates a spray at the end of the capillary upon the application of a strong electric field. The solvent droplets in the spray evaporate and charged analytes either desorb from the surface of the droplets (small molecules) or stay in the droplet until complete evaporation took place (larger (glyco)peptides or proteins) [108]. While MALDI results in singly charged analytes, ESI causes multiple charged ions to arise [129]. This has the advantage that the mass analyzer used is required to cover a narrower m/z range,

however it complicates data analysis as one analyte might be spread over multiple signals (charge states) in the mass spectrum.

A typical ESI-TOF-MS workflow for glycopeptides includes the digestion of (isolated) glycoproteins, the online or offline enrichment or fractionation of the glycopeptides and their subsequent analysis by ESI-TOF-MS [130]. Sialylated glycans and glycoconjugates ionized by ESI suffer less from instability as compared to these analytes ionized by MALDI, and usually no derivatization of glycopeptides is incorporated in the ESI-TOF-MS workflow [131]. However, one should take into account that also with ESI, sialylated species can possibly suffer from ionization biases and salt formation. Additionally, like for MALDI-TOF-MS, linkage-specific sialic acid derivatization in ESI-TOF-MS has the advantage of differentiating between sialic acid linkages without any further separation or fragmentation needed [132, 133].

The online separation of glycopeptides is often achieved by the hyphenation of ESI-TOF-MS to liquid chromatography (LC). A separation step prior to MS enables the analysis of more complex samples and might provide additional structural information on both the peptide and the glycan moiety of the glycopeptides [130]. Reversed-phase (RP)-C18-LC is an often used separation method, which results in clustering of the glycopeptides that share the same peptide moiety and carry equally sialylated glycans. The elution of the sialylated glycopeptides relative to the neutral glycopeptides depends on the ion-pairing agent added to the mobile phase [134, 135]. Simultaneous elution of all glycoforms on a single peptide moiety results in their straightforward identification and relative quantification [25, 130, 131, 136]. LC separation techniques complementary to RP-LC include hydrophilic interaction liquid chromatography (HILIC) and porous graphitized carbon (PGC)-LC. HILIC is especially suitable for the separation of glycopeptides with short peptide sequences, which might not be retained by RP-LC [137] and it allows the efficient separation between glycosylated and non-glycosylated peptides in complex mixtures [134, 138]. Additionally, for sialylated glycopeptides, HILIC enables the differentiation between α 2,3- and α 2,6-linked sialic acids without any prior modification of the molecules [139]. Similar to HILIC, PGC-LC provides a platform for the separation of glycopeptides with short peptide moieties, with the advantage that samples do not have to be loaded in high concentrations of organic solvent, as is the case for HILIC and which might cause solubility issues [23, 140]. However it should be taken into account that both highly sialylated glycopeptides and glycopeptides with longer peptide sequences might be irreversibly retained on the PGC stationary phase [141, 142]. As the three mentioned separation approaches, RP-LC, HILIC and PGC-LC, all have complementary properties, also combinations are used for the characterization of glycopeptides [23, 143-145].

Capillary electrophoresis (CE) provides an additional separation method that is regularly coupled to ESI-TOF-MS. The separation mechanism of CE is complementary to RP-LC as glycopeptides are mainly separated based on their glycan moiety (if the peptide portions are short enough), resulting in the co-elution of similar glycoforms attached to different peptides [146]. Additionally CE-ESI-MS is extremely sensitive, enabling the profiling of glycans on low abundant proteins [146, 147]. While CE-ESI-MS of glycopeptides was reported to be used in combination with sialic acid linkage-specific derivatization [132], it has also been shown that CE is able to distinguish between species with differently linked sialic acids without extra sample preparation after the proteolytic digestion [148].

1.3.4 Mass spectrometric analysis of IgG glycopeptides

Specifically for the analysis of IgG glycopeptides, often trypsin is used for proteolytic cleavage [131, 133]. For the glycosylation site on the C_H2 domain, tryptic digestion results in glycopeptides with the sequences EEQYNSTYR for IgG1, EEQFNSTFR for IgG2, EEQFNSTFR, EEQYNSTFR or TKPWEEQYNSTFR for IgG3 and EEQFNSTYR for IgG4 [22]. The different variants of the IgG3 peptide moieties are a result of the numerous different allotypes known for IgG3, of which the occurrence is dependent on the ethnical background of the population studied. For the Caucasian population it is often assumed that the IgG3 sequence is identical to the IgG2 sequence, resulting in indistinguishable glycosylation profiles on these subclasses. However, it cannot be ruled out that the IgG3 sequence corresponds in mass to the IgG4 sequence (EEQYNSTFR vs. EEQFNSTYR) or has an unique longer sequence (TKPWEEQYNSTFR) as long as the allotypes occurring in the samples are not determined [21].

The MALDI- and ESI-TOF-MS approaches for glycopeptide analysis described above are reported to be used for the glycosylation profiling of IgG glycopeptides. For example, numerous studies report the use of RP-LC-ESI-TOF-MS for the IgG glycosylation profiling of glycopeptides derived from the C_H2 domain [25, 131, 136]. Additionally, CE-ESI-MS showed to be suitable for the highly sensitive analysis of IgG glycopeptides, at the same time being able to differentiate between α 2,3- and α 2,6-linked sialylated species [147, 148]. Specifically for IgG3, PGC- and RP-LC were combined to characterize the *N*-glycosylation of the C_H2 and C_H3 domains and the *O*-glycosylation of the hinge region in the same run, after its non-specific proteolytic treatment with pronase [23]. Finally, for the high-throughput analysis of the tryptic C_H2 domain glycopeptides of IgG, the application of MALDI-TOF-MS methods with or without sialic acid derivatization were reported [114, 120, 127, 128, 131].

1.4 Scope

The reliable characterization of antibody glycosylation is of utmost importance, both in unraveling (patho)physiological processes and in identifying potential clinical markers for disease diagnosis, progression and treatment. The aim of the work described in this thesis is, on the one hand, to develop new methodologies for the analysis of antibody glycosylation, and, on the other hand, the application of glycopeptide profiling methods on clinical samples to gain a better understanding of the behavior and role of antibody glycosylation in health and disease.

In **Chapter 1**, the general concept of protein glycosylation is introduced. Specifically for the antibody IgG, a more in-depth description of its glycosylation features and functions is given. Additionally, the currently used methodologies for the characterization of protein glycosylation are described, with a special focus on the MALDI- and ESI-TOF-MS analysis of glycopeptides, as these technologies are used throughout the presented work.

While MALDI-TOF-MS is a relatively straightforward and rapid manner to study IgG glycopeptides, obtaining an unbiased overview of both the neutral and the sialylated glycopeptides is still a major challenge. In **Chapter 2**, the sialic acid linkage-specific stabilization of sialylated glycoforms, which before was reported for released glycans, is extended to sialic acid linkage-specific IgG Fc glycopeptide derivatization followed by MALDI-TOF-MS analysis.

IgG Fc glycosylation was already extensively studied in various clinical settings, however both the function and regulation of IgG Fc glycosylation is not completely understood as of yet. Additionally, most studies were performed in human adults, while knowledge on pediatric IgG glycosylation is lagging behind. **Chapter 3** uses the MALDI-TOF-MS method developed in **Chapter 2** to characterize the IgG Fc glycosylation of healthy newborns and children. To get an insight into the regulation of IgG Fc glycosylation, in **Chapter 4** this glycosylation is assessed in children in need of a hematopoietic stem cell transplantation, using a previously developed RP-LC-ESI-TOF-MS method. Samples of the patients before and after transplantation are characterized and compared to the profiles of the donors.

One of the aspects of clinical marker development is being able to distinguish between individuals with and without a specific disease. Additionally, it might be very valuable if these markers can also tell something about the subtype and/or severity of the disease, or provide information on disease progression or treatment success, as this offers the opportunity to tailor treatment in an individualized manner. **Chapter 5** deals with the characterization of IgG Fc glycosylation in pediatric meningococcal sepsis. Next to differentiating between diseased and healthy children, glycosylation signatures specific for

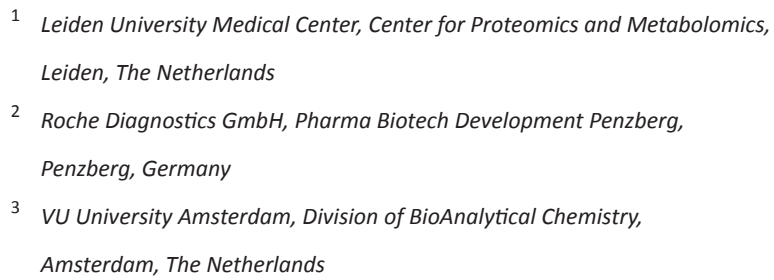
disease severity are assessed and glycosylation features are reported that have the potential to predict disease outcome shortly after patient submission to the hospital.

In **Chapter 6**, IgG Fc glycosylation is evaluated in the case of inflammatory bowel diseases in adults. In this study, specific glycosylation signatures are correlated to disease subtypes (Crohn's disease or ulcerative colitis) and progression. Additionally, the influence of treatment, either by medication or surgery, on the Fc glycosylation profile is described.

The majority of functional studies into IgG Fc glycosylation have been done using mice as model organisms. However, murine IgG glycosylation possesses different characteristics as compared to human IgG glycosylation and hitherto no systematic and subclass-specific profiling of mouse IgG glycosylation has been performed. In **Chapter 7**, the IgG Fc glycosylation of four commonly used mouse strains (both inbred and outbred) is profiled in a subclass- and site-specific manner using RP-LC-ESI-TOF-MS.

While IgG in human plasma is an extensively studied antibody with regard to its Fc glycosylation, information on other antibody subtypes and on antibodies from other sources than plasma is scarce. **Chapter 8** provides a method to isolate both IgG and IgA from human saliva and uses RP-LC-ESI-TOF-MS for their site-specific glycosylation analysis. Finally, a comparison is made between the glycosylation of IgG and IgA derived from saliva and plasma of the same individuals.

The final chapter of this thesis, **Chapter 9**, offers a general discussion of the work described, with a specific focus on mass spectrometric method development for the analysis of antibody glycosylation in a clinical setting.



Linkage-Specific Sialic Acid Derivatization for MALDI-TOF-MS Profiling of IgG Glycopeptides

Noortje de Haan¹, Karli R. Reiding¹, Markus Habberger²,
Dietmar Reusch², David Falck¹ and Manfred Wuhrer^{1,3}

Reprinted and adapted with permission from Anal. Chem.,
2015, 87 (16), pp 8284–8291 DOI: 10.1021/acs.analchem.5b02426 [149].

Copyright © 2015, American Chemical Society.



Glycosylation is a common co- and post-translational protein modification, having a large influence on protein properties like conformation and solubility. Furthermore, glycosylation is an important determinant of efficacy and clearance of biopharmaceuticals such as immunoglobulin G (IgG). Matrix-assisted laser desorption/ionization (MALDI)-time of flight (TOF)-mass spectrometry (MS) shows potential for the site-specific glycosylation analysis of IgG at the glycopeptide level. With this approach however, important information about glycopeptide sialylation is not duly covered because of in-source and metastable decay of the sialylated species.

Here, we present a highly repeatable sialic acid derivatization method to allow subclass-specific MALDI-TOF-MS analysis of tryptic IgG glycopeptides. The method, employing dimethylamidation with the carboxylic acid activator 1-ethyl-3-(3-dimethylamino)propyl)-carbodiimide (EDC) and the catalyst 1-hydroxybenzotriazole (HOBt), results in different masses for the functionally divergent α 2,3- and α 2,6-linked sialic acids. Respective lactonization and dimethylamidation leads to their direct discrimination in MS and importantly, both glycan and peptide moieties reacted in a controlled manner. In addition, stabilization allowed the acquisition of fragmentation spectra informative with respect to glycosylation and peptide sequence. This was in contrast to fragmentation spectra of underivatized samples which were dominated by sialic acid loss. The method allowed the facile discrimination and relative quantitation of IgG Fc sialylation in therapeutic IgG samples. The method has considerable potential for future site- and sialic acid linkage-specific glycosylation profiling of therapeutic antibodies, as well as for subclass-specific biomarker discovery in clinical IgG samples derived from plasma.

2.1 Introduction

Glycosylation is an important and prevalent co- and post-translational protein modification, affecting the physiological and biochemical properties of the conjugate in numerous ways ranging from changes in solubility and half-life to modulation of receptor interaction [150-153]. Protein properties vary not only by glycosylation site occupancy, but also by the type of glycan present on a specific site, and while mammalian glycans are composed of a limited number of monosaccharides, the way in which the monosaccharides can be linked and branched adds considerable complexity to a molecule [154]. One notable example of this is *N*-acetylneuraminic acid. This sugar residue often terminates complex glycan antennae and can be linked either via an α 2,6- or an α 2,3-linkage to the subterminal galactose. On intravenous immunoglobulins (IVIG), the presence of an α 2,6-linked sialic acid reduces inflammation, whereas an α 2,3-linkage does not have this effect [155]. For a commonly used biopharmaceutical protein like immunoglobulin G (IgG), careful analysis and control of glycosylation is a prerequisite to ensure proper conformation, activity and clearance [156-159].

High-throughput analysis of protein glycosylation can be performed by mass spectrometry (MS), matrix-assisted laser desorption/ionization (MALDI)-time of flight (TOF)-MS being a particularly suitable approach [160, 161]. Using this method however, information on monosaccharide linkages is often difficult to obtain, and the analysis of sialylated glycan species is biased by metastable decay and variations in ionization and salt adduction [118, 160]. Derivatization methods are known for released glycans that allow for sialic acid stabilization in MALDI-MS as well as discrimination of sialylation linkage isomers in MS [123, 162]. Previously, we have reported ethyl esterification for this purpose, which is characterized by its facile workflow and high linkage-specificity [29, 124]. The protocol relies on the tendency of α 2,3-linked sialic acids to lactonize, whereas α 2,6-linked sialic acids are more susceptible to reactions with external alcohols or amines. However, as the protocol requires prior release of the glycans from the protein backbone, site-specificity, as well as subclass-specificity in case of IgG, is lost. To retain this information we focus here on the analysis of glycopeptides, which has shown its importance in glycosylation analysis. Notable examples of this include subclass-specific IgG glycosylation profiling and system-wide protein glycosylation mapping [163, 164]. In the case of IgG, glycopeptide analysis makes it possible to differentiate between Fab and Fc glycosylation, which is, amongst others, important in lectin binding studies [29]. Furthermore, because the analysis of glycopeptides gives protein specific information, it can be performed on relatively impure samples. In literature, efforts to stabilize sialylated glycopeptides have included complete methylamidation of all carboxylic acids present on the conjugate using (7-azabenzotriazol-1-yloxy)tripyrrolidinophosphonium hexafluorophosphate as coupling reagent, as well as a direct esterification by 1-pyrenyldiazomethane [128, 165, 166]. While

these approaches have indeed shown improved sialylation analysis by MS, and can achieve recognition of sialic acid linkage upon fragmentation, no report has been made of a glycopeptide derivatization that reacts in a selective way to differently linked sialic acids.

Here, we present a method for the sialic acid linkage-specific stabilization of IgG glycopeptides, which is able to derivatize both *N*-acetylneuraminic acid and *N*-glycolylneuraminic acid and is therefore applicable on samples derived from various sources. Similar to the ethyl esterification reported previously, the method makes use of the carboxylic acid activator 1-ethyl-3-(3-dimethylamino)propyl)carbodiimide (EDC) and the catalyst 1-hydroxybenzotriazole (HOBt) [124]. However, we found that the alcohols used for the previously reported esterification, while linkage-specific for the sialic acid, showed variable reactions on the peptide portion of the glycoconjugate. Testing a range of reagents and conditions yielded a protocol employing dimethylamidation of the glycopeptides, which shows selectivity for the sialic acid linkage as well as for the carboxylic acids on the peptide portion. The protocol proves highly repeatable for the subclass-specific glycosylation analysis of tryptic IgG glycopeptides and provides, next to the sialic acid linkage information directly in MS, the possibility to generate informative MS/MS spectra. Finally, for two monoclonal antibodies with various sialic acid linkages, the profile of the glycopeptides after derivatization was found to be comparable to the analysis of released glycans. The speed and simplicity of the here reported method distinguishes it from other site- and sialic acid-specific methods like LC-MS, capillary electrophoresis (CE)-MS and the use of sialidases.

2.2 Experimental section

2.2.1 Chemicals, reagents, enzymes

The ultrapure deionized water (MQ) used in this study was generated from a Q-Gard 2 system (Millipore, Amsterdam, Netherlands), maintained at ≥ 18 M Ω . Ethanol (EtOH), methanol (MeOH), trifluoroacetic acid (TFA), sodium dodecyl sulfate (SDS), disodium hydrogen phosphate dihydrate (Na₂HPO₄·2H₂O), potassium dihydrogen phosphate (KH₂PO₄) and sodium chloride (NaCl) were purchased from Merck (Darmstadt, Germany). TPCK treated trypsin (from bovine pancreas), HOBt hydrate, dimethyl sulfoxide (DMSO), 50% sodium hydroxide (NaOH), 40% dimethylamine in water, super-DHB, Nonidet P-40 (NP-40), sodium bicarbonate and formic acid (FA) were all purchased from Sigma-Aldrich (Steinheim, Germany) and EDC hydrochloride from Fluorochem (Hadfield, UK). Peptide-*N*-glycosidase F (PNGase F) was acquired from Roche Diagnostics (Mannheim, Germany), 2,5-dihydroxybenzoic acid (2,5-DHB) from Bruker Daltonics (Bremen, Germany), 4-chloro- α -cyanocinnamic acid (Cl-CCA) from Bionet Research (Camelford, Cornwall, UK) and HPLC SupraGradient acetonitrile (ACN) from Biosolve (Valkenswaard, Netherlands). 10x

Phosphate-buffered saline (10x PBS) was made in-house, containing 57 g/L Na₂HPO₄·2H₂O, 5 g/L KH₂PO₄ and 85 g/L NaCl.

2.2.2 Samples

The IgG1 standard from human plasma was acquired from Athens Research (Athens, GA) and IgG from bovine serum from Sigma-Aldrich (Steinheim, Germany). Monoclonal antibodies originating from CHO cells (mAb1), as well as an *in vitro* galactosyl- and sialyltransferase treated variant thereof (mAb2) were provided by Roche Diagnostics. More details about mAb2 production can be found in **S-1.1** and **S-1.2**, Supporting Information. CHO cell-produced BRAD-3 was provided by Sanquin (Amsterdam, The Netherlands). Prior to use, the BRAD-3 sample was affinity purified using protein G Sepharose beads (see **S-1.3**, Supporting Information). Plasma IgG was isolated from human donor plasma by affinity purification also using protein G Sepharose beads (see **S-1.4**, Supporting Information).

The oligosaccharide standards 3'-sialyllactose (Neu5Ac α 2,3Gal β 1,4Glc) sodium salt and 6'-sialyllactose (Neu5Ac α 2,6Gal β 1,4Glc) sodium salt were purchased from Carbosynth (Compton, U.K.) and the 2-aminobenzamide (2-AB) labeled triantennary (A3) glycans were obtained from Ludger (Oxfordshire, U.K.).

2.2.3 Preparation and analysis of glycans and glycopeptides

Digestion of the isolated plasma IgGs (approx. 1 mg/mL) was performed by TPCK treated trypsin, added in a 1:10 (enzyme:substrate) ratio to the sample. The samples were shaken for 10 min at 600 rpm, after which the pH was checked and found to be in a range from pH 6 to 10. Subsequent overnight incubation at 37 °C resulted in a tryptic digest of 0.99 mg/mL plasma IgG. For the IgG1 standard, mAb1, mAb2, the bovine IgG and BRAD-3, the proteins were partially denatured prior to digestion by the addition of 20 μ L 100 mM FA to 1 μ L protein solution, followed by a 15 min incubation at RT. Subsequently, the samples were vacuum dried at 60 °C and dissolved in 50 mM sodium bicarbonate. Trypsin was added in a 1:10 (enzyme:substrate) ratio to the samples and the mixtures were incubated overnight at 37 °C. In this way, tryptic digests were obtained containing 0.23 mg/mL IgG1, 0.25 mg/mL mAb1, 0.19 mg/mL mAb2, 0.25 mg/mL bovine IgG or 0.25 mg/mL BRAD-3. *N*-glycans were released from the IgG samples by PNGase F digestion (see **S-2.1**, Supporting Information)[167] and subjected to linkage-specific derivatization of the sialic acids by ethyl esterification (see **S-2.2**, Supporting Information) [124].

Both glycans and glycopeptides were purified by cotton hydrophilic interaction liquid chromatography (HILIC) solid phase extraction (SPE) (see **S-2.3**, Supporting Information) [168]. Subsequent MALDI-TOF(/TOF)-MS analysis and data analysis were performed as described in **S-3**, **S-4** and **Table S-1**, Supporting Information.

2.2.4 Comparison of different nucleophiles for glycopeptide derivatization

Tryptic IgG glycopeptides derived from human plasma were subjected to derivatization with ethanol, methanol or dimethylamine using EDC and HOBt, to find the most suitable reagent for linkage-specific sialic acid modification with minimal reaction variability on the peptide.

Methyl and ethyl esterifications were performed on 1 μ L tryptic IgG glycopeptides in 20 μ L 250 mM EDC and 250 mM HOBt in the respective alcohol for 1 h at 4 °C and 37 °C, respectively. These are conditions which were reported to result in linkage-specific sialic acid derivatization [124]. After incubation, 20 μ L of ACN was added and the derivatized glycopeptides were purified by HILIC-SPE followed by MALDI-TOF-MS analysis.

To study the use of dimethylamine for the derivatization of IgG glycopeptides, EDC, HOBt and dimethylamine were dissolved in DMSO to concentrations of 50, 150 or 250 mM. Further optimization was performed by increasing the HOBt concentration to 350 and 500 mM while keeping both the EDC and the dimethylamine at 250 mM. Combining 1 μ L of the IgG digest with 20 μ L of the respective reagent mixtures, incubation was performed for 3 h at 60 °C. After addition of 113.3 μ L ACN (yielding a concentration of 85%), derivatized glycopeptides were purified from the mixture by HILIC-SPE, followed by MALDI-TOF-MS analysis.

The level of variability in the modifications on the peptide portion was for all methods determined based on the G1F glycoform. For the ethyl esterification and the dimethylamidation the IgG1 signals with different modifications were extracted from the spectra. For the methyl esterification the IgG2 signals were extracted. Averages and standard deviations were calculated for three replicates.

2.2.5 Dimethylamidation of samples with different sialic acid linkages

To profile the glycosylation of the IgG1 standard, mAb1, mAb2, bovine IgG and BRAD-3 fragment crystallizable region, 1 μ L of their digest was derivatized for 3 h at 60 °C, using 20 μ L of the optimal dimethylamidation reagent (250 mM EDC, 500 mM HOBt and 250 mM dimethylamine in DMSO). Samples were purified by cotton HILIC-SPE and measured by MALDI-TOF-MS.

The 6'- and 3'-sialyllactose standards were 2-AB labeled as described in **S-5**, Supporting Information. These and the 2-AB labeled A3 glycan standard were dimethylamidated, followed by MALDI-TOF-MS measurement.

2.3 Results

Here, we present a method for the derivatization of IgG glycopeptides from both human plasma and biopharmaceutical sources with selective reactivity for different sialic acid linkages, thus allowing IgG subclass- and sialic acid-linkage-specific glycosylation analysis by MALDI-TOF-MS.

2.3.1 IgG glycopeptide derivatization conditions

We previously reported sialic acid linkage-specific esterification of released glycans using the carboxylic acid activator EDC and the catalyst HOBt in ethanol (37 °C) and methanol (4 °C) [124]. These conditions had been optimized to provide selective reaction products for α 2,3-linked and α 2,6-linked sialic acids. Here, these esterification conditions were applied to the derivatization of tryptic glycopeptides derived from human plasma IgG, and the modifications induced in the glycan and peptide moieties were investigated.

All IgG subclasses proved to be recoverable by HILIC-SPE from the 1:1 ethanol/methanol:ACN conditions, and reflectron positive ion mode MALDI-TOF-MS allowed the detection of the native, the ethyl esterified and the methyl esterified glycopeptides as $[M+H]^+$ ions (**Figure 2.1**, for a full listing of peaks detected throughout the experiments after internal calibration see **Table S-2**, Supporting Information). The most intense signals represent core-fucosylated diantennary glycans carrying no galactose (G0F, m/z 2634.044 (IgG1 – native)), one galactose (G1F, m/z 2796.095), or two galactoses (G2F, m/z 2958.150), with other glycan species varying in fucosylation, bisection and sialylation. For the native IgG glycopeptides only a low degree of sialylation was visible (13% of the main peak), as well as metastable signals indicative for sialic acid loss (**Figure 2.1A**). Ethyl and methyl esterification conditions did not show this breakdown, with a concurrent higher degree of sialylation (29% and 31% of the main peak, **Figure 2.1B and 2.1C**).

All IgG subclasses contain three carboxylic acids in their glycopeptide sequence; two on the glutamic acids (E) and one on the C-terminus (IgG1 = EEQYNSTYR, IgG2/3 = EEQFNSTFR, IgG4 = EEQFNSTYR). When comparing the esterified and native conditions, the non-sialylated glycopeptide species show a mass increase corresponding to two times esterification and one loss of water (38.052 Da and 10.021 Da for ethyl and methyl esterification, respectively), likely to be positioned at the carboxylic acids of the peptide portions. The sialylated glycopeptide species (carrying one α 2,6-linked sialic acid) show an additional mass increase upon esterification (28.031 Da or 14.016 Da for ethyl and methyl esterification), suggesting derivatization of the sialic acid as well.

Detrimentially, a byproduct was formed under ethyl and methyl esterification conditions for all glycopeptide species (indicating a peptide-specific effect), corresponding to the

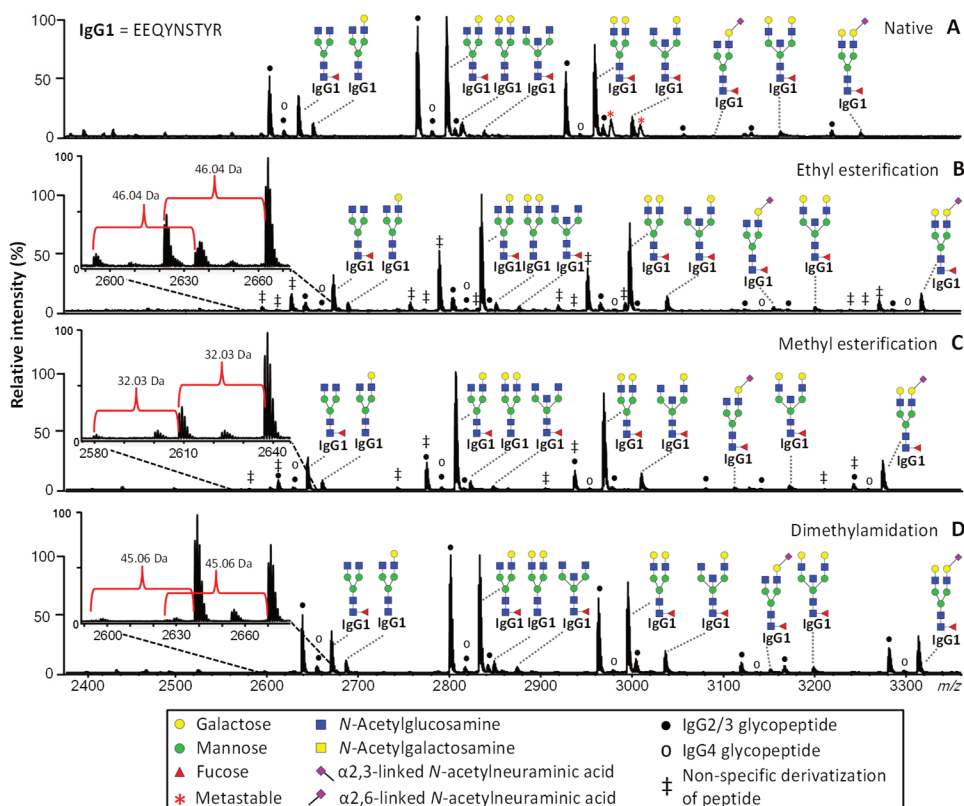


Figure 2.1 MALDI-TOF-MS spectra of plasma IgG glycopeptides. (A) Without derivatization, (B) after ethyl esterification, (C) after methyl esterification and (D) after dimethylamidation. Derivatization (B-D) prevents the formation of metastable signals, and increases the detection of sialylated species. Magnifications of the m/z region corresponding to the G0F-carrying glycopeptides show the variable nucleophilic addition and water loss of the peptide portion after ethyl esterification (-46.042 Da) and methyl esterification (-32.026 Da), with dimethylamidation showing the least side-reactivity (-45.058 Da). Except for the sialic acid linkage, the monosaccharide linkages were not determined. Proposed glycan structures are based on fragmentation and literature [29, 74, 169, 170].

exchange of one esterification for the loss of water (-46.042 Da and -32.026 Da, respectively). When compared to the intensity of the major reaction product, the byproduct showed 10.0% relative abundance (standard deviation (SD) \pm 4.2%) and 33.3% relative abundance (SD \pm 4.6%) for methyl esterification and ethyl esterification respectively. Unfortunately, the resulting mass difference is equal to the mass difference expected between α 2,3- and α 2,6-linked sialylation, preventing potential relative quantification of the sialylation isomers. In addition, while methyl esterification shows the

lowest variability, its relative quantification is further complicated by the fact that the mass difference between methylated and lactonized species (32.026 Da) is very similar to the mass difference between the IgG subclasses IgG1 and IgG2/3 (31.990 Da), resulting in multiple isobaric species.

Next to esterification, the IgG glycopeptides were subjected to amidation with ammonia, methylamine and dimethylamine. Method optimization to maximize specificity of the reaction with respect to both glycan and peptide derivatization resulted in final conditions of 250 mM dimethylamine, 250 mM EDC and 500 mM HOBt in DMSO with incubation for 3 h at 60 °C (**Figures S-1 to S-3**, Supporting Information). Performing reflectron positive mode MALDI-TOF-MS on the dimethylamidated samples showed stabilization of the sialylation (42% of the main peak) and the absence of metastable signals (**Figure 2.1D**). For the peptide portion, two times dimethylamidation and one time water loss was detected, with the α 2,6-linked sialic acids showing dimethylamidation as well. Importantly, the variability seen in the esterified glycopeptide samples is present in only minor amounts for the dimethylamidation condition (1.1% relative abundance; SD \pm 0.2%).

2.3.2 Sialic acid linkage-specificity of dimethylamidation

To assess the selectivity of the dimethylamidation reaction for differently linked sialic acids, two sialyllactose standards with different sialic acid linkages and glycopeptides from four IgG standards were subjected to the dimethylamidation conditions.

Commercially available plasma IgG1, carrying mainly α 2,6-linked sialic acids, showed full dimethylamidation of the sialylated species (m/z 3312.377, **Figure 2.2A**). MAb1, which is known to contain exclusively α 2,3-linked sialic acids [171], showed primarily lactone formation of its sialic acids (m/z 3267.320, **Figure 2.2B**), just like the more highly α 2,3-sialylated BRAD-3 (m/z 3251.326, **Figure S-4**, Supporting Information). In addition, BRAD-3 showed 4.0% dimethylamidation of the sialic acids (+45.058 Da, for observed side reactions see **Table S-3**, Supporting Information). Due to traces of ammonia in the reaction mixture of mAb1, also 10.4% (SD \pm 3.2% for 36 samples) amidation with ammonia was seen for the α 2,3-linked sialic acids (m/z 3284.347). This contaminant most likely comes from the mAb1 sample itself, as BRAD-3 did not show this particular side-reaction. In contrast, the amidation with ammonia was not observed to compete with the lactamization or dimethylamidation on the peptide backbone. The main products after dimethylamidation showed a mass difference of 45.058 Da between the differently linked sialic acids (**Figure 2.3**). This could also be confirmed with sialyllactose standards, showing 99.5% (SD \pm 0.1%) dimethylamidation on 6'-sialyllactose and 92.3% (SD \pm 0.5%) lactone formation on 3'-sialyllactose (**Figure S-5**, Supporting Information). MAb2, derived from mAb1 by modifying its glycosylation in vitro using galactosyltransferases and sialyltransferases, contains glycan structures that are high in

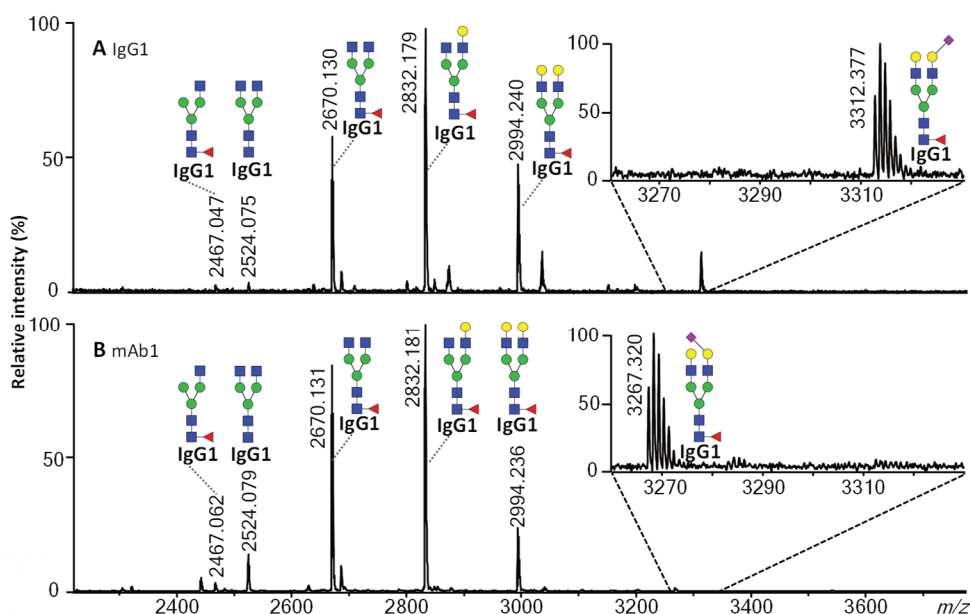


Figure 2.2 MALDI-TOF-MS spectra of the glycopeptide profiles of (A) the IgG1 standard and (B) mAb1 after dimethylamidation. The magnifications focus on the sialylated glycopeptides of the antibodies. Plasma IgG1 mainly carries α 2,6-linked sialic acids, which form a dimethylamide during derivatization (+27.047 Da), while mAb1 mainly carries α 2,3-linked sialic acids, which yields water loss during derivatization (-18.011 Da). After linkage-specific derivatization of the sialic acids, the mass difference between α 2,3- and α 2,6-linked forms is 45.058 Da. For α 2,3-linked sialic acids side products amidated with ammonia (-0.984 Da) were found.

galactosylation and contain both α 2,3- and α 2,6-linked sialic acids. Glycosylation of tryptic mAb2 glycopeptides was analyzed by dimethylamidation using the newly established protocol. The MALDI-TOF-MS profile obtained (**Figure 2.4B**) was compared to a profile resulting from the established method of ethyl esterification after glycan release (**Figure 2.4A**). The profiles were highly comparable for the 19 glycoforms detected (**Figure 2.4C**). The most abundant glycan (G2FS – α 2,6-linked) showed in the released glycan assay an average relative area of 60.0% (SD \pm 0.2%) and in the glycopeptide assay an average relative area of 59.9% (SD \pm 0.9%) across triplicate measurements. The difference across the other species was found to be at most 2.7% of the total relative area (G2FS2). In addition, the obtained glycosylation profile of mAb1 is in very good agreement with the previously published HILIC-UPLC data for released glycans of this same antibody (**Figure S-6**, Supporting Information) [171], proving that possible side reactions do not interfere with the profiling of the glycopeptides.

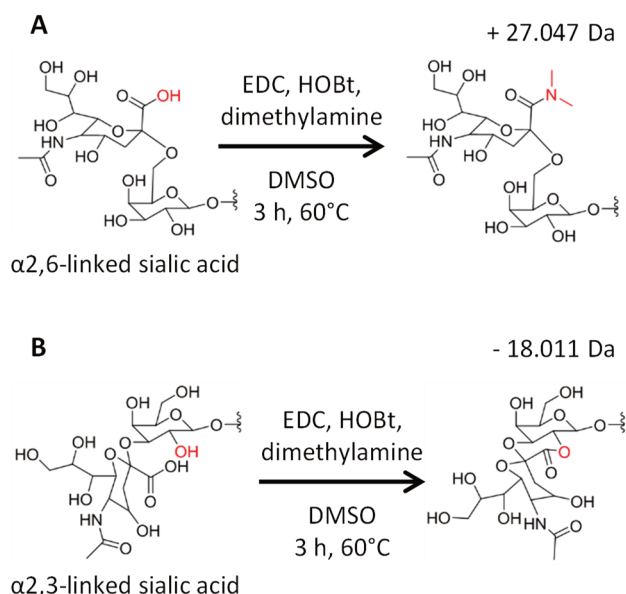


Figure 2.3 Reaction scheme for the derivatization of *N*-acetylneuraminic acid that is either **(A)** α 2,6-linked or **(B)** α 2,3-linked to the subterminal galactose. Under the same conditions, α 2,6-linked sialic acids form a dimethylamide, whereas α 2,3-linked sialic acids react with the neighboring galactose to form a lactone.

The dimethylamine derivatization was additionally performed on a 2-AB labeled triantennary glycan standard containing glycans with a variety of sialic acid linkages. The relative ratio of these species had previously been determined by HILIC-UPLC with exoglycosidase digestion, and shown to correspond to MALDI-TOF-MS analysis of the same sample after ethyl esterification [172]. Comparing esterification with the here described dimethylamidation again shows highly similar ratios and indicates equal response factors for the differentially linked sialic acids after derivatization (**Figure S-7**, Supporting Information). In addition to the stabilization of *N*-acetylneuraminic acids in a linkage specific way, the derivatization method was found to be applicable to IgG glycopeptides containing *N*-glycolylneuraminic acids derived from bovine IgG (**Figures S-8** and **S-9**, Supporting Information).

2.3.3 Repeatability

To demonstrate the robustness of the dimethylamidation protocol, 36 aliquots of the IgG1 standard and mAb1 samples were prepared. On three successive days, 12 aliquots of each antibody were subjected to tryptic digestion, dimethylamidation for 3 h at 60 °C, HILIC-SPE and MALDI-TOF-MS analysis.

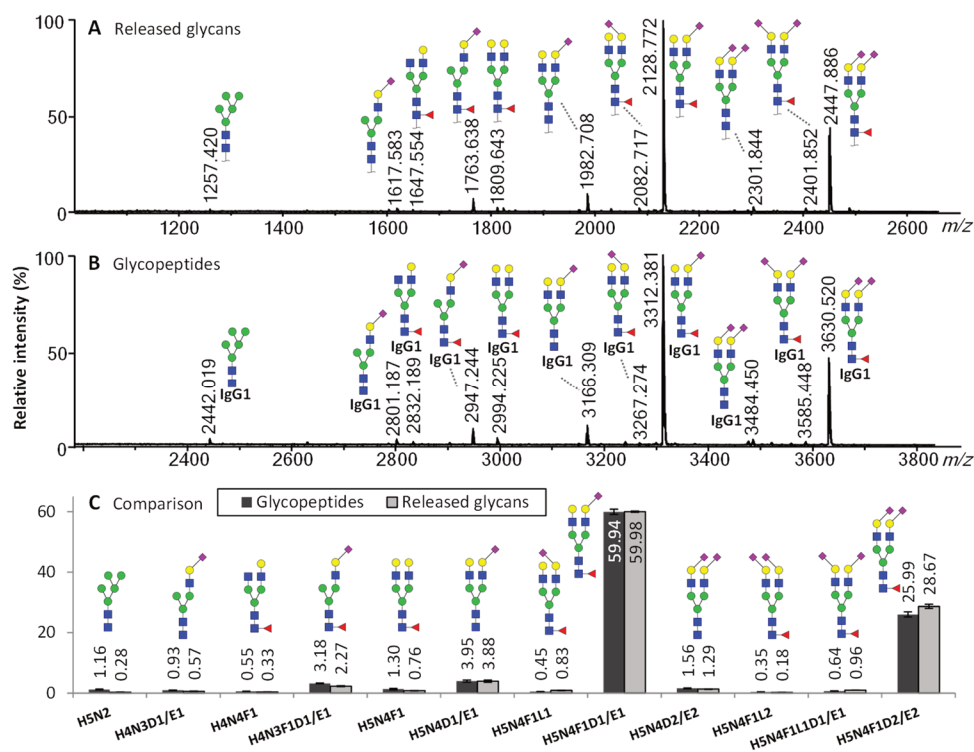


Figure 2.4 MALDI-TOF-MS analysis of mAb2 glycosylation. (A) Profile of the released glycans after ethyl esterification. (B) Profile of the tryptic glycopeptides after dimethylamidation. (C) Average relative intensities for the major glycoforms over three samples per profiling method, with error bars for replicate standard deviation. Abbreviations used are hexose (H), *N*-acetylhexosamine (N), fucose (F), dimethylamidated *N*-acetylneuraminic acid with an α 2,6-linkage (D), ethyl esterified *N*-acetylneuraminic acid with an α 2,6-linkage (E) and lactonized *N*-acetylneuraminic acid with an α 2,3-linkage (L).

The established method with the optimized derivatization procedure showed very good precision, both intra-day and inter-day (**Figure S-10**, Supporting Information). The average relative area of the highest peak for the IgG1 standard (G1F) was 35.2% (SD \pm 0.8%) across all samples, resulting in an average coefficient of variation (CV) of 2.2%. For mAb1 the relative area of the G1F peak was 42.9% (SD \pm 1.1%) with an average CV of 2.5%. Besides the highest signals in the spectra, also the (low abundant) sialylated glycopeptides showed an acceptable CV between 4% and 18%, implying that both α 2,3- and α 2,6-linked sialic acids are stabilized and detected in a repeatable way.

2.3.4 Fragmentation

Both the native form of the IgG1 glycopeptide, carrying G2FS (α 2,6-linked; m/z 3249.248), as well as the dimethylamidated form of this analyte (m/z 3312.384) were subjected to positive ion mode MALDI-TOF/TOF-MS/MS fragmentation to show the effects of sialic acid stabilization in MS/MS. In addition, a derivatized non-sialylated glycopeptide (IgG1 carrying G0F; m/z 2670.134) was fragmented to determine the modifications on the peptide portion of the conjugate.

Fragmentation of native glycopeptides predominantly showed the loss of the labile sialic acid (-291.1 Da) (**Figure 2.5A**). Other minor fragments seen were the peptide portion containing a cross-ring fragment of the Asn-linked *N*-acetylglucosamine (m/z 1271.9) as well as a fragment carrying the innermost *N*-acetylglucosamine with the core fucose (m/z 1538.0).

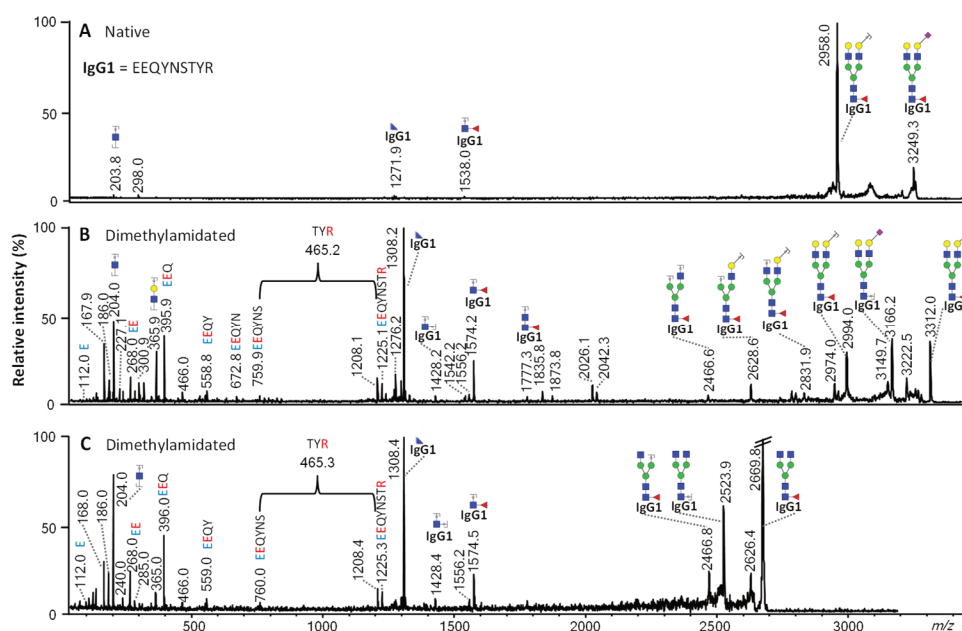


Figure 2.5 MALDI-TOF/TOF-MS/MS spectra of the IgG1 G2FS glycopeptide (A) without derivatization and (B) after dimethylamidation. Whereas the unmodified glycopeptide mainly shows fragmentation of the sialic acid, the derivatized variant shows fragmentation of both the glycan and the peptide moiety. (C) Shows the fragmentation of a non-sialylated IgG1 glycopeptide (G0F) after dimethylamidation, demonstrating the reactions occurring on the peptide portion of the conjugate. Blue: Loss of water. Red: Dimethylamide formation.

After derivatization, the fragmentation spectra were considerably more informative with respect to both glycan and peptide moiety (**Figure 2.5B**), showing not only loss of the dimethylamidated sialic acid (-318.1 Da), but also various other losses indicative for antenna composition. Fragments originating from the peptide portions of both G2FS and G0F (**Figure 2.5B and 2.5C**) show water loss and dimethylamidation on the two N-terminal glutamic acids (m/z 268.0 $[M + H]^+$). This likely reflects pyroglutamic acid formation of the N-terminal glutamic acid and dimethylamidation of the intra-chain glutamic acid. Dimethylamidation at the three most C-terminal amino acids was observed (a loss of 465.2 Da from m/z 1225.1 to m/z 759.9) pointing to the modification of the C-terminal carboxylic acid. Fragmentation of the esterified glycopeptides revealed that the intra-chain glutamic acid is involved in the appearance of the side-reactivity under esterifying conditions (**Figure S-11**, Supporting Information). Lactone formation (-18.01 Da) of α 2,3-linked sialic acids upon derivatization was further established by the fragmentation pattern of the triantennary glycan with two α 2,3-linked and one α 2,6-linked sialic acid from the A3-2-AB glycan standard (**Figure S-12**, Supporting Information).

2.4 Discussion

Derivatization of sialylated glycopeptides for MALDI-TOF(/TOF)-MS analysis has previously been described [128, 166], but the protocol presented here is the first that includes the linkage-specific modification of sialic acids. For free glycans, the possibility to use the difference in reactivity between α 2,3- and α 2,6-linked sialic acids for the specific modification of both isomers has been reported previously [123, 124, 162]. However, the set-up of a protocol for glycopeptides adds complexity due to the presence of peptide moiety carboxylic acids. These acids could participate in a wide range of reactions depending on their local environment. Potential side reactions would include either internal or external esterification, amidation or thioester formation. Furthermore, the behavior of the modified glycoconjugates is likely to be altered with respect to solubility, HILIC retention and ionization. Consequently, the methyl and ethyl esterification of tryptic IgG glycopeptides could not readily be controlled, and heterogeneous reaction products were observed for the peptide portion of the conjugates. Fragmentation shows the N-terminal glutamic acid to mainly lactamize into pyroglutamic acid while the C-terminus forms an alkyl ester. The observed reaction variability seems to be caused by the intra-chain glutamic acid, possibly forming a lactone with a nearby amino acid (e.g. with the serine or threonine hydroxyl group) as a side reaction to the intermolecular ester formation. While some side-reactivity can be allowed, the mass shifts induced by the peptide variability overlap with the mass difference caused by the peptide portion heterogeneity of IgG subclasses, and are equal to the mass shifts observed for differentially linked sialic acids, consequentially prohibiting relative quantification.

As we expected EDC and HOBt to lead to linkage-specific sialic acid modification when presented with a suitably sterically hindered nucleophile [124], we decided to investigate the nucleophile selection rather than, for example, perform an exploration of carboxylic acid activators. Ammonia, methylamine and dimethylamine were all found to stabilize the sialylated glycopeptides for MALDI-TOF(/TOF)-MS measurements, but as expected, the use of the smaller amines caused a decrease in selectivity for the sialic acid linkage (data not shown). The more slowly reacting dimethylamine allowed high sialic acid linkage-specificity of the reaction, and it proved specific for the different peptide carboxylic acids as well. In addition, the use of a secondary amine will also prevent possible cross-linking of several carboxylic acid moieties which may be observed for primary amines or ammonia [173]. The resulting amidation reaction conditions (3 h at 60 °C) are harsher than those previously reported for the ethyl esterification [124], but are still within the scope of published glycan derivatization methodology [123, 174, 175]. For the glycopeptides tested here, no signs of either peptide or glycan degradation were observed.

The reaction with dimethylamine was shown to be highly suitable for the glycosylation profiling of therapeutic monoclonal antibodies as demonstrated for mAb1 and mAb2, resulting in relative ratios comparable to previously established methods [124, 171]. The resolution of the method was sufficient to analyze complex IgG samples with various sialic acid linkages, different subclass peptide sequences, and both *N*-glycolyl- and *N*-acetylneuraminic acids in the structure. With a potential sample throughput of 384 samples a day, the method is rapid compared to existing sialylated glycopeptide profiling methods like LC-MS and CE-MS.

While optimized for IgG glycopeptides carrying α 2,3- or α 2,6-linked *N*-acetyl- and *N*-glycolylneuraminic acids, the effect of the reaction on other sialylation variants is still unknown, examples of this being α 2,8-linkage and *O*-acetylation. In addition, it will be interesting to study the effect of the method on the glycopeptides originating from proteins other than IgG. However, due to the great variability in the amino acid sequence of different glycopeptides, the protocol is expected to require optimization to ensure uniformity in the reactions occurring on the peptide portion of the conjugates.

In conclusion, we presented a method for the stabilization of sialylated glycopeptides for MALDI-TOF(/TOF)-MS analysis, which can be used for the high-throughput linkage-specific analysis of sialylated glycopeptides derived from IgG in a subclass- and site-specific manner. Derivatization induces a mass difference between α 2,3- and α 2,6-linked sialic acids, while peptide modifications are uniform, enabling separation between differently linked sialic acids in MS. Furthermore, highly informative MS/MS spectra of sialylated glycopeptides could be obtained. The method is fast, has excellent intra- and inter-day repeatability and makes use of relatively inexpensive chemicals. A considerable

applicability is expected for the future glycosylation profiling of therapeutic antibodies, as well as for the IgG glycosylation profiling of large clinical cohorts.

Acknowledgements

This work was supported by the European Union Seventh Framework Programmes IBD-BIOM (grant number 305479) and HighGlycan (grant number 278535), as well as by the Netherlands Genomic Initiative Horizon Programme Zenith project (grant number 93511033). Additional financial support was provided by Hoffmann-la Roche. We thank Marco Thomann for providing the experimental section about mAb2 and Gestur Vidarsson for providing BRAD-3.

Supporting Information available

Additional information is available as stated in the text. This information is available free of charge via <https://pubs.acs.org/doi/10.1021/acs.analchem.5b02426>.



- ¹ *Leiden University Medical Center, Center for Proteomics and Metabolomics,
Leiden, The Netherlands*
- ² *Erasmus MC, Pediatrics, Rotterdam, The Netherlands*
- ³ *Erasmus MC, Immunology, Rotterdam, The Netherlands*

Chapter 3

Changes in Healthy Human IgG Fc Glycosylation after birth and during Early Childhood

Noortje de Haan¹, Karli R. Reiding¹, Gertjan J. Driessen²,
Mirjam van der Burg³ and Manfred Wuhrer¹

Reprinted and adapted with permission from J. Proteome Res.,
2016, 15 (6), pp 1853–1861 DOI: 10.1021/acs.jproteome.6b00038 [176].

Copyright © 2016, American Chemical Society.



Glycosylation on the fragment crystallizable (Fc)-region of immunoglobulin G (IgG) has a large influence on the interaction of the antibody with Fc gamma receptors (FcγRs). IgG consists of four subclasses that all have distinct affinities for the different FcγRs. Knowledge about the Fc glycosylation in healthy human is valuable as reference for new biomarkers and in the design of biopharmaceuticals that rely on IgG Fc glycosylation. Previously, subclass-specific characterization of IgG Fc glycosylation was performed for healthy adults, pregnant women and newborns. For young healthy children however, the subclass specific description of IgG Fc glycosylation is still lacking.

Therefore, we performed the IgG subclass-specific analysis of the Fc glycosylation of 130 healthy humans between birth and 40 years of age, including 22 samples derived from the umbilical cords of newborns. The analysis was performed by a previously published matrix assisted laser desorption/ionization (MALDI)-time of flight (TOF)-mass spectrometry (MS) workflow, including a derivatization step for the linkage-specific stabilization of sialic acids.

The characterization revealed that when children start to produce their own IgG they have a decreased galactosylation, sialylation and bisection and an increased fucosylation compared to newborns. During childhood, the fucosylation and sialylation decrease, whereas bisection increases and galactosylation stays constant.

3.1 Introduction

Immunoglobulin G (IgG) is a highly abundant glycoprotein and the most abundant immunoglobulin in the human plasma [177]. It exists in four subclasses (IgG1 to 4), differing in the amino acid sequence of the heavy chain and the number of interchain disulfide bridges. IgG is involved in, amongst others, antigen binding, activation of the complement system and antibody-dependent cell-mediated cytotoxicity (ADCC), and its appearance and biological activity are highly influenced by the *N*-glycan structure on the fragment crystallizable (Fc)-region [177, 178]. Changes in the abundances of different glycan features on the Fc region are reported to associate with age, sex, pregnancy and various autoimmune and infectious diseases, like inflammatory bowel disease and rheumatoid arthritis [28, 29, 85, 95, 179]. For example, galactosylation decreases with increased disease activity and with age, while it increases during pregnancy [28, 29, 85, 95]. Alterations in attached glycan structures change the conformation of the IgG Fc region and with that the possible interactions with Fc receptors (FcγRs) expressed on leukocytes [180, 181]. A notable example is the difference in binding affinity of IgG1 to FcγRIIIa when carrying a glycan that is either fucosylated or nonfucosylated, resulting in enhanced ADCC for antibodies carrying nonfucosylated Fc glycans [182, 183]. To understand biological processes and to search for new biomarkers it is highly relevant to have, next to the diseased situation, also the IgG Fc glycosylation of healthy humans well-characterized. The healthy human IgG Fc glycosylation profile can serve as a base for new diagnostic biomarkers, and is relevant when designing therapeutic antibodies [184].

The topic of healthy human IgG Fc glycosylation is for a large part covered by studies describing levels of glycosylation features in healthy adults of different populations, in children between the age of six and 18 and in healthy pregnant women and newborns [28, 29, 74, 79-81, 83-86, 179]. However, the Fc glycosylation of very young children is yet not comprehensively covered and also information about differences between Fc glycosylation in newborns and young children is lacking. One study reported the decrease of galactosylation in children between one to 18 years old, but was inconclusive about other features [83]. In addition, for children between six and 18 it was found that fucosylation decreases for girls and bisection increases for boys, however these studies describe antibody glycosylation in children based on experiments with released glycans [83, 84]. This approach enhances the chance of biases as no distinction was made between glycans present on the Fc region or the fragment antigen binding (Fab)-part of the antibody. Furthermore, as there are four human IgG subclasses which differ in effector functions, it is interesting to study the glycosylation of the subclasses separately. Especially because it is shown that, for example, FcγRI has a high affinity for IgG1, 3 and 4 but no affinity for IgG2, and also other FcγRs show diverging affinities for the different IgG

subclasses [185]. In addition, not all studies into the modulating effects of glycans are performed for all subclasses of IgG, but often only for IgG1 [58, 186].

We here describe the subclass-specific IgG Fc glycosylation of healthy humans between birth and the age of 40. We analyzed IgG Fc glycopeptides using a previously reported matrix assisted laser desorption/ionization (MALDI)-time of flight (TOF)-mass spectrometry (MS) method [149]. The method includes the derivatization of the IgG glycopeptides to stabilize the sialylated species during MALDI ionization and distinguishes α 2,3- and α 2,6-linked sialic acids by forming a lactone (-18.011 Da) or a dimethylamide (+27.047 Da), respectively. This characterization revealed that when children start to produce their own IgG, about one month after birth [187], their galactosylation, sialylation and bisection decreases and their fucosylation increases compared to IgG found in umbilical cord samples that represent the IgG of both the mothers and the newborns [86]. Furthermore, it was shown that fucosylation and sialylation decrease throughout childhood, whereas bisection increases and galactosylation stays constant.

3.2 Experimental section

3.2.1 Chemicals and enzymes

Disodium hydrogen phosphate dihydrate ($\text{Na}_2\text{HPO}_4 \cdot 2\text{H}_2\text{O}$), potassium dihydrogen phosphate (KH_2PO_4), sodium chloride (NaCl) and trifluoroacetic acid (TFA) were purchased from Merck (Darmstadt, Germany). 1-Hydroxybenzotriazole (HOBt) hydrate, dimethyl sulfoxide (DMSO), 40% dimethylamine in water, sodium bicarbonate, formic acid (FA) and TPCK treated trypsin from bovine pancreas were purchased from Sigma-Aldrich (Steinheim, Germany). 1-Ethyl-3-(3-(dimethylamino)propyl)carbodiimide (EDC) hydrochloride was purchased from Fluorochem (Hadfield, Derbyshire, UK), 4-chloro- α -cyanocinnamic acid (Cl-CCA) from Bionet Research (Camelford, Cornwall, UK) and HPLC SupraGradient acetonitrile (ACN) from Biosolve (Valkenswaard, The Netherlands). Ultra-pure deionized water (MQ) was generated by the Purelab Ultra, maintained at 18.2 M Ω (Veolia Water Technologies Netherlands B.V., Ede, The Netherlands) and phosphate-buffered saline (PBS) was made in-house, containing 5.7 g/L $\text{Na}_2\text{HPO}_4 \cdot 2\text{H}_2\text{O}$, 0.5 g/L KH_2PO_4 and 8.5 g/L NaCl .

3.2.2 Cohort

Peripheral blood samples were collected from 108 healthy donors and 22 blood samples were derived from umbilical cords with approval of the Medical Ethics Committee of the Erasmus MC [188].

The samples were divided over five age categories, namely the newborns (samples from the umbilical cords, UC), the very young children (age 0.1 to 3.9), the young children (age 4 to 9.9), the adolescents (10-17) and the young adults (age 20 to 40; **Table 3.1**). In addition to the biological samples, 30 pooled plasma standards (Visucon-F frozen normal control plasma; Affinity Biologicals 99, Ancaster, Canada) and 12 PBS blanks were included in the cohort to serve as positive and negative controls. All samples were randomized and distributed over two 96-well plates.

Table 3.1 Description of the human sample cohort. UC: samples taken from the umbilical cord.

Age class (age range)	Newborns (UC)	Very young children (0.1 - 3.9)	Young children (4 - 9.9)	Adolescents (10 – 17)	Young adults (20 – 40)	Total
Number of female samples (average age)	14	13 (1.5)	16 (7.2)	15 (12.4)	11 (29.4)	69 (9.3)
Number of male samples (average age)	8	20 (1.9)	16 (5.9)	10 (11.8)	7 (29.5)	61 (7.5)
Total number of samples (average age)	22	33 (1.7)	32 (6.6)	25 (12.2)	18 (29.6)	130 (8.5)

3.2.3 ProtG IgG isolation

IgG1, 2, 3 and 4 were captured from 2 µL plasma using protein G affinity beads (GE Healthcare, Uppsala, Sweden) in a 96-well filter plate (0.7 mL wells, PE frit, Orochem, Naperville, IL) format. The samples were allowed to interact with 15 µL beads in 100 µL PBS for 1 h on a plate shaker (1000 rpm; Heidolph Titramax 100; Heidolph, Kelheim, Germany), after which the beads were washed three times with 200 µL PBS and three times with 200 µL water using a vacuum manifold. Elution was performed with 100 µL 100 mM FA by centrifuging the plate 1 min at 100 g, after which the samples were dried in a vacuum concentrator at 60 °C.

3.2.4 Glycopeptide preparation

Glycopeptides were prepared for MALDI-TOF-MS analysis as described before [149]. Briefly, dried antibodies were dissolved in 20 µL 50 mM sodium bicarbonate buffer (pH 7.9), containing 0.1 mg/mL TPCK treated trypsin (trypsin(w):sample(w) = 1:10) and incubated overnight at 37 °C. To stabilize the sialylated species, 1 µL of each digest was added to 20 µL derivatization reagent (consisting of 250 mM EDC, 500 mM HOBt and 250 mM dimethylamine in DMSO) and the samples were incubated 3 h at 60 °C. After the samples were cooled to room temperature, 113.3 µL ACN (85%) was added and

glycopeptides were enriched by cotton hydrophilic interaction liquid chromatography (HILIC)-solid phase extraction (SPE) [168]. Hand-crafted cotton tips were equilibrated and conditioned with three times 15 μ L mQ and three times 15 μ L 85% ACN respectively. Samples were loaded by pipetting them 20 times through the cotton, after which the tips were washed three times with 15 μ L 85% ACN 1% TFA and three times with 15 μ L 85% ACN. Glycopeptides were eluted in 10 μ L mQ, of which 1 μ L was then applied on a polished steel 384 TF MALDI target (Bruker Daltonics, Bremen, Germany), together with 1 μ L 5 mg/mL Cl-CCA in 70% ACN. The spots were left to dry by air.

3.2.5 MALDI-TOF-MS analysis

The IgG glycopeptides were analyzed with an Ultraflex extreme MALDI-TOF-MS (Bruker Daltonics), operated in positive ion mode and with the reflectron activated. For each sample, 10 000 shots were combined with a frequency of 2 000 Hz and the power of the Smartbeam-II laser was optimized to obtain high intensity signals, while isotopic resolution was maintained. The instrument was controlled by Flexcontrol 3.4 software and the method covered an analysis window from m/z 1000 to 4000. Prior to analyzing the biological samples, the MALDI-TOF-MS was externally calibrated using a peptide calibration standard (Bruker Daltonics).

3.2.6 Data processing

The MALDI-TOF-MS spectra in the figures were smoothed (SavitzkyGolay), baseline subtracted (Top Hat) and internally calibrated using flexAnalysis 3.4, build 76 (Bruker Daltonics). Analytes used for internal calibration are indicated in bold in **Table 3.2**. The glycopeptide compositions were assigned to m/z values based on fragmentation experiments and literature [29, 74]. GlycoWorkbench 2.1, build 146 was used to create the compositional cartoons [189].

Targeted data extraction was performed using MassyTools 0.1.7.2 [190]. This program calibrated the spectra, based on a predetermined list of calibrants (see above) and integrated peak areas of a list with manually determined glycopeptide compositions. For the integration, minimal 95% of the theoretical isotopic pattern was included, and the values were corrected for background, based on local background levels. Furthermore, MassyTools calculated for each analyte the mass error, deviation from the theoretical isotopic pattern and signal-to-noise ratio. These parameters were used for both spectrum and analyte curation, excluding spectra when their “fraction of analyte area above signal-to-noise ratio nine” was above or below the average plus or minus three times standard deviation. In this way, seven spectra were excluded for IgG1 and ten spectra were excluded for IgG2/3. Decisions on the inclusion of certain analytes were based on the mass error of the measured analyte compared to its theoretical mass, and on the deviation of the measured isotopic pattern compared to its theoretical isotopic pattern.

Analyte curation was performed separately for all age categories and glycoforms were included when present in at least one of them. Average mass errors per age category for an analyte to be included were accepted to be between -10 and 10 ppm, and the total isotopic patterns were allowed to deviate on average up to 22%. The absolute intensities of the included analytes were normalized to the total area for IgG1 and IgG2/3 separately. The largest part of the glycopeptides originating from IgG4 could not be extracted as the exact mass of their fucosylated glycopeptides is the same as the nonfucosylated glycopeptides from IgG2/3. The nonfucosylated glycopeptides from IgG4 have the same exact mass as the fucosylated ones from IgG1. Derived traits were calculated for both IgG1 and IgG2/3, showing the fraction of glycoforms that was fucosylated or carried a bisecting *N*-acetylglucosamine. Furthermore, the fraction of galactosylation and sialylation was determined per antenna (**Table S-1**).

Table 3.2 Theoretical m/z values of the glycopeptides extracted for IgG1 and IgG2/3. Glycopeptides used for internal calibration of the spectra are indicated in bold. H: Hexose, N: *N*-Acetylhexosamine, F: Fucose, D: Dimethylamidated α 2,6-linked *N*-acetylneuraminic acid.

IgG1		IgG2/3	
Glycoform	$[M+H]^+$	Glycoform	$[M+H]^+$
H3N3F1	2467.052	H3N4F1	2638.140
H3N4	2524.072	H4N4F1	2800.193
H4N3F1	2629.103	H5N4F1	2962.246
H3N4F1	2670.130	H4N4F1D1	3118.336
H4N4	2686.125	H5N4F1D1	3280.388
H4N4F1	2832.183		
H5N4	2848.178		
H3N5F1	2873.209		
H4N5	2889.204		
H5N4F1	2994.236		
H4N5F1	3035.262		
H4N4F1D1	3150.325		
H5N4D1	3166.320		
H5N5F1	3197.315		
H5N4F1D1	3312.378		
H5N5F1D1	3515.458		
H5N4F1D2	3630.521		

3.2.7 Statistical analysis

For the renormalized glycan species and the derived traits as dependent variables, the distribution per age category was tested to meet normality by the Kolmogorov-Smirnov test, using SPSS 20.0 (IBM, Armonk, NY). As the study population deviates significantly from normality, further statistical analysis was performed using non-parametric tests. Correlation coefficients between glycan traits and age were calculated and tested by the Spearman's rho statistic. Differences in glycan levels between sex and age classes were analyzed using the Mann-Whitney test. The reported *p*-values are two-tailed and, after Bonferroni-correction for 572 tests (with a total of 44 glycan features and derived traits, $5 \times 44 = 220$ tests were performed between the sexes in each age category, $3 \times 44 = 132$ correlation tests were performed, $4 \times 44 = 176$ tests between the UC category and the other age categories were performed and an additional 44 tests were done between the UC category and the female young adults), considered statistically significant when below $8.7 \cdot 10^{-5}$ ($0.05/572$). Both the non-parametric statistical tests and the calculation of the descriptive statistics were performed using R 3.2.2 (R Foundation for Statistical Computing, Vienna, Austria) together with RStudio 0.99.473 (RStudio inc., Boston, MA). Functions used were `wilcox.test`, `quantile`, `cor.test` and `glm`.

3.3 Results

3.3.1 Glycopeptide measurement and data quality

IgG was affinity-purified, and tryptic IgG Fc glycopeptides were derivatized and analyzed by MALDI-TOF-MS for 130 human plasma samples obtained from healthy persons between birth and 40 years of age, including 22 samples derived from the umbilical cords of newborns (**Table 3.1**). After thorough analyte curation, based on mass error, deviation from the theoretical isotopic pattern, and signal-to-noise ratio, 17 glycoforms were extracted from the MS data for IgG1 glycopeptides and five glycoforms for IgG2/3 glycopeptides (**Figure 3.1**, **Table 3.2**). Fucosylated glycoforms of IgG4 have the same exact mass as non-fucosylated glycoforms of IgG2/3 and therefore overlap in the mass spectra. Therefore, IgG4 signals cannot be accurately extracted and only the fucosylated glycoforms of IgG2/3 can be extracted. This overlap is also present between some fucosylated glycoforms of IgG1 and the non-fucosylated glycoforms of IgG4. However, as the relative abundance of IgG1 is about 65% and that of IgG4 about 4% in healthy adults and the IgG4 abundance is even lower in healthy young children [187, 191], the influence of IgG4 glycopeptide signals on IgG1 signals was considered not significant in this situation.

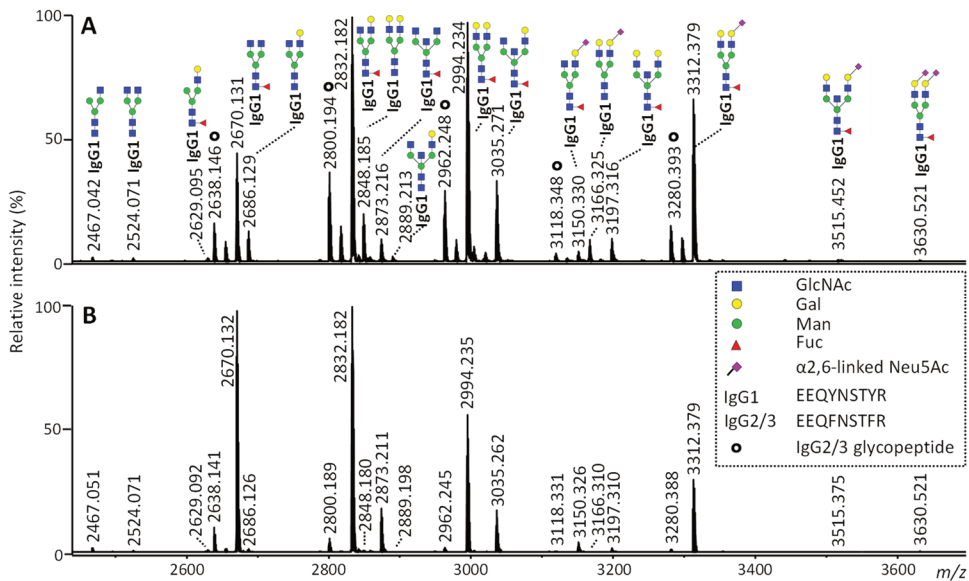


Figure 3.1 MALDI-TOF-MS spectra of tryptic plasma IgG Fc glycopeptides from (A) the umbilical cord of a newborn girl, and (B) a 1.4 year old girl. Assigned are the glycopeptides from IgG1 and IgG2/3, of which the signals were extracted from the data (also see **Table 3.2**). IgG2/3 glycopeptides are 31.99 Da lower in mass than IgG1 glycopeptides, indicated by a circle (*). Except for the sialic acid linkage, the monosaccharide linkages were not determined and proposed glycan structures are based on fragmentation and literature [29, 74]. Blue square: *N*-acetylglucosamine, green circle: mannose, yellow circle: galactose, red triangle: fucose, right pointing pink diamond: α 2,6-linked *N*-acetylneuraminic acid, IgG1: EEQYNSTYR, IgG2/3: EEQFNSTFR. Clear differences can be observed for fucosylation (\uparrow in 1.4 year old), galactosylation (\downarrow in 1.4 year old), sialylation (\downarrow in 1.4 year old) and bisection (\downarrow in 1.4 year old).

In addition to the cohort samples, 30 pooled plasma standards and 12 blanks were randomly distributed over the two sample plates. None of the blanks showed any glycopeptide signals, excluding the presence of measurable cross-contamination between the samples. Furthermore, 29 pooled plasma samples for IgG1 and 28 pooled plasma samples for IgG2/3 which passed the spectrum curation, resulted in highly reproducible glycosylation profiles, showing a coefficient of variation (CV) of only 4.3% for the most abundant IgG1 glycopeptide (average relative intensity: 33.4%, SD \pm 1.5%) and of 2.3% for the most abundant IgG2/3 glycopeptide (40.2%, SD \pm 0.9%; **Figure S-1A** and **B**). These values were slightly higher than the CV of 2.2% reported previously for the most abundant glycopeptide in isolated IgG1 measured 12 times in the same samples, using this method [149]. However, in the method reported before, the isolation of IgG from plasma was not taken into account.

3.3.2 Changes in IgG Fc glycosylation during childhood

The relative abundances of IgG Fc glycans, as well as derived traits like bisection, fucosylation, galactosylation and sialylation were determined for all samples (see **Table S-1** for all derived traits and their calculations). Correlation coefficients between all glycan features and age (0.1 to 17 year) were calculated for male and female samples separately, as well as for the combined data set (multiple testing correction was performed for all tests together; for a complete overview of all correlation tests, see **Figure S-2, S-3** and **Table S-2**). Because IgG glycosylation of the two sexes did not differ significantly within any of the five defined age classes (**Table S-3** and **Figure S-4**), the female and male data sets were combined for further analysis.

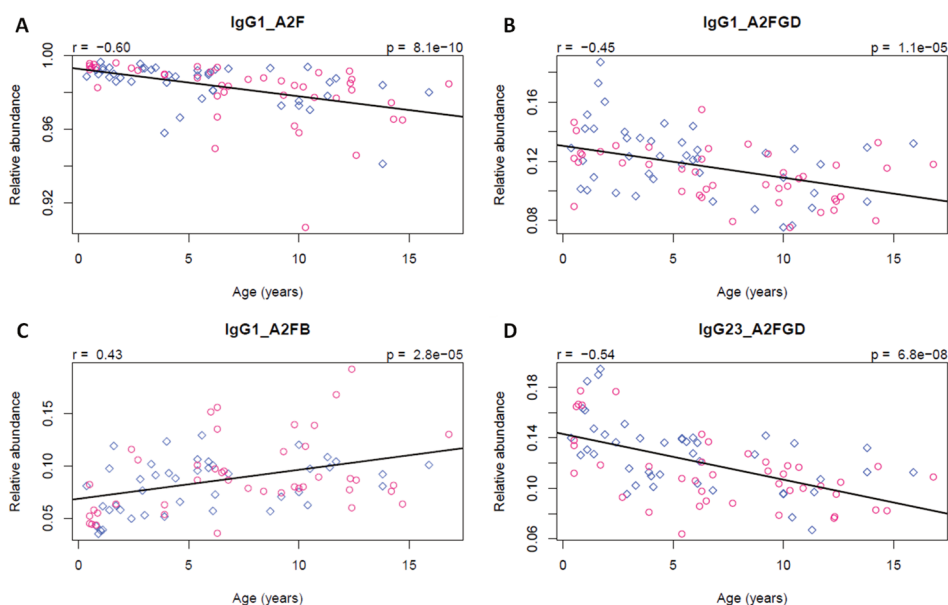


Figure 3.2 (A) Fucosylation of diantennary glycans of IgG1 (IgG1_A2F), (B) sialylation per galactose of diantennary fucosylated glycans of IgG1 (IgG1_A2FGD), (C) bisection of fucosylated diantennary glycans of IgG1 (IgG1_A2FB), and (D) sialylation per galactose on diantennary fucosylated glycans of IgG2/3 (IgG23_A2FGD). These glycan traits correlate significantly with ages between 0.1 and 17. Pink circles: female, blue diamonds: male, r : correlation coefficient for combined female and male samples. The linear line was fitted through combined female and male samples and is not related to the given correlation coefficient, which is based on a Spearman's rho calculation. After Bonferroni correction, p -values below $8.7 \cdot 10^{-5}$ were considered statistically significant.

Galactosylation of IgG1 (IgG1_A2G) did not appear to change within the age range studied, nor did galactosylation of IgG2/3 (IgG23_A2FG). On the other hand, the fucosylation of IgG1 (IgG1_A2F) decreased significantly with age ($r = -0.60$, $p = 8.1 \cdot 10^{-10}$;

Figure 3.2A) and the bisection of fucosylated diantennary glycans (IgG1_A2FB) increased significantly ($r = 0.43$, $p = 2.8 \cdot 10^{-5}$; **Figure 3.2C**). For both IgG1 and IgG2/3, the sialylation of fucosylated diantennary glycans (IgG1_A2FD, IgG23_A2FD) decreases with age, which is even more pronounced when sialylation was considered independent of galactosylation ($\alpha 2,6$ -sialylation per galactose of diantennary fucosylated glycans (A2FGD); IgG1: $r = -0.45$, $p = 1.1 \cdot 10^{-5}$; IgG2/3: $r = -0.54$, $p = 6.8 \cdot 10^{-8}$; **Figure 3.2B** and **D**).

3.3.3 Comparison of IgG Fc glycosylation between age categories

The glycan levels obtained for umbilical cord (UC) plasma samples of newborns were compared to the levels found for very young children (0.1-3.9 years old; see **Figure 3.1** for example spectra of a newborn and a 1.4 year old and **Figure 3.3** and **Table S-4** for a complete overview of all analyses).

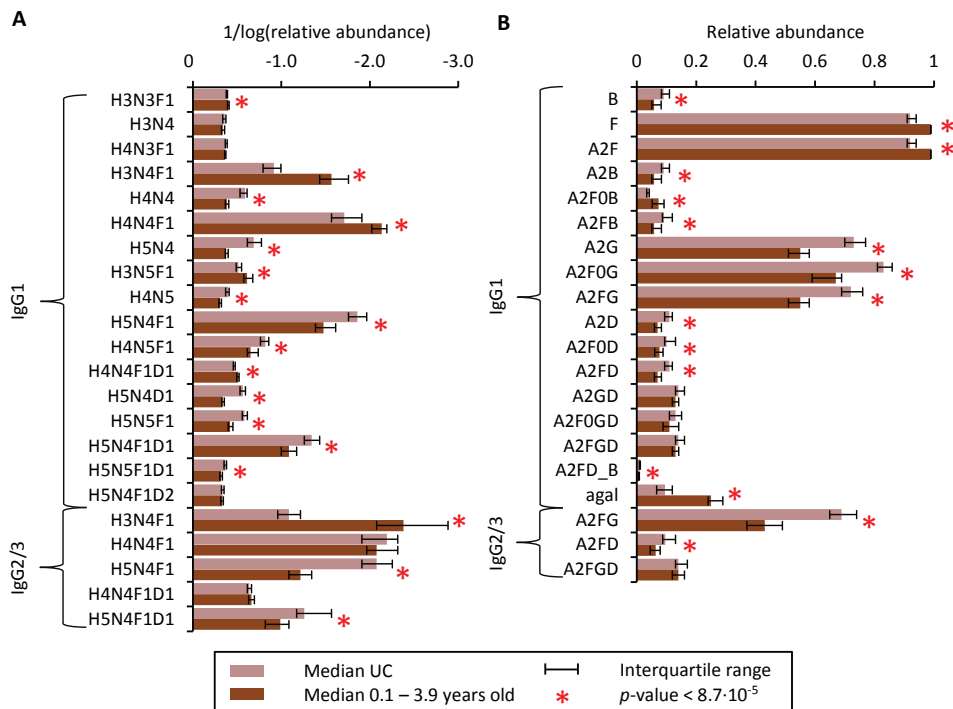


Figure 3.3 Relative abundances of (A) individual IgG Fc glycans and (B) derived glycan traits, found for umbilical cord (UC) samples as compared to the youngest age category (0.1 to 3.9 years old). The median and interquartile range of the relative glycan levels are given for both groups. After Bonferroni correction, p -values below $8.7 \cdot 10^{-5}$ were considered statistically significant (indicated by a red asterisk (*); see **Table S-1** for all derived traits and their calculations).

IgG1 fucosylation (IgG1_A2F) was significantly higher in the young children (median (M) = 0.99) compared to the newborns (M = 0.92; $p = 2.3 \cdot 10^{-14}$; **Figure 3.4A**), whereas bisection (IgG1_A2FB) was found to decrease (M(young children) = 0.058; M(UC) = 0.092; $p = 3.2 \cdot 10^{-6}$; **Figure 3.4C**). Both on IgG1 and IgG2/3, sialylation per galactose (IgG1_A2FGD, IgG23_A2FGD) did not show a significant difference between the UC samples and samples from very young children (**Figure 3.4B and D**). Galactosylation (IgG1_A2G, IgG23_A2FG), however, was significantly lower after birth (IgG1: M(young children) = 0.55; M(UC) = 0.73; $p = 1.4 \cdot 10^{-13}$; IgG2/3: M(young children) = 0.43; M(UC) = 0.69; $p = 2.2 \cdot 10^{-13}$; **Figure 3.5A and B**) and accordingly the sialylation (IgG1_A2D, IgG23_A2FD) went down (IgG1: M(young children) = 0.069; M(UC) = 0.11; $p = 2.4 \cdot 10^{-7}$; IgG2/3: M(young children) = 0.063; M(UC) = 0.096; $p = 1.8 \cdot 10^{-7}$; **Figure 3.5C and D**).

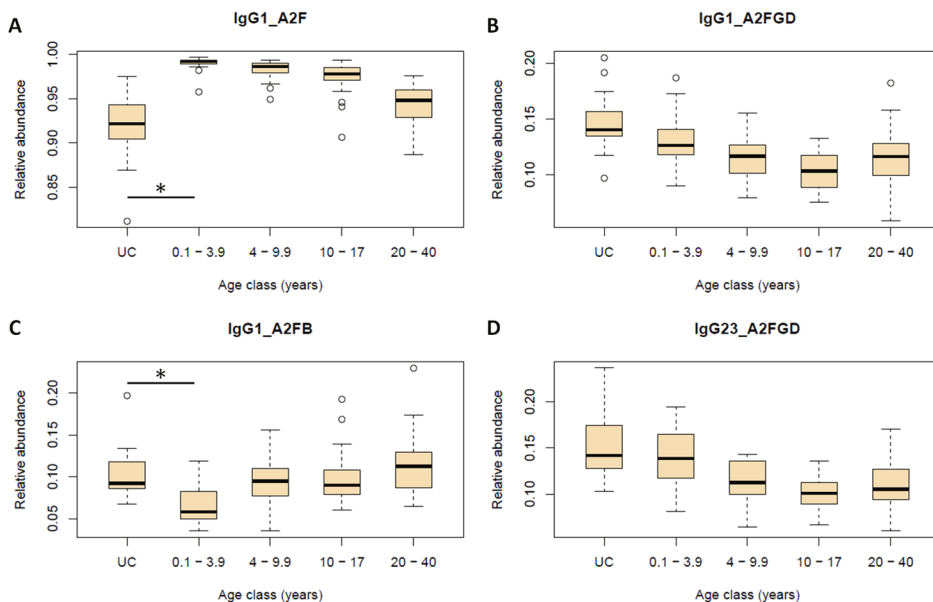


Figure 3.4 (A) Fucosylation of diantennary glycans of IgG1 (IgG1_A2F), (B) sialylation per galactose of diantennary fucosylated glycans of IgG1 (IgG1_A2FGD), (C) bisection of fucosylated diantennary glycans of IgG1 (IgG1_A2FB), and (D) sialylation per galactose of diantennary fucosylated glycans of IgG2/3 (IgG23_A2FGD), per age class. Fucosylation and bisection of fucosylated glycans from IgG1 show significant differences between UC samples and samples from very young children (indicated by the asterisk (*), $p < 8.7 \cdot 10^{-5}$). Sialylation per galactose does not show this difference.

No significant differences were observed for the fucosylation, bisection or sialylation per galactose (IgG1_A2F, IgG1_A2FB, IgG1_A2FGD, IgG23_A2FGD) between UC samples and

samples from young (female) adults (**Figure 3.4, Table S-5**). On the other hand, the galactosylation (IgG1_A2G, IgG23_A2FG) was significantly different between the UC samples and the young adults (IgG1: M(UC) = 0.73; M(young adults) = 0.60; $p = 5.1 \cdot 10^{-7}$; IgG2/3: M(UC) = 0.69; M(young adults) = 0.52; $p = 1.6 \cdot 10^{-7}$; **Figure 3.5**) and when comparing UC samples to the female young adults, the same trends were observed (IgG1: M(UC) = 0.73; M(female young adults) = 0.63; $p = 1.6 \cdot 10^{-4}$; IgG2/3: M(UC) = 0.69; M(female young adults) = 0.57; $p = 4.2 \cdot 10^{-5}$).

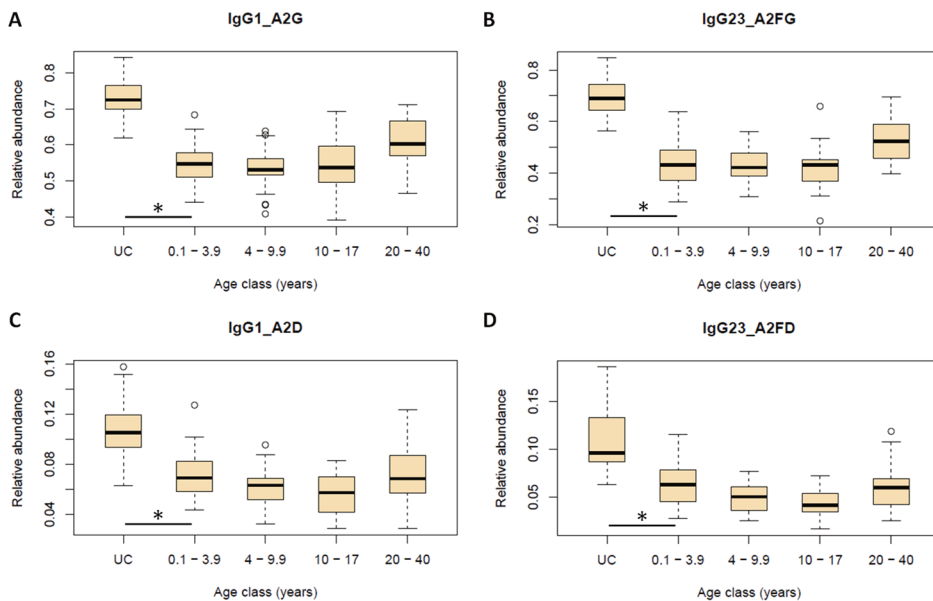


Figure 3.5 (A) Galactosylation of diantennary glycans of IgG1 (IgG1_A2G) and (B) of fucosylated diantennary glycans of IgG2/3 (IgG23_A2FG), (C) sialylation of diantennary glycans of IgG1 (IgG1_A2D) and (D) of fucosylated diantennary glycans of IgG2/3 (IgG23_A2FD), per age class. Both galactosylation and sialylation of IgG1 and IgG2/3 show significant differences between UC samples and samples from very young children (indicated by the asterisk (*), $p < 8.7 \cdot 10^{-5}$).

3.4 Discussion

The plasma IgG Fc glycosylation of 130 healthy individuals between birth and 40 years of age, including 22 samples derived from the umbilical cords of healthy newborns, was analyzed in an IgG subclass specific way. This was accomplished by a previously published, rapid and robust MALDI-TOF-MS workflow in 96-well plate format [149]. Although various

studies describing IgG Fc glycosylation in both healthy and diseased individuals have already been performed [28, 74, 79, 83-86], this is the first study that takes very young children (age 0.1 to 3.9) into account and compares them to newborns. It is also the first study describing Fc glycosylation during childhood in a subclass-specific way, giving a full and specific characterization of IgG1 Fc glycosylation and specific characterization of changes in galactosylation and sialylation of IgG2/3. Herewith, we fill a gap in the characterization of healthy human IgG Fc glycosylation. As is known for IgG, mainly diantennary Fc glycans, with high prevalence of core fucosylation, and possible galactosylation, sialylation and bisection were found [25]. Furthermore, it was observed that almost exclusively α 2,6-linked sialic acids are present on Fc glycans, also in agreement with literature [29, 58]. Levels of sialylation in UC samples reported by our method were comparable to levels reported by the liquid chromatography (LC)-electrospray ionization (ESI)-MS analysis of UC samples and of samples from pregnant women in their 3rd trimester (For IgG1: 21%, 26% and 24% respectively, for IgG2/3: 21%, 27% and 26% respectively [85, 86]; **Table S-6**). This shows that the derivatization in our MALDI-TOF-MS method prevents the vast underestimation of sialylated species due to ionization biases or metastable decay, in contrast to other MALDI-TOF-MS studies [28, 118].

For samples from adult males and females a difference in IgG Fc glycosylation was described before, where females were found to have higher degrees of bisection, galactosylation and sialylation [28, 179]. Furthermore, females age 11 to 14 were found to have lower fucosylation than males and females age 6 to 10 were found to have higher bisection than males [84]. These latter differences, however, were small and not found back in any of the categories between 6 and 18 and are also not supported by our data for children between age 4 and 17 (**Table S-6**). The reason we could not replicate the small differences between sexes in the younger age categories found before, might be due to our smaller sample sizes (31 female and 26 male samples in age class 4 to 17 in our study compared to 63 female and 64 male samples in age class 6 to 14 in Pučić et al. 2013 [84]). On the other hand, the difference in glycoanalytical methods may explain the differences in findings. Specifically, previous literature studied the total of IgG glycosylation, including Fab, whereas our study exclusively considered Fc glycosylation. As we did not observe significant differences between female and male samples in any of the defined age classes between zero and 40, we combined the sexes in all groups.

It is well-known that IgG Fc galactosylation decreases with age during adulthood [28, 81, 83]. Some studies claim a decrease of agalactosylated structures on IgG in children, while mono-galactosylated structures stay constant [83, 84]. Although we found a slightly decreasing trend in agalactosylated structures for children between 0.1 and 17, we observed a significant increase in most mono-galactosylated structures on both IgG1 and IgG2/3. Together with a decreasing trend in total digalactosylated structures, we

concluded that overall galactosylation stayed relatively constant over the age of 0.1 to 17. On the other hand, significant changes in total galactosylation of both IgG1 and IgG2/3 were observed between newborns and very young children, with the newborns having high galactosylation that was comparable to levels reported previously for samples taken from the umbilical cord [86]. Similarly high levels of galactosylation were also found in pregnant women in their 3rd trimester, which is in line with the neonatal Fc receptor (FcRN)-mediated transport of IgG over the placenta without glycosylation bias, resulting in identical IgG Fc glycosylation profiles of mother and baby at birth [84-86]. The young adult women in our study population showed slightly higher galactosylation than the very young children, but significant lower than the newborns. The high galactosylation in newborns and pregnant women is a known anti-inflammatory characteristic of IgG [54, 186], and may therefore contribute to the suppression of the maternal immune response during pregnancy. For example, increased IgG1 Fc galactosylation was reported to enhance signaling via FcγRIIb in combination with dectin-1, thereby blocking the activity of the C5a-receptor and decreasing inflammatory responses [186]. Other glycosylation features that were found to be significantly different between newborns and very young children were fucosylation (increasing after birth) and bisection (decreasing after birth). These features were, however, not significantly different between newborns (and thus pregnant women) and women in their reproductive age. So, low fucosylation and high bisection are features the newborn has adopted from the mother, but which gradually change when the child starts to produce its own IgG one month after birth [187]. Between age 0.1 and 17, fucosylation decreased significantly and bisection increased significantly, which was described before, respectively for girls and boys between age 6 and 18 [84]. Furthermore, it is known that bisection increases with age in adults, starting off at around 10% on IgG1 at the age of 20 [28], which corresponds to the level we found for IgG1 bisection in the age class 20 to 40 (11%). Finally, sialylation per galactose decreases for children between 0.1 and 17, and interestingly, this is not the case when considering sialylation independent from galactosylation. As galactosylation shows to be relatively constant, the decrease of sialylation might be caused by downregulated sialyltransferases, upregulated sialidases, shorter time spend in the Golgi or less available sialic acid donors [192]. On the other hand, for the very young children, the sialylation per galactose does not change compared to the newborns. However, total sialylation does, implying that the decrease observed here is mainly caused by the lower availability of the galactoses [28].

Combining our results with the results from previous studies, we can speculate on the natural progression of IgG Fc glycosylation throughout a human lifetime. At birth, newborns rely exclusively on IgG received from the mother [187], and as IgG passes the placenta via the FcRN independent of Fc glycosylation, the Fc glycosylation of newborns reflects that of the mother [86]. This results in anti-inflammatory IgG glycan profiles, including high galactosylation and sialylation. Furthermore, the newborns express degrees

of fucosylation and bisection that are also found in young adults. Fucosylation increases rapidly as soon as the baby starts to produce its own antibodies, while galactosylation, sialylation and bisection decrease. Fucosylation and sialylation then decrease during childhood, until the levels match those of young adults. Bisection increases and total galactosylation stays constant. During adulthood, bisection keeps increasing with age until it flattens at late adulthood, while fucosylation stays constant after adulthood is reached [28, 79, 82]. Galactosylation and sialylation decrease during adulthood, and both start higher in early adulthood and end lower in late adulthood for women than for men [28, 81]. These differences between sexes were not observed during childhood and are most likely introduced after puberty [84]. All IgG Fc glycan changes reported during adulthood were also shown to be present during inflammation [193].

3.5 Conclusion


We characterized healthy human IgG Fc glycosylation of subjects between birth and 40 years old, including newborns of which we analyzed the umbilical cord plasma. The MALDI-TOF-MS method used did not show a bias towards the sialylated species due to the derivatization step and provided IgG subclass specific information as glycopeptides were analyzed. We revealed a decrease in IgG Fc galactosylation, sialylation and bisection and an increase in fucosylation in very young children compared to newborns, which is the difference between the antibodies the fetus receives from the mother during pregnancy and the IgG the kids make themselves after birth [86]. Furthermore, we showed that fucosylation and sialylation decreased with age 0.1 to 17, whereas bisection increased and galactosylation stayed relatively constant.

Acknowledgements

This work was supported by the European Union Seventh Framework Programmes IBD-BIOM (grant number 305479) and HighGlycan (grant number 278535), as well as by ZonMW (Vidi grant number 91712323).

Supporting Information available

Additional information is available as stated in the text. This information is available free of charge via <https://pubs.acs.org/doi/10.1021/acs.jproteome.6b00038>.

- 
- ¹ *Leiden University Medical Center, Center for Proteomics and Metabolomics, Leiden, The Netherlands*
 - ² *Leiden University Medical Center, Department of Pediatrics, section Immunology, Hematology and Stem Cell Transplantation, Leiden, The Netherlands*
 - ³ *Haga Teaching Hospital, Juliana Children's Hospital, Department of Pediatrics, The Hague, The Netherlands*
 - ⁴ *Erasmus Medical Center, Sophia Children's Hospital, Department of Pediatrics, Rotterdam, The Netherlands*

IgG Fc Glycosylation After Hematopoietic Stem Cell Transplantation is Dissimilar to Donor Profiles

**Noortje de Haan¹, Maarten J.D. van Tol², Gertjan J. Driessen^{3,4},
Manfred Wuhrer¹ and Arjan C. Lankester²**

Reprinted and adapted from Front. Immunol. 9:1238 DOI: 10.3389/fimmu.2018.01238 [194].

Copyright © 2018, de Haan, van Tol, Driessen, Wuhrer and Lankester.



Immunoglobulin G (IgG) fragment crystallizable (Fc) *N*-glycosylation has a large influence on the affinity of the antibody for binding to Fcγ-receptors (FcγRs) and C1q protein, thereby influencing immune effector functions. IgG Fc glycosylation is known to be partly regulated by genetics and partly by stimuli in the microenvironment of the B cell. Following allogeneic hematopoietic stem cell transplantation (HSCT), and in the presence of (almost) complete donor chimerism, IgG is expected to be produced by, and glycosylated in, B cells of donor origin. We investigated to what extent IgG glycosylation in patients after transplantation is determined by factors of the donor (genetics) or the recipient (environment).

Using an IgG subclass-specific liquid chromatography-mass spectrometry method, we analyzed the plasma/serum IgG Fc glycosylation profiles of 34 pediatric patients pre-HSCT and at six and twelve months post-HSCT and compared these to the profiles of their donors and age-matched healthy controls.

Patients treated for hematological malignancies as well as for non-malignant hematological diseases showed after transplantation a lower Fc galactosylation than their donors. Especially for the patients treated for leukemia, the post-HSCT Fc glycosylation profiles were more similar to the pre-HSCT recipient profiles than to profiles of the donors. Pre-HSCT, the leukemia patient group showed as distinctive feature a decrease in sialylation and in hybrid-type glycans as compared to healthy controls, which both normalized after transplantation. Our data suggest that IgG Fc glycosylation in children after HSCT does not directly mimic the donor profile, but is rather determined by persisting environmental factors of the host.

4.1 Introduction

The *N*-glycan attached to the conserved glycosylation site of the fragment crystallizable (Fc) region of immunoglobulin G (IgG) has a large influence on the structure and function of the antibody [49, 195]. The presence or absence of specific monosaccharides have proven to be crucial both in modulating the affinity of IgG binding to Fcγ-receptors (FcγRs) and in the activation of the complement system. For example, the absence of a core fucose on the Fc glycan results in a ten- to twenty-fold increase in binding affinity to the FcγRIIIa and FcγRIIIb and a corresponding increase in antibody-dependent cellular cytotoxicity (ADCC) [37, 49]. For IgG Fc binding to complement factor C1q, galactosylation plays a primary role and is associated positively with binding affinity and downstream complement-dependent cytotoxicity (CDC) [37, 56].

Besides the functional implications of altered IgG Fc glycosylation described above, the IgG Fc glycosylation profile was found to be associated with altered physiological states and disease activity. For example, galactosylation decreases with age in the adult population [28]. In children, on the other hand, Fc galactosylation remains relatively constant with age, while bisection increases and fucosylation and sialylation decrease [176]. Furthermore, in adults, total IgG-Fc galactosylation is decreased in rheumatoid arthritis and active tuberculosis infections [92, 101], but also in different types of cancer, like ovarian cancer and colorectal cancer [102, 103]. Antigen-specific IgG antibodies may display discriminative glycosylation patterns. For example, gp120-specific antibodies in HIV-infected patients show a decrease in fucosylation as compared to the total pool of IgG in these patients [98].

IgG Fc *N*-glycans are co-translationally attached to the protein in the endoplasmic reticulum (ER) of B lymphocytes and enzymatically shaped into their final structure in the ER and Golgi apparatus. This process is dependent on the time the protein spends in the Golgi apparatus, the abundance of monosaccharide donors and presence of specific glycosyltransferases and glycosidases, adding and removing particular monosaccharides to and from the glycoconjugate, respectively [192]. All these factors are known to be partly regulated by the genetics of the B cell [74, 75], and on the other hand, by external stimuli in the microenvironment of the cells, like hormones and cytokines [78, 196]. For example, in *in vitro* experiments, all-*trans* retinoic acid (ATRA) and human interleukin (IL)-21 cause a decrease and increase in both IgG1 Fc galactosylation and sialylation, respectively [78]. However, the exact mechanisms leading to specific IgG Fc glycosylation profiles are not fully understood yet. Unraveling the up-stream factors influencing IgG glycosylation will improve the understanding of changes hereof that are associated with immune-related diseases.

Allogeneic hematopoietic stem cell transplantation (HSCT) is a curative treatment for patients with malignant as well as non-malignant immune-hematological diseases. In

addition to the cure of the primary disease, proper immune reconstitution is an important goal of any HSCT procedure. Previous studies in non-transplant patients have demonstrated that IgG Fc glycosylation patterns are strongly influenced by both B cell intrinsic and (host) environmental factors [74, 78, 196]. HSCT provides a unique setting to study the impact of both determinants on IgG Fc glycosylation in transplanted patients. With this aim we studied a group of pediatric patients that were successfully treated for their initial disease, and in whom (close to) complete donor chimerism was documented at 6 and 12 months post-transplant. Furthermore, the patient group was homogeneous in terms of reaching steady state within this timeframe, *i.e.*, the presence of an uncomplicated clinical condition without requirement of any immunomodulatory medication.

The IgG Fc glycosylation profiles of transplant recipients were analyzed before and after HSCT and compared to the profiles of the donors as well as to those of age-matched healthy controls.

4.2 Materials and Methods

4.2.1 HSCT Patients

In the period 2010-2014, 211 allogeneic HSCT procedures were performed in children at the pediatric transplantation unit of the LUMC. Criteria for exclusion of patients to enroll in the current study were: death within one year after HSCT, an eventful course in the first year after HSCT such as relapse of the original disease, acute graft-versus-host disease (GvHD) grade >1 or extensive chronic GvHD, dependency of IgG supplementation within a period of two months before taking a serum or plasma sample at six and twelve months after HSCT and dependency of immunosuppressive drugs (*i.e.*, cyclosporine A) at seven months after HSCT (median 3.8 months). In addition, patients treated for thalassemia and with a persistent mixed chimerism in peripheral blood mononuclear cells (PBMC) defined as <85% donor origin at 1 year post-HSCT were excluded. Finally, to be included in the study, at least three of the four following serum or plasma samples of a donor-recipient pair should be available: from the graft donor, from the patient before HSCT (and start of the conditioning), and at six and twelve months after HSCT.

The final study cohort consisted of 34 pediatric HSCT recipients. In **Table 4.1**, the characteristics of these patients and their donors are summarized. All transplantation procedures were performed according to national protocols and in line with the recommendations of the European group for Blood and Marrow Transplantation (EBMT).

Table 4.1 Summary of the cohort.

Patients			
Group	Malignant HD ^a	Non-malignant HD ^a	Total
Number (N) of patients	16	18	34
Age at HSCT ^b (median, (range))	9.4 (0.8 to 17.8)	5.7 (0.7 to 14.9)	7.5 (0.7 to 17.8)
Recipient sex (% female)	31.3	16.7	23.5
Donor type ^c : IRD (BM/CB)	4 (4/0)	11 (10/1)	15 (14/1)
MUD (BM/CB)	10 (9/1)	6 (3/3)	16 (12/4)
ORD (PBSC)	2 (2)	1 (1)	3 (3)
Donor age ^b (median, (range))	26.6 (8.9 to 49.0)	17.1 (2.8 to 47.5)	25.6 (2.8 to 49.0)
Donor sex (% female)	12.5	35.7	24.1
Graft: undepl. (N)/CD34- enriched (N)	14/2	17/1	31/3
% chimerism ^d (median, (range))	100 (98 to 100)	100 (87 to 100)	100 (87 to 100)
Acute GvHD ^e (grade 1, N)	2	1	3
Chronic GvHD ^e (limited, N)	1	0	1
1 st sample (N)	16	16	32
1 st sample ^f (median, (range))	-13 (-21 to -6)	-14 (-28 to -6)	-13 (-28 to -6)
2 nd sample (N)	16	18	34
2 nd sample ^f (median, (range))	176 (162 to 199)	183 (158 to 205)	182 (158 to 205)
3 rd sample (N)	16	18	34
3 rd sample ^f (median, (range))	375 (348 to 499)	365 (313 to 431)	372 (313 to 499)
Donor sample (N)	15	14	29
Donor sample ^f (median, (range))	-1 (-159 to 0)	-24 (-43 to 0)	-14 (-159 to 0)
Controls			
Group	Age matched to malignant HD	Age matched to non-malignant HD	Total
Controls (N)	16	18	81
Age (median, (range))	9.3 (0.8 to 16.8)	6.0 (0.6 to 13.8)	6.2 (0.5 to 16.8)
Sex (% female)	68.8	27.8	49.4

^a HD: hematological disease. Malignant HD: acute lymphoblastic leukemia: N = 10; myelodysplastic syndrome/acute myeloblastic leukemia: N = 2; acute myeloblastic leukemia: N = 4. Non-malignant HD: thalassemia: N = 4, Fanconi anemia: N = 3, sickle cell disease: N = 2, severe aplastic anemia: N = 1, progressive bone marrow failure: N = 1, neutropenia congenita: N = 1, Glanzmann thrombasthenia: N = 1, hemophagocytic lymphohistiocytosis: N = 4, X-linked lymphoproliferative disease: N = 1. ^b Age at hematological stem cell transplantation and graft donation (excluding cord blood donors), respectively, in years. ^c IRD: identical related donor; MUD: matched unrelated donor;

(Table 4.1 continued) ORD: other than HLA-genotypically identical related donor; BM: bone marrow; CB: cord blood; PBSC: peripheral blood stem cells. ^d % donor chimerism in peripheral blood mononuclear cells (PBMC) at 1 year post-HSCT. ^e GvHD: graft-versus-host disease. ^f Day of serum/plasma sampling relative to the day of HSCT

4.2.2 Sampling and Study Approval

Serum or plasma samples of HSCT recipients were collected between 6 and 28 days (median 13 days) prior to HSCT, *i.e.*, before start of conditioning, and 6 months (range 158-205 days) and 12 months (range 313-499 days) after HSCT. From 29 of the stem cell donors (excluding umbilical cord donors) a plasma or serum sample was collected between 0 and 159 days (median 14 days) before donation of the graft (Table 4.1). All clinical samples were collected with approval of the Medical Ethics Committee of the LUMC, Leiden (project P01.028) and after receiving written informed consent from the participants. In addition, samples were collected from 81 healthy controls in the same age range as the patients. The healthy control samples were collected with approval of the Medical Ethics Committee of the Erasmus MC, Rotterdam (MEC-2005-137) and after receiving written informed consent from the participants [176, 188].

4.2.3 IgG Glycopeptide Analysis and Data Processing

All 135 clinical samples (patients and donors) were randomized in 96-well plates, together with 12 plasma standards (VisuCon pooled plasma; Affinity Biologicals Inc., Ancaster, ON, Canada) and 5 PBS blanks. Healthy control samples were randomized on separate plates, including 29 plasma standards and 8 PBS blanks. IgG was isolated using Protein G affinity beads (GE Healthcare, Uppsala, Sweden) and digested by trypsin as described before [197], see Supplementary Materials and Methods. The IgG digest was separated and analyzed by nano-liquid chromatography (LC) coupled by electrospray ionization to a Maxis Impact HD quadrupole time-of-flight mass spectrometer (q-TOF-MS; Bruker Daltonics, Bremen, Germany) as described before [197], see Supplementary Materials and Methods. Prior to statistical analysis, raw LC-MS data were extracted and curated using the in-house developed software LacyTools v0.0.7.2 as described previously [197, 198]; for all cohort-specific extraction parameters see Supplementary Materials and Methods.

4.2.4 Statistics

The absolute intensities of the extracted glycoforms (Figure 4.1 and Figure 4.2 and Table S1 in Supplementary information) were total-area normalized per IgG subclass and levels of galactosylation, sialylation, fucosylation as well as other derived traits were calculated (Table 4.2 and Table S2 in Supplementary information). To assess data quality throughout the cohort measurements, the plasma standards were analyzed, revealing highly repeatable glycosylation profiles for all subclasses, with median relative standard deviation of all extracted glycoforms of IgG1, IgG2/3 and IgG4 being 3.4%, 2.7% and 2.1%,

respectively (**Figure S1** in Supplementary information). For three patients, both plasma and serum samples, obtained at corresponding time points, were available. Comparison of these samples showed similar IgG Fc glycosylation profiles for both materials (**Figure S2** in Supplementary information). The difference between measurements in plasma and serum from the same patient was lower than the variation between patients, enabling the use of both materials in this study.

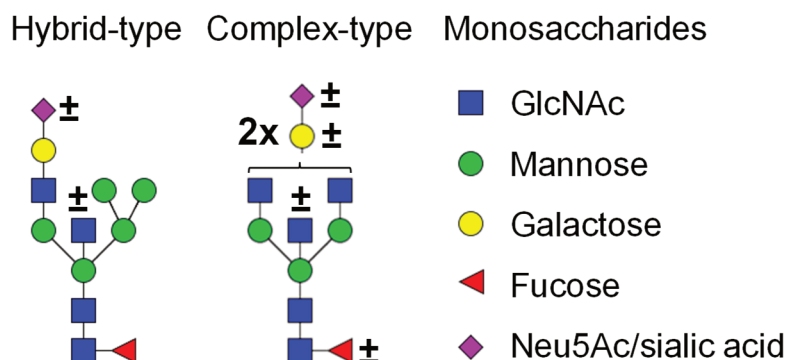


Figure 4.1 Glycan structures found on IgG-Fc. Both hybrid-type and diantennary complex-type glycan structures were found on the IgG Fc glycopeptides in our study. Hybrid-type glycans varied by the presence of a sialic acid and/or a bisecting GlcNAc. Diantennary complex-type glycans were found with zero to two galactoses, zero to two sialic acids and the presence or absence of a bisecting GlcNAc and/or a core fucose. Monosaccharide linkages were based on literature [29, 74, 169, 176]. Green circle: mannose, yellow circle: galactose, blue square: *N*-acetylglucosamine (GlcNAc), red triangle: fucose, pink diamond: *N*-acetylneuraminic acid (Neu5Ac/sialic acid).

Further statistical analysis and data visualization were performed using R 3.1.2 (R Foundation for Statistical Computing, Vienna, Austria) and RStudio 0.98.1091 (RStudio, Inc., Boston, MA). Patients pre- and twelve months post-HSCT, as well as patients and donors, were compared with two-sided Wilcoxon signed-rank tests, healthy controls and patients were compared with two-sided Mann Whitney U tests. The samples of the patients taken six months post-HSCT were left out of the statistical analysis to reduce the data density, but were shown in some figures to illustrate the dynamics of IgG Fc glycosylation profiles after HSCT. Statistical tests were performed for the whole dataset, as well as after stratification on diagnosis: non-malignant hematological disease and malignant hematological disease (**Table 4.1**). For the tests after stratification for diagnosis, subgroups of one-to-one age- matched healthy controls were used. A significance threshold (α) = 0.015 was used throughout the study after correcting for multiple testing using the Benjamini-Hochberg approach with a FDR of 5%.

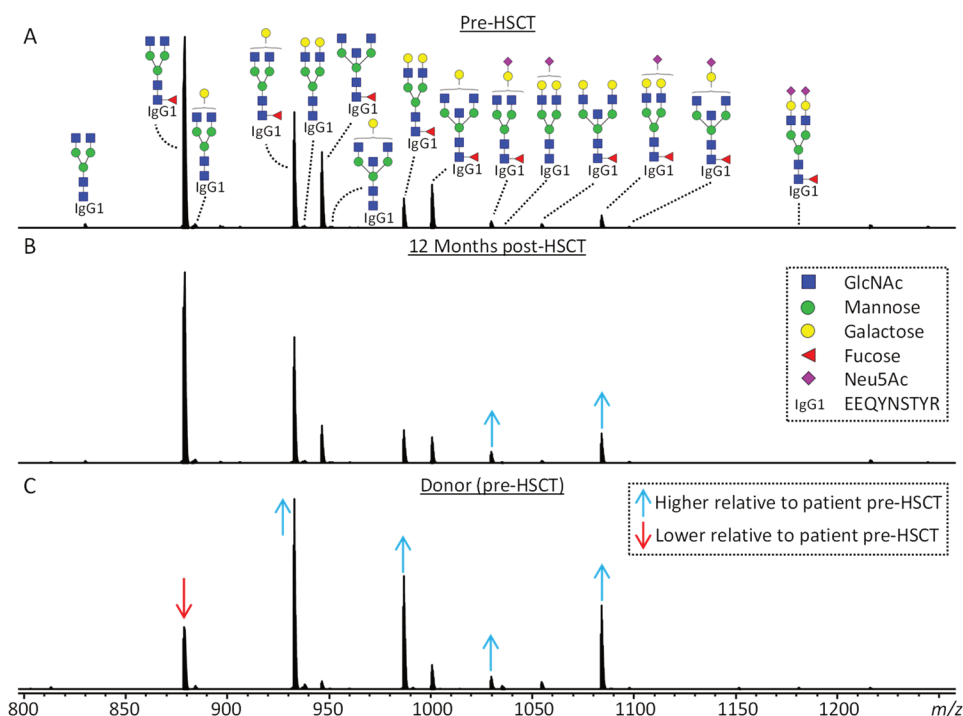


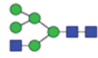
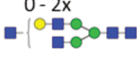
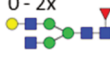
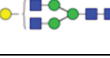
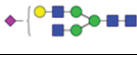

Figure 4.2 Representative mass spectra of IgG1 glycopeptides. Annotated are the 15 most abundant IgG1 glycoforms detected for a 7.5 years old, male, acute myeloid leukemia patient (A) before HSCT, (B) twelve months after HSCT and (C) his 24 years old, healthy, male donor. Triply charged glycopeptides are shown, the proposed glycan structures are based on literature [29, 74, 169, 176]. Green circle: mannose, yellow circle: galactose, blue square: *N*-acetylglucosamine, red triangle: fucose, pink diamond: *N*-acetylneuraminic acid. Differences in relative abundances of glycoforms as compared to the patient pre-HSCT are indicated by red (lower than in pre-HSCT patient) and blue (higher than in pre-HSCT patient) arrows.

4.3 Results

The IgG Fc glycosylation profiles of 34 pediatric HSCT patients were followed over time, starting with a sample prior to the HSCT and followed by two longitudinal samples, six and twelve months post-HSCT. In addition, the IgG Fc glycosylation of the donors prior to the donation of the grafts and of age-matched healthy controls was assessed (Table 4.1). IgG Fc glycopeptides were analyzed by LC-MS, which enabled the detection of 22 glycoforms on IgG1, 16 on IgG2/3 and 11 on IgG4 (Figure 4.1 and 4.2 and Table S1 in Supplementary information). Furthermore, derived glycosylation traits such as levels of galactosylation,

sialylation, fucosylation and bisection were calculated (**Table 4.2** and **Table S2** in Supplementary information).

Table 4.2 Subclass-specific derived traits.

Derived trait ^a	Depiction ^b	Description ^c
Hybrids		Fraction of hybrid-type glycans
Bisection	0 - 2x 	Fraction of glycans with a bisecting <i>N</i> -acetylhexosamine
Fucosylation	0 - 2x 	Fraction of glycans with a core fucose
Galactosylation		Galactosylation per antenna of diantennary glycans
Sialylation	0 - 2x 	Sialylation per antenna of diantennary glycans
Sialylation per galactose	0 - 2x 	Sialylation per galactose of diantennary glycans

^a The individual glycoforms were grouped based on their glycosylation features as described before for IgG glycopeptides in human [176]. ^b Green circle: mannose, yellow circle: galactose, blue square: *N*-acetylglucosamine, red triangle: fucose, pink diamond: *N*-acetylneuraminic acid. The depictions of the derived traits show the minimally required composition to contribute to a trait. ^c For detailed calculations of the traits, see **Table S2** in Supplementary information.

4.3.1 IgG Fc Glycosylation Differences between Patients and Healthy Controls

For the total patient group pre-HSCT, IgG Fc bisection was higher than for healthy controls (e.g. IgG1: 14.8% vs. 10.1%, respectively, $p = 2.5 \times 10^{-7}$; **Table S3** and **Figure S3** in Supplementary information) while IgG1 and IgG2/3 galactosylation and sialylation were lower (e.g. IgG1 galactosylation: 51.9% vs. 59.9%, $p = 3.2 \times 10^{-6}$; **Figure 4.3**, **Table S3** and **Figure S3** in Supplementary information). Furthermore, specifically on IgG1, fucosylation and hybrid-type glycans were lower in patients than in controls (fucosylation: 95.6% vs. 97.5%, $p = 1.1 \times 10^{-5}$, and hybrid-types: 0.3% vs. 0.4%, $p = 6.6 \times 10^{-3}$; **Table S3** and **Figure S3** in Supplementary information).

The patients were grouped according to their diagnosis, resulting in a group with malignant and with non-malignant hematological diseases (**Table 4.1**). These groups differ in disease course and treatment before HSCT, and were hence compared separately to healthy controls with respect to IgG Fc glycosylation (**Table S4** and **Table S5** in

Supplementary information). The pre-HSCT malignant hematological disease group differed in IgG Fc glycosylation from age-matched healthy controls similar to the overall pre-HSCT patient group (**Figure 4.4**, **Figure 4.5** and **Table S4** in Supplementary information). In contrast, the pre-HSCT non-malignant hematological disease group only showed a decrease in IgG1 fucosylation as compared to age-matched healthy controls (**Table S5** and **Figure S5** in Supplementary information).

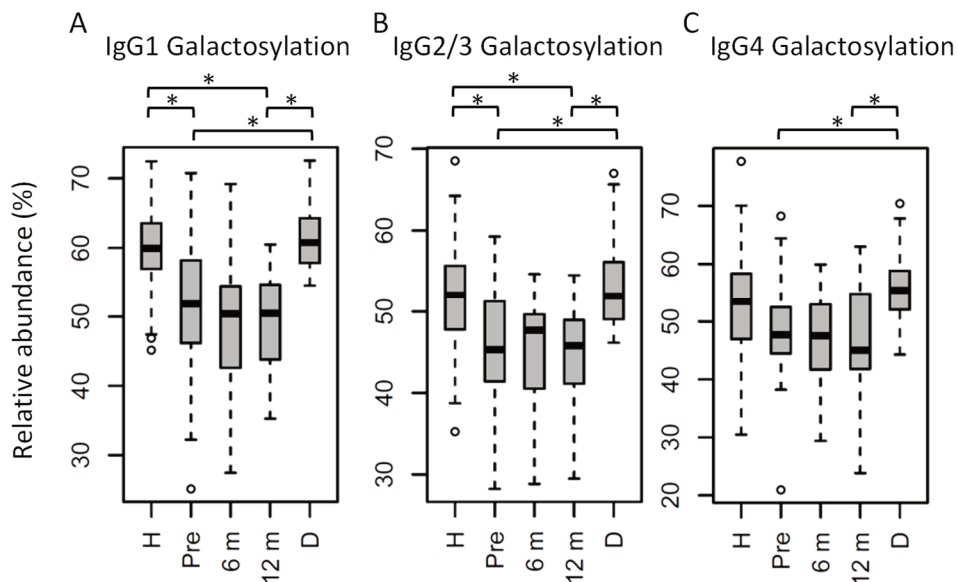


Figure 4.3 IgG Fc galactosylation in all patients, compared to their donors and age-matched healthy controls. IgG Fc Galactosylation on (A) IgG1, (B) IgG2/3 and (C) IgG4 is different between patients before HSCT (Pre) and their donors (D). No changes were observed between patients pre- and twelve months post-HSCT (12 m). In general, patients before and after HSCT have lower galactosylation than age-matched healthy controls (H), although this was not statistically significant for IgG4 galactosylation. 6 m: patients six months after HSCT. Patients and donors were compared by Wilcoxon signed-rank tests, healthy controls and patients with Mann Whitney U tests. p -values < 0.015 were considered statistically significant after 5% FDR correction (as indicated by the asterisks above the plots). For IgG1 galactosylation, n (H, Pre, 6 m, 12 m, D) = 81, 32, 34, 34, 29, for IgG2/3 galactosylation, n (H, Pre, 6 m, 12 m, D) = 69, 32, 32, 33, 29, for IgG4 galactosylation, n (H, Pre, 6 m, 12 m, D) = 59, 27, 15, 17, 28, respectively.

4.3.2 The Impact of HSCT on IgG Fc Glycosylation

In the whole dataset, pre-HSCT IgG Fc glycosylation differed from the corresponding donors (**Table S3** and **Figure S3** in Supplementary information). For all subclasses, IgG galactosylation was higher in donors than in recipients pre-HSCT (IgG1: 60.8% vs. 51.9%, p

= 5.5×10^{-6} ; **Figure 4.3**). In addition, IgG1 fucosylation was lower in donors (94.1%) than in recipients pre-HSCT (95.6%, $p = 1.0 \times 10^{-3}$), while IgG1 sialylation was higher in donors (10.0%) than in recipients (8.5%, $p = 1.5 \times 10^{-3}$; **Table S3** and **Figure S3** in Supplementary information). Both galactosylation and IgG1 sialylation, were still lower in patients twelve months post-HSCT as compared to the donors, and no difference in galactosylation and sialylation was observed between the patients pre-HSCT and twelve months post-HSCT (**Figure 4.3**, **Table S3** and **Figure S3** in Supplementary information). The differences in IgG Fc glycosylation between pre-HSCT patients and healthy controls, as described above, were still observed twelve months post-HSCT, except for IgG1 hybrid-type glycans and IgG2/3 sialylation which both normalized (**Table S3** in Supplementary information).

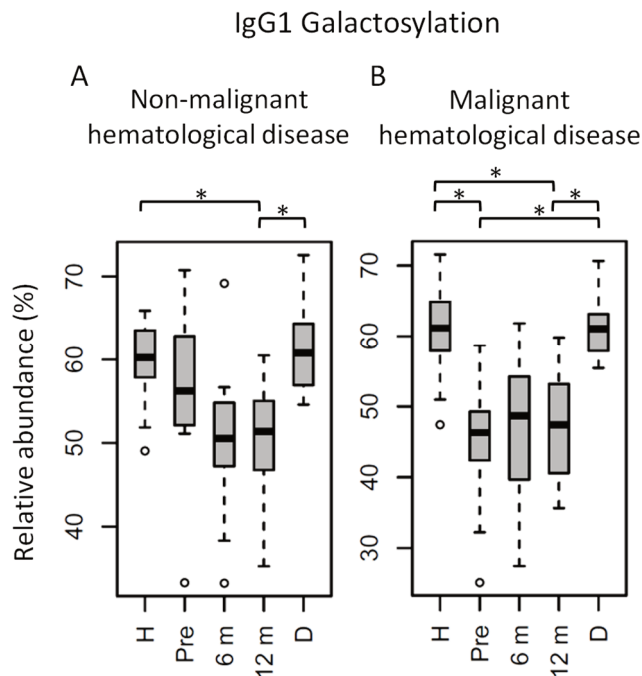


Figure 4.4 IgG1 Fc galactosylation in all patients stratified on diagnose, compared to their donors and age-matched healthy controls. IgG1 Fc galactosylation in children (**A**) with non-malignant hematological diseases and (**B**) with malignant hematological diseases. H: age-matched healthy controls, Pre: patients prior to HSCT, 6 m: patients six months after HSCT, 12 m: patients twelve months after HSCT, D: donors prior to HSCT. Patients and donors were compared by Wilcoxon signed-rank tests, healthy controls and patients with Mann Whitney U tests. p -values < 0.015 were considered statistically significant after 5% FDR correction (as indicated by the asterisks above the plots). For non-malignant hematological diseases, n (H, Pre, 6 m, 12 m, D) = 18, 16, 18, 18, 14, for malignant hematological diseases, n (H, Pre, 6 m, 12 m, D) = 16, 16, 16, 16, 15, respectively.

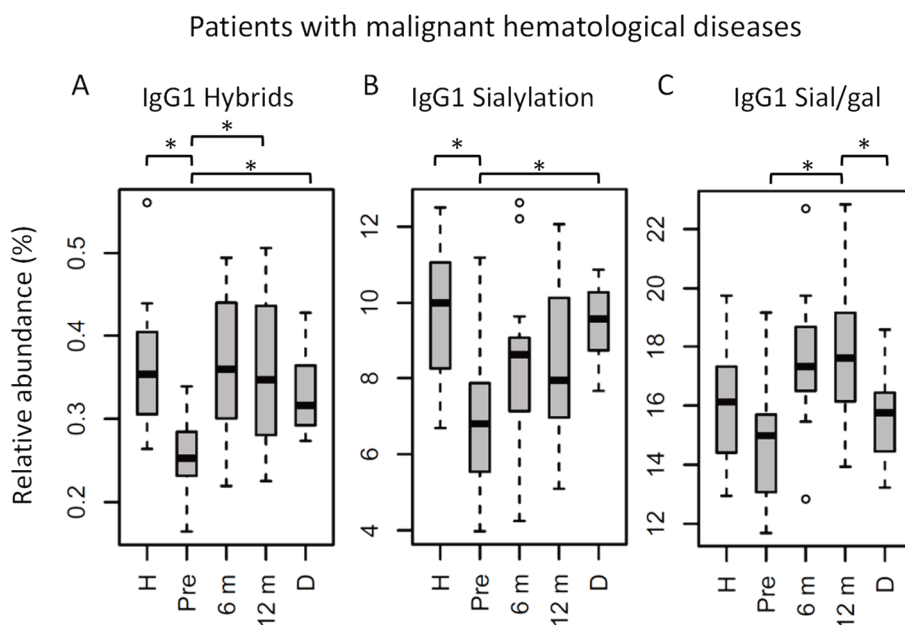


Figure 4.5 IgG1 Fc glycosylation features in patients with malignant hematological diseases, compared to their donors and age-matched healthy controls. IgG1 (A) hybrid-type glycans and (B) sialylation differ between healthy controls (H) and patients before HSCT (Pre). In addition, IgG1 (A) hybrid-type glycans and (B) sialylation are different between patients and donors (D), and IgG1 (A) hybrid-type glycans and (C) sialylation per galactose change within the patients after HSCT. 6 m: patients six months after HSCT, 12 m: patients twelve months after HSCT. Patients and donors were compared by Wilcoxon signed-rank tests, healthy controls and patients with Mann Whitney U tests. p -values < 0.015 were considered statistically significant after 5% FDR correction (as indicated by the asterisks above the plots). For all IgG1 glycosylation features in patients treated for malignant hematological diseases, n (H, Pre, 6 m, 12 m, D) = 16, 16, 16, 16, 15, respectively.

The effect of HSCT on IgG Fc glycosylation was studied additionally for the two diagnosis groups separately (Table S4 and S5 and Figure S4 and S5 in Supplementary information). The observations made on IgG Fc galactosylation in the total data set, were found back in the patients treated for malignant hematological diseases, but only partly in the other subgroup (Figure 4.4). For the patients treated for hematological malignancies, galactosylation was lower for the recipients pre-HSCT (46.3%) than for the donors (IgG1: 61.0%, $p = 1.2 \times 10^{-4}$). The reduced galactosylation in recipients was still observed twelve months post-HSCT (47.4%, $p = 6.1 \times 10^{-5}$), while no difference was observed between patients before and after HSCT (Figure 4.4 and Table S4 in Supplementary information). Another glycosylation trait that was found to be overall low, but significantly lower only in pre-HSCT patients with a hematological malignancy as compared to their donors, was the relative presence of the IgG1 hybrid-type glycans (recipient: 0.25% and donor: 0.32%, $p =$

1.2×10^{-4}). In contrast to galactosylation, the abundance of hybrid-type glycans normalized after HSCT (0.35%; **Figure 4.5A** and **Table S4** in Supplementary information). In addition, IgG1 sialylation was only lower in the patients with a hematological malignancy pre-HSCT (6.8%) as compared to their donors (9.6%, $p = 3.1 \times 10^{-4}$), and showed an increasing trend after HSCT (**Figure 4.5B**). This increase in IgG1 sialylation was more pronounced when assessed per galactose (pre-HSCT: 15.0%, 12 months post-HSCT: 17.6%, $p = 1.5 \times 10^{-3}$) and sialylation per galactose was higher after HSCT (17.6%) than in the corresponding donors (15.8%, $p = 1.2 \times 10^{-4}$; **Figure 4.5C**).

The group treated for non-malignant diseases showed no differences between donors and recipients pre-HSCT (**Figure 4.4** and **Table S5** in Supplementary information). However, a decrease in fucosylation was observed after HSCT (IgG1-pre: 96.3%, post: 95.5%, $p = 1.2 \times 10^{-2}$; **Table S5** and **Figure S5** in Supplementary information). In addition, IgG1 fucosylation and galactosylation were lower post-HSCT than for age-matched healthy controls (fucosylation: 95.5% vs. 97.9%, $p = 6.6 \times 10^{-4}$, and galactosylation: 51.4% vs. 60.2%, $p = 6.0 \times 10^{-6}$; **Figure S5** in Supplementary information), while bisection was higher for the post-HSCT patients as compared to the controls (13.5% and 10.1%, $p = 1.1 \times 10^{-4}$, respectively). Of note, the post-HSCT levels of galactosylation (IgG1: 51.4%) were also lower than those found in the donors (60.8%, $p = 9.8 \times 10^{-4}$; **Figure S5** and **Table S5** in Supplementary information).

4.4 Discussion

4.4.1 Recipient Galactosylation is Different from Donor Galactosylation

Here we studied IgG Fc glycosylation in pediatric patients before and after HSCT as compared to their donors. Looking at the whole data set, the most prominent IgG Fc glycosylation differences between donors and recipients pre-HSCT were observed in the galactosylation, which was lower in the patients as compared to the donors independently of the IgG subclass. This cannot be explained by the age difference between the groups, as galactosylation does hardly differ between children and young adults [84, 176]. Furthermore, a significant difference remained present for the galactosylation of IgG1 and IgG2/3 when comparing recipients pre-HSCT with healthy age-matched controls. Therefore, a low galactosylation state most likely reflects glycosylation changes caused by the disease and/or the treatment thereof. This is supported by the observation that, when the patients were stratified based on diagnosis, only the children treated for hematological malignancies showed a lower galactosylation as compared to both their donors and the healthy age-matched controls. IgG Fc galactosylation was reported before to be lowered in patients with solid tumors [102, 103].

Twelve months after HSCT, the patients treated for hematological malignancies still showed a lower IgG Fc galactosylation as compared to their donors, which indicates that the recipients produce IgG with a Fc glycosylation pattern that partly mimics the profile of the recipient pre-HSCT and not the donor profile. Of note, although for the patient-subgroup treated for non-malignant hematological diseases the pre-HSCT galactosylation level did not differ from the donor, twelve months post-HSCT their galactosylation was also lower than that of the donors. The low level of galactosylation at this stage after HSCT, when all study patients were in a stable and uncomplicated clinical condition, was comparable between the two subgroups. A likely explanation for this aberrant IgG Fc galactosylation is, at least partly, the regulation of this Fc glycosylation trait by host microenvironmental factors like cytokines or hormones which persists for a prolonged period after HSCT. In this respect it would be interesting to study the expression of glycan-modifying enzymes, like glycosyltransferases and glycosidases, and influencers thereof, both before and after HSCT. While the used chemotherapeutic medication (for example clofarabine) has been reported to perform their function through epigenetic mechanisms, it seems unlikely that this influences the IgG production by the donor B cells as these drugs are administered to the patients before the HSCT and are cleared from the circulation rapidly.

4.4.2 Hybrid-type Glycans and Sialylation Increase after HSCT

While aberrant galactosylation in patients treated for hematological malignancies did not change after HSCT, IgG1 hybrid-type glycans and sialylation per galactose increased to a normal level after HSCT in these patients. Although for all samples in the cohort the total relative abundance of the hybrid-type glycans was below 1% of the total glycan profile, still a clear increase was observed in the proportion of hybrid-type glycans after HSCT for hematological malignancies. Hybrid-type structures are an intermediate in the glycosylation biosynthesis, emerging in the medial Golgi with limited α -mannosidase II activity to trim the mannoses on the α 1,6-arm of the glycoconjugate, or upon addition of a bisecting GlcNAc before trimming takes place, as the presence of bisection inhibits the activity of α -mannosidase II [199]. Hybrid-type glycans have been reported to be present on human polyclonal IgG [26, 27], albeit in minor amounts, and little is known of their specific effects on IgG-Fc function.

Similar to galactosylation, IgG1 sialylation was low in patients with hematological malignancies pre-HSCT as compared to both the healthy controls and donors. However, after HSCT, sialylation showed an increase, which was more pronounced when studied relative to the level of galactosylation. While pre-HSCT sialylation was lower than in healthy controls and in donors, post-HSCT no difference was observed between case and control or donor levels. In addition, post-HSCT sialylation per galactose was higher than the levels observed in the donors. While overall sialylation effects might be a possible

side-effect of changing galactosylation (terminal galactoses are a substrate for sialylation), an increase in the amount of sialic acids per galactose is likely to be caused by the up-regulation of the sialyltransferase ST6Gal1 or an increased availability of the substrate CMP-sialic acid [192]. Next to the regulation inside the B cell by genetic and local factors [74, 78, 196], IgG Fc sialylation in mice is also reported to be dynamically regulated independently of the B cell [200]. This is suggested to happen in a stress driven way, with the accumulation of platelets that serve as source of CMP-sialic acid [201]. In murine models an increase in Fc sialylation was reported to act as an anti-inflammatory regulator resulting in up-regulation of the FcγRIIb on macrophages [202]. However, this finding is hard to translate directly to the human situation, due to the differences between mice and men in IgG effector functions [45]. In human *in vitro* models, an increased Fc sialylation on polyclonal IgG was connected to a decreased C1q binding and, consequently, to an impairment of complement-mediated cytotoxicity (CDC) [56].

While various association studies in humans point towards a more pronounced role of galactosylation rather than of sialylation in potentially mediating pro- and anti-inflammatory effects of IgG [54, 97, 203], these studies were all performed in the adult population, while knowledge about the effects in children is limited. A recent study showed the decrease of sialylation per galactose, but not of galactosylation, with age in healthy children [176]. Contrary, for healthy adults it was reported that galactosylation decreases with age, while sialylation per galactose remains stable in males and only slightly decreases in females [28]. These differences in the regulation of IgG galactosylation and sialylation between children and adults warrant further investigation as to the causes as well as downstream effects.

Both IgG1 hybrid-type glycans and sialylation showed a difference between the healthy controls or donors and the recipient treated for hematological malignancies pre-HSCT which was not observed anymore post-HSCT. This might indicate that environmental factors regulating these Fc glycosylation traits have been normalized.

4.4.3 Disease-specific IgG Fc Glycosylation

While for patients treated for hematological malignancies, pre-HSCT, multiple differences in IgG Fc glycosylation were observed as compared to healthy controls, for the group with non-malignant diseases less profound differences were found between cases and controls. Specifically, lower levels of galactosylation and sialylation, as well as lower hybrid-type glycans, were exclusively observed in the group of hematological malignancies. It has previously been reported that IgG galactosylation decreased with different forms of cancer in adults, like ovarian and colorectal cancer [102, 103] while corresponding knowledge on malignancies in children has hitherto been lacking. To our knowledge, the only IgG glycosylation studies performed in diseased children so far were in patients with allergic diseases, asthma and juvenile idiopathic arthritis, showing no associations

between aberrant IgG glycosylation profiles and the two former disorders [76, 105], and a decreased galactosylation and sialylation in juvenile idiopathic arthritis [66]. Here we show that pediatric patients treated for hematological malignancies have an altered IgG Fc glycosylation, which might be specific for their condition or treatment regimens as compared to patients treated for non-malignant hematological diseases.

4.4.4 Conclusion

While the B cells in children after HSCT are mainly of donor origin [204] and patients were investigated after reaching independency of IgG supplementation, we found that IgG Fc glycosylation in our pediatric cohort did not reflect the glycosylation pattern of the donors. Galactosylation was already low pre-HSCT in patients treated for hematological malignancies as compared to their donors and age-matched healthy controls, and remained at this lower level the first year after HSCT. In patients treated for non-malignant hematological diseases, galactosylation showed a strong decrease to similarly low levels after HSCT. These data suggest that external local influences on the IgG Fc glycosylation are operative before HSCT in patients treated for hematological malignancies as well long term after HSCT independently of the original disease. To further identify the external factors influencing IgG glycosylation after HSCT, future research should focus on the expression of glycan-modifying enzymes in the ER and Golgi apparatus, and in addition on the molecules that can influence up- and down-regulation of these enzymes, like cytokines and hormones [78, 196]. Furthermore, antigen-specific IgG glycosylation analysis, for example of anti-pneumococcal or anti-meningococcal antibodies after vaccination or of autoantibodies, might shed light on the influence of antigen stimulation on the IgG glycosylation profile.

Other IgG1 glycosylation features like hybrid-type glycans and sialylation, were also low prior to HSCT in the group treated for hematological malignancies, but normalized after transplantation. This could either be explained by normalization of environmental factors influencing the latter IgG Fc glycosylation traits upon curing the disease or by a reflection of the donor glycosylation status, based on donor genetics. Future studies, in populations that contain both cases with and without post-HSCT complications like immunodeficiencies or antibody mediated autoimmunity, might reveal pathology-specific glycosylation profiles.

Acknowledgements

We would like to thank Anja Janssen-Hoogendijk and Els Jol-van der Zijde for collecting the patient and donor samples and the data of the procedure and outcome of the HSCT. Karli Reiding is acknowledged for his input on the statistical analysis and help with the R scripts. Agnes Hipgrave Ederveen and Carolien Koeleman are acknowledged for their help with

running the LC-MS system. This work was supported by the European Union Seventh Framework Program HighGlycan (278535).

Supporting Information available

Additional information is available as stated in the text. This information is available free of charge via <https://www.frontiersin.org/articles/10.3389/fimmu.2018.01238/full>.

- 
- ¹ *Leiden University Medical Center, Center for Proteomics and Metabolomics, Leiden, The Netherlands*
 - ² *Erasmus MC-Sophia Children's Hospital, University Medical Center Rotterdam, Intensive Care and Department of Pediatric Surgery, Rotterdam, The Netherlands*
 - ³ *Erasmus MC-Sophia Children's Hospital, University Medical Center Rotterdam, Department of Pediatrics, Division of Pediatric Infectious Diseases & Immunology, Rotterdam, The Netherlands*
 - ⁴ *Newcastle University, Institute of Cellular Medicine, Newcastle upon Tyne, United Kingdom*
 - ⁵ *Great North Children's Hospital, Newcastle upon Tyne Hospitals NHS Foundation Trust, Department of Paediatric Immunology, Infectious Diseases & Allergy, Newcastle upon Tyne, United Kingdom*
 - ⁶ *Newcastle University, NIHR Newcastle Biomedical Research Centre, Newcastle upon Tyne, United Kingdom*
 - ⁷ *Erasmus University Medical Center Rotterdam, Department of Public Health, Rotterdam, The Netherlands*
 - ⁸ *Juliana Children's Hospital/Haga Teaching Hospital, Department of Paediatrics, The Hague, The Netherlands*

Differences in IgG Fc Glycosylation are Associated with Outcome of Pediatric Meningococcal Sepsis

Noortje de Haan¹, Navin P. Boeddha^{2,3}, Ebru Ekinci³, Karli R. Reiding¹,
Marieke Emonts^{4,5,6}, Jan A. Hazelzet⁷, Manfred Wuhrer¹
and Gertjan J. Driessen^{3,8}

Reprinted and adapted from mBio 9:3 may/june 2018 DOI:10.1128/mBio.00546-18 [205].
Copyright © 2018, de Haan, Boeddha, Ekinci, Reiding, Emonts, Hazelzet, Wuhrer and Driessen.



Pediatric meningococcal sepsis often results in morbidity and/or death, especially in young children. Our understanding of the reasons why young children are more susceptible to both the meningococcal infection itself and a more fulminant course of the disease is limited. Immunoglobulin G (IgG) is involved in the adaptive immune response against meningococcal infections and its effector functions are highly influenced by the glycan structure attached to the fragment crystallizable (Fc) region.

It was hypothesized that IgG Fc glycosylation might be related to the susceptibility and severity of meningococcal sepsis. Because of this, the differences in IgG Fc glycosylation between 60 pediatric meningococcal sepsis patients admitted to the pediatric intensive care unit and 46 age-matched healthy controls were investigated, employing liquid chromatography with mass spectrometric detection of tryptic IgG glycopeptides. In addition, Fc glycosylation profiles were compared between patients with a severe outcome (death or the need for amputation) and a non-severe outcome.

Meningococcal sepsis patients under the age of 4 years showed lower IgG1 fucosylation and higher IgG1 bisection as compared to age-matched healthy controls. This might be a direct effect of the disease, however, it can also be a reflection of previous immunological challenges and/or a higher susceptibility of these children to develop meningococcal sepsis. Within the young patient group, levels of IgG1 hybrid-type glycans and IgG2/3 sialylation per galactose were associated with illness severity and severe outcome. Future studies in larger groups should explore whether IgG Fc glycosylation could be a reliable predictor for meningococcal sepsis outcome.

5.1 Introduction

Meningococcal infections continue to cause significant mortality and morbidity, despite important reductions in the number of cases as a result of vaccination programs [206, 207]. Several factors associated with susceptibility and/or severity have been identified, e.g. living in crowded conditions, passive smoking and antecedent viral infections [208, 209]. In addition, younger age (<4 years) is an important risk factor for both disease susceptibility and severity, presumably due to an immature immune system [206, 210, 211]. However, the exact mechanism causing young children to be more vulnerable and the factors determining the course of disease are largely unknown [210]. Besides identifying risk factors for the susceptibility of children to be admitted to the pediatric intensive care unit (PICU) with meningococcal sepsis, there is a great interest in identifying prognostic markers to predict the course of the disease and severe outcomes (e.g. death or the need for amputation). These markers would help to decide on appropriate treatment strategies for the individual patients [212]. Several laboratory markers have proven to be of predictive value for the course of meningococcal sepsis, including levels of procalcitonin, C-reactive protein (CRP), leukocytes, thrombocytes, plasminogen activator inhibitor 1 (PAI-1), fibrinogen and various cytokines [213-215]. In addition to the individual markers, predictive scores were developed and validated for the course of meningococcal sepsis, among which the pediatric risk of mortality (PRISM) score [216], the Rotterdam score [214] and the base rate and platelet count (BEP) score [217], all reported to have a good predictive performance for meningococcal sepsis mortality with an AUC between 0.80 and 0.96 [217].

Immunoglobulin G (IgG) plays an essential role in humoral immune responses and is highly involved in the adaptive immune response against meningococcal infections [218, 219]. IgG specific for meningococcal serogroup B is able to initiate complement-dependent lysis of the bacterium and leukocyte-mediated phagocytosis [220, 221]. Both the complement- and the leukocyte-mediated effector functions are mainly induced by IgG1 and IgG3 while the other two IgG subclasses show less activity (IgG2) or no activity at all (IgG4) [219]. It was suggested that the severity of the disease in young children in particular is not determined by the abundance of (certain subclasses of) antimeningococcal-IgG, but rather by either the specificity or affinity of the IgG molecule for the antigen or the IgG receptors [218].

Of great influence on the receptor affinity of IgG is the *N*-glycan on its fragment crystallizable (Fc) at Asn297 [49, 195]. The Fc portion of the IgG molecule is *N*-glycosylated in the endoplasmic reticulum (ER) and Golgi apparatus of B lymphocytes, a process which is under the regulation of both genetic factors and environmental B cell stimuli [74, 78, 196]. Functional studies have shown the effect of alterations in IgG Fc glycosylation on the binding affinity to both Fcγ receptors (FcγR) and complement factor C1q [37]. For

example, increased IgG1 Fc galactosylation showed increased C1q binding and complement-dependent cytotoxicity (CDC) [37, 56]. Of note, afucosylation of IgG1 Fc glycans resulted in substantially increased binding of the antibody to FcγRIIIa and FcγRIIIb, which resulted in increased antibody-dependent cellular cytotoxicity (ADCC) [37, 49].

In addition to the influence of IgG Fc glycosylation on receptor interaction, changes in the glycosylation are also associated with various inflammatory diseases, like active tuberculosis infections [101], HIV [98], alloimmune cytopenias [99, 100], and autoimmune diseases like rheumatoid arthritis [92] and inflammatory bowel disease [95, 222]. Because of the large influence of IgG glycosylation on the antibody function and its association with inflammatory processes, we hypothesize that the fast development of meningococcal sepsis could be associated with Fc glycosylation profiles in the total plasma IgG pool. The aim of this study was to identify differences in IgG Fc glycosylation between pediatric meningococcal sepsis patients and age-matched healthy controls. In addition, we evaluated the potential of specific glycosylation features to serve as a predictive marker for disease outcome.

5.2 Results

IgG Fc glycosylation was analyzed in a subclass-specific way for 60 pediatric patients with a meningococcal infection admitted to the PICU, as well as for 46 age and sex matched healthy controls (**Table 5.1** and **Table S1** in Supplementary Material). For all samples 22 IgG1 Fc glycoforms were quantified, for 57 cases and 34 controls 15 IgG2/3 glycoforms were quantified and for 48 cases and 29 controls 10 IgG4 glycoforms were quantified (**Figure 5.1** and **Table S1** and **S2** in Supplementary Material). From these directly measured glycan traits, derived traits were calculated per IgG subclass. This was done based on glycan type (complex or hybrid-type), bisection, fucosylation, galactosylation and sialylation (**Table 5.2** and **Table S2** in Supplementary Material). The samples of the healthy controls, remeasured in the current study, were a subset of a larger cohort previously analyzed using a different technique, based on the matrix assisted laser/desorption ionization time-of-flight mass spectrometric (MALDI-TOF-MS) detection of derivatized glycopeptides [176]. The healthy controls featured a lower IgG1 fucosylation and IgG1 and IgG2/3 sialylation with higher age as already previously reported for this control cohort (**Figure S1** and **Table S3** in Supplementary Material). In addition, we detected a lower relative abundance of IgG1 and IgG2/3 hybrid-type glycans with higher age in the healthy controls, as well as a higher abundance of bisected glycans on IgG2/3 with higher age, both not previously described for healthy children in this age category (**Figure S1** in Supplementary Material)[84, 176].

Table 5.1 Baseline characteristics of children admitted to PICU with meningococcal sepsis and of their age-matched healthy controls. Median and interquartile ranges are presented unless indicated differently. PRISM: Pediatric risk of mortality [216]; *P* (death Rotterdam): Predicted death rate (%) based on the Rotterdam score [214]; DIC: Disseminated intravascular coagulation [223], PAI-1: Plasminogen activator inhibitor-1; TNF α : Tumor necrosis factor. The number of samples for which specific clinical data was available can be found in **Table S1** in Supplementary Material.

	Patients (n=60)	Patients <4 years (n=37)	Patients \geq4 years (n=22)
Age (years)	2.5 [1.5-8.8]	1.8 [1.2-2.4]	10.1 [6.7-12.3]
Sex (male n, %)	35 (59%)	23 (62%)	12 (55%)
Illness severity			
PRISM score	20 [12-25]	21 [14-25]	19 [9-27]
<i>P</i> (death Rotterdam)	11 [1-82]	32 [2-89]	5 [1-14]
DIC score	5 [4-6]	5 [4-7]	5 [4-7]
Coagulation markers			
Thrombocytes (x10 ⁶ /L)	97 [54-150]	92 [49-166]	109 [82-138]
Fibrinogen (g/L)	2.3 [0.9-3.2]	2.3 [0.9-4.0]	2.2 [1.1-2.9]
PAI-1 (μ g/mL)	4.8 [2.7-6.9]	5.4 [3.6-10.7]	4.3 [1.5-6.0]
Inflammatory markers			
Leukocytes (x10 ⁹ /L)	7.8 [4.0-15.3]	7.1 [3.4-14.3]	11.0 [5.5-17.2]
C-reactive protein (mg/L)	74 [44-119]	60 [39-115]	91 [69-128]
Procalcitonin (ng/mL)	281 [83-482]	361 [145-498]	243 [20-468]
TNF α (pg/mL)	8.4 [5.0-19.8]	12.0 [5.3-23.0]	5.0 [5.0-17.5]
Interleukin-6 (ng/mL)	72 [18-383]	176 [42-723]	38 [1-258]
Interleukin-8 (ng/mL)	20 [4-119]	33 [5-219]	9 [1-58]
Outcome			
Mortality (n, %)	12 (20%)	10 (27%)	2 (9%)
Amputation (n, %)	7 (12%)	2 (5%)	5 (23%)
Severe outcome (n, %)	19 (32%)	12 (32%)	7 (32%)
	Controls (n=46)	Controls <4 years (n=24)	Controls \geq4 years (n=22)
Age (years)	3.9 [1.4-10.0]	1.5 [0.8-2.8]	10.0 [6.7-11.6]
Sex (male n, %)	28 (61%)	15 (63%)	13 (59%)

5.2.1 IgG Fc glycosylation differences between patients with meningococcal sepsis and healthy controls

Comparing the derived glycosylation traits for all IgG subclasses between the meningococcal patients and the healthy controls (**Table S4** in Supplementary Material) revealed a lower IgG1 fucosylation in the children with a meningococcal infection (median

cases: 96.1%, controls: 97.8%; **Figure 5.2A**). When comparing children in the younger age category (< 4 years old) separately from the older children (≥ 4 years old) this effect appeared to be strongly present in the younger children (cases: 96.1%, controls: 98.1%; **Figure 5.2B**, **Table 5.3**), while for the older children the difference in IgG1 fucosylation was only detected as trend (**Figure 5.2C**). Also IgG1 bisection showed to associate with disease in children below 4, being higher in meningococcal patients (11.0%) compared to healthy controls (8.4%; **Figure 5.2E**, **Table 5.3**). In the older age group, a corresponding trend was observed (**Figure 5.2D** and **F**).

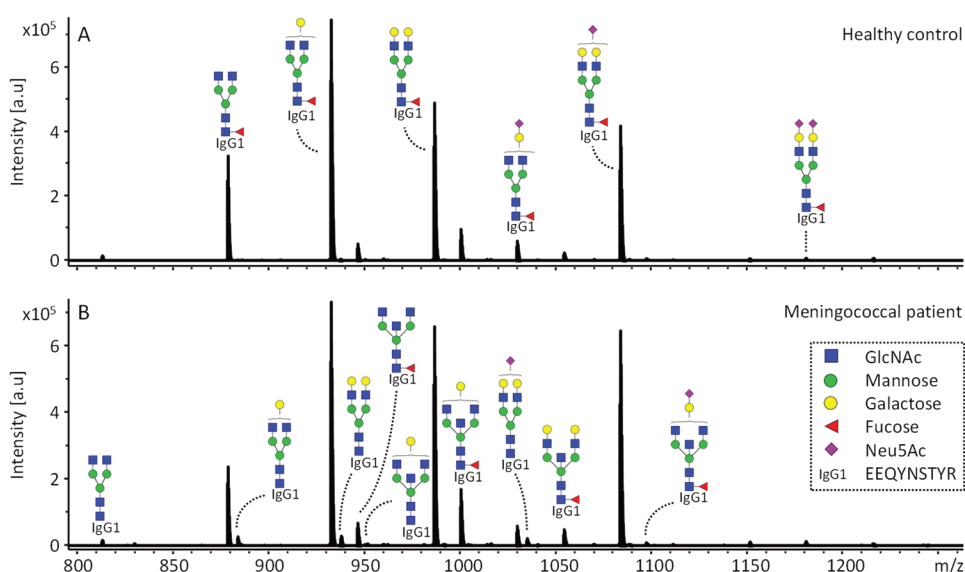

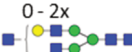
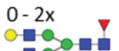


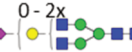


Figure 5.1 IgG1 glycoforms detected in healthy controls and meningococcal patients. Representative mass spectra of a (A) healthy 2.8 year old boy and a (B) 2.8 year old male meningococcal patient. Annotated are the 15 overall most abundant IgG1 glycoforms, the glycoforms that were found to be higher in the meningococcal patients as compared to healthy controls (diantennary glycans without fucose or with a bisecting GlcNAc) are indicated in the spectrum of the patient (B). The proposed glycan structures are based on fragmentation and literature [74, 176]. Green circle: mannose, yellow circle: galactose, blue square: *N*-acetylglucosamine (GlcNAc), red triangle: fucose, pink diamond: *N*-acetylneuraminic acid (Neu5Ac).

Table 5.2 Derived glycosylation traits. The individual glycoforms were grouped based on their glycosylation features as described before for IgG glycopeptides [176]. Green circle: mannose, yellow circle: galactose, blue square: *N*-acetylglucosamine, red triangle: fucose, pink diamond: *N*-acetylneuraminic acid. The depictions of the derived traits show the minimally required composition to contribute to the given trait. For detailed calculations of the traits, see **Table S2** in the Supplementary Material.

Derived trait	Depiction	Description
Hybrid-type		Fraction of hybrid-type glycans
Bisection		Fraction of glycans with a bisecting <i>N</i> -acetylglucosamine
Fucosylation		Fraction of glycans with a core fucose
Galactosylation		Galactosylation per antenna of diantennary glycans
Sialylation		Sialylation per antenna of diantennary glycans
Sialylation per galactose		Sialylation per galactose of diantennary glycans

5.2.2 IgG Fc glycosylation associates with patient outcome in children below 4 years old

IgG Fc glycosylation differences between cases and controls were most pronounced in the young children (below the age of 4 years), a group known to behave clinically different from older meningococcal infected patients [210, 224]. The glycosylation differences between patients with severe disease outcome (death or amputation) and non-severe disease outcome (full recovery) were only compared within this group (**Table 5.3**), as our cohort contained high data density in this age category (**Figure S2** in Supplementary Material). The abundance of hybrid-type structures on IgG1 was found to be overall low (below 1%), however it appeared to be even lower in patients with a severe disease outcome (0.37%) as compared to the patients that fully recovered (0.50%; **Figure 5.3A**). A similar observation was done for the hybrid-type structures on IgG2/3 (**Figure 5.3B**), of which the levels correlated significantly with the levels of IgG1 hybrid-type glycans (**Figure S3** in Supplementary Material). In addition, IgG2/3 sialylation per galactose was lower in patients with a severe disease outcome (19.3%) as compared to the patients with non-severe outcome (21.9%; **Figure 5.3D**). A similar trend was also observed for sialylation per galactose on the other IgG subclasses (**Figure 5.3C and E**), which correlated positively with the levels on IgG2/3 (**Figure S3** in Supplementary Material). The IgG1 hybrid-type glycans,

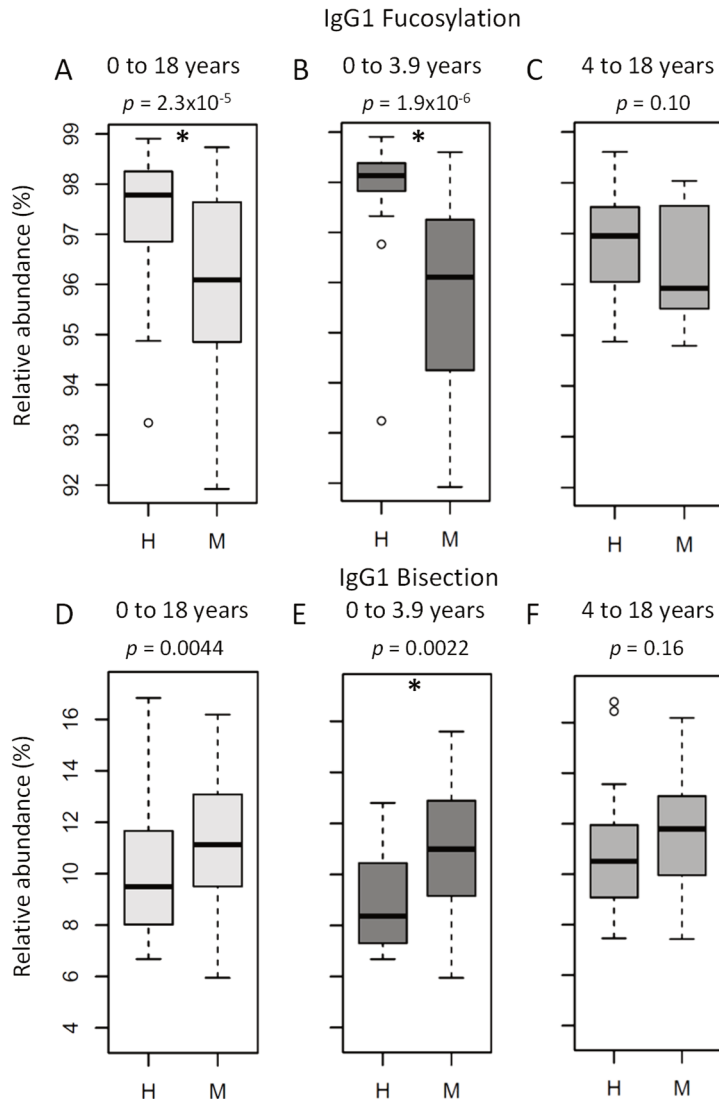


Figure 5.2 IgG1 Fc fucosylation and bisection are different between meningococcal patients (M) and healthy controls (H) below the age of 4. IgG1 Fc fucosylation in meningococcal patients between 0 and 18 (A), 0 and 3.9 (B) and 4 and 18 (C) years old compared to age-matched healthy controls and IgG1 Fc bisection in meningococcal patients between 0 and 18 (D), 0 and 3.9 (E) and 4 and 18 (F) years old compared to age-matched healthy controls. Shown are box and whisker plots, where the boxes represent the inter quartile range (IQR) and the whiskers 1.5xIQR. After multiple testing correction, p -values below 2.7×10^{-3} were considered statistical significant (indicated by an asterisk). The number of samples for which subclass-specific glycosylation data was available can be found in **Table S1** in Supplementary Material.

as well as the sialylation per galactose on IgG2/3 associated negatively with the Rotterdam score (IgG1 hybrid-type correlation coefficient (r) = -0.6, IgG2/3 sialylation per galactose r = -0.7; **Figure 5.4** and **Table S5** in Supplementary Material), known to be predictive for patient outcome [214]. Also IgG1 and IgG2/3 sialylation associated negatively with the Rotterdam score (IgG1 r = -0.5, IgG2/3 r = -0.6). In addition, IgG2/3 sialylation and IgG4 sialylation per galactose associated negatively with the other clinically used predictive score, PRISM (r = -0.6 for both; **Figure 5.4**) [216] which correlated positively with the Rotterdam score (**Figure S3** in Supplementary Material). The described associations were less pronounced in the total dataset, and were not present for the older pediatric patients (**Figure S3** in Supplementary Material).

5.2.3 Associations between IgG Fc glycosylation and inflammatory markers

Various inflammatory markers were measured in the patient samples, including levels of thrombocytes, fibrinogen, PAI-1, CRP, leukocytes, procalcitonin, TNF α and IL-6 and -8. Thrombocyte levels associated positively with IgG1 and IgG2/3 hybrid-type glycans in the young children (r = 0.6 for the hybrid-type glycans on both subclasses; **Figure 5.4** and **Table S5** in Supplementary Material). The same effect was seen for IgG1 hybrid-type glycans and fibrinogen levels (r = 0.6). In addition, IgG2/3 sialylation per galactose correlated positively with fibrinogen and thrombocyte levels (r = 0.6 and 0.7, respectively). Furthermore, IgG2/3 sialylation associated negatively with PAI-1 levels (r = -0.7) and IgG1 fucosylation associated negatively with IL-6 (r = -0.7). In the older pediatric meningococcal patients, leukocyte levels were positively associated with IgG1 and IgG2/3 hybrid-type structures (r = 0.6 for both subclasses) and patients with lower CRP levels had lower levels of IgG2/3 hybrid-type structures (r : 0.7; **Figure S3** and **Table S5** in Supplementary Material).

5.3 Discussion

5.3.1 IgG Fc glycosylation in patients with meningococcal sepsis

Pediatric meningococcal infections resulting in septic shock often occur in young and previously healthy children [206]. The reason why young children are more susceptible to this severe infection and the factors that determine the outcome of disease are largely unknown [210]. In this study, we analyzed the IgG Fc glycosylation of children admitted to the PICU with meningococcal sepsis. Changes in IgG Fc glycosylation are known to have a large influence on the effector function of the antibody and are associated with various inflammatory conditions [37, 49, 56, 92, 101].

Table 5.3 Glycosylation differences between pediatric meningococcal patients (0 to 4 years of age) and age and sex matched healthy controls and between meningococcal patients with a severe and a non-severe disease outcome. Mann Whitney U tests were performed to compare the groups. After multiple testing correction, *p*-values below 2.7×10^{-3} were considered statistically significant (indicated in bold). For detailed calculations of the traits, see **Table S2** in Supplementary Material. The number of samples for which subclass-specific glycosylation data was available can be found in **Table S1** in Supplementary Material.

	Cases and controls <4 years				Meningococcal patients <4 years		
	Healthy	Patients			Non severe	Severe	
Derived trait	Median % (IQR)	Median % (IQR)	<i>p</i> -value		Median % (IQR)	Median % (IQR)	<i>p</i> -value
IgG1 Hybrid-type	0.45 (0.43-0.52)	0.45 (0.41-0.53)	8.0E-01		0.50 (0.44-0.54)	0.37 (0.35-0.43)	2.1E-03
IgG1 Bisection	8.4 (7.4-10.3)	11.0 (9.2-12.9)	2.0E-03		10.0 (9.1-11.8)	13.1 (11.6-14.3)	3.0E-02
IgG1 Fucosylation	98.1 (97.8-98.4)	96.1 (94.2-97.3)	1.9E-06		96.4 (94.6-97.8)	94.5 (93.9-95.8)	2.7E-02
IgG1 Galactosylation	61.9 (56.7-63.6)	61.6 (58.4-63.3)	8.2E-01		62.2 (59.1-63.4)	59.7 (56.9-62.1)	2.1E-01
IgG1 Sialylation	11.3 (10.1-12.8)	10.6 (9.7-11.9)	1.5E-01		11.2 (10.3-11.9)	9.6 (9.2-10.4)	1.8E-02
IgG1 Sialylation per galactose	18.4 (17.7-19.7)	17.8 (16.9-18.7)	3.7E-02		18.2 (17.5-19)	17.2 (15.9-17.6)	1.6E-02
IgG2/3 Hybrid-type	0.43 (0.40-0.54)	0.39 (0.30-0.49)	9.5E-02		0.43 (0.39-0.51)	0.30 (0.25-0.35)	4.8E-03
IgG2/3 Bisection	7.4 (6.3-8.1)	9.7 (8.8-11.2)	4.0E-03		9.2 (8.5-10)	11.1 (9.2-11.6)	1.2E-01
IgG2/3 Fucosylation	98.4 (98.3-98.7)	97.7 (97.5-98.1)	5.7E-03		97.8 (97.5-98.4)	97.5 (97.5-98)	4.6E-01
IgG2/3 Galactosylation	54.5 (46.7-58.1)	51.4 (49.2-53.6)	5.1E-01		51.8 (49.3-54.4)	51.3 (49.8-52.6)	6.1E-01
IgG2/3 Sialylation	13.1 (9.3-14.3)	10.6 (9.7-11.7)	2.1E-01		11.0 (10.5-11.9)	9.6 (9.4-10.3)	8.3E-03
IgG2/3 Sialylation per galactose	23.7 (21.4-24.7)	21.1 (19.5-22.6)	1.4E-02		21.9 (20.5-23.1)	19.3 (18.5-20.9)	2.0E-03
IgG4 Bisection	13.2 (10.6-14.5)	15.5 (13.5-16)	1.7E-01		14.2 (12.4-15.8)	15.9 (15.7-16.1)	3.8E-02
IgG4 Galactosylation	51.6 (44.5-54.9)	54.5 (52.5-58.2)	7.0E-02		55.8 (52.4-59.1)	53.7 (52.7-55.4)	4.5E-01
IgG4 Sialylation	14.1 (11.3-14.9)	13.6 (12.4-14.7)	8.5E-01		14.4 (13.4-15.4)	12.5 (12.3-13)	2.3E-02
IgG4 Sialylation per galactose	26.5 (25.2-28.6)	24.9 (23-26.7)	1.5E-01		25.7 (23.6-27.3)	22.9 (22.6-25.1)	2.7E-02

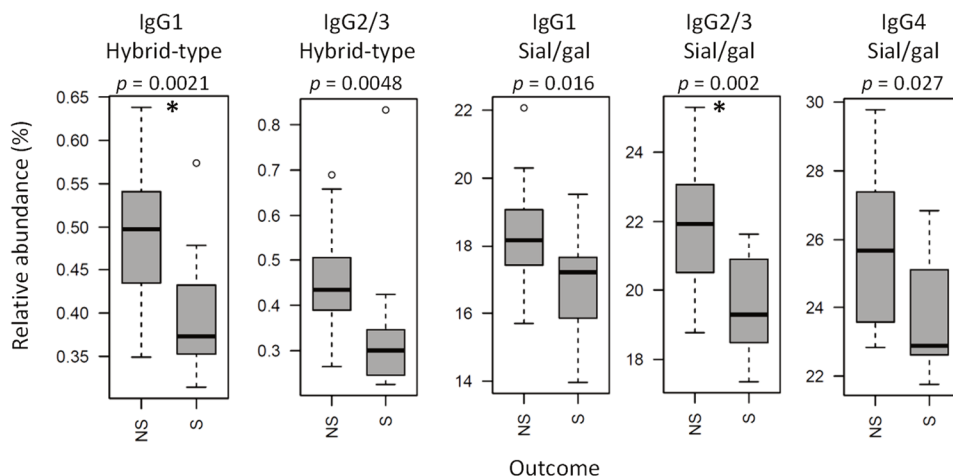


Figure 5.3 Levels of IgG Fc glycosylation features between meningococcal patients below the age of 4 with severe (S) and non-severe (NS) disease outcome. Shown are box and whisker plots of the levels of (A) IgG1 hybrid-type glycans, (B) IgG2/3 hybrid-type glycans, (C) IgG1 sialylation per galactose, (D) IgG2/3 sialylation per galactose, (E) IgG4 sialylation per galactose, where the boxes represent the inter quartile range (IQR) and the whiskers 1.5xIQR. After multiple testing correction, p -values below 2.7×10^{-3} were considered statistically significant (indicated by an asterisk). The number of samples for which subclass-specific glycosylation data was available can be found in **Table S1** in Supplementary Material.

We found IgG1 Fc fucosylation to be lower in patients as compared to age-matched healthy controls. As previous research showed no sex-related IgG glycosylation effects in healthy children between 3 months and 17 years [176], the boys and girls in the current study were not assessed separately. The observed difference between cases and controls was more pronounced in children below the age of 4 years. In addition, in children of this age category, IgG1 Fc bisection was higher in patients as compared to controls. Previous studies reported a different disease course and mortality rate in very young children, showing the relevance of studying this patient group separately from older pediatric meningococcal sepsis patients [206, 210]. Additionally, we found that the cytokine levels in our cohort tended to be higher in younger patients as compared to the older ones. This might be explained by a trend of higher illness severity in young patients and consequently higher cytokine levels. During the maturation of the immune system, when children start to produce their own IgG molecules, the Fc fucosylation is relatively high compared to older children (above the age of 4 years), while the Fc bisection is relatively low [176]. In young children with meningococcal sepsis, a change in the glycosylation of a disease-specific subset of their IgGs might be induced by the meningococcal infection itself in an early stage of the disease. IgG glycosylation is able to change fast as shown in patients experiencing acute systemic inflammation after cardiac surgery, where part of

the patients showed an increased antibody galactosylation the first day after surgery [225]. In addition, studies in mice showed that Fc sialylation could be regulated dynamically, by the interplay of soluble sialyltransferases and the accumulation of platelets providing CMP-sialic acid [200, 201]. The fact that sialyl- and galactosyltransferases are also circulating in the human plasma suggests that glycosylation might be dynamically regulated in humans too [226].

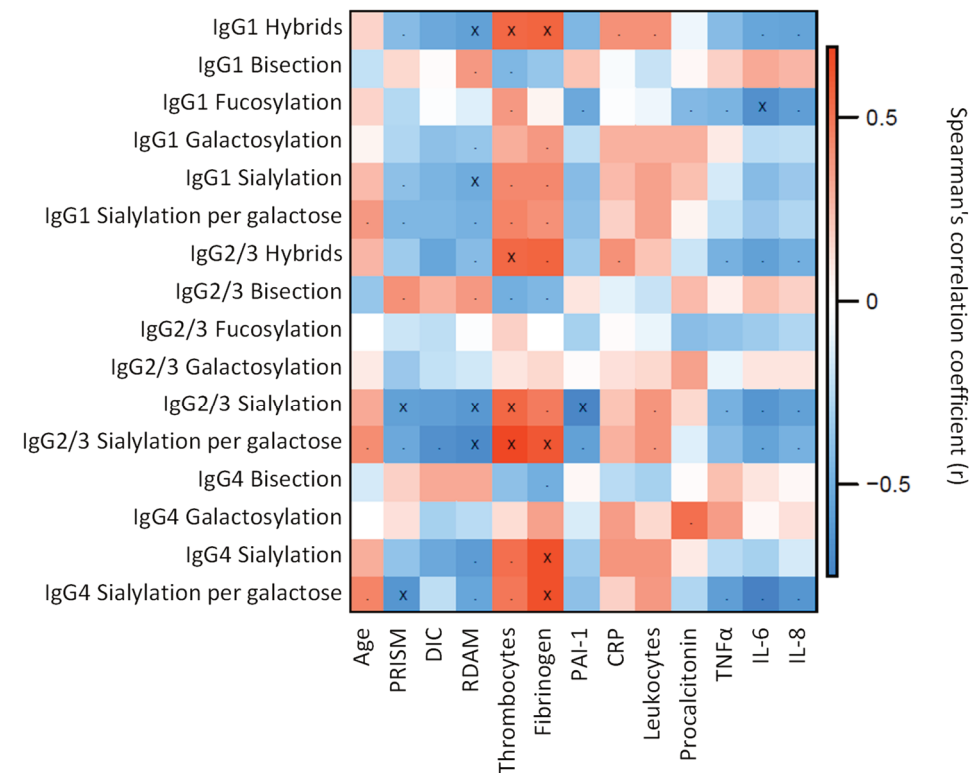


Figure 5.4 Correlation between IgG Fc glycosylation and clinical variables for meningococcal patients between 0 and 3.9 years old. The Spearman correlation coefficient is represented in red for a positive correlation and in blue for a negative correlation between derived glycan trait and the outcome scores and inflammatory markers. Periods (.): $p < 0.05$, crosses (x): $p < 2.7 \times 10^{-3}$ ($\alpha = 2.7 \times 10^{-3}$ adjusted to allow an FDR of 5%).

Alternatively, low Fc fucosylation and high Fc bisection in young patients rather reflect the extent of exposure to previous infections and subsequent adaptive immune responses. Antigen-specific IgG Fc glycosylation was previously shown to differ substantially from the glycosylation of the total pool of IgG. For example gp120-specific IgG in HIV infected patients displays significantly lower Fc fucosylation compared to the total pool of IgG in the infected patients [98]. Furthermore, in alloimmune cytopenias also low levels of Fc fucosylation were observed in anti-HPA-1a and anti-RhD IgGs, as compared to the total IgG pool [99, 100]. Low IgG1 Fc fucosylation (i.e., high afucosylation) enhances binding of IgG to FcγRIIIa and FcγRIIIb 20- to 100-fold [37, 47], thereby increasing antibody-dependent cellular cytotoxicity (ADCC) [37, 49]. The two-fold higher abundance of afucosylated IgGs that we observed for meningococcal sepsis patients might reflect the upregulation of antigen-specific groups of IgG. For IgG specific for meningococcal outer membrane vesicle (OMV) antigens obtained after OMV vaccination, no change in fucosylation was seen over time [227]. However, no comparison was made between total IgG before and after vaccination and glycosylation changes on antigen-specific IgG might be substantially different between vaccinated and naturally infected individuals. We speculate that the low IgG fucosylation observed in young meningococcal patients may reflect a history of exposure to (viral) infections, or in a broader sense antigenic stimuli, resulting in the build-up of low-fucosylation IgG against the respective antigens which manifests itself in a shift of the total IgG pool towards lower fucosylation. Hence, the low fucosylation may be a marker of a history of infections which may *e.g.* reflect a certain proneness to viral or other infectious diseases in these children.

Future studies should elucidate whether skewed IgG Fc glycosylation featuring low fucosylation and high bisection can be identified on meningococcal-specific IgG and whether the deviations from normal are induced by the meningococcal infection or were already present in the children before infection.

5.3.2 IgG Fc glycosylation associates with illness severity

Young patients with severe disease, defined by death or need for amputation, have a lower level of IgG1 hybrid-type glycans and IgG2/3 sialylation per galactose when admitted to the PICU. In addition, these glycosylation features correlate negatively with illness severity, as measured by the Rotterdam score, as well as positively with previously determined predictive factors in meningococcal sepsis, namely levels of thrombocytes and fibrinogen [214], which correlate negatively with severity. Thus, our data suggest that IgG1 hybrid-type glycans and IgG2/3 sialylation per galactose could be a predictor for meningococcal sepsis severity.

Hybrid-type glycans are known to be present on human IgG-Fc in minor amounts, and not much is known about their function [26, 27]. We show here, for the first time, that the

level of hybrid-type glycans on both IgG1 and IgG2/3 correlates negatively with age in healthy children. This is likely connected to maturation of the immune system as hybrid-type glycans are precursors of the usually found complex-type glycans on IgG and might originate from immature B-cells.

In the young patients, IgG2/3 Fc sialylation seems to change independently from the level of Fc galactosylation (serving as a substrate for sialylation), which is likely an effect of the higher availability of sialyltransferase ST6Gal1 or the increased presence of the substrate CMP-sialic acid, either inside the Golgi apparatus or outside the cell [192, 200, 201]. IgG1 Fc sialylation is known to modulate antibody binding to C1q, and subsequent CDC, either positively [37] or negatively [56]. This discrepancy is suggested to be caused by the spatial distribution of the monoclonal antibodies on the cell surface, which depends on the monoclonal antibody studied.

Similar to the glycosylation differences observed between cases and controls, the question is whether the low levels of hybrid-type glycans and sialylation per galactose are emerging during the course of the disease (and are thus meningococcal sepsis specific) or were already present on (a fraction of) the IgG-Fc of patients appearing to have a severe disease outcome. In both situations, the alterations can either be the cause of the severe outcome, or a bystander effect. In either situation IgG Fc glycosylation features have the potential to be used to predict meningococcal sepsis outcome in very young patients, which should be validated in larger study populations.

Interestingly, IgG1 fucosylation associated negatively with IL-6 levels in patients below the age of 4 years, while previous studies in healthy adults showed a positive correlation between IL-6 levels and fucosylation [88]. IL-6 levels have been shown before to be elevated with meningococcal sepsis and to have a potential role in outcome prediction [228]. Furthermore, none of the glycosylation features are associated with levels of CRP in the young patients, while CRP in the healthy adult population does associate with IgG Fc galactosylation (negatively) and Fc fucosylation (positively) [88]. Low CRP levels at the time of admission at the PICU are a known predictor of mortality rate in meningococcal sepsis [214], indicating that the prediction based on CRP is grounded on different mechanisms than the prediction based on glycosylation features. This opens possibilities to combine these factors for an improved prediction tool.

5.3.3 Conclusion

We found IgG1 fucosylation and bisection to be associated with meningococcal sepsis in children below the age of 4 years. Within these young patients we found IgG1 hybrid-type glycans and IgG2/3 sialylation per galactose correlated to the severity of the disease. Further research is needed to determine whether the observed glycosylation differences

between patients and controls are a result of the meningococcal infection itself or rather associated with increased susceptibility to meningococcal septic shock. Furthermore, glycosylation changes associated with illness severity have the potential to be used as outcome predictors, which should be validated in larger study populations.

5.4 Materials and Methods

5.4.1 Patients and controls

In the current retrospective study, plasma or serum samples of prospective cohorts of children with meningococcal sepsis were used. Samples were collected from patients recruited for pediatric meningococcal sepsis studies (1988 to 2005) at the PICU of Erasmus MC-Sophia Children's Hospital (Rotterdam, The Netherlands) [214, 229-231]. These studies were conducted in accordance with the Declaration of Helsinki and Good Clinical Practice guidelines. All individual meningococcal studies as well as the current study were approved by the ethical committee of Erasmus MC (MEC-2015-497), and written informed consent was obtained from parents or legal guardians.

Blood samples from 60 children with meningococcal sepsis were taken within 6 hours after admission to the PICU. All patients fulfilled internationally agreed criteria for sepsis [232]. Most patients already received antibiotics treatment at the moment of sampling and had a central venous catheter *in situ*. In addition, treatment and medication assisting in resuscitation were generally given (such as fluids and inotropes). Samples were processed on ice and were stored at -80 °C until analysis. The samples types comprised a variety of serum, citrate plasma, heparin plasma and EDTA plasma. For several patients, multiple materials taken at the same time point were available.

Plasma samples of 46 healthy controls, selected to be in the same age range as the patients, were collected in accordance with the Declaration of Helsinki and Good Clinical Practice guidelines [176, 188]. The collection of the samples was approved by the ethical committee of Erasmus MC (MEC-2005-137), and written informed consent was obtained from parents or legal guardians.

5.4.2 Clinical data collection

Various clinical data were collected, illness severity was indicated by Pediatric Risk of Mortality (PRISM) [216], predicted death based on the Rotterdam score [214], and the disseminated intravascular coagulation (DIC) score [223]. Coagulation (thrombocytes, fibrinogen and PAI-1) and inflammation (leukocytes, procalcitonin, CRP, tumor necrosis factor (TNF α), interleukins (IL)-6 and -8) markers were measured for clinical reasons or were obtained in previous meningococcal sepsis studies [214, 229, 231]. Patients were

classified to have died if death occurred during PICU-stay. The need for amputation and/or the occurrence of death during the PICU-stay were together classified as a severe disease outcome.

5.4.3 Chemicals

Disodium hydrogen phosphate dihydrate ($\text{Na}_2\text{HPO}_4 \cdot 2\text{H}_2\text{O}$), potassium dihydrogen phosphate (KH_2PO_4), NaCl, and trifluoroacetic acid were purchased from Merck (Darmstadt, Germany). Formic acid, ammonium bicarbonate, and TPCK-treated trypsin from bovine pancreas were obtained from Sigma-Aldrich (Steinheim, Germany). Furthermore, HPLC SupraGradient acetonitrile (ACN) was obtained from Biosolve (Valkenswaard, The Netherlands) and ultra-pure deionized water (MQ) was generated by the Purelab Ultra, maintained at 18.2 M Ω (Veolia Water Technologies Netherlands B.V., Ede, The Netherlands). Phosphate-buffered saline (PBS; pH 7.3) was made in-house, containing 5.7 g/L $\text{Na}_2\text{HPO}_4 \cdot 2\text{H}_2\text{O}$, 0.5 g/L KH_2PO_4 and 8.5 g/L NaCl.

5.4.4 IgG isolation and glycopeptide preparation

The 98 clinical samples and 46 healthy control samples were randomized in a 96-well plate format, together with 32 VisuCon pooled plasma standards (Affinity Biologicals Inc., Ancaster, ON, Canada; eight per plate) and 16 PBS blanks (minimally two per plate). Randomization was performed in a supervised way, selecting an optimal distribution of age, sex and case-control-ratio per plate. IgG was isolated using protein G affinity beads (GE Healthcare, Uppsala, Sweden) as described previously [197]. Briefly, 2 μL of plasma was incubated with 15 μL of beads in 100 μL of PBS for 1 h with agitation. Beads were then washed three times with 200 μL of PBS and three times with 200 μL of MQ, after which the antibodies were eluted with 100 μL 100 mM formic acid. Eluates were dried for 2 h at 60 °C in a vacuum concentrator and dissolved in 40 μL 25 mM ammonium bicarbonate containing 25 ng/ μL trypsin. Samples were shaken for 10 min and incubated at 37 °C for 17 h.

5.4.5 LC-MS analysis of glycopeptides

The IgG digest was separated and analyzed by an Ultimate 3000 high-performance liquid chromatography (HPLC) system (Dionex Corporation, Sunnyvale, CA), coupled to a Maxis Impact HD quadrupole time-of-flight mass spectrometer (q-TOF-MS; Bruker Daltonics) as described before [197] and explained in detail in the Supplementary Materials and Methods (Text S1).

5.4.6 Data processing

The raw LC-MS data was extracted and curated using LacyTools v0.0.7.2 as described previously [197, 198], cohort specific parameters are provided in the Supplementary

Materials and Methods (**Text S1**). Using the described separation methods, glycopeptides with the same peptide portion co-eluted. This resulted in three glycopeptide clusters: one for IgG1, one for IgG4 and one for the combination of IgG2 and 3. As the study population was mainly of the Caucasian ancestry, the tryptic Fc glycopeptides of IgG2 and 3 were assumed to have identical masses, and could therefore not be distinguished by our profiling method. However, it is possible that for part of the samples, the IgG3 glycopeptides are co-analyzed with the ones of IgG4, due to the presence of different IgG3 allotypes [22]. All chromatograms were aligned based on the exact mass and the average retention time of the three most abundant glycoforms of each IgG subclass. After alignment, sum spectra were created per glycopeptide cluster, and then calibrated based on at least five glycopeptides per cluster with a signal-to-noise ratio (S/N) higher than nine. For the targeted extraction, analyte lists were created by manual annotation of summed spectra per biological class (healthy or meningococcal sepsis), covering both doubly charged and triply charged species. Compositional assignments were made on the basis of accurate mass and literature [29, 74]. Glycopeptide signals were integrated by including enough isotopomers to cover at least 95% of the area of the isotopic envelope. Spectra were excluded from further analysis when the total spectrum intensity was below ten times the average spectrum intensity of the blanks. In this way, no spectra were excluded for IgG1, 15 spectra were excluded for IgG2/3 and 29 spectra were excluded for IgG4. Analytes were included in the final data analysis when their average S/N (calculated per biological class) was above nine, their isotopic pattern did not, on average, deviate more than 20% from the theoretical pattern and their average mass error was within ± 10 parts per million (ppm). This resulted in the extraction of 22 IgG1, 15 IgG2/3 and 10 IgG4 glycoforms (**Table S2** in Supplementary Material).

5.4.7 Data analysis

The absolute intensities of the extracted glycoforms were total area normalized per IgG subclass and derived glycan traits were calculated based on specific glycosylation features (**Table 5.2** and **Table S2** in Supplementary Material). Data quality was evaluated based on the 32 pooled plasma standards that were randomly included in the cohort. These resulted in highly repeatable profiles showing a median relative standard deviation of 3.6% for the IgG1 glycopeptides, 2.9% for the IgG2/3 glycopeptides and 2.4% for the IgG4 glycopeptides (**Figure S4** in Supplementary Material). For ten patients, serum, citrate plasma and EDTA plasma of the same time point were available. For these samples, the relative intensities of the individual glycoforms were averaged over the different materials and relative standard deviations were calculated and compared to the standard deviations obtained from the technical replicates. This revealed in general no higher relative standard deviation over the different materials than over the technical replicates (**Figure S4** in Supplementary Material). For patients that had different materials available at the

same time point, the data of the samples were averaged. Statistical analysis was performed using R 3.1.2 (R Foundation for Statistical Computing, Vienna, Austria) and RStudio 0.98.1091 (RStudio, Inc.). First, outliers were removed, which were defined as values outside the 99% confidence interval per biological group (healthy or meningococcal sepsis). Samples were excluded from further statistical analysis when two or more of the derived traits per IgG subclass were marked as outlier. This resulted in the exclusion of one IgG1 and IgG2/3 sample and two IgG4 samples. The derived glycosylation traits per subclass were tested to correlate with age and the continuous clinical variables using Spearman's correlation test. Mann-Whitney U tests were performed to assess glycosylation differences between cases and controls and between patients with a severe and a non-severe disease outcome. All statistical tests were performed both on the whole dataset, and on the subsets of children below the age of 4 and above the age of 4. The tests for disease outcome were exclusively performed on the younger age category (below 4). The significance threshold (α) was adjusted for multiple testing by the Benjamini Hochberg false discovery rate (FDR) method, with an FDR of 5%. This resulted in $\alpha = 0.0027$ throughout the study.

Acknowledgements

The authors would like to thank the Meningococcal Sepsis Research team for the recruitment of the patients. Agnes Hipgrave Ederveen and Carolien Koeleman are acknowledged for their help with running the LC-MS system. This work was supported by the European Union Seventh Framework Programs HighGlycan (278535) and EUCLIDS (279185).

Supporting Information available

Additional information is available as stated in the text. This information is available free of charge via <http://mbio.asm.org/content/9/3/e00546-18.full?sid=0bbb03ae-69be-4a93-8fee-d415309f7cd8>.

- 
- ¹ *University of Zagreb, Faculty of Pharmacy and Biochemistry, Zagreb, Croatia*
 - ² *Leiden University Medical Center, Center for Proteomics and Metabolomics, Leiden, The Netherlands*
 - ³ *Genos Glycoscience Research Laboratory, BIOCentar, Zagreb, Croatia*
 - ⁴ *University of Exeter, Exeter, UK*
 - ⁵ *S. Camillo-Forlanini Hospital, Division of Gastroenterology, Rome, Italy*
 - ⁶ *Casa Sollievo della Sofferenza Hospital, Istituto di Ricovero e Cura a Carattere Scientifico, Division of Gastroenterology, San Giovanni Rotondo, Italy*
 - ⁷ *University Hospital Padua, Division of Gastroenterology, Padua, Italy*
 - ⁸ *Humanitas University, Inflammatory Bowel Disease Center, Department of Gastroenterology, Milan, Italy*
 - ⁹ *Cedars-Sinai Medical Center, F. Widjaja Foundation, Inflammatory Bowel and Immunobiology Research Institute, Los Angeles, California*
 - ¹⁰ *University Hospital Azienda Ospedaliero-Universitaria Careggi, Division of Gastroenterology, Florence, Italy*
 - ¹¹ *Valiant Clinic, Dubai, United Arab Emirates*

Glycosylation of Immunoglobulin G Associates With Clinical Features of Inflammatory Bowel Disease

Mirna Šimurina^{1, #}, Noortje de Haan^{2, #}, Frano Vučković^{3, #},
Nicholas A. Kennedy⁴, Jerko Štambuk³, David Falck², Irena Trbojević-Akmačić³,
Florent Clerc², Genadij Razdorov³, Anna Khon⁵, Anna Latiano⁶,
Renata D’Inca⁷, Silvio Danese⁸, Stephan Targan⁹, Carol Landers⁹,
Marla Dubinsky⁹, The Inflammatory Bowel Disease Biomarkers Consortium,
Dermot P. B. McGovern^{9, §}, Vito Annese^{10,11, §}, Manfred Wuhrer^{2, §}
and Gordan Lauc^{1,3, §}

Authors share co-first authorship; § Authors share co-senior authorship

Reprinted and adapted with permission from Gastroenterology 2018; 154:1320–1333 DOI:

10.1053/j.gastro.2018.01.002 [222]. Copyright © 2018, the AGA Institute.

Background and aims: Causes of inflammatory bowel diseases are not well understood and the most prominent forms, Crohn's disease (CD) and ulcerative colitis (UC), are sometimes hard to distinguish. Glycosylation of IgG has been associated with CD and UC. IgG Fc glycosylation affects IgG effector functions. We evaluated changes in IgG Fc glycosylation associated with UC and CD, as well as with disease characteristics in different patient groups.

Methods: We analyzed 3441 plasma samples obtained from 2 independent cohorts of patients with CD (874 patients from Italy and 391 from the United States (US)) or UC (1056 from Italy and 253 from the US and healthy individuals [controls]; 427 from Italy and 440 from the US). IgG Fc glycosylation (tryptic glycopeptides) was analyzed by liquid chromatography coupled to mass spectrometry. We analyzed associations between disease status (UC vs controls, CD vs controls, and UC vs CD) and glycopeptide traits, and associations between clinical characteristics and glycopeptide traits, using a logistic regression model with age and sex included as covariates.

Results: Patients with CD or UC had lower levels of IgG galactosylation than controls. For example, the odds ratio (OR) for IgG1 galactosylation in patients with CD was 0.59 (95% confidence interval [CI], 0.51-0.69) and for patients with UC was 0.81 (95% CI, 0.71-0.92). Fucosylation of IgG was increased in patients with CD vs controls (for IgG1: OR, 1.27; 95% CI, 1.12-1.44), but decreased in patients with UC vs controls (for IgG23: OR, 0.72; 95% CI, 0.63-0.82). Decreased galactosylation associated with more severe CD or UC, including the need for surgery in patients with UC vs controls (for IgG1: OR, 0.69; 95% CI, 0.54-0.89) and in patients with CD vs controls (for IgG23: OR, 0.78; 95% CI, 0.66-0.91).

Conclusions: In a retrospective analysis of plasma samples from patients with CD or UC, we associated levels of IgG Fc glycosylation with disease (compared to controls) and its clinical features. These findings could increase our understanding of mechanisms of CD and UC pathogenesis and be used to develop diagnostics or guide treatment.

6.1 Introduction

The incidence of inflammatory bowel diseases (IBDs) is increasing [233], and currently affects approximately 1 in 200 people in developed countries [234]. In Europe, IBD has a prevalence of 2.5 to 3 million people [235, 236], with health care costs of €4.6 to 5.2 billion per year [235], while in the United States, the costs for IBD are estimated at US\$11-28 billion per year [237]. The two main types of IBD are Crohn's disease (CD) and ulcerative colitis (UC), which are further subcategorized by the Montreal classification, based on age of onset, disease location, and behavior (CD), and on disease extent and severity (UC) [238].

IBD results from an aberrant host immune response to luminal gut microbiota occurring in genetically susceptible individuals [239]. However, genetic variants associated with IBD explain only 7.5% and 13.6% of UC and CD susceptibility [240], respectively, indicating the importance of studying other factors that contribute to the course of IBD. One of these factors is the regulation of innate and adaptive immunity.

The majority of extracellular and membrane proteins are glycosylated, and glycans are directly involved in the pathophysiology of every major disease [241, 242]. Alternative glycosylation affects the protein structure and its function in a similar manner to mutations in the amino acid sequence [243]. Protein glycosylation has been reported to change significantly in various diseases [96, 103, 244, 245], including cancer [246] and IBD [247-249]. Current strategies for diagnosis, prognosis, and monitoring of IBD are often invasive or lack adequate sensitivity [250, 251], therefore, the measurement of protein glycosylation in serum could be an attractive, minimally invasive biomarker and assist patient stratification for precision medicine.

Recent studies have shown that IgG, which is a key effector of the humoral immune system and has multiple roles in balancing inflammation on the systemic level [252], has altered glycosylation in a number of different diseases [253], including IBD [95, 248, 249]. Additionally, genome-wide association studies of IgG glycosylation have shown pleiotropy with IBD susceptibility loci, suggesting a role for IgG glycosylation in the onset and progression of IBD [240, 254, 255]. However, none of these studies have elucidated the mechanisms behind the observed changes or their clinical relevance.

IgG molecules contain 2 diantennary *N*-glycans covalently attached to conserved *N*-glycosylation sites at Asn-297 on each of its heavy chains. The most complex Fc glycan, FA2BG2S2, is a diantennary (A2) digalactosylated (G2) and disialylated structure with a bisecting b(1,4) *N*-acetylglucosamine (GlcNAc) (B) and an α (1,6) fucose (F) attached to core GlcNAc (**Figure 6.1**) [105, 177]. Other IgG glycans correspond to this complex structure with the lack of one or more sugar units. Fc glycosylation of IgG is complex and

affected by multiple genetic [255], epigenetic [256], and environmental factors [74], resulting in a glycome composition that is very variable between individuals, but stable within an individual in homeostatic conditions [225]. Age is a notable exception that strongly affects the composition of the IgG glycome of an individual [81]. IgG in mice can have pro- and anti-inflammatory activity, depending on its glycosylation status. Sialylation of murine IgG is associated with anti-inflammatory activity [202], while IgG core fucosylation limits IgG-mediated antibody-dependent cellular cytotoxicity (ADCC) [74, 257] and activates complement [258]. Decreased galactosylation of IgG is reported in inflammatory diseases, suggesting an anti-inflammatory role of the attached galactoses [95]. However, pro-inflammatory effects of IgG galactosylation have also been observed [52, 259], hinting at alternative interpretations. The composition of the *N*-glycan attached to the Fc region of IgG affects binding of IgG to both high- and low-affinity Fc gamma receptors [51, 243]. Although the exact molecular mechanism is still elusive [260], the glycans attached to IgG strongly affect immunosuppressive properties of IgG, as exemplified in therapeutic function of intravenously administered immunoglobulins [261]. Inter-individual variability in IgG glycome composition and its changes in disease thus have profound effects on the immune system.

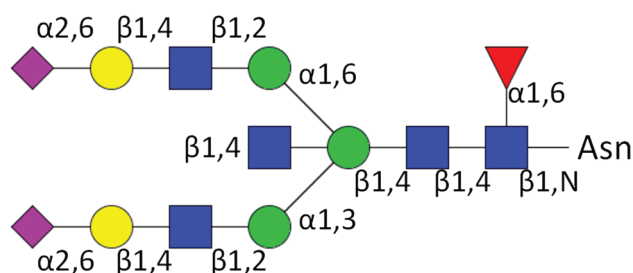


Figure 6.1 The most complex IgG Fc glycan found in our samples: FA2BG2S2. A diantennary (A2) digalactosylated (G2) and disialylated (S2) glycan with a bisecting $\beta(1,4)$ GlcNAc (B) and an $\alpha(1,6)$ fucose (F) attached to core GlcNAc. Linkages and anomeric configurations are shown [105, 177]. Blue square: GlcNAc; red triangle: fucose; green circle: mannose; yellow circle: galactose; pink diamond: *N*-acetylneuraminic acid.

The understanding of functional significance of glycosylation changes in disease are complicated by subclass-specific effects, as demonstrated in different models [36]. Until recently, the IgG glycome in IBD was analyzed on the level of total released glycans [95] by ultraperformance liquid chromatography, which does not discriminate between individual IgG subclasses nor glycan location. Fc and Fab glycosylation of IgG differ significantly and we also demonstrated that disease course can specifically associate with Fc glycosylation

[262]. In this study, we used liquid chromatography coupled to mass spectrometry (LC-MS), that enables high-throughput analysis of IgG Fc glycans in a subclass-specific manner [85, 197] and provides a more detailed insight into IgG glycosylation changes in IBD. By measuring subclass-specific IgG Fc *N*-glycosylation in 3441 IBD patients and controls from two independent cohorts participating in the IBD-BIOM (Inflammatory Bowel Disease Biomarkers) Consortium project, we demonstrated a clear difference in IgG Fc glycosylation between diseased and healthy individuals, but also between the different forms of IBD, and associations with disease severity.

6.2 Materials and Methods

6.2.1 Clinical Samples and Ethical Considerations

Samples were collected from two case-control populations, the Italian cohort (ITA) from Italy ($n = 2357$) and the US cohort from the United States ($n = 1084$), each including CD (ITA: $n = 874$, US: $n = 391$) and UC (ITA: $n = 1056$, US: $n = 253$) patients as well as healthy controls (HC) (ITA: $n = 427$, US: $n = 440$). Both cohorts were collected with the approval of the local ethics committees and informed consent was obtained from all participants. Phenotype was defined using the Montreal classification at the last follow-up [238]. Clinical characteristics were obtained by chart review according to criteria agreed by the clinicians and as described previously [263-265] (**Table 6.1**).

6.2.2 Sample Preparation and Data Preprocessing

Sample preparation and glycopeptide analysis (IgG purification by Protein G affinity chromatography, tryptic digestion, nano-LC-MS analysis, and data preprocessing) were performed separately for the ITA and US cohort [28, 74, 85, 197, 198] (details in the Supplementary Materials and Methods, **Supplementary Table 1**, and **Supplementary Figure 1**). The tryptic Fc glycopeptides for IgG2 and 3 have identical peptide moieties in the Caucasian population and are therefore not distinguishable with our methods [163, 266]. Annotation of the spectra was done based on accurate mass and literature [74, 256]. Using the directly measured glycopeptides, derived glycosylation traits were calculated per IgG subclass (**Supplementary Tables 2 and 3**), which average particular glycosylation features like galactosylation, fucosylation, sialylation, and the presence of a bisecting GlcNAc (bisection).

6.2.3 Statistical Analysis

Data analysis and visualization was performed with R v3.0.1 (R Foundation for Statistical Computing, Vienna, Austria). Association analyses between disease status (UC patients and HC, CD patients and HC and UC and CD patients) and glycopeptide traits as well as

Table 6.1 Demographic Characteristics of American and Italian Inflammatory Bowel Disease Cohorts. E1, proctitis; E2, left-sided UC; E3, extensive UC; IQR, interquartile range. ^a Disease location and behavior are described according to the Montreal classification.

	American cohort			Italian cohort		
	HC ^a	UC	CD	HC	UC	CD
Sample Number	440	253	391	427	1056	874
Age (med/IQR)	46.3 (33.5 - 56.0)	39.4 (29.2 - 54.8)	35.4 (26.0 - 48.4)	44.0 (35.0 – 56.0)	41.0 (31.0 – 52.0)	35.5 (27.0 – 46.0)
Sex (F) (n/%)	254 (57.9%)	129 (51.0%)	169 (43.2%)	145 (34.0%)	423 (40.1%)	368 (42.1%)
Disease Duration (med/IQR) ^b		7.2 (3.3 - 15.4)	8.3 (3.0 - 14.8)		6.0 (2.0 – 13.0)	5.0 (1.0 – 11.0)
Disease Location (CD) (n/%) ^c						
Ileal (L1±L4)	-	-	91 (23.8%)	-	-	327 (38.7%)
Colonic (L2±L4)	-	-	58 (15.2%)	-	-	161 (19.1%)
Ileocolonic (L3±L4)	-	-	233 (61.0%)	-	-	343 (40.6%)
Upper GI (L4 only)	-	-	0 (0%)	-	-	13 (1.5%)
Disease Behaviour (CD) (n/%)						
Inflammatory (B1)	-	-	140 (36.3%)	-	-	504 (58.3%)
Stricturing (B2)	-	-	109 (28.2%)	-	-	237 (27.4%)
Penetrating (B3)	-	-	137 (35.5%)	-	-	124 (14.3%)
Disease Extent (UC) (n/%)						
Proctitis (E1)	-	8 (3.2%)	-	-	115 (11.0%)	-
Left-sided (E2)	-	63 (25.2%)	-	-	489 (47.0%)	-
Extensive (E3)	-	179 (71.6%)	-	-	437 (42.0%)	-
Medication (n/%)						
Mesalazine		-	-		320 (32.5%)	179 (22.7%)
Prednisolone	-	all (100%)	all (100%)	-	360 (36.6%)	229 (29.0%)
Thiopurines (AZA/6MP)	-	84 (36.5%)	71 (18.7%)	-	213 (21.6%)	174 (22.1%)
Anti-TNF	-	146 (63.5%)	309 (81.3%)	-	90 (9.1%)	207 (26.2%)
Surgical resection (n/%)	-	141 (55.7%)	228 (60.6%)	-	81 (8.1%)	327 (37.8%)

within-disease analyses of associations between clinical characteristics and glycopeptide traits were performed using a logistic regression model with age and sex included as additional covariates. For UC, we assessed disease location, duration of the disease, and need for a colectomy. Regarding disease location, we analyzed the differences between Montreal E1 (proctitis) and E2 (left-sided UC) against E3 (extensive UC). For CD, we assessed disease location and behavior, duration of disease, and the need for surgery. For CD behavior, we compared Montreal B2 (stricturing) and B3 (internal penetrating) with B1 (inflammatory disease). For location, we compared Montreal L1 (ileal) against L2 (colonic disease) and L1 against L3 (ileocolonic disease). For both diseases, we used a cutoff of 5 years since diagnosis to stratify disease duration into two groups. In the ITA cohort, for CD as well as for UC, patients treated with the third most potent medication (steroids) were compared to patients treated with mesalazine only and, in addition, patients treated with the first most potent medication (inhibitor of tumor necrosis factor [anti-TNF]) were compared to patients treated with the second most potent medication (azathioprine [AZ] and 6-mercaptopurine [6MP]). These latter tests were also done in the US cohort. Both case-control and within-disease analyses were first performed for each cohort separately and then combined using an inverse variance-weighted meta-analysis approach (R package “metafor” [267]). The false discovery rate was controlled for each analysis using the Benjamini-Hochberg method with false discovery rate set to 0.05. All *P* values were corrected for multiple testing.

For prediction of disease status, a regularized logistic (elastic net) regression model was applied (R package “glmnet” [268]) using direct glycosylation traits as predictors (Supplementary Materials and Methods). Three models were built for each cohort (UC vs HC, CD vs HC, and UC vs CD), using age, sex, and glycopeptide measurements as predictors. To evaluate the performance of the predictive models based on the individual glycoforms, a 10-cross-validation procedure was used. The predictions from each validation round were merged into 1 validation set on which the performance of each model was evaluated based on the area under the curve (AUC) criteria.

6.3 Results

6.3.1 IgG Fc Glycosylation Differences Between Inflammatory Bowel Disease Patients and Healthy Controls

For both CD and UC, we observed an increase in agalactosylated IgG glycopeptides in both cohorts compared to HC and a corresponding decrease of monogalactosylated (not significant for IgG1 in CD patients of the US cohort, but significant in meta-analysis of both cohorts) and digalactosylated IgG glycopeptides (not significant for IgG1 and IgG4 in UC patients of the ITA cohort, but significant in metaanalysis of both cohorts) (**Table 6.2,**

Table 6.2 Associations Between Derived IgG Fc Glycosylation Traits and Inflammatory Bowel Disease in the Italian Cohort. OR, odds ratio. ^a Derived glycosylation traits were calculated as described in **Supplementary Table 3**. ^b To assess differences between HC and UC patients (HC = 0, UC = 1), HC and CD patients (HC = 0, CD = 1), and UC and CD patients (UC = 0, CD = 1), logistic regression was performed using age and sex as co-variables. ^c *P* values are indicated in bold when statistically significant after multiple testing correction (5% false discover rate). Underlined *P* values indicate results that were replicated in the US cohort (**Supplementary Tables 5-7**).

Derived trait ^a	Description	HC vs. UC ^b		HC vs. CD		UC vs. CD	
		OR (95% CI) ^c	<i>p</i> -value ^d	OR (95% CI)	<i>p</i> -value	OR (95% CI)	<i>p</i> -value
IgG1							
IgG1_agal	Fraction of agalactosylatedglycans	1.29 (1.13 - 1.47)	8.9E-05	1.69 (1.46 - 1.96)	2.2E-13	1.23 (1.11 - 1.36)	3.9E-05
IgG1_digal	Fraction of digalactosylatedglycans	0.88 (0.77 - 1.00)	5.7E-02	0.61 (0.52 - 0.70)	2.7E-12	0.71 (0.64 - 0.79)	8.0E-11
IgG1_monogal	Fraction of monogalactosylatedglycans	0.69 (0.61 - 0.79)	5.4E-09	0.69 (0.61 - 0.79)	4.3E-08	1.06 (0.97 - 1.17)	2.0E-01
IgG1_sial	Fraction of sialylatedglycans	1.05 (0.93 - 1.20)	4.1E-01	0.81 (0.70 - 0.92)	1.4E-03	0.78 (0.71 - 0.87)	1.5E-06
IgG1_A2B	Bisection of diantennaryglycans	0.69 (0.61 - 0.78)	3.5E-09	0.91 (0.79 - 1.03)	1.4E-01	1.22 (1.11 - 1.35)	7.8E-05
IgG1_A2F	Fucosylation of diantennaryglycans	0.93 (0.82 - 1.04)	2.1E-01	1.27 (1.12 - 1.44)	2.2E-04	1.36 (1.23 - 1.51)	6.0E-10
IgG1_A2G	Galactosylation per antenna on diantennaryglycans	0.81 (0.71 - 0.92)	1.5E-03	0.59 (0.51 - 0.69)	3.2E-13	0.77 (0.69 - 0.85)	2.5E-07
IgG1_A2S	Sialylation per antenna on diantennaryglycans	1.04 (0.92 - 1.18)	5.1E-01	0.78 (0.68 - 0.90)	3.2E-04	0.77 (0.70 - 0.85)	3.7E-07
IgG1_A2GS	Sialylation per galactose on diantennaryglycans	1.33 (1.18 - 1.51)	3.6E-06	1.15 (1.01 - 1.30)	3.1E-02	0.85 (0.77 - 0.94)	1.1E-03
IgG23							
IgG23_agal	Fraction of agalactosylatedglycans	1.30 (1.14 - 1.50)	1.3E-04	2.76 (2.31 - 3.29)	1.7E-37	2.11 (1.87 - 2.37)	1.2E-40
IgG23_digal	Fraction of digalactosylatedglycans	0.82 (0.71 - 0.94)	3.7E-03	0.41 (0.35 - 0.48)	2.2E-31	0.49 (0.43 - 0.55)	1.0E-36
IgG23_monogal	Fraction of monogalactosylatedglycans	0.77 (0.67 - 0.87)	4.1E-05	0.39 (0.32 - 0.46)	8.5E-34	0.54 (0.48 - 0.60)	8.2E-32
IgG23_sial	Fraction of sialylatedglycans	0.87 (0.76 - 0.99)	2.9E-02	0.53 (0.46 - 0.61)	6.8E-20	0.58 (0.52 - 0.64)	1.0E-24
IgG23_A2B	Bisection of diantennaryglycans	0.62 (0.55 - 0.71)	3.2E-13	0.91 (0.80 - 1.05)	1.9E-01	1.34 (1.21 - 1.48)	8.2E-09
IgG23_A2F	Fucosylation of diantennaryglycans	0.72 (0.63 - 0.82)	3.2E-07	1.12 (0.99 - 1.27)	7.5E-02	1.57 (1.41 - 1.74)	1.6E-18
IgG23_A2G	Galactosylation per antenna on diantennaryglycans	0.79 (0.68 - 0.90)	5.3E-04	0.38 (0.32 - 0.45)	1.9E-35	0.47 (0.42 - 0.53)	4.1E-40
IgG23_A2S	Sialylation per antenna on diantennaryglycans	0.86 (0.76 - 0.98)	2.3E-02	0.52 (0.45 - 0.60)	5.7E-21	0.57 (0.51 - 0.64)	2.4E-25
IgG23_A2GS	Sialylation per galactose on diantennaryglycans	1.02 (0.90 - 1.14)	8.0E-01	1.19 (1.05 - 1.35)	7.6E-03	1.11 (1.01 - 1.22)	2.9E-02
IgG4							
IgG4_agal	Fraction of agalactosylatedglycans	1.30 (1.13 - 1.48)	1.2E-04	2.16 (1.84 - 2.54)	2.3E-24	1.62 (1.46 - 1.80)	3.7E-20
IgG4_digal	Fraction of digalactosylatedglycans	0.89 (0.78 - 1.01)	7.9E-02	0.53 (0.46 - 0.61)	2.8E-18	0.60 (0.53 - 0.67)	1.4E-21
IgG4_monogal	Fraction of monogalactosylatedglycans	0.69 (0.60 - 0.79)	2.0E-08	0.45 (0.38 - 0.53)	7.9E-26	0.68 (0.62 - 0.76)	6.9E-14
IgG4_sial	Fraction of sialylatedglycans	1.01 (0.89 - 1.14)	9.2E-01	0.68 (0.59 - 0.78)	2.2E-08	0.66 (0.60 - 0.74)	3.0E-15
IgG4_A2FB	Bisection of diantennaryglycans	0.79 (0.70 - 0.90)	3.5E-04	0.84 (0.73 - 0.96)	1.1E-02	0.97 (0.88 - 1.08)	5.9E-01
IgG4_A2FG	Galactosylation per antenna on diantennaryglycans	0.81 (0.71 - 0.92)	1.5E-03	0.48 (0.41 - 0.57)	2.2E-22	0.61 (0.55 - 0.68)	5.4E-21
IgG4_A2FS	Sialylation per antenna on diantennaryglycans	1.03 (0.90 - 1.17)	6.8E-01	0.70 (0.61 - 0.80)	1.3E-07	0.67 (0.60 - 0.74)	8.5E-15
IgG4_A2FGS	Sialylation per galactose on diantennaryglycans	1.38 (1.21 - 1.57)	8.5E-07	1.39 (1.22 - 1.60)	7.2E-07	1.00 (0.90 - 1.10)	9.3E-01

Supplementary Tables 5-7, Figure 6.2). In both cohorts, all IgG subclasses showed lower overall galactosylation (A2G) for CD patients compared to UC patients. A decrease in sialylation was also associated with CD in both the US and the ITA cohort, but for UC this effect was only seen in the US cohort. Sialylation per galactose of diantennary glycans (A2GS) increased with disease, or did not change at all. We observed a subclass and disease-specific association for fucosylated IgG glycopeptides (A2F). Increased A2F was associated with CD in the US cohort for both IgG1 and IgG23 and for IgG1 in ITA cohort. Conversely, there was a negative association between IgG23 A2F and UC in both cohorts. Furthermore, both cohorts showed IgG1 and IgG23 A2F to be high in CD patients compared to UC patients. IgG4 bisection (structures with bisecting $\beta(1,4)$ *N*-acetylglucosamine on IgG4) was low for CD and UC compared to HC in both cohorts. A decrease in bisection (A2B) was also observed for the other IgG subclasses in UC patients of the ITA cohort, on the other hand, IgG1 and IgG23 A2B was increased for CD compared to HC in the US cohort. For both cohorts IgG1 and IgG23 A2B was higher in CD compared to UC. Results for the individual IgG glycoforms are shown in **Supplementary Tables 8-11**, and **Supplementary Figure 2**.

6.3.2 Discrimination of Disease Status

The discriminatory performance of individual glycoforms per IgG subclass in distinguishing UC from HC, CD from HC, and UC from CD, was evaluated for ITA and US cohorts separately, using a regularized logistic regression model. The receiver operating characteristic curves for the ITA cohort showed a good performance in discriminating UC from HC (AUC = 0.801; **Figure 6.3A**) and CD from HC (AUC = 0.854; **Figure 6.3B**), and fair performance in discriminating UC from CD (AUC = 0.770; **Figure 6.3C**). This was replicated in the US cohort, showing a good performance in discriminating UC from HC (AUC = 0.814; **Figure 6.3D**) and CD from HC (AUC = 0.849; **Figure 6.3E**), and fair performance in discriminating UC from CD (AUC = 0.746; **Figure 6.3F**). To assess which glycoforms were most important in these models, individual receiver operating characteristic analyses were performed per glycoform per IgG subclass, revealing for example G1 on IgG23 to be in the top 5 of most important glycoforms discriminating UC from HC in both cohorts (**Supplementary Figures 3A and 4A**). In addition, IgG23 and IgG4 G0F were in the top 5 between CD and HC in both cohorts (**Supplementary Figures 5A and 6A**) and IgG23 G0F, G0FN, G2, and G2F were found in both cohorts to be in the top 5 most discriminating glycans between UC and CD (**Supplementary Figures 7A and 8A**). These findings were also reflected in the predictive values of the individual-derived traits (**Supplementary Figures 3-8**, panels B).

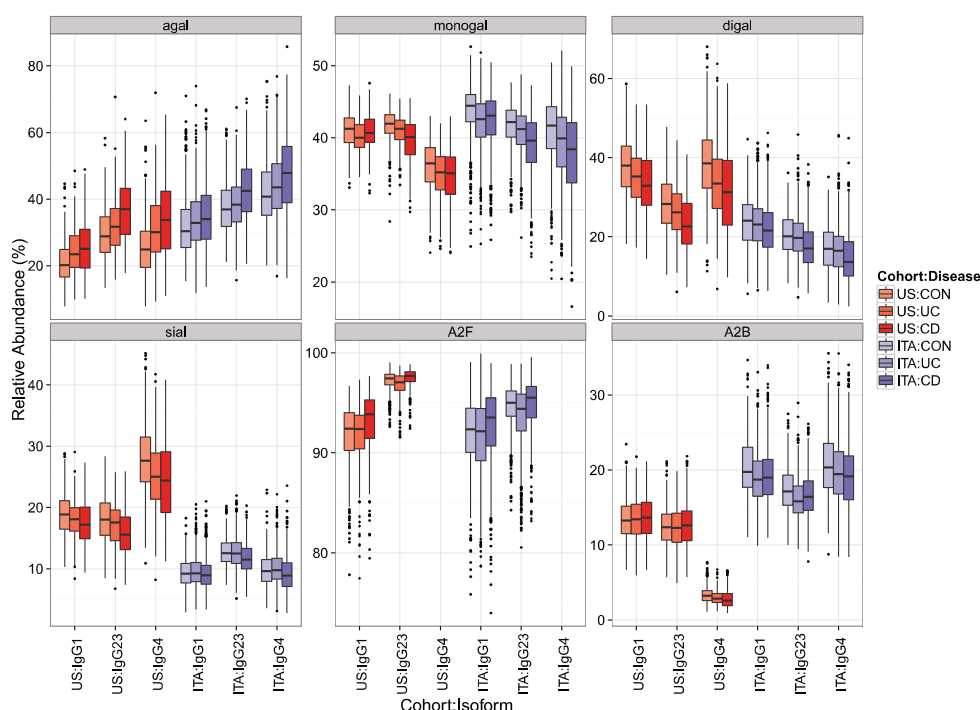


Figure 6.2 Differences in derived IgG Fc glycan traits between HC, UC, and CD for all IgG subclasses in both cohorts. Differences in derived glycan traits for all IgG subclasses between HC, UC, and CD are shown separately for the US (red) and ITA (blue) cohort. Data are shown as box and whiskers plots. Each box represents the 25th to 75th percentiles (interquartile range [IQR]). Lines inside the boxes represent the median. The whiskers represent the lowest and highest values within the boxes $\pm 1.5 \times$ the IQR. Derived glycan traits are listed in **Supplementary Table 2** and **3** and their glycoforms in **Supplementary Table 8**. Analysis of the differences in glycan traits between UC and HC, CD and HC, and UC and CD, were performed using a logistic regression model with age and sex included as additional covariates (**Table 6.2**, **Supplementary Tables 5-7**).

6.3.3 Disease Behavior, Location, and Classification

In the ITA cohort (and the meta-analysis of both cohorts) an increase in agalactosylated IgG glycopeptides and a decrease in digalactosylated IgG glycopeptides were associated with extensive UC and the need for surgery in UC. In addition, the need for surgery was associated with less sialylated glycans on all IgG subclasses. In both cohorts, agalactosylated IgG1 glycopeptides decreased and monogalactosylated IgG1 glycopeptides increased with the duration of UC (**Supplementary Table 12** and **Figure 6.4**). In addition, for surgery in CD patients, the IgG23 agalactosylation increased in both cohorts, while IgG23 digalactosylation was decreased. Furthermore, IgG23 sialylation decreased in the ITA cohort (and the meta-analysis of both cohorts). Also a worse disease behavior

(Montreal B2 + B3 vs B1) was associated with increased IgG23 agalactosylation and decreased IgG23 digalactosylation and sialylation in the ITA cohort (and the meta-analysis of both cohorts), while a more extensive CD (ileal [L1] vs ileocolonic [L3]) was associated with increased IgG1 agalactosylation in the US cohort (and the meta-analysis of both cohorts; **Supplementary Tables 13** and **Figure 6.5**). Results for the individual IgG glycoforms are shown in **Supplementary Tables 14** and **15**.

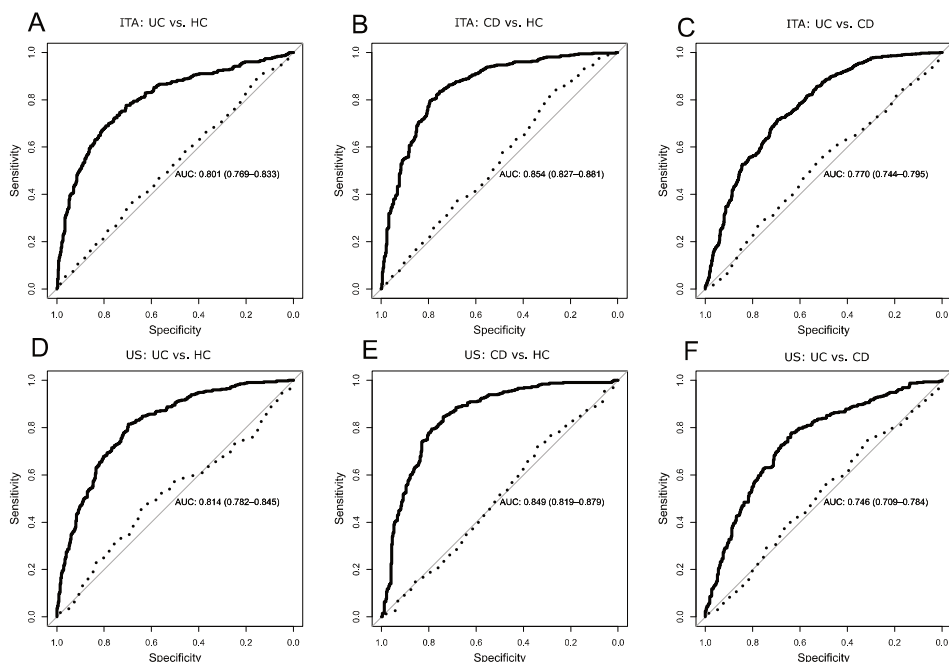


Figure 6.3 Receiver operating characteristic curves illustrating the discriminative power of individual glycoforms per IgG subclass. Prediction of disease status was performed using a logistic (elastic net) regression model for the ITA cohort between UC and HC (**A**), CD and HC (**B**), UC and CD (**C**), and for the US cohort between UC and HC (**D**), CD and HC (**E**), and UC and CD (**F**). While models based only on age and sex did not show predictive power (dotted line), addition of individual glycoforms increased the predictive power of the models (solid line).

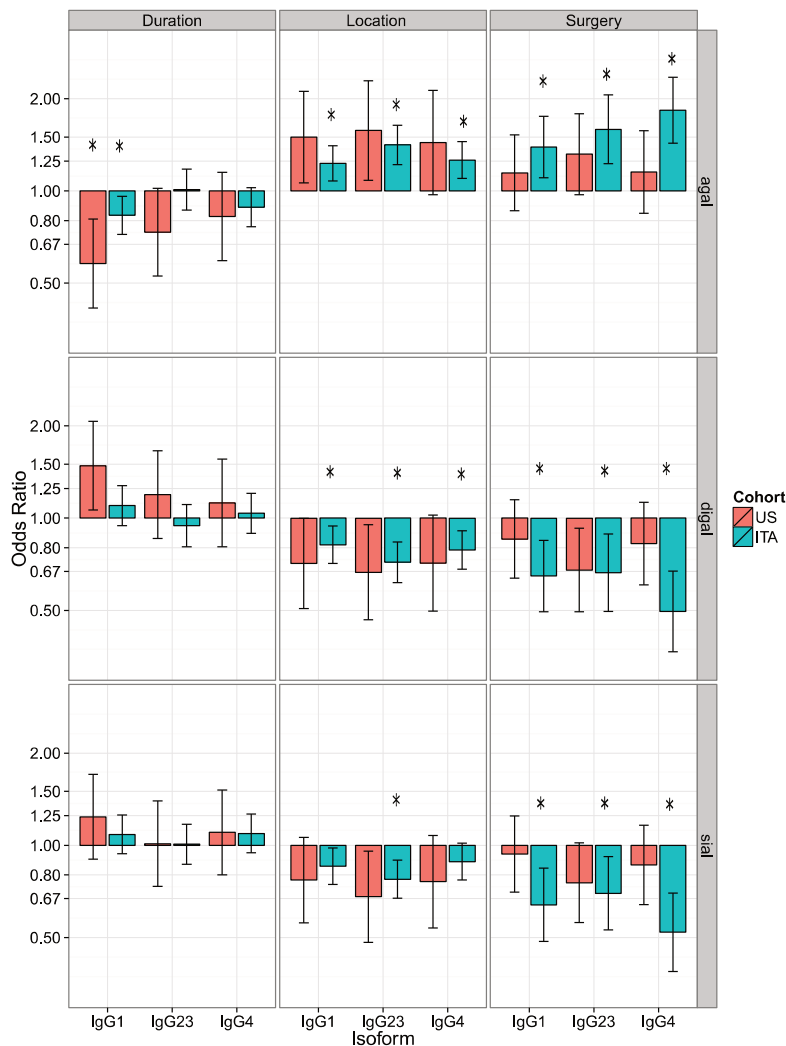


Figure 6.4 Associations between derived IgG Fc glycan traits and clinical characteristics in UC (duration, location, and surgery). Odds ratios for the associations between derived glycan traits and clinical traits in UC (duration of disease: <5 years = 0, >5 years = 1, disease location: E1 (proctitis) + E2 (left-sided UC) = 0, E3 (extensive UC) = 1, and surgery: no = 0, yes = 1) for all IgG subclasses are shown for the ITA cohort (green) and the US cohort (red). Bars indicate odds ratios. Derived glycan traits are explained in **Supplementary Tables 2 and 3** and their glycoforms in **Supplementary Table 8**. Analysis of the association between derived glycan traits and clinical characteristics in UC were performed using a logistic regression model, with age and sex included as additional covariates, statistically significant findings are indicated with an asterisk (*) (**Supplementary Table 12**).

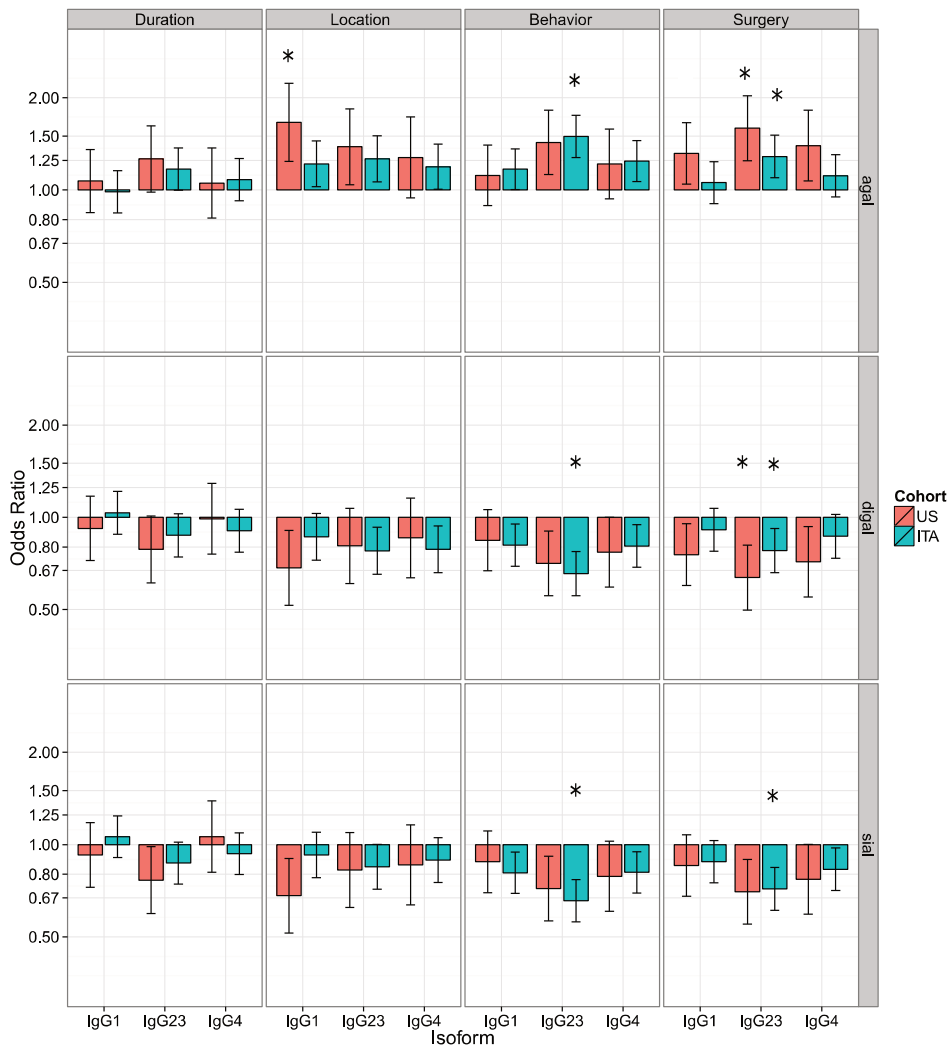


Figure 6.5 Associations between derived IgG Fc glycan traits and clinical characteristics in CD (duration, location, behavior, and surgery). Odds ratios for the associations between derived glycan traits and clinical characteristics in CD (duration of disease: <5 years = 0, >5 years = 1, disease location: L1 [ileal CD] = 0, L3 [ileocolonic CD] = 1, behavior: B1 [inflammatory CD] = 0, B2 [structuring CD] + B3 [penetrating CD] = 1, and surgery: no = 0, yes = 1) for all IgG subclasses are shown for the ITA cohort (green) and the US cohort (red). Bars indicate positive/negative odds ratios. Derived glycan traits are explained in **Supplementary Table 2** and **3** and their glycoforms in **Supplementary Table 8**. Analysis of the association between derived glycan traits and clinical characteristics in CD were performed using a logistic regression model, with age and sex included as additional covariates, statistically significant findings are indicated with an asterisk (*) (**Supplementary Table 13**).

6.3.4 Use of Medication

For UC patients in the ITA cohort, an increase in overall agalactosylation was associated with the use of steroids compared to mesalazine. This difference was not observed for CD patients in the ITA cohort (**Supplementary Tables 16 and 17**). In the US cohort, UC patients treated with anti-TNF showed a decrease in overall galactosylation, and IgG1 and IgG4 sialylation when compared to patients treated with AZA/6MP. This was not replicated in the ITA cohort. However, the same observation was made for CD patients in the US cohort (and the meta-analysis of both cohorts), where a decrease in overall galactosylation was associated with treatment with anti-TNF compared to treatment with AZA/6MP. Results for the individual IgG glycoforms are shown in **Supplementary Tables 18 and 19**.

6.4 Discussion

In this study, we analyzed subclass-specific IgG Fc glycosylation in IBD in two independent cohorts, using a nano-LC-MS method [85]. The importance of altered glycosylation in IBD has been reported before in different models [247, 269] and specifically IgG Fc glycosylation was found to play an important role in a number of inflammatory processes [270], including the course of IBD [95].

6.4.1 Associations Between IgG Fc glycosylation and Inflammatory Bowel Disease

Although observed for both diseases, associations between galactosylation and sialylation and disease were consistently more pronounced in CD than in UC. IgG Fc galactosylation was decreased in IBD patients compared to HC. This decrease was previously found in the total IgG *N*-glycome [95], and we revealed that this change is not subclass-specific (**Figure 6.2**). Decreased IgG Fc galactosylation has been reported in different inflammatory diseases [95]. Because IgG galactosylation has been shown to also decrease with aging [256], observed changes in galactosylation are most likely connected to inflammation in general and are not IBD-specific. On the other hand, decreased galactosylation on antigen-specific antibodies in rheumatoid arthritis precedes onset of the disease [93, 271], which indicates that the individual differences in IgG galactosylation could be associated with predisposing factors for the development of inflammatory disease, including IBD [272].

In addition, sialylation was decreased in IBD, which was previously observed in CD but not UC [95]. This effect was less pronounced than the galactosylation effect and it was also not replicated in both cohorts for all IgG subclasses. Likely, the decrease in sialylation is a by-effect of the observed decrease in galactosylation, as galactosylation is required for the addition of a sialic acid to a glycan. This is supported by our observation that sialylation

per galactose (derived trait A2GS) did not show a difference between either CD or UC and HC, or increased with disease. Various studies in humans have shown the predominant role of galactosylation rather than sialylation in the regulation of pro- and anti-inflammatory effects of IgG [52, 54, 97].

Recently, it was discovered that 5 genetic loci associated with IgG glycosylation showed pleiotropy with IBD, suggesting the role of IgG glycosylation in the development and course of IBD [240, 254, 255]. Mutations in these genetic loci associated with IgG galactosylation, fucosylation, and bisection, features also significantly changing with IBD as found in the current study. As multiple-derived glycosylation traits were associated with IBD, we hypothesized that IgG Fc glycosylation might be used as tool to discriminate between IBD patients and HC. Our prediction models were based on the individual glycoforms per IgG subclass and showed an improved discriminatory performance compared to previously published models based on individual glycoforms [95], this is likely due to the higher number of individual glycoforms included in our model and the subclass specificity of our analysis. For example, in both cohorts, IgG23 and IgG4 glycoforms showed the largest effect size between HC and IBD patients. IgG23 and IgG4 are less abundant in human plasma than IgG1 [191], likely causing the effect of their glycoforms to be partly masked during released glycan analysis. Despite the differences between the two cohorts in terms of disease behavior in CD and disease extent in UC (both more severe in the US cohort, likely due to a longer disease duration) and collection of the samples (a single tertiary/quaternary IBD center for the US cohort and multiple primary centers for the ITA cohort), we still found equally performing models for both of them.

These findings suggest possible clinical utility of glycans as minimally invasive diagnostic markers. However, future studies confirming these findings and contrasting/combining these markers with others minimally invasive prognostic markers are warranted [273-275]. Previous studies have identified IBD-associated serologies, transcriptomics, and genetics. Especially the comparative utility of IgG Fc glycosylation as peripheral biomarker compared to IBD-associated serologies, which measure antibodies to commensal flora (eg, ASCA, anti-CBIR1, and ANCA) [264, 273, 276, 277], should be evaluated. The preferred study design for this would be a prospective longitudinal study that further explores the impact of changes in disease severity and progression over time. Previously, it was suggested that the IgG glycome of healthy individuals is stable over time [90], although influenced by changes in lifestyle and environmental factors [90]. In the context of IBD, it is likely to change with disease activity.

6.4.2 Differences Between Crohn's Disease and Ulcerative Colitis

Reliable differentiation between UC and CD is currently done by colonoscopy (invasive) or radiology (radiation exposure) [278]. Current methods based on serology markers, like

antibodies specific for microbial antigens, still do not reach the specificity and sensitivity demanded for a diagnostic test [279]. In addition, the differences in mechanisms leading to the development of these diseases remain unclear [280]. Lower IgG galactosylation was more pronounced in CD than in UC, which might indicate a more severe inflammatory response in CD [186]. Fucosylation was decreased in UC, but increased in CD, suggesting different regulation mechanisms. The absence of a fucose on an IgG Fc glycan has shown to improve Fc binding to Fcγ receptor III, thereby enhancing ADCC [47]. As an increased galactosylation also enhances the ADCC activity of antibodies in in vitro models, the combination of a lower fucosylation and higher galactosylation in UC compared to CD might result in higher ADCC activity in UC than in CD [259]. IgG Fc bisection was also different between UC and CD patients, showing a higher bisection in CD than in UC. This was consistent with the previous observation that IgG bisection was higher in CD, but not in UC, compared to HC [95]. Although bisection has a large influence on the structure of a glycan, its effect on antibody function is largely unknown [74]. Various studies report an increased bisection to be related to a higher antibody affinity for Fcγ receptor III and, therefore, an associated increase of ADCC [62, 281].

6.4.3 Associations Between IgG Fc Glycosylation and Disease Status

The potential role of IgG Fc glycosylation in the course and development of IBD has been consolidated through confirming, for the first time, the changes in IgG Fc glycosylation with clinical subphenotypes of UC and CD. The increase of aglycosylated glycoforms with more severe disease and the need for surgery in both UC and CD might suggest that when the disease involves more of the colon (more extensive [E3] UC or ileocolonic [L3] CD) and is more severe (there is a need for surgery), IgG has less possibilities to suppress the inflammation [89]. With longer duration of UC, on the other hand, a decrease in agalactosylation was observed, which was not detected with duration in CD. This can be connected to the different disease behaviors, as for UC, it is known that disease activity can decrease over time, while CD usually has a pattern of worsening activity [282].

The treatment exposures in the two cohorts were different, IBD patients in the US cohort had all been exposed to corticosteroids, which was not the case in the ITA cohort, where the patients on and off corticosteroids were compared. In both cohorts, patients on anti-TNF therapy (more severe cases) were compared to the ones exposed to AZA/6MP (less severe cases) [283, 284]. In the US cohort, we observed increased agalactosylation for all subclasses in IBD patients on anti-TNF therapy compared to patients on AZA/6MP. This was not replicated in the ITA cohort, which likely reflects the heterogeneity of the two cohorts in terms of treatment guidelines. However, in the ITA cohort, an increase in agalactosylated structures was found with the use of corticosteroids as most potent treatment, compared to the less potent one with mesalazine. Steroids compared to mesalazine and anti-TNF compared to AZA/6MP might be considered surrogate markers

for disease severity, as they are used when the disease progresses [283, 284]. This corresponds to our findings that more severe disease was also associated with a decrease in IgG Fc galactosylation. Although corticosteroids have an anti-inflammatory effect [285], our findings suggest that the observed glycosidic changes are not an effect of therapy, but are rather connected to a more severe disease.

6.5 Conclusions

In this study, we confirmed previous associations of reduced galactosylation in IBD compared to HC. In addition, it was demonstrated that this same glycosylation trait was associated with more extensive and progressive disease, suggesting a potential role of IgG Fc glycosylation as diagnostic and/or prognostic tool. Furthermore, we found the IgG glycosylation features fucosylation, galactosylation, and bisection to be different between UC and CD patients. Individual glycoforms showed good performance for distinguishing both UC and CD from HCs and fair performance for distinguishing UC from CD, which gave an insight into the difference in mechanisms behind the two diseases. The reported differences in IgG Fc glycans might influence the development and behavior of IBD through affecting binding of IgG to FcγRs [51, 243]. Furthermore, individual differences in IgG glycosylation might affect efficacy of therapeutic monoclonal antibodies, which have to compete with circulating IgG to activate effector functions [286]. The reported changes in IgG Fc glycosylation in the current study give guidelines for future, prospective studies that should elucidate the longitudinal relationship between changes in IgG Fc glycans and development of disease, and disease progression, as well as their role in predicting treatment response. Clinical exploitation of these glycan markers will be facilitated by the existing broad application in clinical laboratories of mass spectrometry or capillary electrophoresis, which show great potential for glycomics assays [287, 288].

Acknowledgements


The Inflammatory Bowel Disease Biomarkers Consortium: Harry Campbell, Vlatka Zoldoš, Iain K. Permberton, Daniel Kolarich, Daryl L. Fernandes, Evropi Theodorou, Victoria Merrick, Daniel I. Spencer, Richard A. Gardner, Ray Doran, Archana Shubhakar, Ray Boyapati, Igor Rudan, Paolo Lionetti, Jasminka Krištić, Mislav Novokmet, Maja Pučić-Baković, Olga Gornik, Angelo Andriulli, Laura Cantoro, Giancarlo Sturniolo, Gionata Fiorino, Natalia Manetti, Ian D. Arnott, Colin L. Noble, Charlie W. Lees, Alan G. Shand, Gwo-Tzer Ho, Malcolm G. Dunlop, Lee Murphy, Jude Gibson, Louise Evenden, Nicola Wrobel, Tamara Gilchrist, Angie Fawkes, Guinevere S.M. Kammeijer, Aleksandar Vojta, Ivana Samaržija,

Dora Markulin, Marija Klasić, Paula Dobrinić, Yurii Aulchenko, Tim van den Heuve, Daisy Jonkers, and Marieke Pierik.

This was supported by the European Union Seventh Framework Programmes Inflammatory Bowel Disease Biomarkers (contract 305479), H2020 grants SYSCID (contract 733100), GlySign (contract 722095), and IMForFuture (contract 721815); by the European Structural and Investment Funds IRI (grant KK.01.2.1.01.0003), and Croatian National Centre of Research Excellence in Personalized Healthcare (grant KK.01.1.1.01.0010); as well as by The Netherlands Genomic Initiative Horizon Programme Zenith project (grant no. 93511033). Research at the Inflammatory Bowel Disease Center at Cedars-Sinai is supported by National Institutes of Health grants including U01DK062413 (DPBM), P01DK046763 (SRT, DPBM), R01HS021747 (DPBM), and U01AI067068 (DPBM).

Supporting Information available

Additional information is available as stated in the text. This information is available free of charge via [https://www.gastrojournal.org/article/S0016-5085\(18\)30012-X/fulltext](https://www.gastrojournal.org/article/S0016-5085(18)30012-X/fulltext).

- 
- ¹ *Leiden University Medical Center, Center for Proteomics and Metabolomics,
Leiden, The Netherlands*
- ² *Genos, Glycoscience research laboratory, Zagreb, Croatia*

The *N*-glycosylation of Mouse Immunoglobulin G (IgG) Fragment Crystallizable Differs Between IgG Subclasses and Strains

Noortje de Haan¹, Karli R. Reiding¹, Jasminka Krištić²,
Agnes L. Hipgrave Ederveen¹, Gordan Lauc² and Manfred Wuhrer¹

Reprinted and adapted from Front. Immunol. 8:608 DOI: 10.3389/fimmu.2017.00608 [289].

Copyright © 2017, de Haan, Reiding, Krištić, Hipgrave Ederveen, Lauc and Wuhrer.



N-linked glycosylation of the Fc region of IgG is known to have a large influence on the activity of the antibody, an effect reported to be IgG subclass-specific. This situation applies both to humans and mice. The mouse is often used as experimental animal model to study the effects of Fc glycosylation on IgG effector functions, and results are not uncommonly translated back to the human situation. However, while human IgG Fc glycosylation has been extensively characterized in both health and disease, this is not the case for mice.

To characterize the glycosylation profile of murine IgG-Fc and in addition evaluate the systematic glycosylation differences between mouse strains, sexes and IgG subclasses, we used nanoLC-MS(/MS) to look at the subclass-specific IgG Fc glycopeptides of male and female mice from the strains BALB/c, C57BL/6, CD-1 and Swiss Webster.

The structural analysis revealed the presence of predominantly fucosylated, diantennary glycans, with varying amounts of galactosylation and α 2,6-sialylation. In addition, we report glycosylation features not previously reported in an Fc specific way on murine IgG, including monoantennary, hybrid, and high mannose structures, as well as diantennary structures without a core fucose, with a bisecting GlcNAc, or with α 1,3-galactosylation.

Pronounced differences were detected between strains and the IgG subclasses within each strain. Especially the large spread in galactosylation and sialylation levels found between both strains and subclasses may vastly influence IgG effector functions. Mouse strain-based and subclass-specific glycosylation differences should be taken into account when designing and interpreting immunological and glycobiological mouse studies involving IgG effector functions.

7.1 Introduction

Immunoglobulin G (IgG) is the most abundant antibody in human plasma and plays a crucial role in the humoral immune response [290]. Various effector functions of IgG are affected by its fragment crystallizable (Fc)-glycosylation, which has shown to influence the binding of IgG-Fc to e.g. Fc γ -receptors (Fc γ R) and C-type lectins [58, 186, 252]. Changes in IgG Fc glycosylation are associated with various diseases and physiological processes. For example, galactosylation on total IgG is decreased in rheumatoid arthritis and active tuberculosis infections and increases with pregnancy [54, 92, 101]. Fucosylation on the other hand, is decreased on alloantibodies against red blood cells and platelets as well as on gp120-specific antibodies in HIV-infected patients [98, 99, 291]. Modification of IgG Fc glycosylation has also shown to be a suitable measure to improve the efficacy of therapeutic monoclonal antibodies [292].

Mice are often used as experimental animal models to study the effects of Fc glycosylation on IgG effector functions [45, 252]. Various mouse strains are established for different research areas, for example outbred strains like CD-1 or Swiss Webster are used frequently for toxicological and pharmaceutical studies [293]. In addition, because CD-1 mice are efficient breeders, they are regularly used in genetic experiments [294]. On the other hand, inbred strains like BALB/c and C57BL/6 are often used to study infectious diseases and cancer [295, 296].

Contrary to the human IgG Fc glycosylation, mice predominantly express the sialic acid *N*-glycolylneuraminic acid (Neu5Gc), while humans exclusively express *N*-acetylneuraminic acid (Neu5Ac) [42]. Furthermore, as IgG Fc glycosylation is partly genetically determined [256], and partly influenced by environmental factors like exposure to immunological challenges [297], baseline Fc glycosylation may play a role in the outcome of an immunological study, and may confound the potential translation to the human situation. Differences in total plasma *N*-glycosylation between mouse strains were demonstrated before [298]. Interestingly, glycans that are for humans known to be predominantly derived from IgG [299] showed both sex and strain specific differences in the murine total plasma *N*-glycome study. For example, galactosylation of diantennary fucosylated species, which is a known immune modulator on IgGs [186], was reported to be higher for BALB/c and C57BL/6 mice, as compared to CD-1 and Swiss Webster [298].

In contrast to human IgG, which can be divided into four subclasses (IgG1 to 4), murine IgG only knows three subclasses (IgG1 to 3) [300]. In addition, murine IgG2 can be split in the isotypes IgG2a, 2b and 2c, of which IgG2a and 2c are allelic variants and further sequence variants are known for IgG1 and IgG2b [44, 301]. Like for human IgG, the affinity of murine IgG for the various Fc γ Rs differs per subclass [22, 300, 302, 303]. For example, defucosylation of IgG Fc glycans has been found to improve the Fc γ R-mediated pro-

inflammatory activity of murine IgG2b, while this is not the case for murine IgG1 [304]. Despite its importance and some previous descriptions of single case murine IgG glycosylation [44], no comprehensive strain- and subclass-specific characterization was hitherto performed.

We used nano-liquid chromatography (nanoLC) coupled to electrospray ionization (ESI)-mass spectrometry (MS) to analyze glycopeptides derived from murine IgG. In this way, we were able to separate the *N*-glycosylation present on IgG1 and its sequence variant (IgG1i), as well as on IgG2b, IgG2a/c, and IgG3, and to perform a subclass-specific relative quantification thereof. The glycosylation profiling of mice from each of the commonly used strains BALB/c, C57BL/6, CD-1 and Swiss Webster revealed significant differences between both the mouse strains and the subclasses within the strains. In addition, nanoLC-MS/MS allowed the characterization of glycan structures which, to our knowledge, were not previously reported on polyclonal murine IgG-Fc. These included high-mannose structures, hybrid structures, and structures with a bisecting *N*-acetylglucosamine (GlcNAc), without a core fucose, or with α 1,3-linked galactose attached to the β -linked-galactose. Next to Neu5Gc, we detected Neu5Ac on several of the subclasses. Finally, previously reported matrix-assisted laser desorption/ionization (MALDI)-time-of-flight (TOF)-MS(/MS) [124, 298] and ultra-performance liquid chromatography (UPLC)-fluorescence [74, 305] methods allowed to differentiate between respectively sialic acid linkages and antenna galactosylation in monogalactosylated species.

7.2 Materials and Methods

7.2.1 Chemicals

Ultra-pure deionized water was generated by the Purelab Ultra, maintained at 18.2 M Ω (Veolia Water Technologies Netherlands B.V., Ede, The Netherlands) and used throughout. Disodium hydrogen phosphate dihydrate (Na₂HPO₄·2H₂O), potassium dihydrogen phosphate (KH₂PO₄), NaCl, sodium dodecyl sulfate (SDS), ethanol, glacial acetic acid and trifluoroacetic acid were purchased from Merck (Darmstadt, Germany). 1-Hydroxybenzotriazole hydrate, dimethyl sulfoxide (DMSO), ammonium bicarbonate, formic acid, Nonidet P-40 substitute (NP-40), super-DHB, NaOH and tosyl phenylalanyl chloromethyl ketone (TPCK)-treated trypsin from bovine pancreas were purchased from Sigma-Aldrich (St. Louis, MO), 1-ethyl-3-(3-(dimethylamino)propyl)carbodiimide hydrochloride from Fluorochem (Hadfield, Derbyshire, UK) and HPLC SupraGradient acetonitrile (ACN) from Biosolve (Valkenswaard, The Netherlands). Recombinant peptide-*N*-glycosidase F (PNGaseF) was obtained from Roche Diagnostics (Mannheim, Germany).

Phosphate-buffered saline (PBS) was made in-house, containing 5.7 g/L $\text{Na}_2\text{HPO}_4 \cdot 2\text{H}_2\text{O}$, 0.5 g/L KH_2PO_4 and 8.5 g/L NaCl.

For specifically the ultra-performance liquid chromatography (UPLC)-fluorescence analysis of the 2-aminobenzamide (2-AB) labeled glycans, ultra-pure deionized water was generated by the Millipore Synergy Ultrapure Water Purification System, maintained at $\geq 18.2 \text{ M}\Omega$ at 25 °C (Merck Millipore, Billerica, MA), whereas formic acid was purchased from Merck, ethanol from Carlo Erba Reagents (Val de Reuil, France) and 2-AB, DMSO, 2-picoline borane and ACN from Sigma-Aldrich (St. Louis, MO).

7.2.2 Samples

The disodium EDTA plasma of 40 individual mice was purchased from BioChemed Services (Winchester, VA). The mice, aged between 8 and 12 weeks, originated from the strains BALB/c, C57BL/6, CD-1 and Swiss Webster. Of each strain, five male and five female mice were included in the study. Four pooled disodium EDTA plasma samples (one male and one female) of the same strains were purchased from Seralab (West-Sussex, U.K.; **Figure 7.1**; [298]).

7.2.3 IgG isolation from murine plasma

Murine IgG was captured from 2 μL (for the glycopeptide workflow) or 100 μL (for the released glycan workflow) plasma, using respectively 15 μL or 500 μL protein G affinity beads (GE Healthcare, Uppsala, Sweden) in 100 μL or 1000 μL PBS. Proteins were allowed to interact with the beads while shaken for 1 h, after which the beads were washed three times with PBS and three times with water. IgG was eluted in 100 μL 100 mM FA, by incubating the beads 15 min at room temperature with agitation. Eluates were dried for 2 h in a vacuum concentrator at 60 °C.

7.2.4 Preparation glycopeptides

Glycopeptide analysis was performed for all 40 individual mouse samples and in addition for six technical replicates of the four pooled samples in a randomized 96-well plate format. Six blanks were included to serve as negative control. Dried IgG samples (between 3 and 5 μg based on SDS-PAGE-gel analysis; **Figure S1** in Supplementary Material) were dissolved in 40 μL 25 mM ammonium bicarbonate (pH 8) with 1 μg TPCK-treated trypsin and incubated for 17 h at 37 °C. Before nano-liquid chromatography (nanoLC)-mass spectrometry (MS) analysis all samples were diluted 20 times in ultra-pure water.

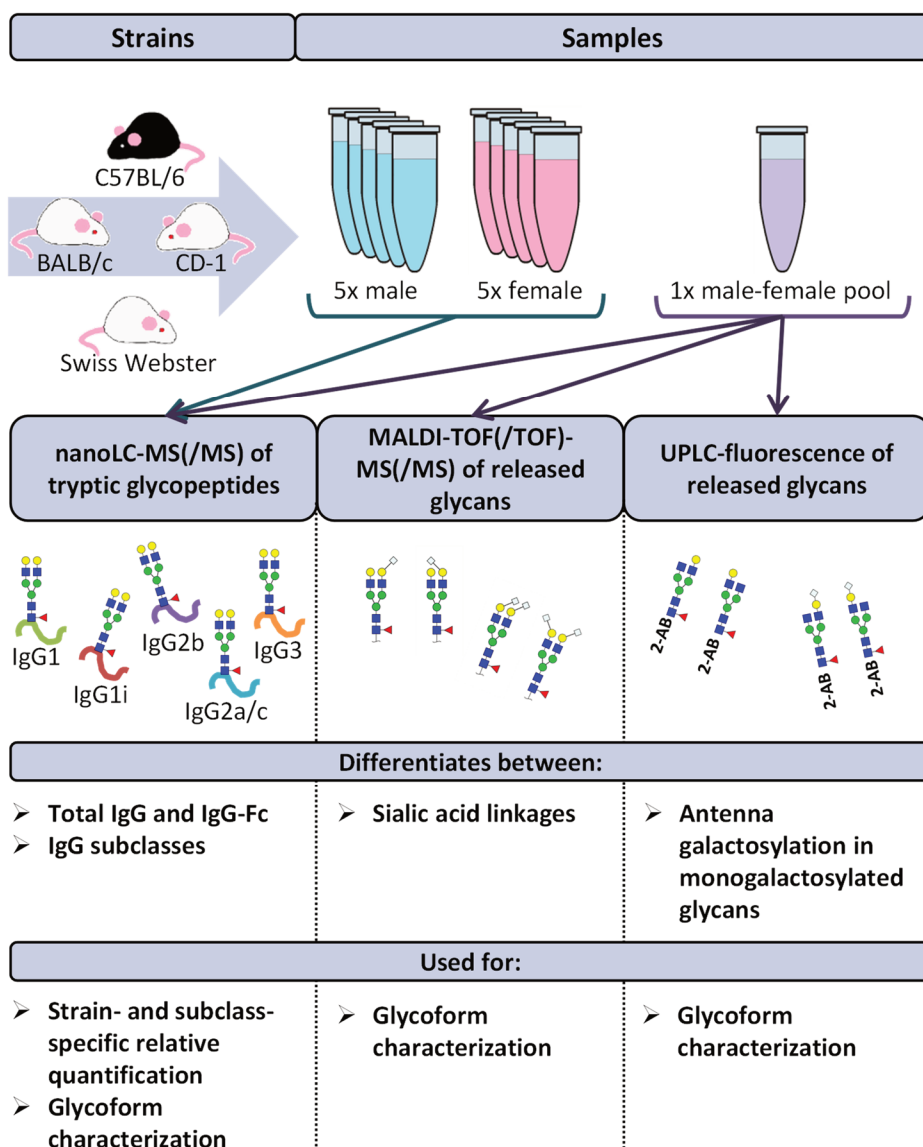


Figure 7.1 Schematic representation of the study design. The IgG glycopeptides of 40 individual mice were analyzed by nanoLC-MS(/MS). The mice originated from the strains BALB/c, C57BL/6, CD-1 and Swiss Webster. Of each strain, five male and five female mice were included. Based on these analyses, relative quantification of the glycoforms was performed in a strain- and subclass-specific way. In addition, released IgG glycans of four pooled plasma samples (one male and one female) of the same strains were analyzed by nanoLC-MS(/MS), MALDI-TOF(/TOF)-MS(/MS) and UPLC-fluorescence for further structural elucidation of the glycoforms.

7.2.5 Preparation of released glycans

Released glycan analysis was performed for the four pooled samples. The complete sample preparation was carried out in triplicate. Dried IgG samples (between 150 and 250 µg based on SDS-PAGE-gel analysis; **Figure S1** in Supplementary Material) were dissolved in 20 µL water and 40 µL 2% SDS and incubated for 10 min at 60 °C. *N*-Glycans were released by adding 40 µL release mixture (2 mU PNGase F and 2% NP-40 in 2.5x PBS) and incubating for 17 h at 37 °C.

Prior to matrix-assisted laser desorption/ionization (MALDI)-time-of-flight (TOF)-MS analysis, sialic acids were stabilized in a linkage-specific way by ethyl esterification [124]. 2 µL of the released glycans was added to 20 µL derivatization reagent (250 mM 1-ethyl-3-(3-(dimethylamino)propyl)carbodiimide and 250 mM 1-hydroxybenzotriazole in ethanol) and incubated for 1 h at 37 °C. 20 µL ACN was added and derivatized glycans were enriched by cotton hydrophilic-interaction liquid chromatography (HILIC)-solid phase extraction (SPE) as described before, and eluted in 10 µL water [124, 168].

Prior to UPLC analysis, the released glycans were labeled at the reducing end with 2-AB. 90 µL of the released glycans was dried and reconstituted in 50 µL of water. The labeling mixture was freshly prepared by dissolving 19.2 mg/mL 2-AB and 44.8 mg/mL 2-picoline borane in DMSO and glacial acetic acid (70:30, v/v). 25 µL of labeling mixture was added to each sample in a 96-well plate format and the plate was sealed using adhesive tape. Samples were mixed by a 10 min shaking step, followed by 2 h incubation at 65 °C. After incubation, samples were left to cool down to room temperature for 30 min. The samples (in a volume of 75 µL) were mixed with 700 µL of cold 100% ACN. Free label and reducing agent were removed from the samples using HILIC-SPE on a 0.2 µm GHP filter plate (Pall Corporation, Ann Arbor, MI, USA). Solvent was removed by a vacuum manifold (Millipore Corporation, Billerica, MA, USA). All wells were prewashed using 200 µL of 70% ethanol, followed by 200 µL of water and equilibrated with 200 µL of cold 96% ACN. The samples were loaded onto GHP filter plate and incubated for 2 min before the vacuum application. The wells were subsequently washed 5 times using 200 µL of cold 96% ACN. The last washing step was followed by centrifugation at 1000 rpm for 5 min. Glycans were eluted two times with 90 µL of water after 15 min of shaking at room temperature followed by centrifugation at 1000 rpm for 5 min. The combined eluates were stored at -20 °C until usage.

7.2.6 nanoLC-MS(/MS) analysis of glycopeptides

The 20 times diluted tryptic digests of the IgG samples were separated with an Ultimate 3000 RSLCnano system (Dionex/Thermo Scientific, Breda, The Netherlands) equipped with an Acclaim PepMap 100 trap column (100 µm x 20mm, particle size 5 µm, Dionex/Thermo Scientific) and an Acclaim PepMap RSLC C18 nano-column (75 µm x 150 mm, particle size

2 μ m, Dionex/Thermo Scientific). 2 μ L sample was injected and separated with a gradient from 97% solvent A (0.1% formic acid in water) and 3% solvent B (95% ACN) to 27% solvent B over 15 min, with a flow rate of 700 nL/min. The nanoLC was coupled to a MaXis HD quadrupole time-of-flight-MS (q-TOF-MS; Bruker Daltonics) via an electrospray ionization (ESI) interface, equipped with the CaptiveSpray and nanoBooster technologies (Bruker Daltonics), using ACN-doped nebulizing gas. Profile spectra were recorded in m/z range 550 to 1800 with a frequency of 1 Hz. The collision energy was 5 eV, the transfer time 130 μ s, and the pre-pulse storage 10 μ s. The total analysis time per sample was 19 min. The nanoLC system and the q-TOF-MS were operated under Chromeleon Client version 6.8 and otofControl version 4.0.15, respectively. For a closer examination of the glycoforms present, nanoLC-MS/MS was performed on a pooled sample of the undiluted digests of all 40 individual mouse samples. 5 μ L of the pooled sample was injected and all putative glycopeptides peaks were selected for MS/MS fragmentation analysis by collision-induced dissociation.

7.2.7 MALDI-TOF(/TOF)-MS(/MS) analysis of released glycans

MALDI-TOF(/TOF)-MS(/MS) analysis was performed on an UltrafleXtreme (Bruker Daltonics) operated under flexControl 3.3 (Build 108; Bruker Daltonics). 1 μ L of the enriched ethyl-esterified glycans was spotted on a MALDI target (MTP AnchorChip 800/384 TF; Bruker Daltonics) together with 1 μ L 5 mg/mL super-DHB in 50% ACN and 1 mM NaOH. The spots were dried by air at room temperature. For each spot, a mass spectrum was recorded from m/z 1 000 to 3 000, combining 10 000 shots in a random walk pattern at 1 000 Hz and 100 shots per raster spot. Prior to the analysis of the samples, the instrument was calibrated using peptide calibration standard (Bruker Daltonics). MALDI-TOF(/TOF)-MS(/MS) of the most abundant peaks was performed by laser-induced dissociation.

7.2.8 UPLC-fluorescence analysis of released glycans

Fluorescently labeled *N*-glycans were separated by HILIC on a Waters Acquity UPLC instrument (Milford, MA, USA) consisting of a quaternary solvent manager, sample manager and a FLR fluorescence detector set with excitation and emission wavelengths of 250 and 428 nm, respectively. The instrument was under the control of Empower 3 software, build 3471 (Waters, Milford, MA, USA). The UPLC system was equipped with a Waters BEH Glycan chromatography column (100 \times 2.1 mm i.d., 1.7 μ m BEH particles). 40 μ L (80% ACN:20% water) sample was injected and separated with a gradient of 75% solvent B (100% ACN; solvent A: 100 mM ammonium formate pH 4.4) to 62% solvent B over 27 min, with a flow of 0.4 ml/min. Solvent B was maintained at 62% for an additional 5 min. Samples were maintained at 10 $^{\circ}$ C before injection, and the separation temperature was 60 $^{\circ}$ C. The system was calibrated using an external standard of

hydrolyzed and 2-AB labeled glucose oligomers from which the retention times for the individual glycans were converted to glucose units (GU).

7.2.9 Data processing

For automated relative quantification of the glycopeptides by LaCyTools (version 1.0.1, build 8) [198], the nanoLC-MS files were converted to mzXML files. Chromatograms were aligned based on at least six glycopeptide signals with a signal-to-noise ratio (S/N) above nine, covering the full elution range of the glycopeptides (412 to 716 s; **Table S1** in Supplementary Material). Targeted peak integration was performed on doubly, triply and quadruply charged species. Twelve chromatographic glycopeptide clusters were defined, one per IgG subclass (IgG1, IgG1i, total IgG2, IgG3) and within each subclass, one per degree of sialylation (zero, one or two sialic acids; **Table S2A** and **Figure S2** in Supplementary Material). Sum spectra were created for these clusters and signals were integrated to include at least 85% of the theoretical isotopic pattern. The actual presence of a glycopeptide was assessed based on the mass accuracy (between -20 and 20 ppm), the deviation from the theoretical isotopic pattern (IPQ; below 25%) and the S/N (above nine) of an integrated signal. Analytes were included for all samples when present in at least 50% of the spectra of one biological group (vendor, strain and sex). For the glycopeptides that passed analyte curation for total IgG2, new extraction clusters were defined to separate IgG2b glycoforms from IgG2a/c glycoforms (two clusters per analyte; **Table S2B** in Supplementary Material). Again, glycoforms were included when meeting the requirements described above. Glycopeptide signals were corrected for the actual percentage of isotopic pattern integrated, the included charge states were summed per analyte and absolute values were normalized to the total signal intensity per IgG subclass. For the in-depth analysis of compositional features, derived traits were calculated (**Table S3** in Supplementary Material, [176, 298]).

For automated relative quantification of the released glycans analyzed by MALDI-TOF-MS, using MassyTools (version 0.1.8.1.)[190], the MALDI-TOF-MS files were converted to text files. Spectra were calibrated based on at least six glycan signals with a S/N above nine, covering the full *m/z* range of the glycans (**Table S4** in Supplementary Material). Targeted peak integration was performed for an extensive, visually determined, list of glycans, including at least 95% of the theoretical isotopic pattern. The actual presence of a glycan was assessed based on the mass accuracy (between -20 and 20 ppm), the IPQ (below 25%) and the S/N (above nine) of an integrated signal. Analytes were included for all samples when present in at least two-thirds of one of the technical triplicates. Glycan signals were normalized to the total signal intensity.

The chromatographic glycan peaks resulting from the UPLC-fluorescence analysis were integrated using an automatic processing method with the “Traditional integration

algorithm” after which each chromatogram was manually corrected to maintain the same intervals of integration for all samples. In this way, all chromatograms were separated into 27 peaks and the amount of glycans in each peak was expressed as a percentage of the total integrated area. Assignment of the glycans structures in all major UPLC peaks was based on previous analysis [305].

7.2.10 Data analysis

Statistical analysis of the glycopeptide data was performed using R 3.1.2 (R Foundation for Statistical Computing, Vienna, Austria) and RStudio 0.98.1091(RStudio, Inc.). Because of the small sample sizes (between 5 and 40 cases) and the skewing in the distribution of some of the glycosylation traits, non-parametric Mann-Whitney U tests were performed to assess sex-, strain- and subclass-specific glycosylation differences. Multiple testing was accounted for by Bonferroni-correction of the significance threshold (α) per biological question. Differences between the sexes were assessed based on the combined strains (47 tests; $\alpha = 0.05/47 = 1.1 \times 10^{-3}$; **Table S5** in Supplementary Material), as well as for the individual strains (168 tests; $\alpha = 3.0 \times 10^{-4}$; **Table S5** in Supplementary Material). Subsequently, the sexes were combined to compare the glycosylation between the different strains (222 tests; $\alpha = 2.3 \times 10^{-4}$; **Table S6** in Supplementary Material), between the different subclasses of the combined strains (87 tests; $\alpha = 5.7 \times 10^{-4}$; **Table S7** in Supplementary Material), and between the different subclasses of the individual strains (87 tests each; $\alpha = 5.7 \times 10^{-4}$; **Table S8** in Supplementary Material).

7.3 Results

7.3.1 Glycoform characterization

The IgG Fc glycosylation of 40 individual mice of four strains (BALB/c, C57BL/6, CD-1 and Swiss Webster) and both sexes (five mice per strain per sex) was analyzed by nanoLC-MS(/MS) of tryptic glycopeptides in a subclass-specific manner. In addition, the strain-specific IgG Fc glycosylation was studied for four plasma pools of one male and one female mouse per strain (**Figure 7.1; Figure 7.2A**). A total of 32 different glycan compositions was detected on the combination of IgG subclasses, whereof 27 on IgG1, 22 on IgG1i, 24 on IgG2b, 25 on IgG2a/c and 21 on IgG3, showing a vast overlap of the glycoforms present per subclass (**Table 7.1; Figure S2, S3, S4 and S5** in Supplementary Material). In addition to the nanoLC-MS(/MS) analysis of glycopeptides, the total IgG glycans of the four pooled samples (one of each strain) were enzymatically released and analyzed by both MALDI-TOF(/TOF)-MS(/MS) after sialic acid linkage-specific derivatization and UPLC-fluorescence after 2-AB labeling. The latter two methods allowed the distinction between $\alpha 2,3$ - and

α 2,6-linked sialic acids and α 1,3- and α 1,6-antenna galactosylation, respectively (Figure 7.2B and C).

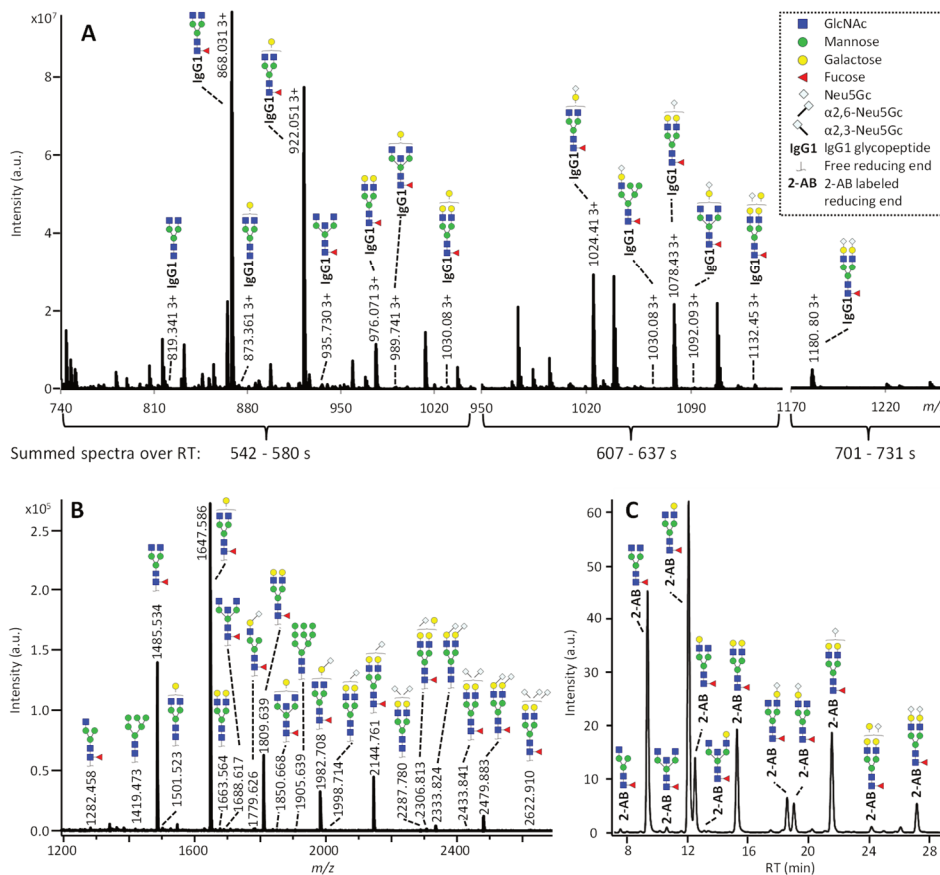


Figure 7.2 Glycoforms detected by the three synergetic analysis methods. Representative data and analytes detected in the analysis of the pooled CD-1 sample, showing (A) IgG1 Fc glycopeptides analyzed by nanoLC-MS, (B) the 20 most abundant released glycans of total IgG analyzed by MALDI-TOF-MS after linkage-specific sialic acid derivatization, and (C) released glycans of total IgG analyzed by UPLC-fluorescence after 2-AB labeling. Except for the sialic acid linkage in the MALDI-TOF-MS analysis (B), and the antenna galactosylation in the UPLC-fluorescence analysis (C) the monosaccharide linkages were not determined. The proposed glycan structures are based on fragmentation and literature [42, 44, 306, 307].

Table 7.1 Detected glycoforms per IgG subclass by nanoLC-MS.

Glycoform composition ^a	Depiction ^b	IgG1 ^c	IgG1i	IgG2b	IgG2a/c	IgG3
H2N3F1		X	X	X	X	
H5N2		X	X			X
H3N3F1		X	X	X	X	X
H3N4		X	X			X
H6N2		X				
H4N3F1		X	X	X	X	X
H3N4F1		X	X	X	X	X
H4N4		X	X	X	X	X
H5N3F1			X	X	X	
H4N4F1		X	X	X	X	X
H5N4		X		X	X	X
H3N5F1		X	X		X	
H4N5						X
H4N3F1G1		X	X	X	X	X
H4N4G1			X			
H5N4F1		X	X	X	X	X
H4N5F1		X		X	X	X
H5N3F1G1		X	X	X	X	
H4N4F1G1		X	X	X	X	X
H5N4G1		X	X	X	X	X
H6N4F1		X	X	X	X	X
H5N5F1		X				X
H6N3F1G1		X	X	X	X	X
H5N4F1G1		X	X	X	X	X
H6N4G1		X				
H4N5F1G1		X	X	X	X	X
H5N4G2				X	X	
H6N4F1G1		X	X	X	X	X
H5N5F1G1		X		X	X	
H5N4F1G1S1				X	X	
H5N4F1G2		X	X	X	X	X
H5N5F1G2		X		X	X	

^a H: hexose, N: *N*-acetylhexosamine, F: fucose, G: *N*-glycolylneuraminic acid, S: *N*-acetylneuraminic acid. ^b Symbols used: green circle: mannose, yellow circle: galactose, blue square:

(Table 7.1 continued) *N*-acetylglucosamine, red triangle: fucose, white diamond: *N*-glycolylneuraminic acid (Neu5Gc). The proposed glycan structures are based on fragmentation and literature [42, 44, 306, 307]. See also Table S9 in Supplementary Material. ^c Peptide sequence of IgG1: EEQFNSTFR, IgG1i: EEQINSTFR, IgG2b: EDYNSTIR, IgG2a/c: EDYNSTLR, IgG3: EAQYNSTFR.

For all subclasses and in all mice the most abundant glycoforms (approximately 90% of the total area) included diantennary glycans with zero, one or two galactoses, a core fucose, and zero, one or two α 2,6-linked sialic acids, all in agreement with literature [42, 44]. In all samples, the sialic acids proved to be mainly *N*-glycolylneuraminic acid (Neu5Gc) [42, 44], with only the IgG2 isotypes showing the additional presence of *N*-acetylneuraminic acid (Neu5Ac) (IgG2a/b/c glycoform H5N4F1G1S1; H: hexose, N: *N*-acetylhexosamine, F: fucose, G: Neu5Gc, S: Neu5Ac; Table S9 in Supplementary Material). The presence of these minor amounts of Neu5Ac was also registered by MALDI-TOF/TOF-MS/MS analysis (H5N4F1E1Ge1; E: α 2,6-linked Neu5Ac, Ge: α 2,6-linked Neu5Gc; Table S9 in Supplementary Material). In addition to the α 2,6-linked Neu5Gc, the MALDI-TOF-MS method showed α 2,3-linked Neu5Gc to be present in the form of H5N4F1G1I, H5N4G1IGe1 and H5N4F1G1IGe1 (GI: α 2,3-linked Neu5Gc; Table S9 in Supplementary Material).

Next to the fucosylated diantennary glycans described above, also variants without core fucose, with bisecting GlcNAc or with α 1,3-galactosylation on the β -linked-galactoses were detected on mouse IgG-Fc. Bisection was confirmed by nanoLC-MS/MS analysis of the H4N5F1G1 glycoform on IgG1 (Table S9 in Supplementary Material) and in accordance with literature [42, 307]. The presence of an extra hexose on diantennary, digalactosylated structures was indicated by nanoLC-MS/MS analysis of the glycan composition H6N4F1G1 on IgG1 (Table S9 in Supplementary Material). In line with literature, this structure, as well as H6N4F1 and H6N4G1, were assigned to diantennary structures that carry an α 1,3-galactose on one of their antennae (Table S9 in Supplementary Material) [43, 306, 308].

Besides diantennary glycans, also monoantennary, high mannose and hybrid structures were detected on the IgG Fc glycopeptides. While monoantennary glycans were reported before on mouse IgG [42], high mannose and hybrid structures were not. Both H5N2 and H6N2 were detected at the glycopeptides level (Table S9 in Supplementary Material), H8N2 was additionally observed in the MALDI-TOF-MS analysis (Table S9 in Supplementary Material). The presence of hybrid structures was confirmed by nanoLC-MS/MS of H6N3F1G1 on IgG1 (Table S9 in Supplementary Material).

7.3.2 Sex- and strain-specific IgG Fc glycosylation

Based on the glycopeptide analysis of the 40 individual mice, it was shown that the two isotypes of IgG1, i.e. IgG1 (UniProt entry P01868 [309]) and IgG1i (A0A075B5P4), were simultaneously present in four of the CD-1 mice and five of the Swiss Webster mice, while

the others expressed exclusively one of the two forms. In addition, BALB/c and C57BL/6 showed solely the respective presence of IgG1 and IgG1i. IgG2b (P01867/A0A075B5P3), IgG3 (P03987) and IgG2a (P01863/P01864) and/or IgG2c (A0A0A6YY53) glycopeptides were observed in all mice, although no distinction could be made between the IgG2a and IgG2c isotypes, as they resulted in the same tryptic glycopeptides (**Table 7.1; Table S10** in Supplementary Material).

For the relative quantification of the glycoforms, absolute intensities were normalized per subclass. In addition, derived traits were calculated based on compositional features (**Table 7.2; Table S3** in Supplementary Material). The derived traits per IgG subclass, such as overall galactosylation and sialylation, were compared between the four strains using Mann-Whitney U tests. As no difference was found between sexes for any of the testing groups, male and female mice were pooled for all subsequent analyses (**Table S5** in Supplementary Material).

Many glycosylation traits showed to differ between strains, one of the most pronounced differences being the relative abundance of bisecting GlcNAc on diantennaries (A2B). A2B was low throughout, but clearly higher in BALB/c and C57BL/6 (e.g. IgG2b medians of 1.0% and 0.7%) than in CD-1 and Swiss Webster (0.3% and 0.2%; for statistical test outcomes see **Table 7.3, Table S6** in Supplementary Material and **Figure 7.3A**). This difference was detected for all IgG subclasses except IgG3, where the A2B was found to be similarly low for BALB/c (IgG3 BALB/c: 1.9%, C57BL/6: 5.0%, CD-1: 2.3% and SW: 2.6%).





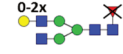
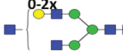
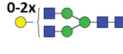
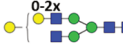
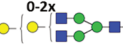
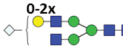
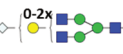
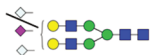
All strains had low levels of afucosylated glycans, with BALB/c and C57BL/6 having a slightly higher relative abundance of afucosylated diantennaries (A2aF) on IgG2a/c (1.0% and 1.3%) than CD-1 (0.7%; **Table S6** and **Figure S6** in Supplementary Material). This trend appeared similar for IgG1, IgG1i and IgG3 (**Figure 7.3B; Table S6** and **Figure S6** in Supplementary Material).

Differences in antenna galactosylation (A2G) between the four strains were specifically observed for IgG2a/c and IgG3. On IgG2a/c, galactosylation was high for C57BL/6 (61%), as compared to all other strains (e.g. BALB/c: 44%; **Table S6** and **Figure S6** in Supplementary Material). On IgG3, high galactosylation was seen in BALB/c and C57BL/6 (38% and 42%), as compared to CD-1 and Swiss Webster (31% and 30%; **Figure 7.3C**). UPLC-fluorescence analysis showed furthermore the galactose on the monogalactosylated species to be between 78% and 85% on the α 1,6-antenna for H4N4F1 and between 51% and 62% on the α 1,6-antenna for H4N4F1G1 (**Figure S7** in Supplementary Material). Sialylation (A2S) followed the same behavior as the galactosylation on IgG3 and IgG2a/c, showing IgG3 A2S to be higher for BALB/c and C57BL/6 (9.2% and 11%) than for CD-1 (6.7%), and IgG2a/c A2S to be higher for C57BL/6 (18%) than for all other strains (e.g. BALB/c: 7.5%; **Table S6**

and **Figure S6** in Supplementary Material). In addition A2S on IgG2b was lower for CD-1 (13%) than for C57BL/6 (20%; **Figure 7.3D**).

Finally, strain-specific differences were found for the relative abundance of hybrid structures (Hy) on the two isotypes of IgG2, namely a high degree of hybrid structures on IgG2a/c for BALB/c and C57BL/6 (both 0.8%) as compared to CD-1 and Swiss Webster

Table 7.2 Derived glycosylation traits.

Derived trait	Depiction ^a	Description
Total		Sum of all glycans
M		Fraction of high mannose glycans
Hy		Fraction of hybrid glycans
A1		Fraction of N3 glycans (non-hybrid)
A2aF		Afucosylation of diantennary glycans
A2B		Bisection of diantennary glycans
A2G		Galactosylation per antenna of diantennary glycans
A2Ga		α 1,3-galactosylation per antenna of diantennary glycans
A2GGa		α 1,3-galactosylation per β -galactose of diantennary glycans
A2S		Sialylation per antenna of diantennary glycans
A2GS		Sialylation per β -galactose of diantennary glycans
S2Sa		Fraction of Neu5Ac on disialylated, diantennary glycans

^a The depictions of the derived traits show the minimally required composition to contribute to a trait. Symbols used: green circle: mannose, yellow circle: galactose, blue square: *N*-acetylglucosamine, red triangle: fucose, white diamond: *N*-glycolylneuraminic acid (Neu5Gc), pink diamond: *N*-acetylneuraminic acid (Neu5Ac). For exact calculations per IgG subclass, see Table S3 in Supplementary Material.

(both 0.2%), and on IgG2b for BALB/c (0.6%) as compared to CD-1 and Swiss Webster (0.2% and 0.1%; **Table S6** and **Figure S6** in Supplementary Material).

No significant differences were found between the strains for the glycosylation traits on IgG1i, likely due to a reduced statistical power as IgG1i was only present in five of the studied CD-1 and six of the studied Swiss Webster mice. However, the IgG1i derived glycosylation traits followed the trends observed for the IgG2 and IgG3 traits between the strains (**Table 7.3**, **Table S6** in Supplementary Material). None of the derived glycosylation traits appeared to be different between CD-1 and Swiss Webster.

Table 7.3 Fold differences in the derived glycosylation traits between the strains.

Derived trait ^a	C57BL/6 / BALB/c ^b	CD-1 / BALB/c	SW / BALB/c	CD-1 / C57BL/6	SW / C57BL/6	CD-1 / SW
IgG1						
A2B	n.d.	0.22	0.27	n.d.	n.d.	1.22
A2GS	n.d.	0.68	0.75	n.d.	n.d.	1.10
IgG2b						
Hy	0.56	0.29	0.20	0.53	0.36	0.69
A1	0.56	1.33	1.08	2.36	1.92	0.82
A2aF	0.80	1.09	0.96	1.35	1.20	0.88
A2B	0.74	0.29	0.24	0.39	0.33	0.84
A2S	1.14	0.75	0.82	0.66	0.72	1.09
A2GS	1.10	0.80	0.87	0.73	0.79	1.08
S2Sa	0.36	0.55	0.37	1.53	1.03	0.68
IgG2a/c						
Hy	0.98	0.23	0.19	0.23	0.19	0.83
A2aF	1.27	0.71	0.75	0.56	0.59	1.05
A2B	1.92	0.23	0.20	0.12	0.10	0.87
A2G	1.39	1.02	1.06	0.74	0.76	1.04
A2Ga	1.93	0.98	0.98	0.51	0.51	1.00
A2S	2.33	1.16	1.46	0.50	0.63	1.27
A2GS	1.65	1.09	1.26	0.66	0.76	1.15
IgG3						
A1	1.18	0.72	0.73	0.61	0.62	1.01
A2B	2.63	1.19	1.36	0.45	0.52	1.14
A2G	1.10	0.81	0.79	0.74	0.72	0.97
A2S	1.14	0.73	0.77	0.64	0.68	1.06

^a For an explanation of the derived traits, see **Table 7.2** and **Table S3** in Supplementary Material. ^b Presented values indicate the fold difference between the group medians of strain A / strain B (indicated above each column). Values in **bold**: statistically significant, n.d.: not determined.

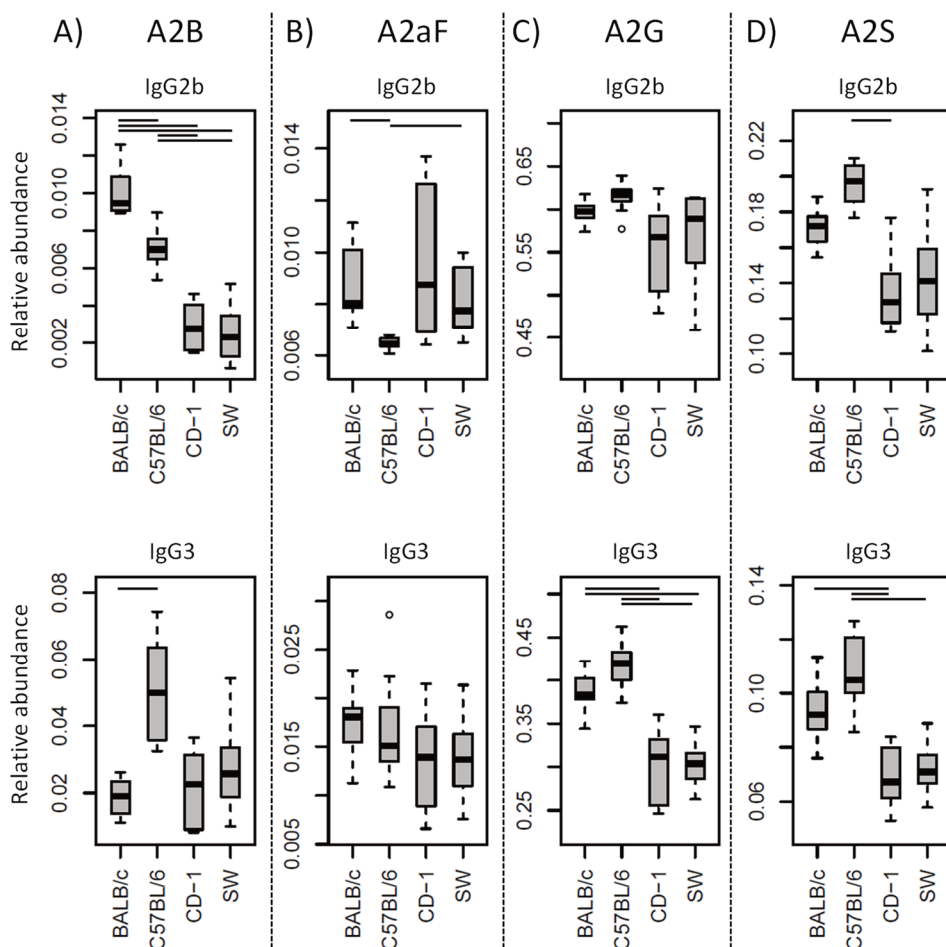


Figure 7.3 Differences in the relative abundances of glycosylation traits between strains. Relative abundances of the derived glycosylation traits (A) bisection (A2B), (B) afucosylation (A2aF), (C) galactosylation (A2G) and (D) sialylation (A2S) on IgG2b and IgG3 for the four different mouse strains: BALB/c, C57BL/6, CD-1 and Swiss Webster (SW). Significant differences between strains are indicated by black lines above the boxes. Boxes represent the interquartile range (IQR) and median value, whiskers represent the first and the third quartiles respectively minus or plus 1.5 times the IQR.

7.3.3 Subclass-specific glycosylation

Glycosylation differences between subclasses were assessed for the 40 mice of the combined strains using the Mann-Whitney U test (Table 7.4, Table S7 in Supplementary Material). In addition, all glycosylation differences between the subclasses were

confirmed by the analysis of the four pooled plasma samples (**Figure S8** in Supplementary Material).

Table 7.4 Fold differences in the derived glycosylation traits between the IgG subclasses.

Derived trait ^a	IgG1i / IgG1 ^b	IgG2b / IgG1	IgG2a/c / IgG1	IgG3 / IgG1	IgG2b / IgG1i	IgG2a/c / IgG1i	IgG3 / IgG1i	IgG2a/c / IgG2b	IgG3 / IgG2b	IgG3 / IgG2a/c
Hy	1.09	0.35	0.42	n.d.	0.32	0.38	n.d.	1.18	n.d.	n.d.
A1	2.66	0.40	0.82	1.89	0.15	0.31	0.71	2.05	4.73	2.30
A2aF	0.87	0.39	0.47	0.77	0.45	0.54	0.89	1.20	1.97	1.64
A2B	0.39	0.20	0.24	0.98	0.51	0.62	2.51	1.22	4.95	4.04
A2G	0.76	1.77	1.38	1.04	2.33	1.82	1.37	0.78	0.59	0.75
A2Ga	3.04	2.13	1.70	2.37	0.70	0.56	0.78	0.80	1.11	1.39
A2GGa	3.33	1.26	1.19	2.05	0.38	0.36	0.62	0.94	1.63	1.73
A2S	0.53	1.53	0.89	0.78	2.90	1.67	1.46	0.58	0.51	0.88
A2GS	0.83	0.91	0.68	0.79	1.10	0.82	0.95	0.75	0.87	1.16

^a For an explanation of the derived traits, see **Table 2** and **Table S3** in Supplementary Material.

^b Presented values indicate the fold difference between the group medians of IgG A / IgG B (indicated above each column). Values in **bold**: statistically significant, n.d.: not determined.

One of the most noticeable differences between subclasses was the level of A2G, which proved highest on IgG2b (median 60%), followed by IgG2a/c (47%), IgG3 (35%) and IgG1 (34%), and IgG1i (26%; **Figure 7.4A**). A2S showed a similar pattern, being highest on IgG2b (17%) followed by IgG1 (11%), IgG2a/c (9.6%) and IgG3 (8.4%), and IgG1i (5.7%; **Figure 7.4B**). Also the sialylation per galactose (A2GS) was not the same for all subclasses, namely higher on IgG1 (31%) and IgG2b (28%) as compared to IgG3 (24%) and IgG2a/c (21%; **Figure 7.4C**). This effect could specifically be attributed to BALB/c, which showed low IgG2a/c A2GS (18%) and high IgG1 A2GS (40%, **Table S8** in Supplementary Material).

For the overall sample set, the abundance of A2aF was higher for IgG1 (2.0%), IgG1i (1.7%) and IgG3 (1.5%) than for IgG2a/c (0.9%; **Figure 7.4D**). Furthermore, A2B, was consistently low on both IgG2 isotypes (IgG2b: 0.5%, IgG2a/c: 0.7%), as well as on IgG1i (1.0%), compared to IgG1 (2.7%) and IgG3 (2.6%; **Figure 7.4E**). The presence of α 1,3-galactosylation on diantennaries (A2Ga) was relatively constant over all subclasses (IgG2a/c: 0.7%, IgG2b: 0.8%, IgG3: 0.9% and IgG1i: 1.2%), except on IgG1 (0.4%), on which it was significantly lower than on all others (**Figure 7.4F**). This effect was even more pronounced when studied for BALB/c specifically (IgG1: 0.4% and e.g. IgG2b: 0.9%; **Table S8** in Supplementary Material).

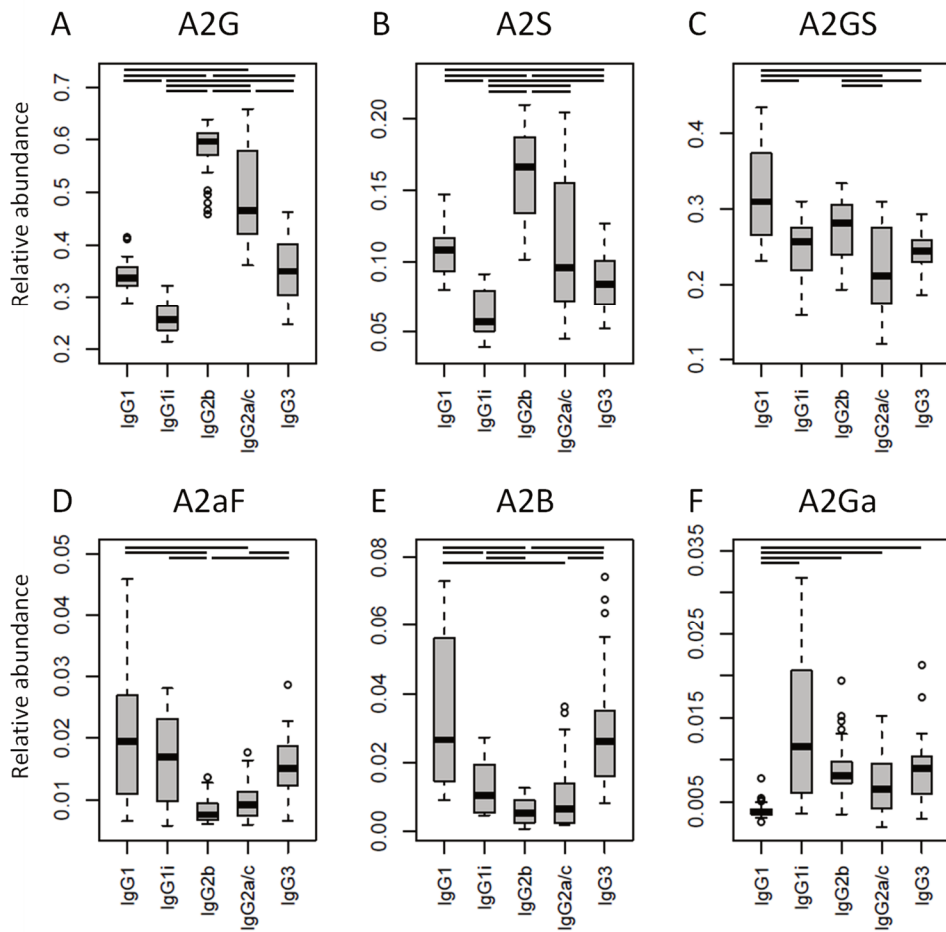


Figure 7.4 Differences in the relative abundances of glycosylation traits between the IgG subclasses. Relative abundances of the derived glycosylation traits (A) galactosylation (A2G), (B) sialylation (A2S), (C) sialylation per galactose (A2GS), (D) afucosylation (A2aF), (E) bisection (A2B), and (F) α 1,3-galactosylation (A2Ga) on the different IgG subclasses studied for the 40 individual mice of all strains. Significant differences between subclasses are indicated by black lines above the boxes. Box and whisker plots as described in Figure 7.3.

7.4 Discussion

In this research we present, to our knowledge, the most in-depth characterization of mouse IgG Fc glycosylation conducted to date. Next to thorough IgG glycoform characterization, we provide the subclass-specific comparison of the IgG Fc glycosylation of several commonly used mouse strains. Previous studies into the characterization of

mouse IgG glycosylation made use of enzymatically released glycans from isolated IgG, losing both Fc and subclass-specificity [42, 307]. Here, IgG Fc glycosylation profiling was achieved in a subclass-specific way by analyzing tryptic glycopeptides by nanoLC-MS(/MS). The methodology was reported before, but never applied to multiple mice of different strains and sexes [44]. We included in our study five male and five female mice of the commonly used strains BALB/c, C57BL/6, CD-1 and Swiss Webster. On top of the nanoLC-MS(/MS) method, we used two additional techniques for the in-depth characterization of the released IgG *N*-glycans, namely MALDI-TOF(/TOF)-MS(/MS) and UPLC-fluorescence.

7.4.1 Detected glycoforms

Consistent with literature, our methods revealed the presence of mainly fucosylated, diantennary glycans with zero to two galactoses and sialic acids [42, 44, 307]. The sialic acids were predominantly found as α 2,6-Neu5Gc, but the presence of minor amounts of α 2,6-Neu5Ac was detected as well. As CMP-Neu5Ac is the precursor for the CMP-Neu5Gc synthesis the presence of this substrate may be assumed in murine plasma cells [310]. Next to α 2,6-Neu5Gc, also α 2,3-Neu5Gc was present in low abundances, although this feature could not be assigned to the Fc portion specifically, as the sialic acid linkage-differentiation was only achieved on the released glycan level (**Figure 7.1**). Furthermore, on the released glycan level, we performed with UPLC-fluorescence a relative quantification of α 1,6-antenna galactosylation, as compared to the α 1,3-antenna galactosylation for monogalactosylated glycans. The α 1,6-antenna showed to be preferably galactosylated, consistent with literature on both human and mouse IgG glycosylation [42, 74]. Interestingly, the α 1,6-antenna preference was lower for the sialylated H4N4F1G1 as compared to nonsialylated H4N4F1, which might be explained by steric constraints of the α 1,6-antenna availability for processing as soon as it is galactosylated [311]. On the other hand, this ratio might be influenced by varying distributions of these glycoforms over the subclasses, in combination with unequal IgG subclass abundances.

The presence of afucosylated diantennaries as well as that of a bisecting GlcNAc on the diantennaries is well-known for human IgG-Fc [25, 74, 84, 176], but has not yet been reported in an Fc specific way for mouse IgG before [44]. Interestingly, we identified both afucosylation and bisection on all IgG subclasses. The enzyme catalyzing the addition of a bisecting GlcNAc to the β -mannose in the *N*-glycan core, GlcNAc-transferase III, was reported to be expressed in human B lymphocytes [312] and murine brain and kidney tissues [313, 314], making the bisection on mouse IgG-Fc not unimaginable. In addition, both bisection and afucosylation were reported before for glycans released from isolated murine IgG [42].

Whereas α 1,3-galactosylation was previously only reported on monoclonal IgG produced in the mouse cell-lines SP2/0 and J558L [306, 308], we here demonstrate its presence on polyclonal murine IgG-Fc. α 1,3-Galactosylation is immunogenic in human, in which the α 1,3-galactosyltransferase is not functionally expressed [315]. For mice, α 1,3-galactosylation is a known glycosylation feature [43].

Next to the diantennary glycan variants described, also high-mannose, hybrid and monoantennary structures were identified specifically on the mouse Fc. Where monoantennary glycans were already reported on murine IgG before, both high mannoses and hybrids were not [42]. These glycoforms can be expected as they are precursors of the complex diantennary glycans [316].

7.4.2 Strain and subclass differences

Interestingly, not all IgG subclasses were detected equivalently between the mouse strains and even individuals. We revealed the presence of IgG2b and IgG3 in all mice studied. However, the inbred BALB/c and C57BL/6 mice respectively expressed only IgG1 or IgG1i, while several individuals of outbred CD-1 and Swiss Webster mice showed both isotypes at the same time, which would suggest IgG1 and IgG1i to be allelic variants. This situation was prior reported for IgG2a and IgG2c showing IgG2a to be exclusively present in BALB/c and IgG2c in C57BL/6 [44, 301]. However, we were not able to assess this, as the tryptic digestion of IgG2a and IgG2c resulted in the same glycopeptides which were detected in all mice.

When comparing the glycosylation traits between the strains, we observed galactosylation and sialylation to have a lower variation between the individual mice of BALB/c and C57BL/6, as compared to CD-1 and Swiss Webster. As outbred strains are expected to have a wider genetic background than inbred strains, this suggests that there is a strong genetic influence on IgG Fc glycosylation [255, 293, 294]. Next to the genetics, also environmental factors might play a role in the differences between the strains, like exposure to pathogens and health status. For example, the high levels of IgG1 bisection and afucosylation and low levels of IgG1 galactosylation in BALB/c mice, as compared to the other strains in this study, may well represent a more proinflammatory phenotype [193, 304, 317].

The difference in variation between the mouse strains was observed before in the analysis of the murine total plasma *N*-glycome [298]. Diantennary, fucosylated glycans in the total plasma *N*-glycome, for healthy humans known to be almost exclusively derived from IgG [299], showed a larger biological variation in the strains CD-1 and Swiss Webster as compared to C57BL/6 and BALB/c. To the contrary, whereas for the total IgG glycans in the total plasma *N*-glycome a clear difference was observed between male and female CD-

1 and Swiss Webster mice, this was not the case in the current IgG subclass specific glycopeptide analysis. This might be explained by an interplay between, on the one hand, IgG subclass abundances between the sexes, and on the other hand, glycosylation differences between the IgG subclasses. In addition, other, hitherto unidentified glycoproteins than IgG that show a pronounced sex-specificity may overlap with the IgG glycans in the total plasma *N*-glycome. Other sex-related glycosylation differences observed in the total plasma *N*-glycome study are in glycans that are derived from proteins other than IgG and might indeed have a sex-influenced glycosylation pattern.

Both galactosylation and sialylation of IgG Fc glycans are established traits involved in the anti-inflammatory activity of IgG [186, 202, 318]. On the one hand, sialylation has been reported to dampen immune responses in an antigen-independent way by binding SIGN-R1 (mouse) and DC-SIGN (human) [58, 200], is suggested to be involved in the inhibition of B-cell activation in mice [319] and is in addition able to decrease complement-mediated cytotoxicity via C1q binding [56]. An increased galactosylation, on the other hand, causes improved binding of mouse IgG1 to the FcγRIIB and subsequent downregulation of proinflammatory activities [186]. Of note, the latter phenomenon is observed for IgG1, but not for IgG2a, emphasizing the differences between the IgG subclasses [186].

Another trait known to influence antibody activity in both humans and mice is afucosylation. An increased afucosylation on human IgG1 and murine IgG2a and IgG2b is known to result in an improved binding to specific FcγRs (FcγRIII in humans and FcγRIIB and FcγRIV in mice) and thereby increasing antibody-dependent cellular cytotoxicity (ADCC) [47, 304]. Similar to the galactosylation described above, it is relevant to study afucosylation in a subclass-specific way to predict its effect. As IgG subclasses have varying binding affinities for the FcγRs, differential afucosylation can alter the ratio between activating and inhibiting FcγR stimulation. For example, the *in vivo* effect of mouse IgG2b afucosylation on ADCC is larger than that of IgG2a [304].

7.4.3 Translation of murine IgG-Fc glycosylation to the human system

In terms of glycan structures identified, our mouse data match the glycoforms reported on human IgG-Fc to a large extent, but several pronounced and relevant difference were also observed. One example of this is the earlier-reported difference between the most abundant sialic acid structure, namely Neu5Gc in the mouse and Neu5Ac in man [42, 44, 45, 307], and another is the alternative termination of murine glycans by α1,3-galactosylation instead of (or next to) sialylation. Both factors are important in assessing the suitability of mice for immunological studies, as they might change the interaction between IgG-Fc and effector proteins. For example, it was shown that not the mouse sialic acid-binding Ig-like lectin CD22, but only the human CD22 is able to bind Neu5Ac on intravenous immunoglobulin [45, 46].

Of importance for interpretation of the data is that mouse IgG-subclass nomenclature does not match that of humans, human IgG1 and IgG3 are often directed against protein antigens, while for mice this is the case for IgG2a and IgG2b [22, 320]. In addition, human IgG4 is similar to mouse IgG1 in its involvement in responses to allergens and mast-cell binding, and human IgG2 is similar to mouse IgG3 in the recognition of carbohydrate antigens [22, 320, 321]. Furthermore, the affinity for FcγRs is not consistent between mouse and human IgG subclasses, as human IgG1 has a broad affinity for all FcγRs, while for the mouse this is achieved by IgG2a and IgG2b [185, 322]. In addition, the inhibitory FcγRIIB binds in mice to IgG1, 2a and 2b, while in human it binds to IgG1, 3 and 4 [300].

The mice we studied were aged between eight and twelve weeks and considered young adults [323]. Comparing their IgG2b and IgG2a/c galactosylation to that found previously on IgG1 in healthy human between 20 and 40 years, similar levels were observed [28]. The other murine IgG subclasses showed considerably lower levels of galactosylation. The murine IgG2a/c and 2b sialylation, on the other hand, was found to be high in mice, as compared to overall human IgG Fc sialylation. In addition, the overall bisection and afucosylation were lower on all subclasses in mice than in humans [28, 74]. This latter finding might be related to the infrequent immunological challenges lab mice experience. The same phenomenon was observed before in very young children (aged between 0.3 and 4 years), showing low levels of afucosylated IgGs, which increased with age (and likely immunological challenges) [176]. In addition, high levels of afucosylated antibodies were observed before in human on antigen specific antibodies against, amongst others, HIV gp120, human platelet antigen and red blood cells [98, 99, 291]. Interestingly, the mice showed no differences for the Fc glycosylation features between the sexes. This is different from what is known for human (young) adult IgG glycosylation, where significant differences were reported for IgG Fc galactosylation and sialylation [28].

7.5 Conclusion

We report pronounced differences of IgG Fc glycosylation in mice between both subclass and strains. Especially galactosylation and sialylation showed a large variation in their abundance. In addition, the levels of hybrid structures, α1,3-galactosylation, afucosylation and bisection, all not previously reported on murine IgG in an Fc specific way, showed to differ between the subclasses and strains. Noticeable variations were observed for the murine Fc glycosylation, as compared to prior-reported human Fc glycosylation, for example in terms of sialic acids present (respectively Neu5Gc and Neu5Ac in mice and humans). Also levels of glycosylation traits that are recognized as important immune modulators, including galactosylation, sialylation, afucosylation and bisection deviated between humans and mice. When considering mouse models for immunological research,


a careful selection should be made both on the mouse strain and on the IgG subclasses used, taking into account the baseline glycosylation profiles and biological engagement.

Acknowledgements

This work was supported by the European Union Seventh Framework Programmes IBD-BIOM (grant number 305479) and HighGlycan (grant number 278535).

Supporting Information available

Additional information is available as stated in the text. This information is available free of charge via <https://www.frontiersin.org/articles/10.3389/fimmu.2017.00608/full>.



¹ *Leiden University Medical Center, Center for Proteomics and Metabolomics,
Leiden, The Netherlands*

Comparative Glycomics of Immunoglobulin A and G from Saliva and Plasma Reveals Biomarker Potential

**Rosina Plomp^{1, #}, Noortje de Haan^{1, #}, Albert Bondt¹, Jayshri Murli¹,
Viktoria Dotz¹ and Manfred Wuhrer¹**

Authors contributed equally

Reprinted and adapted from Front. Immunol. 9:2436. DOI: 10.3389/fimmu.2018.02436 [324].

Copyright © 2018, Plomp, de Haan, Bondt, Murli, Dotz and Wuhrer.



The *N*-glycosylation of immunoglobulin (Ig) G, the major antibody in the circulation of human adults, is well known for its influences on antibody effector functions and its alterations with various diseases. In contrast, knowledge on the role of glycans attached to IgA, which is a key immune defense agent in secretions, is very scarce. In this study we aimed to characterize the glycosylation of salivary (secretory) IgA, including the IgA joining chain (JC) and secretory component (SC) and to compare IgA and IgG glycosylation between human plasma and saliva samples to gain a first insight into oral cavity-specific antibody glycosylation.

Plasma and whole saliva were collected from 19 healthy volunteers within a two-hour time window. IgG and IgA were affinity-purified from the two biofluids, followed by tryptic digestion and nanoLC-ESI-QTOF-MS(/MS) analysis.

Saliva-derived IgG exhibited a slightly lower galactosylation and sialylation as compared to plasma-derived IgG. Glycosylation of IgA1, IgA2 and the JC showed substantial differences between the biofluids, with salivary proteins exhibiting a higher bisection, and lower galactosylation and sialylation as compared to plasma-derived IgA and JC. Additionally, all seven *N*-glycosylation sites, characterized on the SC of secretory IgA in saliva, carried highly fucosylated and fully galactosylated diantennary *N*-glycans. This study lays the basis for future research into the functional role of salivary Ig glycosylation as well as its biomarker potential.

8.1 Introduction

Using saliva for diagnostic purposes has gained increasing popularity due to its various advantages over plasma or serum. First, saliva can be easily and painlessly collected from donors without the need for specialized equipment or training. Second, next to proteins derived from serum (ca. 27% of total salivary proteins), saliva also contains locally produced proteins which might reflect diseases that affect the oral cavity, such as Sjögren's syndrome, or oral cancer [325-327]. Saliva assays are already available on the market, e.g. for the detection of antibodies against HIV [325]. Moreover, numerous potential salivary protein-, DNA-, RNA-, and small-molecule-based biomarkers for various diseases have been proposed, as recently reviewed [328]. Furthermore, two studies using global lectin-based profiling of glycans in saliva revealed associations with breast cancer and Sjögren's syndrome [329, 330].

Glycosylation is a prevalent posttranslational modification which heavily influences the structure and function of proteins, as is well known for plasma-derived immunoglobulin (Ig) G. The glycosylation of the fragment crystallizable (Fc) portion of IgG has been shown to influence binding to Fcγ receptors (FcγRs) and complement factors [37]. Moreover, plasma IgG glycosylation has been associated with various diseases and could, therefore, be exploited for diagnostic and therapeutic approaches in the future [331-333]. In contrast, for other Igs, such as IgA, way less is known about the relationship between their glycosylation and effector functions. Although IgA *N*-glycosylation was shown to influence the IgA transport from circulation to mucosal tissue [334] and the *O*-glycosylation of IgA1 is considered a major factor in the pathogenesis of IgA nephropathy [335], the absence of the Fc *N*-glycosylation of IgA1 had no effect on FcαR binding [336]. Site-specific investigation of antibody glycosylation in human samples other than plasma has been limited to cerebrospinal fluid and synovial fluid for IgG [337, 338] and colostrum for IgA [339, 340]. The glycosylation of saliva-derived IgG and IgA has only been crudely examined using lectin binding assays, and without a direct comparison to blood [341, 342].

The lack of knowledge about salivary antibody glycosylation is mainly due to the fact that the antibody concentrations are much lower than in plasma, posing a major challenge for their in-depth characterization. Plasma contains approximately 12.5 mg/mL IgG and 2.2 mg/mL IgA, while the concentrations for unstimulated whole saliva are estimated at approximately 0.014 mg/mL and 0.19 mg/mL for IgG and IgA, respectively [343, 344]. Salivary IgG is thought to mainly be derived from circulation, while a minority (< 20%) is produced by local plasma cells in gingival lesions or salivary glands [343, 345]. In contrast, more than 95% of salivary IgA is produced locally by plasma cells in various glands, where it can form a dimeric complex via the associated joining chain (JC) [346]. Secretion of dimeric IgA across the epithelial layer is enabled by the polymeric Ig receptor (pIgR), of which a part remains bound to the IgA and is known as the secretory component (SC). As a

consequence, secretory (S)IgA as a complex of dimeric IgA covalently linked to the JC and SC (**Figure 8.1**), makes up for more than 80% of the salivary IgA pool, while plasma IgA is predominantly (~90%) monomeric [343, 347]. In addition, the ratio between IgA1 and IgA2 is dependent on the source of IgA: while saliva contains approximately 35% IgA2, around 20% IgA2 is found in serum [343, 347]. In contrast to IgG, which only contains one, or two in the case of some IgG3 variants [23], *N*-glycosylation sites at the constant domain, the IgA1 and IgA2 constant domains contain two up to five potential *N*-glycosylation sites, respectively, and IgA1 carries up to six *O*-glycans in the hinge region [177, 348] (**Figure 8.1**). In addition, the JC has one *N*-glycosylation site and the SC seven (**Figure 8.1**). This further complicates detailed (S)IgA glycosylation analysis. However, in recent years great progress has been made with respect to both measurement sensitivity and data analysis tools in the field of glycoproteomics, facilitating site-specific glycosylation analysis of minute amounts of Igs [133, 198, 349, 350].

Here, we developed a method for the analysis of IgG and (S)IgA glycosylation in whole saliva using bead-based affinity chromatography purification, followed by tryptic digestion and analysis with nano liquid chromatography (nanoLC)-electrospray ionization (ESI)-quadrupole time-of-flight (QTOF)-mass spectrometry (MS). The method can be used in a 96-well plate format and was applied to characterize and compare the glycosylation of both IgG and (S)IgA in saliva and plasma of 19 healthy individuals. To the best of our knowledge we are the first to report site-specific glycoprofiling of antibodies in saliva.

8.2 Material and Methods

8.2.1 Collection of biofluids and preprocessing

Nineteen healthy donors (18 Caucasians and 1 of South Asian ancestry) were recruited to donate blood and saliva. The study population included 13 females and 6 males, with an average age of 28.4 years (range: 20-42). All donors gave informed consent, and the study was approved by the Medical Ethics Commission of the Leiden University Medical Center (P16.189). Both biofluids were collected between 10:30 A.M. and 12:30 P.M. on the same day. Donors were instructed to rinse their mouth with water an hour prior to collection of saliva and abstain from food and beverages until sample collection was finished. Saliva was collected by unstimulated drooling into a 5-mL Eppendorf tube for approximately 10 min, and immediately frozen at -20 °C. Subsequently, 10 mL of venous blood was collected in an EDTA vial. The blood was centrifuged at $3184 \times g$ for 5 min and the clear upper fraction, consisting of plasma, was collected and frozen at -20 °C.

Saliva samples underwent a preprocessing step to reduce viscosity: After thawing, the samples were centrifuged at $3184 \times g$ at 4 °C for 30 min. Four hundred μ L of supernatant

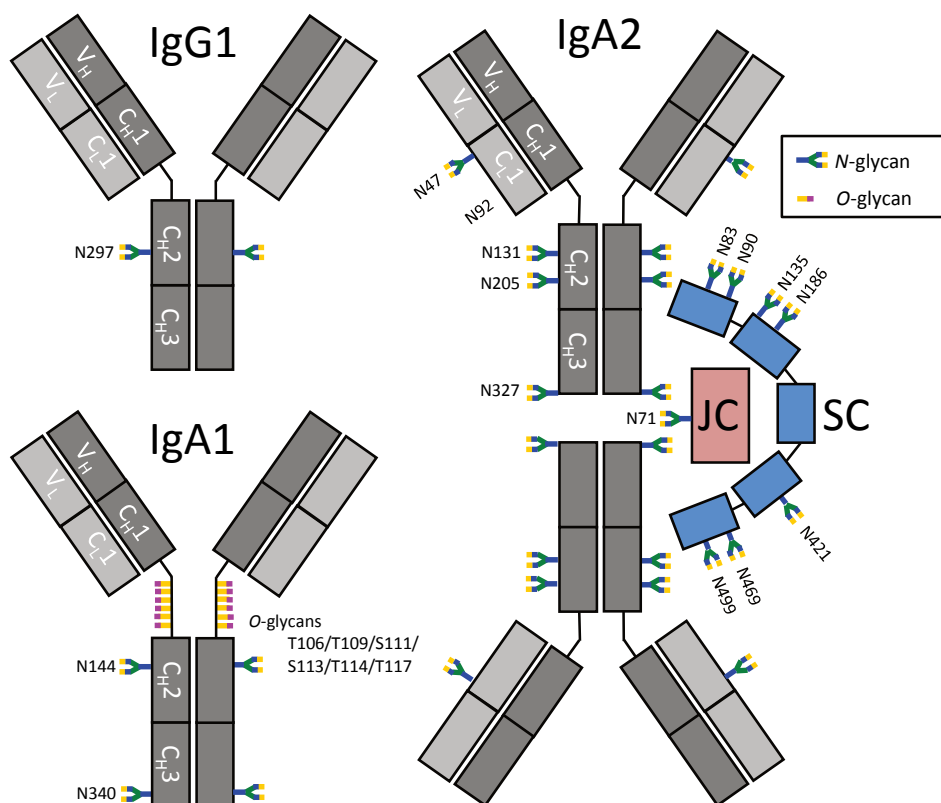


Figure 8.1 Schematic representation of IgG1, IgA1 and SIgA2 and their glycosylation sites. IgA2 is shown in its dimeric form, in a complex with a joining chain (JC; red) and a secretory component (SC; blue). The JC and SC are covalently linked to IgA by disulfide bonds (not shown). Each Ig monomer is composed of two heavy chains (dark grey) and two light chains (light grey), again connected by disulfide bonds. The chains are further subdivided as constant (C) and variable (V) domains. N-glycosylation sites on IgG are indicated by their amino acid number according to the nomenclature used by conventional literature, e.g. [177], while IgA, the JC and SC have UniProt numbering [309]. N92 on IgA2 was previously reported to be glycosylated, however, N92 on the IgA2 allotype found in our samples (A2m(1)) was not incorporated in a N-glycosylation consensus sequence and was found to be non-glycosylated.

was collected from each sample and dispersed over 4 aliquots of 100 μ L (for IgG and IgA purification each in duplicate), which were added to a 96-well filter plate with a 10 μ m pore frit (Orochem, Naperville, IL). The samples were centrifuged at 200 $\times g$ for 1 min, and flow-throughs were used for IgG and IgA affinity purification immediately after.

8.2.2 Purification and digestion of immunoglobulins from donor plasma and saliva

IgG and IgA were each purified in duplicate on separate plates using affinity bead chromatography, based on a protocol described previously [29]. For IgG purification, 15 μ L of Protein G Sepharose 4 Fast Flow beads (GE Healthcare, Uppsala, Sweden) were added per well on an Orochem filter plate and washed three times with phosphate-buffered saline (PBS). For IgA purification, the same procedure was followed using 2 μ L CaptureSelect IgA Affinity Matrix beads (Thermo Fisher Scientific, Breda, The Netherlands). For IgG purification, either 100 μ L of saliva or 2 μ L of plasma was added to each well, while 100 μ L of saliva or 5 μ L of plasma was used for IgA purification. Sample volumes were brought to a total of 200 μ L by the addition of PBS. The plates were incubated for 1 h while shaking at 750 rpm with 1.5 mm orbit (Heidolph Titramax 100; Heidolph, Kelheim, Germany) to accommodate binding.

Using a vacuum manifold, the samples were washed 3 times by adding 400 μ L PBS, followed by 3 times 400 μ L of MilliQ-purified water (Purelab Ultra, maintained at 18.2 M Ω ; Veolia Water Technologies Netherlands B.V., Ede, The Netherlands). The antibodies were eluted from the beads by adding 100 μ L of 100 mM formic acid (Sigma-Aldrich, Zwijndrecht, The Netherlands), incubating for 5 min at 750 rpm, and centrifuging at 100 \times g for 2 min. Samples were dried for 2 h at 60 $^{\circ}$ C in a vacuum centrifuge.

The IgG samples were resolubilized in 20 μ L 50 mM ammonium bicarbonate (Sigma-Aldrich) while shaking for 5 min at 750 rpm. Twenty μ L of 0.05 μ g/ μ L tosyl phenylalanyl chloromethyl ketone (TPCK)-treated trypsin (Sigma-Aldrich) in ice-cold MilliQ-purified water was added per well, and the samples were incubated at 37 $^{\circ}$ C overnight.

In contrast to tryptic IgG digestion to obtain Fc glycopeptides, IgA molecules need to be reduced and alkylated prior to digestion to obtain peptides covering all glycosylation sites. IgA samples were resolubilized in 30 μ L 30 mM ammonium bicarbonate, 12.5% acetonitrile (Biosolve, Valkenswaard, the Netherlands) while shaking for 5 min at 750 rpm. Subsequently, 5 μ L of 35 mM dithiothreitol (Sigma-Aldrich) was added, followed by 5 min incubation at room temperature on a shaker (750 rpm) and 30 min incubation at 60 $^{\circ}$ C in an oven. After cooling to room temperature, 5 μ L of 125 mM iodoacetamide (Sigma-Aldrich) was added and the samples were incubated in the dark while shaking for 30 min. Two μ L of 100 mM dithiothreitol was added to quench the iodoacetamide. Finally, 8 μ L of 0.08 μ g/ μ L TPCK-treated trypsin in ice-cold MilliQ-purified water was added per well, and the samples were incubated at 37 $^{\circ}$ C overnight. Before LC-MS analysis, IgA and IgG samples derived from plasma were diluted twice and 20-times, respectively, with MilliQ-purified water, whereas saliva-derived samples were not diluted. Assuming no losses and prior concentrations of 12.5 mg/mL plasma IgG, 0.014 mg/mL saliva IgG, 2.2 mg/mL plasma IgA and 0.19 mg/mL saliva IgG [343, 344], the concentrations of the final digests

were 0.031 mg/mL, 0.035 mg/mL, 0.110 mg/mL and 0.380 mg/mL for plasma IgG, saliva IgG, plasma IgA and saliva IgA, respectively.

8.2.3 Digestion and *N*-glycan release of IgA samples for MS/MS analysis

For the fragmentation analysis by MS/MS of the IgA glycopeptides, a separate purification and tryptic digestion of IgA was done in triplicate on two saliva samples from two donors from the study described above, a pooled-plasma standard from a minimum of 20 human donors (VisuCon-F Frozen Normal Control Plasma; Affinity Biologicals, Ancaster, Canada), 10 µg of a human plasma-derived IgA standard (Lee Biosolutions, Maryland Heights, MO), and a human colostrum-derived SIgA standard (Athens Research and Technology, Athens, GA). The procedure was similar to what is described above, except that 1 µg trypsin per sample was used instead of 0.64 µg. Twenty µL of trypsin-digested sample was collected and heated to 95 °C to inactivate the trypsin. After cooling to room temperature, 1 µL of *N*-glycosidase F (Roche Diagnostics, Mannheim, Germany) was added and the samples were incubated at 37 °C overnight. The samples obtained from the pooled-plasma standard were diluted twice and the (S)IgA standard samples thrice with MilliQ-purified water, whereas the saliva-derived samples were not diluted.

8.2.4 NanoLC-ESI-QTOF-MS(/MS) analysis

IgG and IgA samples were present on separate plates and measured on different days. Each pair of plasma and saliva sample of the same donor was analyzed successively, but the duplicate pair of the same donor was measured at a later time point. Blanks consisting of MilliQ-purified water were run after every 20 samples. Two hundred nL of each sample was injected into an Ultimate 3000 RSLCnano system (Dionex/Thermo Scientific, Breda, the Netherlands) coupled to a quadrupole-TOF-MS (MaXis HD; Bruker Daltonics, Bremen, Germany). The LC system was equipped with an Acclaim PepMap 100 trap column (particle size 5 µm, pore size 100 Å, 100 µm × 20 mm, Dionex/Thermo Scientific) and an Acclaim PepMap C18 nano analytical column (particle size 2 µm, pore size 100 Å, 75 µm × 150 mm, Dionex/Thermo Scientific). A mixture of solvent A (0.1% formic acid in MilliQ-purified water) and solvent B (95% acetonitrile) was applied with a constant flow of 0.7 µL/min using a linear gradient: t (min) = 0, %B = 3; t = 5, %B = 3; t = 35, %B = 53; with washing and equilibration starting at t = 36, %B = 70; t = 38, %B = 70; t = 39, %B = 3; t = 58, %B = 3. The sample was ionized in positive-ion mode using a CaptiveSprayer (Bruker Daltonics) electrospray source at 1300 V. A nanoBooster (Bruker Daltonics) was used to enrich the nitrogen gas with acetonitrile to enhance ionization efficiency. Mass spectra were acquired with a frequency of 1 Hz and the MS ion detection window was set at mass-to-charge ratio (m/z) 550-1800. Fragmentation by collision-induced dissociation MS/MS used an ion detection window of m/z 50-2800.

8.2.5 Data processing

LC-MS(/MS) data were first examined manually using DataAnalysis (Bruker Daltonics). Glycopeptides were identified based on their m/z and literature (**Supplemental Table S1**) [26, 29, 74, 85, 107, 340, 351-353]. In the following, glycosylation site numbering for IgG is based on conventions commonly used in literature, e.g. [177], and for IgA1, IgA2, the JC and the SC, UniProt numbering is used (**Figure 8.1**)[309]. For each glycopeptide cluster, here defined as a group of glycopeptides sharing the same peptide portion, e.g. IgA2 N205, at least one glycopeptide was characterized by MS/MS fragmentation, elucidating the glycan composition and the identity of the peptide (**Supplemental Figure S1**). In order to provide information on the peptide sequence of the IgA glycopeptides, a proteomics analysis (MASCOT Deamon version 2.2.2; Matrix Science, London, UK) was run on the LC-MS/MS data of the *N*-glycosidase F-digested IgA samples, in which the *N*-glycans had been released. The following settings were used: database: SwissProt (2017_09); taxonomy: *Homo sapiens*; enzyme: trypsin; fixed modifications: carbamidomethyl (C); variable modifications: oxidation (M), deamidated (NQ) and Gln→pyro-Glu (N-term Q); maximal amount of missed cleavages: 2; peptide tolerance MS: 0.05 Da; peptide tolerance MS/MS: 0.07 Da (**Supplemental Table S2**). The peptides covering IgA2 N47 and N92 were not recognized by the software, but could still be manually identified (**Supplemental Figure S2**).

For IgA1/2 N340/N327, two different peptide sequences were identified in *N*-glycosidase F-treated samples: the expected LAGKPTHVNVSVVMAEVDGTCY and the truncated LAGKPTHVNVSVVMAEVDGTC, lacking the C-terminal tyrosine, as described before by Bondt *et al.* [351]. Both of these peptides eluted at two different retention times: a minor peak (< 20%) first, and a higher peak eluting one minute later. The same pattern could be seen in samples that were not treated with *N*-glycosidase F. For data analysis, only the higher, later-eluting peak was included, since the lower peak was often of too low signal quality.

LC-MS data were calibrated in DataAnalysis based on a list of the expected m/z values of either IgG1 N297 or IgA N205 glycopeptides. The data files were then converted to mzXML format using the MSconvert program from the ProteoWizard 3.0 suite. Alignment of the time axis of the data and extraction of glycopeptide signal intensities, based on sum spectra, was done using the in-house developed LacyTools software, with a list of manually compiled glycopeptides and their retention times as input [198]. For signal extraction, area integration was performed within an m/z window of ± 0.05 Th around each isotopic peak (with the minimum theoretical % of signal intensity covered by the sum of the integrated isotopic peaks at 85%) within an individually specified time window surrounding the retention time. This resulted in background-corrected signal areas for each glycopeptide per charge state ($[M+2H]^{2+}$ to $[M+7H]^{7+}$). Whether an analyte was

present in a sample, was determined based on the signal-to-noise ratio (S/N ; > 9), the isotopic pattern quality score (IPQ; < 0.2) and the mass accuracy (< 10 ppm deviation) of each signal per charge state. Data of specific glycopeptide clusters were excluded for further processing when either the total number of analytes detected was $< 50\%$ of the maximum number detected for that cluster, or when the summed absolute intensity of the detected analytes was $< 5\%$ of the maximum sum observed for that cluster. This assessment was performed separately for samples obtained from saliva or plasma. Subsequently, individual analytes were subjected to quality control criteria to determine which were of sufficient quality for relative quantification. Glycopeptides in specific charge states were included for relative quantification if their signal showed a $S/N > 9$, $IPQ < 0.2$ and an absolute mass error < 10 ppm in at least 25% of either all plasma or all saliva samples. Finally, all included charge state signals for the same glycopeptide were summed and absolute abundances were corrected for the fraction of isotopes integrated. The glycopeptide signals were normalized on the total signal intensity per glycopeptide cluster, resulting in the relative quantification of each glycopeptide.

Based on the *N*-glycan monosaccharide compositions, glycoforms were categorized as bisected, high-mannose or hybrid, and, in addition, the number of fucoses, galactoses and sialic acids was determined (**Supplemental Table S1**). This was used for the calculation of several glycosylation features per glycosylation site, based on total-area normalized data. Fucosylation represents the number of fucoses per complex-type *N*-glycan, i.e. $\text{sum}((\text{complex-type species with } n \text{ fucoses}) * n) / \text{sum}(\text{complex-type species})$. Bisection represents the fraction of bisected complex-type *N*-glycans, i.e. the sum of all structures presumed to carry a $\beta 1-4$ -linked *N*-acetylglucosamine (GlcNAc) on the innermost mannose, divided by the sum of all complex-type glycoforms. Galactosylation was calculated as the number of galactoses per complex-type *N*-glycan, i.e. $\text{sum}((\text{complex-type species with } n \text{ galactoses}) * n) / \text{sum}(\text{complex-type species})$. Sialylation was calculated as the number of sialic acids per complex-type *N*-glycan, i.e. $\text{sum}((\text{complex-type species with } n \text{ sialic acids}) * n) / \text{sum}(\text{complex-type species})$. Sialylation/Galactose represents the number of sialic acids per galactose on complex-type species, i.e. sialylation divided by galactosylation. High-mannose represents the fraction of high-mannose type *N*-glycans, i.e. sum of all structures where the core is elongated only by mannoses, while hybrid-type glycans represent the structures that are either hybrid-type or have only one antenna. In addition, for the *O*-glycosylation on IgA1, glycosylation features were defined as follows. #HexNAc represents the number of *N*-acetylhexosamines per *O*-glycopeptide, i.e. $\text{sum}((\text{species with } n \text{ } N\text{-acetylhexosamines}) * n)$. #Hex represents the number of hexoses per *O*-glycopeptide, i.e. $\text{sum}((\text{species with } n \text{ hexoses}) * n)$. #SA represents the number of sialic acids per *O*-glycopeptide, i.e. $\text{sum}((\text{species with } n \text{ sialic acids}) * n)$. Hex/HexNAc represents the number of hexoses per *N*-acetylhexosamine, i.e. #Hex divided by #HexNAc. Finally, SA/Hex represents the number of sialic acids per hexose, i.e. #SA divided by #Hex.

8.2.6 Statistical analysis

From each duplicate pair of samples, the sample with the higher absolute signal intensity per glycopeptide cluster was used for statistical analyses (**Supplemental Table S3**). The IgG and IgA glycosylation features in plasma and saliva originating from the same donor were compared using the Wilcoxon signed rank test (wilcox.test function from the MASS package) in R (v3.1.2; R Foundation for Statistical Computing, Vienna, Austria [354]) and RStudio (v0.98.1091; RStudio, Inc.; **Supplemental Table S4**). Correlation analysis was performed between the saliva and plasma samples using the cor.test function from the R stats package (use=pairwise.complete.obs, method=spearman) to obtain the correlation coefficient (rho) and associated *p*-value (**Table 8.1**). The Wilcoxon signed rank test and correlation analysis were only performed when data from at least 11 paired (plasma and saliva from the same donor) samples were available, which was the case for IgG1 N297, IgG2/3 N297, IgG4 N297, IgA2 N205 and IgA2 N47. Bonferroni correction was performed to account for multiple testing, resulting in a *p*-value threshold for significance of $0.05/28 = 0.00179$. Graphs were created either in Microsoft Excel 2010 or Graphpad Prism 7.

Table 8.1 Correlation of derived glycan traits between saliva and plasma samples as shown by the Spearman's correlation coefficient (rho) and associated *p*-values. The numbers of included pairs are listed under 'N_{pair}'. *p*-values significant after Bonferroni correction are shown in bold ($\alpha = 1.79 \times 10^{-3}$). The correlation for IgA1/2 N144/131 and N340/327, JC N71, the SC *N*-glycosylation and the IgA1 *O*-glycosylation was not assessed because this data was present for less than 11 paired samples (plasma and saliva from the same individual).

protein	site	peptide	N _{pair}	Fucosylation		Bisection		Galactosylation		Sialylation		Sialic acid/ galactose	
				rho	<i>p</i> -value	rho	<i>p</i> -value	rho	<i>p</i> -value	rho	<i>p</i> -value	rho	<i>p</i> -value
IgG1	N297	EEQYNSTYR	17	0.973	4.7E-06	0.877	< 1E-07	0.627	0.0084	0.843	9.7E-07	0.961	4.6E-07
IgG2/3	N297	EEQFNSTFR	17	0.716	0.0017	0.936	< 1E-07	0.699	0.0025	0.748	8.4E-04	0.885	< 1E-07
IgG4	N297	EEQFNSTYR	12	NA	NA	0.965	< 1E-07	0.706	0.013	0.762	0.0059	0.434	0.16
IgA2	N205	TPLTANITK	16	0.232	0.39	0.474	0.066	-0.0529	0.85	0.191	0.48	0.232	0.39
IgA2	N47	SESGQNVTAR	13	NA	NA	0.412	0.16	-0.242	0.43	0.181	0.55	0.423	0.15

8.3 Results

Paired plasma and saliva samples were collected from 19 healthy donors. From these samples, IgG and IgA were separately purified in duplicate using bead-based affinity chromatography. Samples were trypsin-digested and analyzed by nanoLC-ESI-QTOF-MS. Glycopeptides were identified on the basis of the registered *m/z*, tandem mass spectrometric analyses as well as literature information on immunoglobulin glycosylation

(**Supplemental Table S1** and **Supplemental Figure S1** and **S3**). Glycosylation features were calculated for each glycosylation site of IgG, IgA, JC and SC (**Supplemental Table S3**).

8.3.1 IgG *N*-glycosylation

For IgG1 N297, 27 different glycan compositions were quantified in both the plasma and saliva samples. For IgG2/3 N297, also 27 different glycoforms were quantified and 13 for IgG4 N297 (**Supplemental Figure S3A** and **Supplemental Table S1A**). IgG1 and IgG4 derived from saliva showed a slightly lower degree of galactosylation and sialylation as compared to plasma (for example, 1.1 and 1.3 times lower medians for IgG1 and IgG4 galactosylation, respectively). In contrast, high-mannose and hybrid-type glycans were more abundant in salivary IgG1 and IgG2/3, as compared to plasma (for example, 2.7 and 3.4 times higher medians for IgG1 and IgG2/3 high-mannose type glycans, respectively; **Figure 8.2** and **Supplemental Table S4**). For IgG1 and IgG2/3, a significant correlation was observed for the fucosylation, bisection, sialylation and sialylation/galactose between plasma and saliva (**Table 8.1**), showing the similarities in glycosylation features between the two biofluids to be conserved across the different donors. IgG4 showed similar behavior (**Table 8.1**).

8.3.2 IgA *N*-glycosylation

For IgA2 N205 and N47, 15 and 10 different glycoforms were quantified, respectively, in both the saliva and the plasma samples (**Supplemental Figure S3B** and **Supplemental Table S1B**). The *N*-glycans were of the complex-type and mainly diantennary (> 98% of total abundance). Two to five fold differences were observed in the relative abundances of the different glycan types present on plasma- vs. saliva-derived IgA2: salivary *N*-glycans at both N205 and N47 showed a higher degree of bisection and a lower degree of galactosylation, sialylation and sialylation/galactose (**Figure 8.2** and **Supplemental Table S4**). None of the tested glycosylation traits on IgA2 showed a significant correlation between plasma and saliva samples (**Table 8.1**). Of note, for IgA2 *N*-glycosylation site N47 a truncated glycopeptide, i.e. (W)SESGQN₄₇VTAR(N), was registered. This peptide features a tryptic C-terminal cleavage while the *N*-terminus stems from a chymotryptic cleavage site. The predicted tryptic peptide (K)VFPLSLDSTPQDNVVVACL VQGFFPEPLSVT WSESGQN₄₇VTAR(N) was not observed.

The glycopeptides with the peptide moieties LAGKPTHVNVSVVMAEVDGTCY and LAGKPTHVNVSVVMAEVDGTC (truncated; t) were assigned to both IgA1 and IgA2 covering the glycosylation sites N340 and IgA2 N327, respectively, as these peptide portions are common to both IgA subclasses (**Supplemental Table S2**). The previously reported sequence variant of IgA2 N327, MAGKPTHIN₃₂₇VSVVMAEADGTC(Y), was not observed in

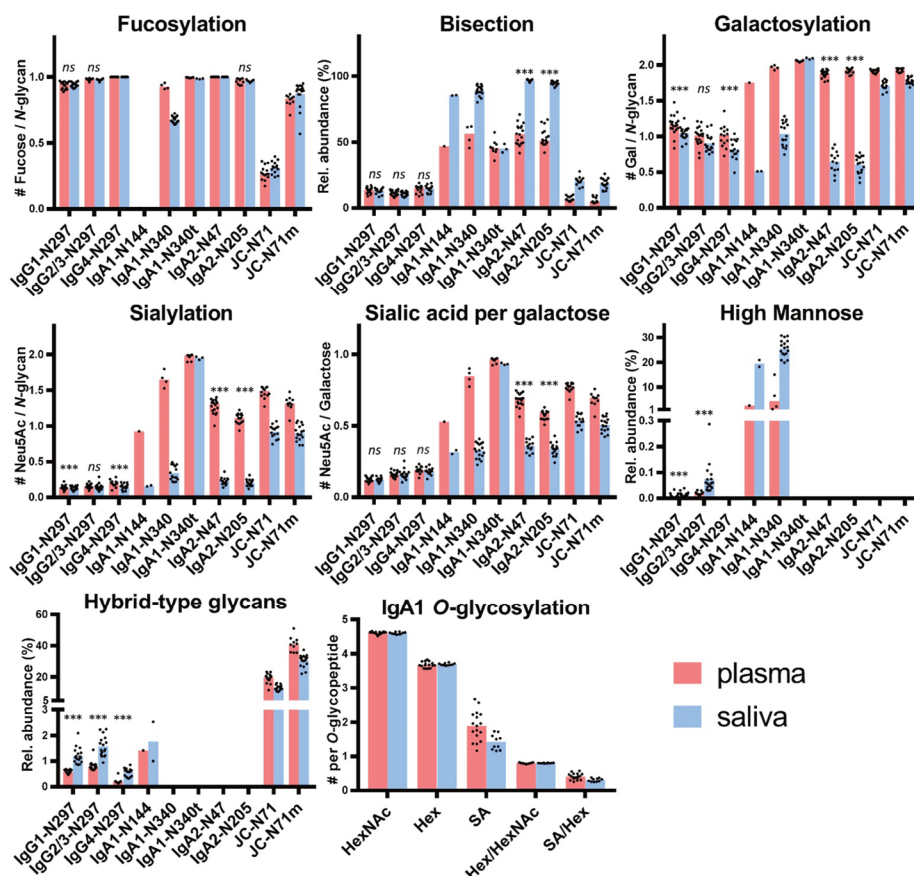


Figure 8.2 Glycosylation features for each of the glycosylation sites found in IgG, IgA and the JC. The bar graphs represent the medians per glycosylation site (red for plasma and blue for saliva) and the black dots represent the individual data points for each donor. A Wilcoxon signed rank test was performed between paired samples from plasma and saliva when the total number of pairs was > 10 (**Supplemental Table S4**). Significant differences are denoted by ***, non-significant differences are denoted by *ns*. IgA1-N340t is the C-terminally-truncated version of IgA1-N340 and JC-N71m is the miscleavage variant of JC-N71. IgA1-N144 also represents IgA2-N131, and IgA1-N340 and -N340t also represent IgA2-N327 and -N327t.

our samples, also not with the naturally occurring polymorphisms I326→V and A335→V [340, 355, 356]. The absolute MS signals of the truncated variant were higher in plasma samples, while those relating to the sequence including the C-terminal tyrosine were higher in saliva (**Supplemental Table S3**). Twenty-one and eight different glycoforms could be quantified on the full-length and the truncated sequence, respectively (**Supplemental** 162

Table S1B). Furthermore, trends of lower fucosylation (1.4 times lower), galactosylation (2 times lower) and sialylation (5 times lower) and higher bisection (1.7 times higher) in saliva as compared to plasma were observed for IgA1/2 N340/327, but not for IgA1/2 N340/327t (**Figure 8.2, Supplemental Table S4**).

IgA1 N144 and IgA2 N131 share the same tryptic glycopeptide sequence LSLHRPALEDLLLGSEAN_{144/131}LTCTLTGLR. While nearly all samples failed to provide data of sufficient quality to derive a glycosylation profile, the three samples which did pass data curation (one from plasma and two from saliva, not paired) showed up to 20% high-mannose type glycans and up to 3% hybrid-type/mono-antennary glycans, in addition to the complex-type *N*-glycans (**Figure 8.2**). In contrast to other IgA *N*-glycosylation sites, glycans at N144/131 were almost entirely afucosylated (< 1% fucosylation; **Supplemental Table S3** and **Supplemental Table S4**).

For IgA2 N92, in all samples only non-glycosylated peptides with the sequence HYTN₉₂PSQDVTVPVPPPPPCCHPR (allotype A2m(1)) were observed. Moreover, samples treated with *N*-glycosidase F did not show deamidated forms of this peptide, indicating that no glycosylated variants of N92 were present prior to *N*-glycosidase F digestion (**Supplemental Table S2**).

8.3.3 IgA1 *O*-glycosylation

The potential *O*-glycosylation sites located within the IgA1 hinge region were part of one large tryptic peptide: HYTNPSQDVTVPVSTPPTPSPSTPPTPSPSCCHPR. Forty-two *O*-glycopeptides were quantified. The collective glycan composition consisted of two to five hexoses, three to six HexNAcs and zero to five *N*-acetylneuraminic acids, likely distributed over three to six *O*-glycans (**Supplemental Table S1B**). Only a minor trend of lower (1.4 times lower) salivary *O*-glycan sialylation was observed as compared to plasma (**Figure 8.2**).

8.3.4 Joining chain (JC) *N*-glycosylation

The single *N*-glycosylation site N71 at the JC was observed on two tryptic peptides: EN₇₁ISDPTSPLR (JC N71) and the miscleaved IIVPLNNREN₇₁ISDPTSPLR (JC N71m). In general, this glycosylation site contained a higher fraction of monoantennary and hybrid-type glycans than the IgA heavy chain *N*-glycosylation sites (between 20 and 50%; **Supplemental Table S1C**). Furthermore, for this site similar differences between saliva and plasma were observed as for the IgA1 and IgA2 heavy chain *N*-glycosylation sites, namely a higher bisection (3.2 times higher) and lower galactosylation (1.1 times lower) and sialylation (1.7 times lower) in the saliva-derived samples (**Figure 8.2** and **Supplemental Table S4**). The miscleaved glycopeptides showed a higher abundance of fucosylation as

compared to the expected tryptic glycopeptides (3.2 times higher in plasma and 2.9 times higher in saliva; **Figure 8.2**).

8.3.5 Secretory component (SC) *N*-glycosylation

All seven *N*-glycosylation sites of the SC were detected after tryptic digestion of salivary SigA. Low-intensity signals of SC glycopeptides were also seen in a few plasma samples (**Supplemental Table S3**). *N*-glycans at N135, N186, N421 and N469 were determined to be complex-type and diantennary, furthermore the antennae were fully galactosylated and partially sialylated (**Supplemental Table S1D**, **Supplemental Figure S4**). In addition, on N499, mono-antennary species were identified. The observed glycoforms carried zero to five fucoses, and tandem mass spectrometry indicated the presence of both core and antennary fucosylation (**Figure 8.3** and **Supplemental Figure S1**). On N135, N469 and N499 between 1% and 4% bisection was observed (**Supplemental Figure S4**). The glycosylation sites N83 and N90 were present on the same tryptic peptide, and the joint glycan composition $H_{10}N_8F_{2-8}S_{0-3}$ indicated that the glycans at these two sites were similar to those on other SC sites.

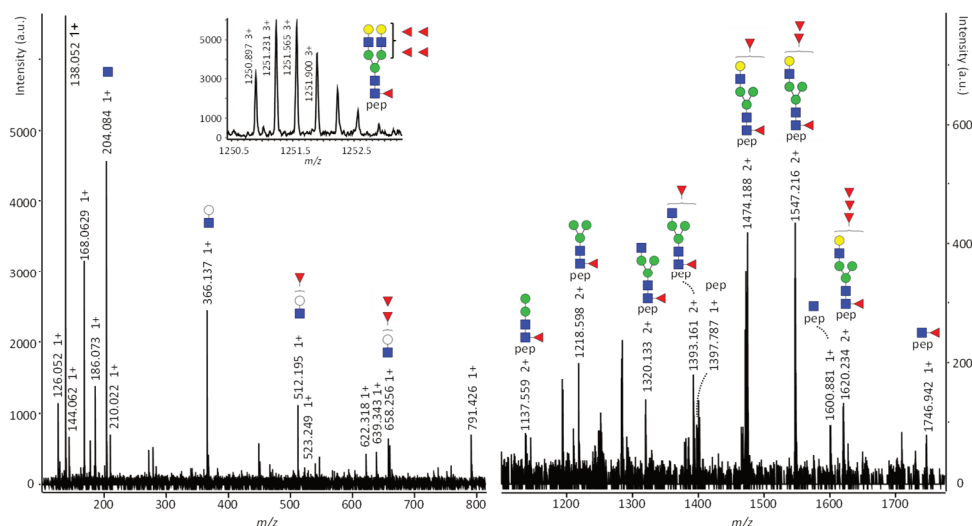


Figure 8.3 Fragmentation spectrum of SC N469 H5N4F5S0. The parent ions were detected at m/z 1250.895 at a retention time of 13.1 min and were assigned as the triply charged variant of $[M] = 3749.664$ Da, representing SC N469 H5N4F5S0. The structure carries both core and antenna fucosylation, as the former proven by $[M+H]^+ = 1746.942$, representing the peptide sequence VPGN₄₆₉VTAVLGETLK plus a GlcNAc and a fucose, and the latter by $[M+H]^+ = 512.195$ and 658.256, representing the antenna oxonium ions with one or two fucoses, respectively. pep: VPGN₄₆₉VTAVLGETLK, white circle: hexose, green circle: mannose, yellow circle: galactose, blue square: *N*-acetylglucosamine, red triangle: fucose.

8.4 Discussion

Here we present the first site-specific glycosylation analysis of antibodies in human saliva. IgG and IgA were purified from the plasma and saliva of 19 healthy individuals, and analyzed by LC-MS(/MS). Similar to previous studies on human serum and colostrum IgG or IgA glycosylation which used a comparable analytical methodology [85, 107, 340, 351], we observed glycopeptides covering the *N*-glycosylation sites of IgG1, 2/3 and 4 at N297, IgA1 at N340 and N144, IgA2 at N327, N205 and N131, and of the IgA-associated JC at N71, and the *O*-glycosylation sites in the IgA1 hinge region. We report several non-sialylated glycoforms on the JC that have not been described previously. Moreover, in both plasma and saliva samples we characterized the glycosylation at IgA2 *N*-glycosylation site N47, which had not extensively been described in literature [107, 340]. Finally, we provide an overview of the *N*-glycans at all 7 glycosylation sites of the SC in saliva including hitherto unreported molecular species, such as glycoforms with four or five fucoses.

The region surrounding IgA2 N92 is polymorphic and can produce two types of tryptic peptides, HYTN₉₂PSQDVTVPVPPPPPCCHPR (allotype A2m(1)) and HYTN₉₂SSQDVTVPCR (allotype A2m(2)) [357]. Since we detected the tryptic IgA2 peptide HYTN₉₂PSQDVTVPVPPPPPCCHPR in saliva and plasma samples from all individuals included in our study, we conclude that all carry at least one allele of IgA2 allotype A2m(1). This was expected, given that this allele has a frequency of 0.985 in the Caucasian population [357, 358]. Allotype A2m(2) peptides were not observed in our samples. Two previous studies reported the NPS sequence on the A2m(1) allotype to be *N*-glycosylated [339, 359], even though the proline following the N92 in A2m(1) does not match the consensus sequence for *N*-glycosylation. Here, however, we found that IgA2 N92 was not glycosylated in either plasma or saliva, in accordance with a previous report on colostrum SigA [340]. In future research also donors expressing the A2m(2) allotype should be included to obtain a complete characterization of IgA glycosylation.

In the current study, we did not detect the (glyco)peptides covering IgA2 N327 when searching for the expected tryptic peptide sequence obtained from UniProt entry IGHA2_HUMAN (P01877) or its naturally occurring variants. However, instead of the methionine in position 319 on IgA2 [309], a leucine was previously reported in allotype A2m(1) [355, 356], resulting in identical peptide sequences for both IgA2 N327 and IgA1 N340. Our observation that all individuals studied expressed IgA2 allotype A2m(1), made us conclude that the glycopeptides that we detected with peptide sequences LAGKPTHVNVSVVMAEVDGTCY and LAGKPTHVNVSVVMAEVDGTC (truncated [351, 360]) represented a mixture of IgA1 N340 and IgA2 N327.

The two differentially cleaved peptide sequences covering N71 of the JC showed a large variation in their glycan fucosylation, with the miscleaved variant having about 3 times

higher fucosylation than the expected peptide. This indicates that the core fucose might interfere with tryptic cleavage at R69. Similar differences in fucosylation were found previously [340].

Saliva collection has multiple advantages over the collection of plasma, for example, it is painless and does not require special instrumentation or trained personnel. Specialized devices for saliva collection making use of swabs or chewing on paraffin wax do exist [325, 343]. However, we utilized the simplest method, i.e. unassisted, unstimulated drooling, and found that this was sufficient to obtain IgG and IgA for a thorough glycomic analysis. A limitation of the current method might be that only solubilized antibodies were obtained, while the fraction associated to, for example, mucins was precipitated during the sample preparation. Furthermore, before saliva can be used as a potential diagnostic fluid, further research is necessary to evaluate robustness in terms of sample collection mode, time point and sample storage. Finally, although the current method can be performed in a 96-well plate format and has the potential to be automated, for its application in a routine laboratory or diagnostic setting further technological development is required that allows the specific quantification of glycoforms of interest, identified in the discovery phase. Despite the mentioned limitations, using saliva Ig glycosylation might have a potential in medical research in two different contexts: i) as a proxy for plasma Ig glycosylation reflecting systemic conditions, and ii) as a biomarker (panel) or therapeutic target for local perturbations in the oral cavity.

8.4.1 Saliva Ig glycosylation as proxy for plasma Ig glycosylation

The glycosylation of, in particular, IgG as the most abundant Ig in plasma has been proposed as a biomarker for various physiological and pathological states in multiple large-scale studies [74, 81, 255]. Similarly, IgA1 *O*-glycosylation associates with IgA nephropathy and IgA1 *N*- and *O*-glycosylation showed to alter with pregnancy and rheumatoid arthritis [335, 351, 361]. The vast majority of salivary IgG is thought to originate from plasma, and thus differences in glycosylation between plasma- and saliva-derived IgG likely originate from the minority (< 20%) of locally produced IgG [343, 345]. Here we found salivary IgG at N297 to exhibit a slightly lower galactosylation and sialylation, and a slightly higher abundance of high-mannose and hybrid-type glycans as compared to plasma. However, most IgG glycosylation features, except galactosylation, correlated well between plasma and saliva. This indicates that these features have potential as plasma IgG proxies and, thus, as biomarkers for the systemic health status. Low galactosylation and sialylation of plasma IgG are associated with inflammation and various autoimmune diseases [88, 362]. Additionally, galactosylation and sialylation are known to influence the binding of IgG to FcγRs and the C1q protein [37, 56]. This suggests that the slight IgG glycosylation differences we found between the two biofluids from healthy individuals may arise from the locally higher inflammatory state in the oral cavity,

since it is constantly exposed to pathogens. This aspect should be taken into account when further exploring the use of salivary IgG glycosylation as biomarker for systemic diseases, with special attention regarding possible co-occurring oral inflammatory conditions, such as periodontitis (gum disease). In contrast to IgG, the *N*-glycosylation of IgA was not correlated between plasma and saliva in our study. This is likely due to either the different origin of plasma cells producing the two pools of IgA proteins or to a difference in processing, such as dimerization and J-chain binding, or their translocation through the epithelial cell layer. Our findings in healthy individuals aged between 20-42 years suggest that salivary IgA cannot be used as a proxy for plasma IgA *N*-glycosylation.

8.4.2 Saliva Ig glycosylation as a biomarker (panel) or therapeutic target for local perturbations in the oral cavity

Differences of Ig glycosylation in locally produced biofluids can be exploited as biomarkers for local pathological processes. Accordingly, IgG glycosylation in cerebrospinal and synovial fluid from multiple sclerosis and rheumatoid arthritis patients, respectively, revealed biofluid-specific associations with disease [337, 338]. In addition, patients with advanced periodontitis were reported to exhibit a lower salivary IgG galactosylation than healthy individuals [341]. Our data suggest that salivary IgA *N*-glycosylation analysis also provides a promising tool to detect local glycosylation perturbations in the oral cavity which might reflect pathological processes. IgA is the most abundant antibody in human saliva, and SIgA is regarded as an important first line of defense against pathogens on mucosal surfaces [334, 343, 344]. Interestingly, the *N*-glycosylation profile reported for colostrum-derived SIgA [340] is similar to our data on salivary SIgA, in terms of a high abundance of glycoforms carrying a bisecting GlcNAc, contrary to plasma-derived IgA. This suggests that in healthy individuals, SIgA shares a common *N*-glycosylation profile, whether it originates from the salivary or mammary glands, but differs from the IgA glycosylation profile in the circulation. This might be related to the fact that both salivary and milk SIgA enter the gastrointestinal tract via the same route, and can exert similar functions while passing the oral cavity and the gastrointestinal tract.

Salivary IgA and JC showed a considerably higher bisection and lower galactosylation and sialylation at all observed sites of *N*-glycosylation, except for the truncated variants of IgA1 N340 and IgA2 N327 lacking the C-terminal tyrosine, which had a similar glycosylation profile in plasma and saliva. Moreover, the truncated version was low-abundant in saliva and highly abundant in plasma. Therefore we hypothesize that the truncated form originates from circulation and is present in saliva due to leakage or transport from the circulation [345], while the full-length variant might mainly be produced and secreted locally in the oral cavity. The majority of salivary IgA and JC is produced locally in plasma B cells of the glandular stroma [343, 347]. This suggests that changes in the glycosylation machinery of specifically these cells are the cause for the substantial glycosylation

differences between plasma and saliva. For example, an upregulation of beta-1,4-*N*-acetylglucosaminyltransferase III (GnT-III/MGAT3) and a downregulation of beta-1,4-galactosyltransferase (B4GalT) and beta-galactoside-alpha-2,6-sialyltransferase (St6Gal) 1 in the glandular stroma B cells could be responsible for the observed differences in IgA *N*-glycosylation. Alternatively, the pIgR-enabled transport of IgA across the epithelium, the dimerization of IgA, and the binding of the J-chain might be selective for certain glycoforms of IgA. However, for the binding to the pIgR this appears unlikely taking into account a previous study which reported that the removal of either the *N*- or *O*-glycans of polymeric IgA had no influence on pIgR-mediated transcytosis [363]. Finally, it could be speculated that asialoglycoprotein receptors, which are located primarily in the liver, could alter the overall glycosylation of plasma IgA by specifically removing non-sialylated proteins from circulation [364], thus leading to a higher level of sialylation compared to saliva. However, this would not explain the differences in the levels of bisection between plasma and saliva. The functional consequences of differences in IgA *N*-glycosylation are at this point not well understood: The *N*-glycans on the constant region of IgA do not seem to be essential for FcR binding, in contrast to the ones on IgG [336]. However, IgA sialylation has been shown to be required for dectin-1-mediated transport of SIgA across the epithelium of intestinal cells [334]. Furthermore, in addition to the Fab-binding sites, SIgA fucosylation and sialylation enable the binding of the antibody to pathogenic bacteria, acting as a decoy to prevent bacterial adhesion to the epithelium and subsequent infection [365-367]. Finally, the C-terminal *N*-glycan sialic acids have recently been reported to directly inhibit sialic acid-binding viruses like influenza [368].

The fact that we did not find differences between salivary and plasma IgA1 *O*-glycosylation, except for a slight trend of lower sialylation in saliva, is likely due to their inherently different biosynthetic pathways as compared to *N*-glycans, involving distinct glycosyltransferases [369]. Additionally, we here evaluated all *O*-glycosylation sites simultaneously at the same glycopeptide, of which we could imagine that it provides less resolution than when the analysis would have been done on the single-structure level. Thus, it is difficult to judge on the usefulness of IgA *O*-glycosylation as a potential diagnostic biomarker based on our data. However, future investigations should further assess IgA *O*-glycosylation in a specific disease context, since in plasma it has been associated with pathologies, such as IgA nephropathy and Sjögren's syndrome [335, 370, 371].

A comparison of the salivary IgA SC with plasma was not possible, due to insufficient signal intensities of the plasma SC from most individuals in our study, most likely due to its low abundance in plasma. *N*-glycans on the SC have been shown to be crucial for various functional aspects of SIgA [367]. For example, SC glycosylation enables the innate protection against mucosal pathogens [372]. Furthermore, SC glycans are essential for a

correct localization of IgA in the mucosal lining, resulting in protection from bacterial infection in the respiratory tract of mice [373]. Because of the important and diverse role of SC glycosylation, future studies should examine whether salivary SC glycosylation is associated with, for example, periodontitis, to explore its potential as a diagnostic biomarker or therapeutic target.

8.4.3 Conclusions

Large differences were found between the glycosylation of plasma- and saliva-derived IgA and its JC, while this was not the case for IgG. This suggests that the SIgA, locally produced by plasma B cells in the glandular stroma, differs in glycosylation from IgA of the circulation, that presumably is largely produced by circulating plasma cells, pointing towards distinct regulatory mechanisms. An alternative explanation is that SIgA dimerization or transport into the oral cavity might be glycoform-specific, or that certain IgA-producing B cells, expressing a specific glycosylation repertoire, may be relocated to the glandular stroma after activation. The observed differences between plasma and salivary IgA make biofluid-specific analysis of SIgA glycosylation (including the JC and SC) a promising tool for mucosal disease-related biomarker research. IgG glycosylation, on the other hand, showed a good correlation between plasma and saliva in healthy individuals, indicating that salivary IgG might be a proxy to study plasma IgG in situations where a healthy oral environment can be assumed.

Acknowledgments

We would like to thank Shivani Kapoerchan and Lisette den Hertog for their help with initial method development. Agnes Hipgrave Ederveen and Carolien Koeleman are acknowledged for their help with running the LC-MS system. This work was supported by the European Union Seventh Framework Program HighGlycan (278535).

Supporting Information available

Additional information is available as stated in the text. This information is available free of charge via <https://www.frontiersin.org/articles/10.3389/fimmu.2018.02436/full>.



Chapter 9

Discussion and Perspectives



The highly diverse glycan structures present on glycoproteins in human body fluids provide a rich source of information on the biological processes taking place in the body. This information can provide insights into the mechanisms behind diseases and has high potential for pharmaceutical and clinical applications, for instance by revealing new therapeutic targets and disease-associated markers. However, the in-depth characterization of protein glycosylation is not straightforward as one protein might carry multiple glycosylation sites. Furthermore, these sites are not always occupied by a glycan, and the glycans attached show many different structures, which are often isomeric. The presented work deals with, on the one hand, the development of analytical methods for analyzing the glycosylation of antibodies, which represent a major group of human glycoproteins, and, on the other hand, the application of these methods to characterize glycosylation profiles specific for certain organisms, body fluids, or medical conditions. Both of these aspects will be discussed in the following sections, with a focus on their current challenges and future applications.

9.1 Technological challenges and considerations

9.1.1 Protein- and site-specificity

The specific isolation of proteins from a biofluid of interest, for example by affinity chromatography, is an often used approach to reduce sample complexity, thus simplifying its glycoproteomic characterization. In the current work, this approach was applied for the protein-specific glycoprofiling of the antibodies immunoglobulin G (IgG; **Table 9.1; Chapters 2 through 8**) [149, 176, 194, 205, 222, 289] and immunoglobulin A (IgA; **Table 9.1; Chapter 8**). IgG can be subdivided into four subclasses (IgG1 to 4) and IgA into two (IgA1 and 2). Obtaining subclass-specific antibody glycosylation profiles is relevant as the subclasses have distinct functions and vary in their affinities for interaction partners [34, 185]. After isolation of the antibodies, site- and subclass-specific glycosylation information can be derived from the analysis of glycopeptides using mass spectrometry (MS; **Table 9.1**). However, obtaining glycopeptides with peptide moieties fully specific for the antibody subclass and glycosylation site remains a challenging task. This was exemplified by the isomeric or identical tryptic glycopeptides obtained from: 1) the human IgG3 and IgG2 or IgG4 C_H2 domains which are observed depending on the IgG3 allotype (**Table 9.1; Chapters 2 to 6 and 8**) [149, 176, 194, 205, 222], 2) the IgA1 and IgA2 C_H2 and C_H3 domains (**Table 9.1; Chapter 8**) and 3) the murine IgG2a, b and c C_H2 domains (**Table 9.1; Chapter 7**) [289]. These challenges might be partly overcome by the use of proteases with a different specificity as compared to trypsin, as they might result in larger and more specific protein fragments. An example of a suitable enzyme would be GluC, which preferably cuts proteins at the C-terminus of glutamic acid residues while also showing

some reactivity C-terminally of aspartic acid residues. For isomeric peptide moieties, optimization of the separation conditions, prior to mass spectrometric detection, might provide a suitable approach to enable subclass-specific analysis, as was shown in **Chapter 7** for the differentiation between murine IgG2b and IgG2a/c Fc glycopeptides (**Table 9.1**) [289]. This might also be a solution for the isomeric glycopeptides obtained from human IgG4 and specific allotypes of IgG3 (**Table 9.1**) [22]. So far, glycopeptides from these subclasses were not shown to be separated under the chromatographic conditions used.

9.1.2 Mass spectrometric instrumentation

The research performed in this thesis made use of two kinds of mass spectrometers. In **Chapters 2** and **3**, matrix-assisted laser desorption/ionization (MALDI)-time of flight (TOF)-MS was applied for the analysis of glycopeptides [149, 176, 374], while in **Chapters 4** through **8**, glycopeptides were analyzed by electrospray ionization (ESI)-TOF-MS coupled to reversed-phase (RP)-liquid chromatography (LC) [194, 197, 205, 222, 289]. The MALDI-TOF-MS workflow included the purification of IgG, its tryptic digestion, the linkage-specific sialic acid derivatization of the glycopeptides, purification of the glycopeptides, and their analysis by MALDI-TOF-MS. For the LC-ESI-MS workflow, the proteins were isolated and digested, after which the glycopeptides were separated by RP-LC and analyzed by on-line ESI-TOF-MS. Both approaches have their own advantages in terms of resolution, throughput and obtained information content: The MALDI-TOF-MS method demonstrated a high sample throughput, enabling the preparation and analysis of approximately 384 samples in two working days. As proven previously for the analysis of released glycans, the method may potentially encompass an even higher sample throughput by the automation of the sample preparation [375]. Furthermore, the sialic acid linkage specificity of the derivatization adds information on the presence of sialic acid isomers. Although this method requires multiple sample preparation steps, it showed to have a high inter- and intra-day repeatability, suitable to pick up the biological variation in IgG glycosylation between individuals [176]. Method repeatability might be further improved by automated sample preparation [375].

The reversed phase-LC-ESI-MS approach requires a similar amount of time for the preparation of 384 samples as the MALDI method, after which approximately 96 samples can be analyzed per 24 hours. The chromatographic separation of the glycopeptides, prior to their separation in the m/z dimension, resulted in the clustering of glycopeptides with the same peptide sequence. For human IgG this has the advantage that, based on their retention time, the afucosylated glycoforms of IgG4/3 can be distinguished from the isomeric fucosylated glycoforms of IgG1 with one hexose less. Similarly, the afucosylated glycoforms of IgG2/3 can be distinguished from the fucosylated glycoforms of IgG4/3 with one hexose less. In both cases, the overlapping masses are caused by a difference of one

Table 9.1 Peptide moieties, and their masses, of the tryptic glycopeptides of human and murine IgG and human IgA.

Protein	Glycosylation site		Tryptic peptide sequence (<u>glycosylation site</u>)	Peptide mass [M] (Da)
	Consensus numbering, e.g. [177]	UniProt [309]		
Human IgG1	N297	N180	EEQY <u>N</u> STYR	1188.5047
Human IgG2	N297	N176	EEQF <u>N</u> STFR	1156.5149
Human IgG3	TH2-7/TH3-7/TH4-7	T122/T137/T152	SCD <u>I</u> PPPCPR	1071.4478
Human IgG3	N297	N227	EEQF <u>N</u> STFR ^a	1156.5149 ^a
			EEQY <u>N</u> STFR ^a	1172.5098 ^a
			TKPWEEQY <u>N</u> STFR ^a	1684.7845 ^a
Human IgG3	N392	N322	GFYPSDIAVEWESSGQPENN Y <u>N</u> TPPMLSDSGSFLLYSK	4388.9372
Human IgG4	N297	N177	EEQF <u>N</u> STYR	1172.5098
Murine IgG1	-	N173	EEQF <u>N</u> STFR ^b EEQI <u>N</u> STFR ^b	1156.5149 ^b 1122.5306 ^b
Murine IgG1	-	N278 ^c	NTQPIMNT <u>N</u> GSYFVYSK ^c	1962.9145 ^c
Murine IgG2a	-	N180/185 ^d	EDY <u>N</u> STLR	996.4512
Murine IgG2b	-	N185	EDY <u>N</u> STIR	996.4512
Murine IgG2c	-	N185	EDY <u>N</u> STLR	996.4512
Murine IgG3	-	N179	EAQY <u>N</u> STFR	1114.5043
Murine IgG3	-	N322 ^c	<u>N</u> LSR ^c	488.2707 ^c
Murine IgG3	-	N332 ^c	SPELE <u>L</u> NETCAEAQDGELDGL WTTITIFISLFLLSVCYSASVTLF ^c	5066.5072 ^c
Human IgA1	T225/T228/S230/ S232/T233/T236	T106/T109/S111/ S113/T114/T117	HYTNPSQDVTVPVPS <u>I</u> P P <u>I</u> PS <u>P</u> STPPTSPSCCHPR	4135.8826
Human IgA1	N263	N144	LSLHRPALEDLLLGSEAN <u>L</u> TCLTGLR	2962.5909
Human IgA1	N459	N340 ^e	LAGKPTHV <u>N</u> VSVVMAEVDGTC(Y) ^e	2183.0714 (2346.1348) ^e
Human IgA2	N166	N47	VFPLSLDSTPQDNVVVACLQ GFFPEPLSVTWSESGQ <u>N</u> VTAR	4533.252616
Human IgA2	N211	N92 ^f	HYTNSSQDVTVP <u>C</u> R ^f	1605.720554 ^f
Human IgA2	N263	N131	LSLHRPALEDLLLGSEAN <u>L</u> TCLTGLR	2962.5909
Human IgA2	N337	N205	TPLTAN <u>I</u> TK	957.5495
Human IgA2	N459	N327 ^e	LAGKPTHV <u>N</u> VSVVMAEVDGTC(Y) ^{e/g}	2183.0714 ^g (2346.1348) ^e
			MAGKPTHI <u>N</u> VSVVMAEADGTC(Y) ^{e/g}	2129.9908 ^g (2293.0541) ^e
Human J-chain	N49	N71	ENISDPT <u>S</u> PLR	1227.6095
Human SC ^h	-	N83 + N90	ANLTNFPEN <u>G</u> TFVVNIAQLSQDDSGR	2806.3522
Human SC	-	N135	GLSFDVSLEVSQGP <u>L</u> NDTK	2175.1059
Human SC	-	N186	QIGLYPVLVIDSSGYVNP <u>N</u> YTGR	2524.2961
Human SC	-	N421	LSLLEPGN <u>G</u> FTFVILNQLTSR	2401.2852
Human SC	-	N469	VPGN <u>V</u> TAVLGETLK	1396.7925
Human SC	-	N499	WNNTGCQALPSQDEGPSK	1987.8694

^a Depending on the IgG3 allotype [22]. ^b Depending on the IgG1 allotype [44, 289]. ^c N-glycosylation motive, not reported to be glycosylated. ^d Depending on the IgG2a allotype [309]. ^e This glycosylation site is naturally found on a peptide with and without the C-terminal tyrosine [351, 360]. ^f This glycosylation site is only present on the IgA2 allotype A2m(1) [357]. ^g Depending on the IgA2 allotype. Additional naturally occurring polymorphisms are known for this peptide portion: I326→V and A335→V [340, 356, 357]. ^h SC: secretory component.

oxygen atom in the peptide moiety (phenylalanine instead of tyrosine) and the compositional difference between a hexose and a fucose, which is also one oxygen ($C_6H_{12}O_6$ vs. $C_6H_{12}O_5$). The described separation possibilities make LC-ESI-MS the preferred approach for the analysis of samples of polyclonal IgG in which all subclasses are present. MALDI-TOF-MS may be used, for example, for the characterization of biopharmaceutical products, which often consist of monoclonal IgG, or for the analysis of purified polyclonal IgG subclasses. Furthermore, the LC-ESI-MS method can be applied on the tryptic digest of other antibody isotypes with minor adaptations. In contrast, the derivatization required for the MALDI-TOF-MS workflow has to be optimized for each protein separately, in order to minimize heterogeneity due to side reactions in the peptide portion (see optimization for IgG glycopeptides; **Chapter 2**) [149].

9.1.3 Technical variation and the use of external standards

The here-reported antibody glycosylation profiling of hundreds up to thousands of samples resulted in repeatable outcomes for the included technical standards, with median relative standard deviations between 5% and 12% per glycosylation site. The technical variation introduced within a study usually proved to be considerably lower than the biological variation of interest [176, 194, 205, 222, 289].

However, in the larger studies, including thousands of samples and covering several weeks of measurement time, the technical variability was noticeably higher as compared to smaller studies [205, 222]. Additional batch effects were observed when comparing the results of two (or more) studies that were prepared and analyzed separately. This often hampers the direct integration of two datasets. Enhancing the repeatability and reproducibility of the IgG glycopeptide workflows will aid future research, for example, by ensuring a higher comparability between studies, allowing the integration of datasets and enabling the reuse of data obtained from precious samples. In **Chapters 4** and **5**, the samples from the healthy children studied in **Chapter 3** [176] were reused (and remeasured) as control samples [194, 205]. Samples from healthy children are precious, as it is hard to obtain them due to ethical constraints. Both timewise and because of limited sample amounts, it would have been beneficial to be able to reuse the data obtained in one of the studies and integrate them with the data from the later studies. Furthermore, data comparability over a long period is important with regard to longitudinal study designs and the integration of glycomic analysis in a clinical laboratory, which is further elaborated on in the section below (**Chapter 9.2** on IgG Fc glycosylation as clinical marker).

External standards are an essential component of a good glycomic and glycoproteomic study design and can account for a large part of the introduced technological variability. In the presented work two types of external standards were used. One type consisted of material representative for the biological samples, and was randomly included throughout

the analysis to be subjected to the complete sample preparation. The second external standard, the system suitability standard consisting of isolated human IgG, was separately prepared and only introduced during LC-MS analysis. While the first standard provided the technical variation over the complete workflow, the latter independently evaluated the performance of the MS. Keeping both standards constant over time, studies and labs, will allow to monitor a large part of the variation introduced by the profiling workflows and might allow the mathematical correction of batch-related biases. However, biases caused by differences between samples, for example, in the concentration of the analyte of interest or the sample matrix, will not be accounted for by these standards. For this purpose, the use of internal standards is required, preferably in the form of heavy isotope-labeled analyte analogues.

9.1.4 Towards the use of internal standards

Heavy isotope-labeled internal standards are already commonly used in (clinical) small molecule-, lipidomic- and proteomic-based MS workflows [376-378]. These kind of standards are a key component of the analysis, both in controlling for inter-sample technical variation and to perform absolute quantification of the analytes of interest. However, the use of these standards lags behind in the field of glyc(oprote)omics. The reason for this is 1) the demand for a wide variety of standards, covering the different glycoforms present at one protein glycosylation site or in one biological sample, and 2) the laborious process of producing (heavy-labeled) glycoconjugate standards in relevant amounts. Ideally, a heavy-labeled variant of every glycoform of interest would be available. In exploratory studies, as described in this thesis, a wider range needs to be covered. In a future clinical setting (See **Chapter 9.2** on IgG Fc glycosylation as clinical marker), the panel of glycoforms of interest may be considerably be brought down on the basis of the glycosylation biomarker identified in the exploratory phase.

Isotope labeled internal standards enable both the control of technical variability and the absolute quantification of the analytes in case the concentration of the added standard is known. Current glycosylation profiling techniques are dependent on some form of normalization to assess changes in the profiles. The most commonly used normalization method is the total area normalization, representing the abundance of a glycoform relative to the total abundance of all glycoforms. A disadvantage of this technique is that no distinction can be made between the increasing abundance of a certain glycoform and the decreasing abundance of others. Comparing absolute glycoform abundancies to the ones from added internal standards, results in a quantification per glycoform that is independent of the other glycoforms [379]. Additional information on the absolute amount of antibody subclasses can be obtained by the inclusion of heavy-labeled analogues of protein- and subclass-specific peptides (nonglycosylated). The absolute quantification of IgG subclasses might reveal concentration-dependent glycosylation

changes [380]. Additionally, combining glycosylation profiling and antibody quantification in the same analysis provides an advantage in terms of time and sample usage [381]. The latter is especially important in cases where sample amounts are limited and alternative techniques, like immunoassays, are not applicable.

Ideally, an internal standard covers the variability introduced during the complete IgG glycopeptide profiling workflow. For this purpose, a standard should be mixed with each sample as early in the process as possible. An intact heavy-labeled monoclonal IgG, like the SILuTMMAB molecule [382, 383], might be spiked into the samples prior to affinity purification of the antibodies. These glycoproteins are expressed by cells grown in ¹³C₆, ¹⁵N₄-arginine and ¹³C₆, ¹⁵N₂ lysine-enriched medium. Their tryptic glycopeptides always contain either a heavy arginine or lysine residue at the C-terminus [382, 383]. Currently, these monoclonals are produced in CHO cells, hence they do not resemble human-like glycosylation (e.g., α2,3-linked sialylation instead of α2,6-linked and limited bisection). Although they are suitable to monitor IgG isolation and digestion, in their current form these heavy-labeled glycoproteins cannot be used to correct for, or quantify, all human IgG glycoforms. When the four human IgG subclasses were covered and the heavy labeled antibodies were expressed with a more humanized glycosylation repertoire, these would be suitable standards to support both subclass and glycoform quantification. Additionally, such standards would allow to largely correct for the technical variation introduced during the complete experimental procedure. However, one should keep in mind that such a procedure does not cover for variability in the preparation or addition of the internal standard itself. Furthermore, sample handling steps occurring prior to the addition of the standards are not taken into account. These steps might include specific storage conditions and possibly sample concentration via evaporation. To account for the latter, an internal standard is preferably added during or right after sample collection.

To monitor specific steps later in a profiling workflow, (additional) standards could either be added after the affinity purification or after protein digestion. In the first case this could be in the form of an intact antibody or a panel of glycopeptides with extended peptide moieties surrounding the tryptic cleavage sites. In the second case this could be a panel of glycopeptides, representing the glycoforms of interest. For the current exploratory profiling methods, every added standard is a step forward in managing the experimental variation and/or obtaining quantitative subclass or glycoform information. However, a combination of multiple standards is expected to be essential for the incorporation of MS-based glycopeptide profiling in a clinical laboratory.

The combination of chemical, chemoenzymatic or cell culturing metabolic approaches recently accelerated the availability of heavy labeled glycans and glycoconjugates, as exemplified by the heavy-labeled glycosylated antibody described above [382, 383].

However, it remains challenging to cover the complete repertoire of glycoforms assessed in one glycoproteomic study [379, 384-386]. Alternative methods to obtain heavy-labeled glycoconjugate standards are based on the introduction of an external heavy (for the internal standard) or light (for the studied samples) label to the analytes. For released glycans, for example, this was done via glycosylamine or aldehyde labeling at the reducing end [387-389], permethylation of the carboxyl, hydroxyl and amine groups [120, 390] or amidation of the sialic acids [391]. These approaches might offer a promising solution as they provide a lot of freedom in the selection of the heavy-labeled glycan analogues, which could therefore provide a true representation of the samples under study. Similar strategies could be considered for the labeling of glycopeptides. Additionally, (IgG) glycopeptides have the advantage of the peptide portion possessing functional groups that can be subjected to derivatization, like primary amines and carboxyl groups [392, 393]. Via these groups, glycopeptides can alternatively be modified by isobaric labels. An example is the tandem mass tag (TMT) approach, that labels different samples with different isobaric tags and allows the multiplexing of samples and their quantification after MS fragmentation [394]. The downside of external labeling approaches is the introduction of extra steps in the experimental procedure, possibly causing a lower robustness and introducing (biased) sample losses. Furthermore, samples and standards can only be mixed after the labeling procedure, which means that an extra standard, controlling for labelling efficiency, is potentially necessary. Though, when carefully designed, also external labeling approaches might find their way to be applied in the absolute quantification of glycopeptides.

9.2 IgG Fc glycosylation as clinical marker

Despite the pending challenges in antibody glycosylation analysis, the methods presented in this thesis resulted in a wealth of information, which was linked to various (patho)physiological processes [176, 194, 205, 222]. For example, IgG galactosylation correlated with disease behavior in patients suffering from inflammatory bowel disease (IBD; **Chapter 6**) and IgG sialylation per galactose associated with disease outcome in patients with meningococcal sepsis (**Chapter 5**). These relations suggest that antibody glycosylation might be of use in a clinical setting. Specifically, perturbations in antibody glycosylation profiles can be considered as clinical markers for potential use in diagnosis, prognosis or treatment monitoring. Most promising is the use of antibody glycosylation for fine-tuning diagnosis and treatment strategies. The major concern in the identification of clinical markers (or biomarkers) is the lack of sensitivity and specificity of an identified marker, resulting in false negative and false positive test outcomes, respectively. Considering the fact that Fc glycosylation on IgG was reported before to be altered in a wide variety of diseases, care should be taken not to overinterpret differences observed

between a specific group of patients and the healthy population. For example, a lower Fc galactosylation and sialylation on total plasma IgG was reported for patients suffering from, amongst others, IBD (**Chapter 6**) [95, 222], rheumatoid arthritis [92-94], lupus [96], active tuberculosis infection [101], visceral leishmaniasis [395], colorectal cancer [103] and ovarian cancer [102]. Following this, one cannot claim the biomarker potential of a lower Fc galactosylation or sialylation for the diagnosis of any of these diseases, as it is simply not specific enough. Low IgG galactosylation, and the low sialylation that usually results from the lower availability of the antennary galactose substrate, is often an indication of an ongoing inflammatory process. This is supported by the fact that supposedly healthy individuals with relatively high levels of inflammatory markers like C-reactive protein and interleukin (IL)-6 show low levels of galactosylation and sialylation [88]. Furthermore, galactosylation and sialylation of IgG naturally decrease with aging, which is in turn associated with an increase of inflammatory processes [28, 79, 81, 193, 396]. A possible mechanism via which the low total IgG galactosylation is involved in the inflammatory process, is via its effect on IgG binding to Fc γ -receptors (Fc γ R) and C1q. An increased galactosylation enhances binding affinity in both cases (for Fc γ R binding, this is mainly/only valid for the afucosylated subset of the IgG glycome) [37, 41, 52, 397]. This might play a role in the non-specific blocking of the effector molecules, thus influencing their competition with disease specific antibodies [398]. Alternatively (or additionally), in mouse models, a higher galactosylation showed to attenuate the inflammatory response via complex formation between dectin-1 and the inhibitory Fc γ RIIb [186]. While it seems unlikely, it cannot be ruled out that changes in total IgG galactosylation are merely a bystander effect of other pro- and anti-inflammatory processes in the body.

Hence, the power of using IgG glycosylation in a clinical setting does likely not lie in the direct diagnosis of certain pathologies, but rather in the fine-tuning thereof. An example can be found in the predictive value of IgG Fc galactosylation observed in patients suffering from anti-neutrophil cytoplasmic antibody (ANCA)-associated vasculitis (AAV), and who are in remission [97]. A rise in their ANCA levels might indicate a future relapse of the disease, however with poor specificity (i.e., a large part of the patients that shows an ANCA rise does not relapse). An additional low Fc galactosylation of the total IgG improves the specificity of the prediction and can forecast a reactivation of the disease already eight months prior to its actual occurrence [97]. This indicates that the longitudinal follow-up of IgG glycosylation in patients with confirmed (autoimmune) diseases might be a valuable approach to exploit antibody glycosylation in a clinical setting. In **Chapter 6** of this thesis, it was shown that the glycosylation patterns of the total plasma IgG pool associated with IBD disease characteristics like severity and subtype [222]. Lower levels of galactosylation were observed in patients with a more extensive and more severe disease. This indicates that, also in the case of IBD, the level of IgG galactosylation might be used to evaluate disease progression and treatment success in a longitudinal follow-up. However, to

validate this hypothesis, a study setup different from the present one is required, including multiple samples per patient over an extended period of time.

In addition to the longitudinal evaluation of IgG Fc glycosylation, a one-time measurement at the time of diagnosis might give information on the subtype or expected outcome of a disease. For example, in **Chapter 6**, it was shown that the level of galactosylation and fucosylation together were able to discriminate between the IBD subtypes Crohn's disease (CD) and ulcerative colitis (UC) [222]. Although the sensitivity and specificity of this discrimination by glycosylation was not sufficient to be used on its own, the data might have added value when combined with other serology markers that can discriminate between CD and UC, like levels of ANCA and anti-*Saccharomyces cerevisiae* antibodies (ASCAs) [399]. Furthermore, in **Chapter 5**, IgG Fc glycosylation was investigated for pediatric meningococcal sepsis patients admitted to the intensive care unit. This study showed the levels of hybrid-type glycans and sialylation per galactose to be lower at disease onset in patients that eventually showed a more severe disease outcome, as compared to patients that showed a non-severe disease outcome [205]. Such information, when obtained early in the disease process, might be used for patient stratification. However, in this specific case, the findings should be validated in a larger replication cohort, and comparisons, with regard to sensitivity and specificity, should be made to existing prediction scores and to a combination of glycosylation with existing markers.

While the research in this thesis focused on the evaluation of total plasma (or serum) IgG to find disease subtype-specific glycosylation profiles, another promising approach is the assessment of antibodies specific for disease-related antigens. In various situations, these disease-specific antibodies have shown to exhibit glycosylation patterns that are vastly different from those of total IgG [97-100]. An example in which this differential glycosylation appeared to be an attractive indicator of disease severity can be found in the anti-D IgGs occurring in pregnant women with hemolytic disease of the fetus and newborn (HDFN) [99]. In this condition, anti-D alloantibodies from the mother are transferred across the placenta and attack the red blood cells of the fetus. While HDFN disease severity correlates poorly with anti-D antibody titers, a low fucosylation on these antibodies was connected to increased ADCC and a more severe disease [99]. This observation is in line with an enhanced binding affinity of afucosylated antibodies for the FcγRIIIa and subsequent induction of antibody-dependent cell-mediated cytotoxicity (ADCC) [37, 47-49]. With regard to the findings presented in **Chapter 5**, it is interesting to investigate the glycosidic differences of meningococcus-specific IgG between patients with severe and non-severe disease outcomes. A glycosylation profile that makes the specific antibodies more potent to interact with their effector molecules (inducing FcγR effector functions and/or complement activation), possibly determines how well a disease is kept under control. While afucosylation of HIV-specific IgGs that increase FcγRIII effector

functions were associated with containment of disease progression [98], the opposite was true for dengue fever where a disease exacerbation was observed [400].

In all, despite the high variability in IgG Fc glycosylation between individuals and its dependency on age, sex and environmental factors, information on the general inflammatory proneness, or state, of an individual can be obtained when looking at Fc galactosylation. This can be of particular clinical value when studied 1) in a longitudinal manner using earlier time points of the same patient as a reference, and 2) in the context of a previously confirmed pathology to stratify for, for example, disease severity, subtype or chance to relapse. Other glycosylation features, when studied on total IgG, appear to contain less clear information on disease status or progression. Sialylation often follows the trends observed for galactosylation, however showing less pronounced effects [54, 97, 222]. The fraction of afucosylated glycoforms was shown to be related to the maturation of the immune system in children, and/or the immunological challenges they encountered (**Chapter 3**) [176]. A lower fucosylation in older children might be a result of the higher abundance of disease-specific antibodies. Following this reasoning, a low IgG fucosylation at young age might reflect either an ongoing infection or a buildup of multiple previous immunizations. However, to make these kind of observations clinically relevant, their origin needs to be studied further. In addition to the analysis of total IgG Fc glycosylation, the evaluation of Fc glycosylation features on the level of the disease-specific IgGs might be exploited as a clinical tool. Mainly antigen-specific IgG fucosylation has been shown to correlate with distinct disease phenotypes [98-100]. Furthermore, fucosylation demonstrated to influence the potency of antibodies to activate effector pathways via FcγRIIIa [37, 48, 49]. Even more clearly than for the total IgG glycosylation, future tests based on antigen-specific IgG glycosylation will be valuable in the context of fine-tuning a diagnosis or prognosis, rather than in the disease diagnosis itself.

9.3 Studying the regulatory mechanisms of IgG Fc glycosylation

As detailed in **Chapter 1**, protein *N*-glycosylation is mainly regulated in the endoplasmic reticulum (ER) and Golgi apparatus of the cells where the protein is produced [55], which for IgG are the plasma B cells. The composition and structure of the Fc glycan is, amongst others, dependent on the availability of specific glycosidases, glycosyltransferases and nucleotide sugar donors in the B cell. Furthermore, the glycan repertoire is influenced by the turnover rate of specific glycoforms and the enzymatic modifications that might take place in the circulation. While the involved enzymes are under direct (epi)genetic regulation, the availability of nucleotide sugars additionally depends on their metabolic pathways and transport into the relevant cellular compartments of the Golgi. Mutations in the genes encoding for many of the aforementioned components have shown to have

tremendous effects on general protein glycosylation [316]. However, a lot remains unclear regarding the fine-tuning of the regulation of the glycosylation machinery in a situation where all components are initially in place. Specifically, for the regulation of IgG Fc glycosylation, examples of some urgent questions are: 1) What is the effect of the B cell microenvironment? 2) What is the source and function of the large glycan microheterogeneity? 3) What is the effect of the antigen?

There are roughly three ways to study the regulation of antibody glycosylation: in humans, model organisms or using cell culture systems. Very often the mouse is used as model organism to study the regulation of IgG Fc glycosylation. These studies, for example, revealed that Fc sialylation was affected by specific cytokines, like IL-21, -22 and -23 [318], the involvement of T cells [319, 401] and the antigen based on which the B cells were matured [402]. Studies in mice have a large advantage over studies in humans, as various experimental conditions can be controlled, and the function of specific genes and proteins can be assessed by genetic manipulation. However, profound differences between mouse and human glycosylation, which had previously been shown for plasma protein *N*-glycosylation [298], were accordingly found for IgG Fc glycosylation in this thesis (**Chapter 7**) [289]. Firstly, murine Fc glycans carry predominantly the sialic acid *N*-glycolylneuraminic acid, while humans exclusively express *N*-acetylneuraminic acid [42, 289]. Secondly, mice can terminate their *N*-glycans with an α 1,3-linked galactose, a feature which is naturally absent and immunogenic in humans [315]. Thirdly, the relative glycan abundances between subclasses in mice are very different, while glycan profiles are rather comparable for the four human IgG subclasses [88, 289, 402]. Finally, the incidence of afucosylated and bisected glycoforms on murine IgG is noticeably lower as compared to human IgG [28, 289]. In addition, the IgG receptors and their cellular and tissue distribution are different between humans and mice [60, 300]. This means that, although experiments in murine models can provide unique opportunities to study the regulation of IgG Fc glycosylation, care should be taken in translating findings obtained in mice directly to the human situation [45].

In contrast, exploiting specific health-related situations in humans might provide the opportunity to get a direct insight into the regulation of IgG Fc glycosylation. An example is the work performed in **Chapter 4**, where individuals in need of a hematopoietic stem cell transplantation were studied in a longitudinal manner [194]. Comparing the Fc glycosylation of the donors to that of the recipients, pre- and post-transplantation, revealed the transplanted cells to mimic the glycosylation of the recipients, not the donor. This indicates that there is no conserved, epigenetic memory that determines the glycosylation in donor cells, but rather a large influence of the microenvironment of the B cells. An alternative study design to explore the regulation of antibody glycosylation directly in humans is the longitudinal assessment of total IgG glycosylation pre- and post-

infection, vaccination or drug treatment in clinical trials [196, 227, 403]. Such a study design, for example, revealed the effect of hormone levels on Fc galactosylation [196]. Comparing antibody responses between vaccination and infection with the same pathogen might give an insight into the antigen-dependent regulation of antigen-specific IgGs [404, 405]. For example, it was shown that antibodies specific against hepatitis B virus exhibited a slightly lower fucosylation when derived from infected individuals, as compared to vaccinated individuals [405]. Furthermore, both antigen-specific and total IgG glycosylation can be compared between different body fluids or tissues. This might reveal the tissue- or fluid-specific regulation of Fc glycosylation, as was already proven for IgG derived from cerebrospinal or synovial fluid [337, 338]. Notably, in **Chapter 8**, it was reported that the glycosylation on IgG showed distinct profiles when produced in the circulation or secreted in saliva, a finding that was even more pronounced on IgA. This is likely to be dependent on the specific antigens the antibody producing cells encounter in the different body compartments.

Finally, the use of cultured human B cells provides the means to study the direct effect of soluble factors in the microenvironment of B cells on the regulation of their IgG Fc glycosylation. For example, the addition of IL-21 and all-trans retinoic acid showed to respectively increase and decrease Fc galactosylation when added during the activation and differentiation of cultured human B cells [78]. Even more exciting would be the analysis of IgGs produced by a single activated B cell, various single B cells from the same clone, and different clones with the same antigen-specificity. These types of experiment will provide insight into the regulation of the glycan microheterogeneity. Specifically, the question can be answered whether one B cell produces IgG with one glycoform or the whole repertoire of glycans. Furthermore, one can get information on whether the cells from one B cell clone or clones with very similar specificity all produce the same glycosylation profile. While single cell analysis is relevant to obtain insights into the regulatory mechanisms of one cell, the characterization of IgG produced by one clone or pool of antigen-specific B cells might be more relevant for the functional translation, as this is what is present during an immune response in the body.

9.4 Conclusion

In this thesis, methods were developed, and antibody glycosylation was characterized in order to further the clinical application of antibody glycosylation analysis. New mass spectrometric workflows were introduced in **Chapters 2** and **8**. **Chapter 7** showed the differential characteristics of murine IgG glycosylation of different strains and highlighted the profound differences between humans and mice, with regard to IgG glycosylation. **Chapters 4** and **8** showed the use of controlled human situations to study the regulatory

mechanisms of IgG and IgA glycosylation. Finally, **Chapters 3, 5 and 6**, identified glycosidic differences with specified (patho)physiological conditions, which might be exploited for patient stratification in the future.

The clinical application of antibody glycomics by mass spectrometry requires further technological developments and mechanistic insights in order to be exploited to its full potential. Preferred study designs involve the longitudinal monitoring of antibody glycosylation in humans, the analysis of antigen-specific antibodies, and the use of human B cell cultures and single B cell analysis. Finally, sets of glycoforms should be identified which can serve as clinical biomarkers and can be monitored in a clinical test. To make all this technically feasible, it is essential to have mass spectrometric techniques that are robust over a long period of time and over a large range of analyte concentrations and matrix variations. Therefore, internal standards should be introduced in glycopeptide profiling workflows.

Addendum

References

1. Khoury, G.A., R.C. Baliban, and C.A. Floudas, *Proteome-wide post-translational modification statistics: frequency analysis and curation of the swiss-prot database*. Sci Rep, 2011. **1**.
2. Varki, A., *Essentials of Glycobiology*, in *Essentials of Glycobiology*, rd, et al., Editors. 2015: Cold Spring Harbor (NY).
3. Spiro, R.G., *Protein glycosylation: nature, distribution, enzymatic formation, and disease implications of glycopeptide bonds*. Glycobiology, 2002. **12**(4): p. 43R-56R.
4. Lis, H. and N. Sharon, *Protein glycosylation. Structural and functional aspects*. Eur J Biochem, 1993. **218**(1): p. 1-27.
5. Van Breedam, W., et al., *Bitter-sweet symphony: glycan-lectin interactions in virus biology*. FEMS Microbiol Rev, 2014. **38**(4): p. 598-632.
6. Crocker, P.R. and A. Varki, *Siglecs in the immune system*. Immunology, 2001. **103**(2): p. 137-45.
7. Garcia-Vallejo, J.J. and Y. van Kooyk, *The physiological role of DC-SIGN: a tale of mice and men*. Trends Immunol, 2013. **34**(10): p. 482-6.
8. Marshall, R.D., *Glycoproteins*. Annu Rev Biochem, 1972. **41**: p. 673-702.
9. Bause, E. and G. Legler, *The role of the hydroxy amino acid in the triplet sequence Asn-Xaa-Thr(Ser) for the N-glycosylation step during glycoprotein biosynthesis*. Biochem J, 1981. **195**(3): p. 639-44.
10. Zielinska, D.F., et al., *Precision mapping of an in vivo N-glycoproteome reveals rigid topological and sequence constraints*. Cell, 2010. **141**(5): p. 897-907.
11. Kornfeld, R. and S. Kornfeld, *Assembly of asparagine-linked oligosaccharides*. Annu Rev Biochem, 1985. **54**: p. 631-64.
12. Schauer, R., *Chemistry, metabolism, and biological functions of sialic acids*. Adv Carbohydr Chem Biochem, 1982. **40**: p. 131-234.
13. McNaught, A.D., *International Union of Pure and Applied Chemistry and International Union of Biochemistry and Molecular Biology. Joint Commission on Biochemical Nomenclature. Nomenclature of carbohydrates*. Carbohydr Res, 1997. **297**(1): p. 1-92.
14. Seeberger, P.H., *Monosaccharide Diversity*, in *Essentials of Glycobiology*, rd, et al., Editors. 2015: Cold Spring Harbor (NY). p. 19-30.
15. Prestegard, J.H., J. Liu, and G. Widmalm, *Oligosaccharides and Polysaccharides*, in *Essentials of Glycobiology*, rd, et al., Editors. 2015: Cold Spring Harbor (NY). p. 31-40.
16. Bennett, E.P., et al., *Control of mucin-type O-glycosylation: a classification of the polypeptide GalNAc-transferase gene family*. Glycobiology, 2012. **22**(6): p. 736-56.
17. Brockhausen, I. and P. Stanley, *O-GalNAc Glycans*, in *Essentials of Glycobiology*, rd, et al., Editors. 2015: Cold Spring Harbor (NY). p. 113-123.
18. Jensen, P.H., D. Kolarich, and N.H. Packer, *Mucin-type O-glycosylation--putting the pieces together*. FEBS J, 2010. **277**(1): p. 81-94.
19. Hanisch, F.G., *O-glycosylation of the mucin type*. Biol Chem, 2001. **382**(2): p. 143-9.
20. Murphy, K. and C. Weaver, *Antigen Recognition by B-cell and T-cell Receptors*, in *Janeway's Immunobiology 9th edition*. 2017, Garland Science: New York and London. p. 139-172.
21. Dard, P., et al., *DNA sequence variability of IGHG3 alleles associated to the main G3m haplotypes in human populations*. Eur J Hum Genet, 2001. **9**(10): p. 765-72.
22. Vidarsson, G., G. Dekkers, and T. Rispens, *IgG subclasses and allotypes: from structure to effector functions*. Front Immunol, 2014. **5**: p. 520.
23. Stavenhagen, K., R. Plomp, and M. Wührer, *Site-Specific Protein N- and O-Glycosylation Analysis by a C18-Porous Graphitized Carbon-Liquid Chromatography-Electrospray Ionization Mass Spectrometry Approach Using Pronase Treated Glycopeptides*. Anal Chem, 2015. **87**(23): p. 11691-9.

24. Hulsmeier, A.J., et al., *Glycosylation site occupancy in health, congenital disorder of glycosylation and fatty liver disease*. Sci Rep, 2016. **6**: p. 33927.
25. Wuhrer, M., et al., *Glycosylation profiling of immunoglobulin G (IgG) subclasses from human serum*. Proteomics, 2007. **7**(22): p. 4070-81.
26. Flynn, G.C., et al., *Naturally occurring glycan forms of human immunoglobulins G1 and G2*. Mol Immunol, 2010. **47**(11-12): p. 2074-82.
27. Maier, M., et al., *Applying mini-bore HPAEC-MS/MS for the characterization and quantification of Fc N-glycans from heterogeneously glycosylated IgGs*. J Chromatogr B Analyt Technol Biomed Life Sci, 2016. **1033-1034**: p. 342-352.
28. Bakovic, M.P., et al., *High-throughput IgG Fc N-glycosylation profiling by mass spectrometry of glycopeptides*. J Proteome Res, 2013. **12**(2): p. 821-31.
29. Bondt, A., et al., *Immunoglobulin G (IgG) Fab glycosylation analysis using a new mass spectrometric high-throughput profiling method reveals pregnancy-associated changes*. Mol Cell Proteomics, 2014. **13**(11): p. 3029-39.
30. Liu, T., et al., *Human plasma N-glycoproteome analysis by immunoaffinity subtraction, hydrazide chemistry, and mass spectrometry*. J Proteome Res, 2005. **4**(6): p. 2070-80.
31. Plomp, R., et al., *Hinge-Region O-Glycosylation of Human Immunoglobulin G3 (IgG3)*. Mol Cell Proteomics, 2015. **14**(5): p. 1373-84.
32. van de Bovenkamp, F.S., et al., *Adaptive antibody diversification through N-linked glycosylation of the immunoglobulin variable region*. Proc Natl Acad Sci U S A, 2018. **115**(8): p. 1901-1906.
33. van de Bovenkamp, F.S., et al., *The Emerging Importance of IgG Fab Glycosylation in Immunity*. J Immunol, 2016. **196**(4): p. 1435-41.
34. Murphy, K. and C. Weaver, *The Humoral Immune Response*, in *Janeway's Immunobiology 9th edition*. 2017, Garland Science: New York and London. p. 399-444.
35. Krapp, S., et al., *Structural analysis of human IgG-Fc glycoforms reveals a correlation between glycosylation and structural integrity*. J Mol Biol, 2003. **325**(5): p. 979-89.
36. Kao, D., et al., *A Monosaccharide Residue Is Sufficient to Maintain Mouse and Human IgG Subclass Activity and Directs IgG Effector Functions to Cellular Fc Receptors*. Cell Rep, 2015. **13**(11): p. 2376-2385.
37. Dekkers, G., et al., *Decoding the Human Immunoglobulin G-Glycan Repertoire Reveals a Spectrum of Fc-Receptor- and Complement-Mediated-Effector Activities*. Front Immunol, 2017. **8**: p. 877.
38. Mimura, Y., et al., *Role of oligosaccharide residues of IgG1-Fc in Fc gamma RIIb binding*. J Biol Chem, 2001. **276**(49): p. 45539-47.
39. Allhorn, M., et al., *Human IgG/Fc gamma R interactions are modulated by streptococcal IgG glycan hydrolysis*. PLoS One, 2008. **3**(1): p. e1413.
40. Buck, P.M., S. Kumar, and S.K. Singh, *Consequences of glycan truncation on Fc structural integrity*. MAbs, 2013. **5**(6): p. 904-16.
41. Li, T., et al., *Modulating IgG effector function by Fc glycan engineering*. Proc Natl Acad Sci U S A, 2017. **114**(13): p. 3485-3490.
42. Raju, T.S., et al., *Species-specific variation in glycosylation of IgG: evidence for the species-specific sialylation and branch-specific galactosylation and importance for engineering recombinant glycoprotein therapeutics*. Glycobiology, 2000. **10**(5): p. 477-86.
43. Tearle, R.G., et al., *The alpha-1,3-galactosyltransferase knockout mouse. Implications for xenotransplantation*. Transplantation, 1996. **61**(1): p. 13-9.
44. Maresch, D. and F. Altmann, *Isotype-specific glycosylation analysis of mouse IgG by LC-MS*. Proteomics, 2016. **16**(9): p. 1321-30.
45. Tjon, A.S., et al., *Differences in Anti-Inflammatory Actions of Intravenous Immunoglobulin between Mice and Men: More than Meets the Eye*. Front Immunol, 2015. **6**: p. 197.

46. Brinkman-Van der Linden, E.C., et al., *Loss of N-glycolylneuraminic acid in human evolution. Implications for sialic acid recognition by siglecs*. J Biol Chem, 2000. **275**(12): p. 8633-40.
47. Shields, R.L., et al., *Lack of fucose on human IgG1 N-linked oligosaccharide improves binding to human Fcγ₃RIII and antibody-dependent cellular toxicity*. J Biol Chem, 2002. **277**(30): p. 26733-40.
48. Iida, S., et al., *Nonfucosylated therapeutic IgG1 antibody can evade the inhibitory effect of serum immunoglobulin G on antibody-dependent cellular cytotoxicity through its high affinity binding to Fcγ₃RIIIa*. Clin Cancer Res, 2006. **12**(9): p. 2879-87.
49. Ferrara, C., et al., *Unique carbohydrate-carbohydrate interactions are required for high affinity binding between Fcγ₃RIII and antibodies lacking core fucose*. Proc Natl Acad Sci U S A, 2011. **108**(31): p. 12669-74.
50. Subedi, G.P., Q.M. Hanson, and A.W. Barb, *Restricted motion of the conserved immunoglobulin G1 N-glycan is essential for efficient Fcγ₃RIIIa binding*. Structure, 2014. **22**(10): p. 1478-88.
51. Subedi, G.P. and A.W. Barb, *The immunoglobulin G1 N-glycan composition affects binding to each low affinity Fcγ₃ receptor*. MAbs, 2016. **8**(8): p. 1512-1524.
52. Thomann, M., et al., *In vitro glycoengineering of IgG1 and its effect on Fc receptor binding and ADCC activity*. PLoS One, 2015. **10**(8): p. e0134949.
53. Pace, D., et al., *Characterizing the effect of multiple Fc glycan attributes on the effector functions and Fcγ₃RIIIa receptor binding activity of an IgG1 antibody*. Biotechnol Prog, 2016. **32**(5): p. 1181-1192.
54. Bondt, A., et al., *Association between galactosylation of immunoglobulin G and improvement of rheumatoid arthritis during pregnancy is independent of sialylation*. J Proteome Res, 2013. **12**(10): p. 4522-31.
55. Stanley, P., N. Taniguchi, and M. Aebi, *N-Glycans*, in *Essentials of Glycobiology*, rd, et al., Editors. 2015: Cold Spring Harbor (NY). p. 99-111.
56. Quast, I., et al., *Sialylation of IgG Fc domain impairs complement-dependent cytotoxicity*. J Clin Invest, 2015. **125**(11): p. 4160-70.
57. Sondermann, P., et al., *General mechanism for modulating immunoglobulin effector function*. Proc Natl Acad Sci U S A, 2013. **110**(24): p. 9868-72.
58. Anthony, R.M., et al., *Identification of a receptor required for the anti-inflammatory activity of IVIG*. Proc Natl Acad Sci U S A, 2008. **105**(50): p. 19571-8.
59. Yu, X., et al., *Dissecting the molecular mechanism of IVIg therapy: the interaction between serum IgG and DC-SIGN is independent of antibody glycoform or Fc domain*. J Mol Biol, 2013. **425**(8): p. 1253-8.
60. Bayry, J., et al., *DC-SIGN and α₂,6-sialylated IgG Fc interaction is dispensable for the anti-inflammatory activity of IVIg on human dendritic cells*. Proc Natl Acad Sci U S A, 2009. **106**(9): p. E24; author reply E25.
61. Nagae, M., et al., *Atomic visualization of a flipped-back conformation of bisected glycans bound to specific lectins*. Sci Rep, 2016. **6**: p. 22973.
62. Ferrara, C., et al., *Modulation of therapeutic antibody effector functions by glycosylation engineering: influence of Golgi enzyme localization domain and co-expression of heterologous β₁, 4-N-acetylglucosaminyltransferase III and Golgi α-mannosidase II*. Biotechnol Bioeng, 2006. **93**(5): p. 851-61.
63. Harpaz, N. and H. Schachter, *Control of glycoprotein synthesis. Processing of asparagine-linked oligosaccharides by one or more rat liver Golgi α-D-mannosidases dependent on the prior action of UDP-N-acetylglucosamine: α-D-mannoside β-2-N-acetylglucosaminyltransferase I*. J Biol Chem, 1980. **255**(10): p. 4894-902.
64. Dashivets, T., et al., *Multi-Angle Effector Function Analysis of Human Monoclonal IgG Glycovariants*. PLoS One, 2015. **10**(12): p. e0143520.

65. Franco, A., et al., *Human Fc receptor-like 5 binds intact IgG via mechanisms distinct from those of Fc receptors*. J Immunol, 2013. **190**(11): p. 5739-46.
66. Cheng, H.D., et al., *High-throughput characterization of the functional impact of IgG Fc glycan aberrancy in juvenile idiopathic arthritis*. Glycobiology, 2017. **27**(12): p. 1099-1108.
67. Ghetie, V., et al., *Abnormally short serum half-lives of IgG in beta 2-microglobulin-deficient mice*. Eur J Immunol, 1996. **26**(3): p. 690-6.
68. Williams, P.J., et al., *Short communication: selective placental transport of maternal IgG to the fetus*. Placenta, 1995. **16**(8): p. 749-56.
69. Wilcox, C.R., B. Holder, and C.E. Jones, *Factors Affecting the FcRn-Mediated Transplacental Transfer of Antibodies and Implications for Vaccination in Pregnancy*. Front Immunol, 2017. **8**: p. 1294.
70. Jefferis, R., *Isotype and glycoform selection for antibody therapeutics*. Arch Biochem Biophys, 2012. **526**(2): p. 159-66.
71. Ashwell, G. and A.G. Morell, *The role of surface carbohydrates in the hepatic recognition and transport of circulating glycoproteins*. Adv Enzymol Relat Areas Mol Biol, 1974. **41**(0): p. 99-128.
72. Naso, M.F., et al., *Engineering host cell lines to reduce terminal sialylation of secreted antibodies*. MAbs, 2010. **2**(5): p. 519-27.
73. Alessandri, L., et al., *Increased serum clearance of oligomannose species present on a human IgG1 molecule*. MAbs, 2012. **4**(4): p. 509-20.
74. Pucic, M., et al., *High throughput isolation and glycosylation analysis of IgG-variability and heritability of the IgG glycome in three isolated human populations*. Mol Cell Proteomics, 2011. **10**(10): p. M111 010090.
75. Wahl, A., et al., *Genome-Wide Association Study on Immunoglobulin G Glycosylation Patterns*. Front Immunol, 2018. **9**: p. 277.
76. de Jong, S.E., et al., *IgG1 Fc N-glycan galactosylation as a biomarker for immune activation*. Sci Rep, 2016. **6**: p. 28207.
77. Wahl, A., et al., *IgG glycosylation and DNA methylation are interconnected with smoking*. Biochim Biophys Acta, 2018. **1862**(3): p. 637-648.
78. Wang, J., et al., *Fc-glycosylation of IgG1 is modulated by B-cell stimuli*. Mol Cell Proteomics, 2011. **10**(5): p. M110 004655.
79. Chen, G., et al., *Human IgG Fc-glycosylation profiling reveals associations with age, sex, female sex hormones and thyroid cancer*. J Proteomics, 2012. **75**(10): p. 2824-34.
80. Keusch, J., et al., *Analysis of different glycosylation states in IgG subclasses*. Clin Chim Acta, 1996. **252**(2): p. 147-58.
81. Kristic, J., et al., *Glycans are a novel biomarker of chronological and biological ages*. J Gerontol A Biol Sci Med Sci, 2014. **69**(7): p. 779-89.
82. Yamada, E., et al., *Structural changes of immunoglobulin G oligosaccharides with age in healthy human serum*. Glycoconj J, 1997. **14**(3): p. 401-5.
83. Parekh, R., et al., *Age-related galactosylation of the N-linked oligosaccharides of human serum IgG*. J Exp Med, 1988. **167**(5): p. 1731-6.
84. Pucic, M., et al., *Changes in plasma and IgG N-glycome during childhood and adolescence*. Glycobiology, 2012. **22**(7): p. 975-82.
85. Selman, M.H., et al., *Fc specific IgG glycosylation profiling by robust nano-reverse phase HPLC-MS using a sheath-flow ESI sprayer interface*. J Proteomics, 2012. **75**(4): p. 1318-29.
86. Einarsdottir, H.K., et al., *Comparison of the Fc glycosylation of fetal and maternal immunoglobulin G*. Glycoconj J, 2013. **30**(2): p. 147-57.
87. Jansen, B.C., et al., *MALDI-TOF-MS reveals differential N-linked plasma- and IgG-glycosylation profiles between mothers and their newborns*. Sci Rep, 2016. **6**: p. 34001.
88. Plomp, R., et al., *Subclass-specific IgG glycosylation is associated with markers of inflammation and metabolic health*. Sci Rep, 2017. **7**(1): p. 12325.

89. Gornik, O., T. Pavic, and G. Lauc, *Alternative glycosylation modulates function of IgG and other proteins - implications on evolution and disease*. Biochim Biophys Acta, 2012. **1820**(9): p. 1318-26.
90. Gornik, O., et al., *Stability of N-glycan profiles in human plasma*. Glycobiology, 2009. **19**(12): p. 1547-53.
91. Hennig, R., et al., *Towards personalized diagnostics via longitudinal study of the human plasma N-glycome*. Biochim Biophys Acta, 2016. **1860**(8): p. 1728-38.
92. Parekh, R.B., et al., *Association of rheumatoid arthritis and primary osteoarthritis with changes in the glycosylation pattern of total serum IgG*. Nature, 1985. **316**(6027): p. 452-7.
93. Ercan, A., et al., *Aberrant IgG galactosylation precedes disease onset, correlates with disease activity, and is prevalent in autoantibodies in rheumatoid arthritis*. Arthritis Rheum, 2010. **62**(8): p. 2239-48.
94. van de Geijn, F.E., et al., *Immunoglobulin G galactosylation and sialylation are associated with pregnancy-induced improvement of rheumatoid arthritis and the postpartum flare: results from a large prospective cohort study*. Arthritis Res Ther, 2009. **11**(6): p. R193.
95. Trbojevic Akmacic, I., et al., *Inflammatory bowel disease associates with proinflammatory potential of the immunoglobulin G glycome*. Inflamm Bowel Dis, 2015. **21**(6): p. 1237-47.
96. Vuckovic, F., et al., *Association of systemic lupus erythematosus with decreased immunosuppressive potential of the IgG glycome*. Arthritis Rheumatol, 2015. **67**(11): p. 2978-89.
97. Kemna, M.J., et al., *Galactosylation and Sialylation Levels of IgG Predict Relapse in Patients With PR3-ANCA Associated Vasculitis*. EBioMedicine, 2017. **17**: p. 108-118.
98. Ackerman, M.E., et al., *Natural variation in Fc glycosylation of HIV-specific antibodies impacts antiviral activity*. J Clin Invest, 2013. **123**(5): p. 2183-92.
99. Kapur, R., et al., *Low anti-RhD IgG-Fc-fucosylation in pregnancy: a new variable predicting severity in haemolytic disease of the fetus and newborn*. Br J Haematol, 2014. **166**(6): p. 936-45.
100. Sonneveld, M.E., et al., *Glycosylation pattern of anti-platelet IgG is stable during pregnancy and predicts clinical outcome in alloimmune thrombocytopenia*. Br J Haematol, 2016. **174**(2): p. 310-20.
101. Lu, L.L., et al., *A Functional Role for Antibodies in Tuberculosis*. Cell, 2016. **167**(2): p. 433-443 e14.
102. Qian, Y., et al., *Quantitative analysis of serum IgG galactosylation assists differential diagnosis of ovarian cancer*. J Proteome Res, 2013. **12**(9): p. 4046-55.
103. Vuckovic, F., et al., *IgG Glycome in Colorectal Cancer*. Clin Cancer Res, 2016. **22**(12): p. 3078-86.
104. Simon, A.K., G.A. Hollander, and A. McMichael, *Evolution of the immune system in humans from infancy to old age*. Proc Biol Sci, 2015. **282**(1821): p. 20143085.
105. Pezer, M., et al., *Effects of allergic diseases and age on the composition of serum IgG glycome in children*. Sci Rep, 2016. **6**: p. 33198.
106. Wuhrer, M., et al., *Glycoproteomics based on tandem mass spectrometry of glycopeptides*. J Chromatogr B Analyt Technol Biomed Life Sci, 2007. **849**(1-2): p. 115-28.
107. Hinneburg, H., et al., *The Art of Destruction: Optimizing Collision Energies in Quadrupole-Time of Flight (Q-TOF) Instruments for Glycopeptide-Based Glycoproteomics*. J Am Soc Mass Spectrom, 2016. **27**(3): p. 507-19.
108. de Hoffmann, E. and V. Stroobant, *Mass Spectrometry Principles and Applications Third Edition*. 2007, West Sussex, England: John Wiley & Sons Ltd.
109. Cotter, R.J., *Peer Reviewed: The New Time-of-Flight Mass Spectrometry*. Anal Chem, 1999. **71**(13): p. 445A-51A.
110. Wiley, W. and I.H. McLaren, *Time-of-flight mass spectrometer with improved resolution*. Review of scientific instruments, 1955. **26**(12): p. 1150-1157.

111. Mamyrin, B., et al., *The mass reflectron, a new non-magnetic time-of-flight mass spectrometer with high resolution*. Zh. Eksp. Teor. Fiz, 1973. **64**: p. 82-89.
112. Karas, M., et al., *Matrix-assisted ultraviolet laser desorption of non-volatile compounds*. International journal of mass spectrometry and ion processes, 1987. **78**: p. 53-68.
113. Knochenmuss, R., *A quantitative model of ultraviolet matrix-assisted laser desorption/ionization*. J Mass Spectrom, 2002. **37**(8): p. 867-77.
114. Selman, M.H., et al., *MALDI-TOF-MS analysis of sialylated glycans and glycopeptides using 4-chloro-alpha-cyanocinnamic acid matrix*. Proteomics, 2012. **12**(9): p. 1337-48.
115. Harvey, D.J., *Analysis of carbohydrates and glycoconjugates by matrix-assisted laser desorption/ionization mass spectrometry: an update for 2009-2010*. Mass Spectrom Rev, 2015. **34**(3): p. 268-422.
116. Wührer, M., C.H. Hokke, and A.M. Deelder, *Glycopeptide analysis by matrix-assisted laser desorption/ionization tandem time-of-flight mass spectrometry reveals novel features of horseradish peroxidase glycosylation*. Rapid Commun Mass Spectrom, 2004. **18**(15): p. 1741-8.
117. Thaysen-Andersen, M., S. Mysling, and P. Hojrup, *Site-specific glycoprofiling of N-linked glycopeptides using MALDI-TOF MS: strong correlation between signal strength and glycoform quantities*. Anal Chem, 2009. **81**(10): p. 3933-43.
118. Powell, A.K. and D.J. Harvey, *Stabilization of sialic acids in N-linked oligosaccharides and gangliosides for analysis by positive ion matrix-assisted laser desorption/ionization mass spectrometry*. Rapid Commun Mass Spectrom, 1996. **10**(9): p. 1027-32.
119. Kang, P., Y. Mechref, and M.V. Novotny, *High-throughput solid-phase permethylation of glycans prior to mass spectrometry*. Rapid Commun Mass Spectrom, 2008. **22**(5): p. 721-34.
120. Shajahan, A., et al., *Tool for Rapid Analysis of Glycopeptide by Permethylation via One-Pot Site Mapping and Glycan Analysis*. Anal Chem, 2017. **89**(20): p. 10734-10743.
121. Gil, G.C., et al., *High throughput quantification of N-glycans using one-pot sialic acid modification and matrix assisted laser desorption ionization time-of-flight mass spectrometry*. Anal Chem, 2010. **82**(15): p. 6613-20.
122. Liu, X., et al., *Methylamidation for sialoglycomics by MALDI-MS: a facile derivatization strategy for both alpha2,3- and alpha2,6-linked sialic acids*. Anal Chem, 2010. **82**(19): p. 8300-6.
123. Wheeler, S.F., P. Domann, and D.J. Harvey, *Derivatization of sialic acids for stabilization in matrix-assisted laser desorption/ionization mass spectrometry and concomitant differentiation of alpha(2 --> 3)- and alpha(2 --> 6)-isomers*. Rapid Commun Mass Spectrom, 2009. **23**(2): p. 303-12.
124. Reiding, K.R., et al., *High-throughput profiling of protein N-glycosylation by MALDI-TOF-MS employing linkage-specific sialic acid esterification*. Anal Chem, 2014. **86**(12): p. 5784-93.
125. Li, H., et al., *MALDI-MS analysis of sialylated N-glycan linkage isomers using solid-phase two step derivatization method*. Anal Chim Acta, 2016. **924**: p. 77-85.
126. Nishikaze, T., et al., *Differentiation of Sialyl Linkage Isomers by One-Pot Sialic Acid Derivatization for Mass Spectrometry-Based Glycan Profiling*. Anal Chem, 2017. **89**(4): p. 2353-2360.
127. Gomes de Oliveira, A.G., et al., *A systematic study of glycopeptide esterification for the semi-quantitative determination of sialylation in antibodies*. Rapid Commun Mass Spectrom, 2015. **29**(19): p. 1817-26.
128. Nishikaze, T., S. Kawabata, and K. Tanaka, *In-depth structural characterization of N-linked glycopeptides using complete derivatization for carboxyl groups followed by positive- and negative-ion tandem mass spectrometry*. Anal Chem, 2014. **86**(11): p. 5360-9.
129. Mann, M., C.K. Meng, and J.B. Fenn, *Interpreting mass spectra of multiply charged ions*. Analytical Chemistry, 1989. **61**(15): p. 1702-1708.

130. Thaysen-Andersen, M., N.H. Packer, and B.L. Schulz, *Maturing Glycoproteomics Technologies Provide Unique Structural Insights into the N-glycoproteome and Its Regulation in Health and Disease*. Mol Cell Proteomics, 2016. **15**(6): p. 1773-90.
131. Reusch, D., et al., *Comparison of methods for the analysis of therapeutic immunoglobulin G Fc-glycosylation profiles-Part 2: Mass spectrometric methods*. MAbs, 2015. **7**(4): p. 732-42.
132. Khatri, K., et al., *Microfluidic Capillary Electrophoresis-Mass Spectrometry for Analysis of Monosaccharides, Oligosaccharides, and Glycopeptides*. Anal Chem, 2017. **89**(12): p. 6645-6655.
133. Plomp, R., et al., *Recent Advances in Clinical Glycoproteomics of Immunoglobulins (Igs)*. Mol Cell Proteomics, 2016. **15**(7): p. 2217-28.
134. Palmisano, G., et al., *Structural analysis of glycoprotein sialylation-part II: LC-MS based detection*. Rsc Advances, 2013. **3**(45): p. 22706-22726.
135. Wuhrer, M., A.M. Deelder, and C.H. Hokke, *Protein glycosylation analysis by liquid chromatography-mass spectrometry*. J Chromatogr B Analyt Technol Biomed Life Sci, 2005. **825**(2): p. 124-33.
136. Stadlmann, J., et al., *Analysis of immunoglobulin glycosylation by LC-ESI-MS of glycopeptides and oligosaccharides*. Proteomics, 2008. **8**(14): p. 2858-71.
137. Zauner, G., et al., *Protein glycosylation analysis by HILIC-LC-MS of Proteinase K-generated N- and O-glycopeptides*. J Sep Sci, 2010. **33**(6-7): p. 903-10.
138. Ding, W., et al., *Identification and quantification of glycoproteins using ion-pairing normal-phase liquid chromatography and mass spectrometry*. Mol Cell Proteomics, 2009. **8**(9): p. 2170-85.
139. Takegawa, Y., et al., *Simple separation of isomeric sialylated N-glycopeptides by a zwitterionic type of hydrophilic interaction chromatography*. J Sep Sci, 2006. **29**(16): p. 2533-40.
140. Thaysen-Andersen, M., et al., *Site-specific characterisation of densely O-glycosylated mucin-type peptides using electron transfer dissociation ESI-MS/MS*. Electrophoresis, 2011. **32**(24): p. 3536-45.
141. Stavenhagen, K., D. Kolarich, and M. Wuhrer, *Clinical Glycomics Employing Graphitized Carbon Liquid Chromatography-Mass Spectrometry*. Chromatographia, 2015. **78**(5-6): p. 307-320.
142. Alley, W.R., Jr., Y. Mechref, and M.V. Novotny, *Use of activated graphitized carbon chips for liquid chromatography/mass spectrometric and tandem mass spectrometric analysis of tryptic glycopeptides*. Rapid Commun Mass Spectrom, 2009. **23**(4): p. 495-505.
143. Zhao, Y., et al., *Online two-dimensional porous graphitic carbon/reversed phase liquid chromatography platform applied to shotgun proteomics and glycoproteomics*. Anal Chem, 2014. **86**(24): p. 12172-9.
144. Liu, M., et al., *Efficient and accurate glycopeptide identification pipeline for high-throughput site-specific N-glycosylation analysis*. J Proteome Res, 2014. **13**(6): p. 3121-9.
145. Khatri, K., et al., *Confident assignment of site-specific glycosylation in complex glycoproteins in a single step*. J Proteome Res, 2014. **13**(10): p. 4347-55.
146. Heemskerk, A.A., et al., *Coupling porous sheathless interface MS with transient-ITP in neutral capillaries for improved sensitivity in glycopeptide analysis*. Electrophoresis, 2013. **34**(3): p. 383-7.
147. Kammeijer, G.S., et al., *Dopant Enriched Nitrogen Gas Combined with Sheathless Capillary Electrophoresis-Electrospray Ionization-Mass Spectrometry for Improved Sensitivity and Repeatability in Glycopeptide Analysis*. Anal Chem, 2016. **88**(11): p. 5849-56.
148. Kammeijer, G.S.M., et al., *Sialic acid linkage differentiation of glycopeptides using capillary electrophoresis - electrospray ionization - mass spectrometry*. Sci Rep, 2017. **7**(1): p. 3733.
149. de Haan, N., et al., *Linkage-specific sialic acid derivatization for MALDI-TOF-MS profiling of IgG glycopeptides*. Anal Chem, 2015. **87**(16): p. 8284-91.

150. Crocker, P.R., J.C. Paulson, and A. Varki, *Siglecs and their roles in the immune system*. Nature reviews. Immunology, 2007. **7**(4): p. 255-66.
151. Muramatsu, T., *Essential roles of carbohydrate signals in development, immune response and tissue functions, as revealed by gene targeting*. Journal of biochemistry, 2000. **127**(2): p. 171-6.
152. Wormald, M.R. and R.A. Dwek, *Glycoproteins: glycan presentation and protein-fold stability*. Structure, 1999. **7**(7): p. R155-60.
153. Apweiler, R., H. Hermjakob, and N. Sharon, *On the frequency of protein glycosylation, as deduced from analysis of the SWISS-PROT database*. Biochimica et biophysica acta, 1999. **1473**(1): p. 4-8.
154. in *Essentials of Glycobiology*, A. Varki, et al., Editors. 2009: Cold Spring Harbor (NY).
155. Anthony, R.M., et al., *Recapitulation of IVIG anti-inflammatory activity with a recombinant IgG Fc*. Science, 2008. **320**(5874): p. 373-6.
156. Jefferis, R., *Glycosylation as a strategy to improve antibody-based therapeutics*. Nature reviews. Drug discovery, 2009. **8**(3): p. 226-34.
157. Huang, L., et al., *Impact of variable domain glycosylation on antibody clearance: an LC/MS characterization*. Analytical biochemistry, 2006. **349**(2): p. 197-207.
158. Coloma, M.J., et al., *Position effects of variable region carbohydrate on the affinity and in vivo behavior of an anti-(1-->6) dextran antibody*. Journal of immunology, 1999. **162**(4): p. 2162-70.
159. Hayes, J.M., et al., *Fc gamma receptor glycosylation modulates the binding of IgG glycoforms: a requirement for stable antibody interactions*. Journal of proteome research, 2014. **13**(12): p. 5471-85.
160. Harvey, D.J., *Analysis of carbohydrates and glycoconjugates by matrix-assisted laser desorption/ionization mass spectrometry: An update covering the period 1999-2000*. Mass spectrometry reviews, 2006. **25**(4): p. 595-662.
161. Huffman, J.E., et al., *Comparative performance of four methods for high-throughput glycosylation analysis of immunoglobulin G in genetic and epidemiological research*. Molecular & cellular proteomics : MCP, 2014. **13**(6): p. 1598-610.
162. Alley, W.R., Jr. and M.V. Novotny, *Glycomic analysis of sialic acid linkages in glycans derived from blood serum glycoproteins*. Journal of proteome research, 2010. **9**(6): p. 3062-72.
163. Selman, M.H., et al., *Immunoglobulin G glycopeptide profiling by matrix-assisted laser desorption ionization Fourier transform ion cyclotron resonance mass spectrometry*. Anal Chem, 2010. **82**(3): p. 1073-81.
164. Thaysen-Andersen, M. and N.H. Packer, *Advances in LC-MS/MS-based glycoproteomics: getting closer to system-wide site-specific mapping of the N- and O-glycoproteome*. Biochim Biophys Acta, 2014. **1844**(9): p. 1437-52.
165. Amano, J., et al., *Derivatization with 1-pyrenyldiazomethane enhances ionization of glycopeptides but not peptides in matrix-assisted laser desorption/ionization mass spectrometry*. Analytical chemistry, 2010. **82**(20): p. 8738-43.
166. Nishikaze, T., et al., *Negative-ion MALDI-MS2 for discrimination of alpha2,3- and alpha2,6-sialylation on glycopeptides labeled with a pyrene derivative*. Journal of chromatography. B, Analytical technologies in the biomedical and life sciences, 2011. **879**(17-18): p. 1419-28.
167. Ruhaak, L.R., et al., *Hydrophilic interaction chromatography-based high-throughput sample preparation method for N-glycan analysis from total human plasma glycoproteins*. Analytical chemistry, 2008. **80**(15): p. 6119-26.
168. Selman, M.H., et al., *Cotton HILIC SPE microtips for microscale purification and enrichment of glycans and glycopeptides*. Analytical chemistry, 2011. **83**(7): p. 2492-9.

169. Stumpo, K.A. and V.N. Reinhold, *The N-glycome of human plasma*. Journal of proteome research, 2010. **9**(9): p. 4823-30.
170. Thanabalasingham, G., et al., *Mutations in HNF1A result in marked alterations of plasma glycan profile*. Diabetes, 2013. **62**(4): p. 1329-37.
171. Reusch, D., et al., *Comparison of methods for the analysis of therapeutic immunoglobulin G Fc-glycosylation profiles--part 1: separation-based methods*. MAbs, 2015. **7**(1): p. 167-79.
172. Shubhakar, A., et al., *High-Throughput Analysis and Automation for Glycomics Studies*. Chromatographia, 2015. **78**(5-6): p. 321-333.
173. Kloos, D., et al., *Derivatization of the tricarboxylic acid cycle intermediates and analysis by online solid-phase extraction-liquid chromatography-mass spectrometry with positive-ion electrospray ionization*. Journal of chromatography. A, 2012. **1232**: p. 19-26.
174. Ruhaak, L.R., et al., *2-picoline-borane: a non-toxic reducing agent for oligosaccharide labeling by reductive amination*. Proteomics, 2010. **10**(12): p. 2330-6.
175. Morelle, W. and J.C. Michalski, *Analysis of protein glycosylation by mass spectrometry*. Nat Protoc, 2007. **2**(7): p. 1585-602.
176. de Haan, N., et al., *Changes in Healthy Human IgG Fc-Glycosylation after Birth and during Early Childhood*. J Proteome Res, 2016. **15**(6): p. 1853-61.
177. Arnold, J.N., et al., *The impact of glycosylation on the biological function and structure of human immunoglobulins*. Annu Rev Immunol, 2007. **25**: p. 21-50.
178. Chan, A.C. and P.J. Carter, *Therapeutic antibodies for autoimmunity and inflammation*. Nat Rev Immunol, 2010. **10**(5): p. 301-16.
179. Ruhaak, L.R., et al., *Decreased levels of bisecting GlcNAc glycoforms of IgG are associated with human longevity*. PLoS One, 2010. **5**(9): p. e12566.
180. Shields, R.L., et al., *High resolution mapping of the binding site on human IgG1 for Fc gamma RI, Fc gamma RII, Fc gamma RIII, and FcRn and design of IgG1 variants with improved binding to the Fc gamma R*. J Biol Chem, 2001. **276**(9): p. 6591-604.
181. Jefferis, R. and J. Lund, *Interaction sites on human IgG-Fc for Fc gamma R: current models*. Immunol Lett, 2002. **82**(1-2): p. 57-65.
182. Yamane-Ohnuki, N. and M. Satoh, *Production of therapeutic antibodies with controlled fucosylation*. MAbs, 2009. **1**(3): p. 230-6.
183. Matsumiya, S., et al., *Structural comparison of fucosylated and nonfucosylated Fc fragments of human immunoglobulin G1*. J Mol Biol, 2007. **368**(3): p. 767-79.
184. Reusch, D. and M.L. Tejada, *Fc glycans of therapeutic antibodies as critical quality attributes*. Glycobiology, 2015. **25**(12): p. 1325-34.
185. Bruhns, P., et al., *Specificity and affinity of human Fc gamma receptors and their polymorphic variants for human IgG subclasses*. Blood, 2009. **113**(16): p. 3716-25.
186. Karsten, C.M., et al., *Anti-inflammatory activity of IgG1 mediated by Fc galactosylation and association of Fc gamma RIIB and dectin-1*. Nat Med, 2012. **18**(9): p. 1401-6.
187. Morell, A., et al., *IgG subclasses: development of the serum concentrations in "normal" infants and children*. J Pediatr, 1972. **80**(6): p. 960-4.
188. Driessen, G.J., et al., *Common variable immunodeficiency and idiopathic primary hypogammaglobulinemia: two different conditions within the same disease spectrum*. Haematologica, 2013. **98**(10): p. 1617-23.
189. Ceroni, A., et al., *GlycoWorkbench: a tool for the computer-assisted annotation of mass spectra of glycans*. J Proteome Res, 2008. **7**(4): p. 1650-9.
190. Jansen, B.C., et al., *MassyTools: A High-Throughput Targeted Data Processing Tool for Relative Quantitation and Quality Control Developed for Glycomic and Glycoproteomic MALDI-MS*. J Proteome Res, 2015.
191. Shakib, F. and D.R. Stanworth, *Human IgG subclasses in health and disease. (A review). Part II*. Ric Clin Lab, 1980. **10**(4): p. 561-80.

192. Varki, A., *Factors controlling the glycosylation potential of the Golgi apparatus*. Trends Cell Biol, 1998. **8**(1): p. 34-40.
193. Dall'Olio, F., et al., *N-glycomic biomarkers of biological aging and longevity: a link with inflammaging*. Ageing Res Rev, 2013. **12**(2): p. 685-98.
194. de Haan, N., et al., *Immunoglobulin G Fragment Crystallizable Glycosylation After Hematopoietic Stem Cell Transplantation Is Dissimilar to Donor Profiles*. Front Immunol, 2018. **9**: p. 1238.
195. Caaveiro, J.M., M. Kiyoshi, and K. Tsumoto, *Structural analysis of Fc/FcγR complexes: a blueprint for antibody design*. Immunol Rev, 2015. **268**(1): p. 201-21.
196. Ercan, A., et al., *Estrogens regulate glycosylation of IgG in women and men*. JCI Insight, 2017. **2**(4): p. e89703.
197. Falck, D., et al., *High-Throughput Analysis of IgG Fc Glycopeptides by LC-MS*. Methods Mol Biol, 2017. **1503**: p. 31-47.
198. Jansen, B.C., et al., *LaCyTools: A Targeted Liquid Chromatography-Mass Spectrometry Data Processing Package for Relative Quantitation of Glycopeptides*. J Proteome Res, 2016. **15**(7): p. 2198-210.
199. in *Essentials of Glycobiology*, A. Varki, et al., Editors. 2015: Cold Spring Harbor (NY).
200. Jones, M.B., et al., *B-cell-independent sialylation of IgG*. Proc Natl Acad Sci U S A, 2016. **113**(26): p. 7207-12.
201. Manhardt, C.T., et al., *Extrinsic sialylation is dynamically regulated by systemic triggers in vivo*. J Biol Chem, 2017.
202. Kaneko, Y., F. Nimmerjahn, and J.V. Ravetch, *Anti-inflammatory activity of immunoglobulin G resulting from Fc sialylation*. Science, 2006. **313**(5787): p. 670-3.
203. Plomp, H., *Glycoproteomics characterization of immunoglobulins in health and disease*. 2017.
204. van Tol, M.J., et al., *The origin of IgG production and homogeneous IgG components after allogeneic bone marrow transplantation*. Blood, 1996. **87**(2): p. 818-26.
205. de Haan, N., et al., *Differences in IgG Fc Glycosylation Are Associated with Outcome of Pediatric Meningococcal Sepsis*. MBio, 2018. **9**(3).
206. Stoof, S.P., et al., *Disease Burden of Invasive Meningococcal Disease in the Netherlands Between June 1999 and June 2011: A Subjective Role for Serogroup and Clonal Complex*. Clin Infect Dis, 2015. **61**(8): p. 1281-92.
207. ECDC. *Surveillance Atlas of Infectious Diseases*. 2017; Available from: <http://atlas.ecdc.europa.eu/public/index.aspx>.
208. MacNeil, J.R., et al., *Epidemiology of infant meningococcal disease in the United States, 2006-2012*. Pediatrics, 2015. **135**(2): p. e305-11.
209. Hadjichristodoulou, C., et al., *A Case-Control Study on the Risk Factors for Meningococcal Disease among Children in Greece*. PLoS One, 2016. **11**(6): p. e0158524.
210. Maat, M., et al., *Improved survival of children with sepsis and purpura: effects of age, gender, and era*. Crit Care, 2007. **11**(5): p. R112.
211. Rivero-Calle, I., et al., *The Burden of Pediatric Invasive Meningococcal Disease in Spain (2008-2013)*. Pediatr Infect Dis J, 2016. **35**(4): p. 407-13.
212. Montero-Martin, M., et al., *Prognostic markers of meningococcal disease in children: recent advances and future challenges*. Expert Rev Anti Infect Ther, 2014. **12**(11): p. 1357-69.
213. Hatherill, M., et al., *Procalcitonin and cytokine levels: relationship to organ failure and mortality in pediatric septic shock*. Crit Care Med, 2000. **28**(7): p. 2591-4.
214. Kornelisse, R.F., et al., *Meningococcal septic shock in children: clinical and laboratory features, outcome, and development of a prognostic score*. Clin Infect Dis, 1997. **25**(3): p. 640-6.

215. Carrol, E.D., et al., *A predominantly anti-inflammatory cytokine profile is associated with disease severity in meningococcal sepsis*. Intensive Care Med, 2005. **31**(10): p. 1415-9.
216. Pollack, M.M., U.E. Ruttimann, and P.R. Getson, *Pediatric risk of mortality (PRISM) score*. Crit Care Med, 1988. **16**(11): p. 1110-6.
217. Couto-Alves, A., et al., *A new scoring system derived from base excess and platelet count at presentation predicts mortality in paediatric meningococcal sepsis*. Crit Care, 2013. **17**(2): p. R68.
218. Pollard, A.J., et al., *Humoral immune responses to Neisseria meningitidis in children*. Infect Immun, 1999. **67**(5): p. 2441-51.
219. Vidarsson, G., et al., *Activity of human IgG and IgA subclasses in immune defense against Neisseria meningitidis serogroup B*. J Immunol, 2001. **166**(10): p. 6250-6.
220. Aase, A. and T.E. Michaelsen, *Opsonophagocytic activity induced by chimeric antibodies of the four human IgG subclasses with or without help from complement*. Scand J Immunol, 1994. **39**(6): p. 581-7.
221. Bredius, R.G., et al., *Fc gamma receptor IIa (CD32) polymorphism in fulminant meningococcal septic shock in children*. J Infect Dis, 1994. **170**(4): p. 848-53.
222. Simurina, M., et al., *Glycosylation of Immunoglobulin G Associates With Clinical Features of Inflammatory Bowel Diseases*. Gastroenterology, 2018. **154**(5): p. 1320-1333 e10.
223. Khemani, R.G., et al., *Disseminated intravascular coagulation score is associated with mortality for children with shock*. Intensive Care Med, 2009. **35**(2): p. 327-33.
224. Sharip, A., et al., *Population-based analysis of meningococcal disease mortality in the United States: 1990-2002*. Pediatr Infect Dis J, 2006. **25**(3): p. 191-4.
225. Novokmet, M., et al., *Changes in IgG and total plasma protein glycomes in acute systemic inflammation*. Sci Rep, 2014. **4**: p. 4347.
226. Lee-Sundlov, M.M., et al., *Circulating blood and platelets supply glycosyltransferases that enable extrinsic extracellular glycosylation*. Glycobiology, 2017. **27**(2): p. 188-198.
227. Vestreim, A.C., et al., *A pilot study showing differences in glycosylation patterns of IgG subclasses induced by pneumococcal, meningococcal, and two types of influenza vaccines*. Immun Inflamm Dis, 2014. **2**(2): p. 76-91.
228. Vermont, C.L., et al., *CC and CXC chemokine levels in children with meningococcal sepsis accurately predict mortality and disease severity*. Crit Care, 2006. **10**(1): p. R33.
229. de Kleijn, E.D., et al., *Activation of protein C following infusion of protein C concentrate in children with severe meningococcal sepsis and purpura fulminans: a randomized, double-blinded, placebo-controlled, dose-finding study*. Crit Care Med, 2003. **31**(6): p. 1839-47.
230. Emonts, M., et al., *Thrombin-activatable fibrinolysis inhibitor is associated with severity and outcome of severe meningococcal infection in children*. J Thromb Haemost, 2008. **6**(2): p. 268-76.
231. Hermans, P.W., et al., *4G/5G promoter polymorphism in the plasminogen-activator-inhibitor-1 gene and outcome of meningococcal disease*. Meningococcal Research Group. Lancet, 1999. **354**(9178): p. 556-60.
232. Goldstein, B., et al., *International pediatric sepsis consensus conference: definitions for sepsis and organ dysfunction in pediatrics*. Pediatr Crit Care Med, 2005. **6**(1): p. 2-8.
233. Burisch, J., et al., *East-West gradient in the incidence of inflammatory bowel disease in Europe: the ECCO-EpiCom inception cohort*. Gut, 2014. **63**(4): p. 588-97.
234. Molodecky, N.A., et al., *Increasing incidence and prevalence of the inflammatory bowel diseases with time, based on systematic review*. Gastroenterology, 2012. **142**(1): p. 46-54 e42; quiz e30.
235. Burisch, J., et al., *The burden of inflammatory bowel disease in Europe*. J Crohns Colitis, 2013. **7**(4): p. 322-37.
236. Burisch, J. and P. Munkholm, *Inflammatory bowel disease epidemiology*. Curr Opin Gastroenterol, 2013. **29**(4): p. 357-62.

237. Crohn's and Colitis Foundation of America. *The facts about inflammatory bowel diseases*. 17-02-2017]; Available from: <http://www.crohnscolitisfoundation.org/assets/pdfs/updatedibdfactbook.pdf>.
238. Satsangi, J., et al., *The Montreal classification of inflammatory bowel disease: controversies, consensus, and implications*. Gut, 2006. **55**(6): p. 749-53.
239. Xavier, R.J. and D.K. Podolsky, *Unravelling the pathogenesis of inflammatory bowel disease*. Nature, 2007. **448**(7152): p. 427-34.
240. Jostins, L., et al., *Host-microbe interactions have shaped the genetic architecture of inflammatory bowel disease*. Nature, 2012. **491**(7422): p. 119-24.
241. in *Transforming Glycoscience: A Roadmap for the Future*. 2012: Washington (DC).
242. Kristic, J. and G. Lauc, *Ubiquitous Importance of Protein Glycosylation*. Methods Mol Biol, 2017. **1503**: p. 1-12.
243. Subedi, G.P. and A.W. Barb, *The Structural Role of Antibody N-Glycosylation in Receptor Interactions*. Structure, 2015. **23**(9): p. 1573-1583.
244. Gornik, O. and G. Lauc, *Glycosylation of serum proteins in inflammatory diseases*. Dis Markers, 2008. **25**(4-5): p. 267-78.
245. Hauselmann, I. and L. Borsig, *Altered tumor-cell glycosylation promotes metastasis*. Front Oncol, 2014. **4**: p. 28.
246. Pinho, S.S. and C.A. Reis, *Glycosylation in cancer: mechanisms and clinical implications*. Nat Rev Cancer, 2015. **15**(9): p. 540-55.
247. Dias, A.M., et al., *Dysregulation of T cell receptor N-glycosylation: a molecular mechanism involved in ulcerative colitis*. Hum Mol Genet, 2014. **23**(9): p. 2416-27.
248. Dube, R., et al., *Agalactosyl IgG in inflammatory bowel disease: correlation with C-reactive protein*. Gut, 1990. **31**(4): p. 431-4.
249. Shinzaki, S., et al., *IgG oligosaccharide alterations are a novel diagnostic marker for disease activity and the clinical course of inflammatory bowel disease*. Am J Gastroenterol, 2008. **103**(5): p. 1173-81.
250. Lichtenstein, G.R. and D.P. McGovern, *Using markers in IBD to predict disease and treatment outcomes: rationale and a review of current status*. The American Journal of Gastroenterology Supplements, 2016. **3**(3): p. 17.
251. Panes, J., V. Jairath, and B.G. Levesque, *Advances in Use of Endoscopy, Radiology, and Biomarkers to Monitor Inflammatory Bowel Diseases*. Gastroenterology, 2017. **152**(2): p. 362-373 e3.
252. Schwab, I. and F. Nimmerjahn, *Intravenous immunoglobulin therapy: how does IgG modulate the immune system?* Nat Rev Immunol, 2013. **13**(3): p. 176-89.
253. Lauc, G., et al., *Mechanisms of disease: The human N-glycome*. Biochim Biophys Acta, 2016. **1860**(8): p. 1574-82.
254. Franke, A., et al., *Genome-wide meta-analysis increases to 71 the number of confirmed Crohn's disease susceptibility loci*. Nat Genet, 2010. **42**(12): p. 1118-25.
255. Lauc, G., et al., *Loci associated with N-glycosylation of human immunoglobulin G show pleiotropy with autoimmune diseases and haematological cancers*. PLoS Genet, 2013. **9**(1): p. e1003225.
256. Menni, C., et al., *Glycosylation of immunoglobulin g: role of genetic and epigenetic influences*. PLoS One, 2013. **8**(12): p. e82558.
257. Scanlan, C.N., D.R. Burton, and R.A. Dwek, *Making autoantibodies safe*. Proc Natl Acad Sci U S A, 2008. **105**(11): p. 4081-2.
258. Gasdaska, J.R., et al., *An afucosylated anti-CD20 monoclonal antibody with greater antibody-dependent cellular cytotoxicity and B-cell depletion and lower complement-dependent cytotoxicity than rituximab*. Mol Immunol, 2012. **50**(3): p. 134-41.
259. Thomann, M., et al., *Fc-galactosylation modulates antibody-dependent cellular cytotoxicity of therapeutic antibodies*. Mol Immunol, 2016. **73**: p. 69-75.

260. Schwab, I., A. Lux, and F. Nimmerjahn, *Pathways Responsible for Human Autoantibody and Therapeutic Intravenous IgG Activity in Humanized Mice*. Cell Rep, 2015. **13**(3): p. 610-620.
261. Washburn, N., et al., *Controlled tetra-Fc sialylation of IVIg results in a drug candidate with consistent enhanced anti-inflammatory activity*. Proc Natl Acad Sci U S A, 2015. **112**(11): p. E1297-306.
262. Bondt, A., et al., *Fab glycosylation of immunoglobulin G does not associate with improvement of rheumatoid arthritis during pregnancy*. Arthritis Res Ther, 2016. **18**(1): p. 274.
263. Cleynen, I., et al., *Inherited determinants of Crohn's disease and ulcerative colitis phenotypes: a genetic association study*. Lancet, 2016. **387**(10014): p. 156-67.
264. Dubinsky, M.C., et al., *Multidimensional prognostic risk assessment identifies association between IL12B variation and surgery in Crohn's disease*. Inflamm Bowel Dis, 2013. **19**(8): p. 1662-70.
265. Haritunians, T., et al., *Genetic predictors of medically refractory ulcerative colitis*. Inflamm Bowel Dis, 2010. **16**(11): p. 1830-40.
266. Balbin, M., et al., *DNA sequences specific for Caucasian G3m(b) and (g) allotypes: allotyping at the genomic level*. Immunogenetics, 1994. **39**(3): p. 187-93.
267. Viechtbauer, W., *Conducting meta-analyses in R with the metafor package*. Journal of statistical software, 2010. **36**(3).
268. Friedman, J., T. Hastie, and R. Tibshirani, *Regularization Paths for Generalized Linear Models via Coordinate Descent*. J Stat Softw, 2010. **33**(1): p. 1-22.
269. Shinzaki, S., et al., *Altered oligosaccharide structures reduce colitis induction in mice defective in beta-1,4-galactosyltransferase*. Gastroenterology, 2012. **142**(5): p. 1172-82.
270. Anthony, R.M., F. Wermeling, and J.V. Ravetch, *Novel roles for the IgG Fc glycan*. Ann N Y Acad Sci, 2012. **1253**: p. 170-80.
271. Rombouts, Y., et al., *Anti-citrullinated protein antibodies acquire a pro-inflammatory Fc glycosylation phenotype prior to the onset of rheumatoid arthritis*. Ann Rheum Dis, 2015. **74**(1): p. 234-41.
272. Ito, K., et al., *Lack of galactosylation enhances the pathogenic activity of IgG1 but Not IgG2a anti-erythrocyte autoantibodies*. J Immunol, 2014. **192**(2): p. 581-8.
273. Dubinsky, M.C., et al., *Serum immune responses predict rapid disease progression among children with Crohn's disease: immune responses predict disease progression*. Am J Gastroenterol, 2006. **101**(2): p. 360-7.
274. Lee, J.C., et al., *Genome-wide association study identifies distinct genetic contributions to prognosis and susceptibility in Crohn's disease*. Nat Genet, 2017. **49**(2): p. 262-268.
275. Marigorta, U.M., et al., *Transcriptional risk scores link GWAS to eQTLs and predict complications in Crohn's disease*. Nat Genet, 2017. **49**(10): p. 1517-1521.
276. Siegel, C., et al., *A validated web-based tool to display individualised Crohn's disease predicted outcomes based on clinical, serologic and genetic variables*. Alimentary pharmacology & therapeutics, 2016. **43**(2): p. 262-271.
277. Yoon, S.M., et al., *Colonic Phenotypes Are Associated with Poorer Response to Anti-TNF Therapies in Patients with IBD*. Inflamm Bowel Dis, 2017. **23**(8): p. 1382-1393.
278. Soubieres, A.A. and A. Poullis, *Emerging Biomarkers for the Diagnosis and Monitoring of Inflammatory Bowel Diseases*. Inflamm Bowel Dis, 2016. **22**(8): p. 2016-22.
279. Bennike, T., et al., *Biomarkers in inflammatory bowel diseases: current status and proteomics identification strategies*. World J Gastroenterol, 2014. **20**(12): p. 3231-44.
280. Panaccione, R., *Mechanisms of inflammatory bowel disease*. Gastroenterol Hepatol (N Y), 2013. **9**(8): p. 529-32.
281. Zou, G., et al., *Chemoenzymatic synthesis and Fcγ receptor binding of homogeneous glycoforms of antibody Fc domain. Presence of a bisecting sugar moiety enhances the*

- affinity of Fc to FcγIIIa receptor. *Journal of the American Chemical Society*, 2011. **133**(46): p. 18975-18991.
282. Cosnes, J., et al., *Epidemiology and natural history of inflammatory bowel diseases*. *Gastroenterology*, 2011. **140**(6): p. 1785-94.
 283. D'Haens, G.R., et al., *The London Position Statement of the World Congress of Gastroenterology on Biological Therapy for IBD with the European Crohn's and Colitis Organization: when to start, when to stop, which drug to choose, and how to predict response?* *Am J Gastroenterol*, 2011. **106**(2): p. 199-212; quiz 213.
 284. Mowat, C., et al., *Guidelines for the management of inflammatory bowel disease in adults*. *Gut*, 2011. **60**(5): p. 571-607.
 285. Liu, D., et al., *A practical guide to the monitoring and management of the complications of systemic corticosteroid therapy*. *Allergy Asthma Clin Immunol*, 2013. **9**(1): p. 30.
 286. Fiebiger, B.M., et al., *Protection in antibody- and T cell-mediated autoimmune diseases by antiinflammatory IgG Fcs requires type II FcRs*. *Proc Natl Acad Sci U S A*, 2015. **112**(18): p. E2385-94.
 287. Jannetto, P.J. and R.L. Fitzgerald, *Effective Use of Mass Spectrometry in the Clinical Laboratory*. *Clin Chem*, 2016. **62**(1): p. 92-8.
 288. Vanderschaeghe, D., et al., *High-throughput profiling of the serum N-glycome on capillary electrophoresis microfluidics systems: toward clinical implementation of GlycoHepatoTest*. *Analytical chemistry*, 2010. **82**(17): p. 7408-7415.
 289. de Haan, N., et al., *The N-Glycosylation of Mouse Immunoglobulin G (IgG)-Fragment Crystallizable Differs Between IgG Subclasses and Strains*. *Front Immunol*, 2017. **8**: p. 608.
 290. Murphy, K. and C. Weaver, *Janeway's immunobiology*. 9th ed. 2016: Garland Science.
 291. Kapur, R., et al., *A prominent lack of IgG1-Fc fucosylation of platelet alloantibodies in pregnancy*. *Blood*, 2014. **123**(4): p. 471-80.
 292. Iida, S., et al., *Two mechanisms of the enhanced antibody-dependent cellular cytotoxicity (ADCC) efficacy of non-fucosylated therapeutic antibodies in human blood*. *BMC Cancer*, 2009. **9**: p. 58.
 293. Chia, R., et al., *The origins and uses of mouse outbred stocks*. *Nat Genet*, 2005. **37**(11): p. 1181-6.
 294. Aldinger, K.A., et al., *Genetic variation and population substructure in outbred CD-1 mice: implications for genome-wide association studies*. *PLoS One*, 2009. **4**(3): p. e4729.
 295. Cheemarla, N.R. and A. Guerrero-Plata, *Immune Response to Human Metapneumovirus Infection: What We Have Learned from the Mouse Model*. *Pathogens*, 2015. **4**(3): p. 682-96.
 296. Walrath, J.C., et al., *Genetically engineered mouse models in cancer research*. *Adv Cancer Res*, 2010. **106**: p. 113-64.
 297. Azuma, K., et al., *Twin studies on the effect of genetic factors on serum agalactosyl immunoglobulin G levels*. *Biomed Rep*, 2014. **2**(2): p. 213-216.
 298. Reiding, K.R., et al., *Murine Plasma N-Glycosylation Traits Associated with Sex and Strain*. *J Proteome Res*, 2016. **15**(10): p. 3489-3499.
 299. Clerc, F., et al., *Human plasma protein N-glycosylation*. *Glycoconj J*, 2016. **33**(3): p. 309-43.
 300. Bruhns, P., *Properties of mouse and human IgG receptors and their contribution to disease models*. *Blood*, 2012. **119**(24): p. 5640-9.
 301. Zhang, Z., T. Goldschmidt, and H. Salter, *Possible allelic structure of IgG2a and IgG2c in mice*. *Mol Immunol*, 2012. **50**(3): p. 169-71.
 302. Hamaguchi, Y., et al., *Antibody isotype-specific engagement of Fcγ receptors regulates B lymphocyte depletion during CD20 immunotherapy*. *J Exp Med*, 2006. **203**(3): p. 743-53.
 303. Nimmerjahn, F., et al., *FcγR4: a novel FcR with distinct IgG subclass specificity*. *Immunity*, 2005. **23**(1): p. 41-51.

304. Nimmerjahn, F. and J.V. Ravetch, *Divergent immunoglobulin g subclass activity through selective Fc receptor binding*. Science, 2005. **310**(5753): p. 1510-2.
305. Kristic, J., et al., *Profiling and genetic control of the murine immunoglobulin G glycome*. Nat Chem Biol, 2018. **14**(5): p. 516-524.
306. Lund, J., et al., *Control of IgG/Fc glycosylation: a comparison of oligosaccharides from chimeric human/mouse and mouse subclass immunoglobulin Gs*. Mol Immunol, 1993. **30**(8): p. 741-8.
307. Mahan, A.E., et al., *A method for high-throughput, sensitive analysis of IgG Fc and Fab glycosylation by capillary electrophoresis*. J Immunol Methods, 2015. **417**: p. 34-44.
308. Chung, C.H., et al., *Cetuximab-induced anaphylaxis and IgE specific for galactose-alpha-1,3-galactose*. N Engl J Med, 2008. **358**(11): p. 1109-17.
309. UniProt. [cited 2018 25-07-2018]; Available from: <https://www.uniprot.org/>.
310. Varki, A., *Multiple changes in sialic acid biology during human evolution*. Glycoconj J, 2009. **26**(3): p. 231-45.
311. Wormald, M.R., et al., *Variations in oligosaccharide-protein interactions in immunoglobulin G determine the site-specific glycosylation profiles and modulate the dynamic motion of the Fc oligosaccharides*. Biochemistry, 1997. **36**(6): p. 1370-80.
312. Narasimhan, S., et al., *Beta-1,4-mannosyl-glycoprotein beta-1,4-N-acetylglucosaminyltransferase III activity in human B and T lymphocyte lines and in tonsillar B and T lymphocytes*. Biochem Cell Biol, 1988. **66**(8): p. 889-900.
313. Priatel, J.J., et al., *Isolation, characterization and inactivation of the mouse Mgat3 gene: the bisecting N-acetylglucosamine in asparagine-linked oligosaccharides appears dispensable for viability and reproduction*. Glycobiology, 1997. **7**(1): p. 45-56.
314. Bhaumik, M., M.F. Seldin, and P. Stanley, *Cloning and chromosomal mapping of the mouse Mgat3 gene encoding N-acetylglucosaminyltransferase III*. Gene, 1995. **164**(2): p. 295-300.
315. Lanteri, M., et al., *A complete alpha1,3-galactosyltransferase gene is present in the human genome and partially transcribed*. Glycobiology, 2002. **12**(12): p. 785-92.
316. Freeze, H.H., *Genetic defects in the human glycome*. Nat Rev Genet, 2006. **7**(7): p. 537-51.
317. Davies, J., et al., *Expression of GnTIII in a recombinant anti-CD20 CHO production cell line: Expression of antibodies with altered glycoforms leads to an increase in ADCC through higher affinity for FC gamma RIII*. Biotechnol Bioeng, 2001. **74**(4): p. 288-94.
318. Pfeifle, R., et al., *Regulation of autoantibody activity by the IL-23-TH17 axis determines the onset of autoimmune disease*. Nat Immunol, 2017. **18**(1): p. 104-113.
319. Hess, C., et al., *T cell-independent B cell activation induces immunosuppressive sialylated IgG antibodies*. J Clin Invest, 2013. **123**(9): p. 3788-96.
320. Hussain, R., et al., *Selective increases in antibody isotypes and immunoglobulin G subclass responses to secreted antigens in tuberculosis patients and healthy household contacts of the patients*. Clin Diagn Lab Immunol, 1995. **2**(6): p. 726-32.
321. Burton, D.R., *Immunoglobulin G: functional sites*. Mol Immunol, 1985. **22**(3): p. 161-206.
322. Mancardi, D.A., et al., *FcgammaRIV is a mouse IgE receptor that resembles macrophage FcepsilonRI in humans and promotes IgE-induced lung inflammation*. J Clin Invest, 2008. **118**(11): p. 3738-50.
323. Sengupta, P., *The Laboratory Rat: Relating Its Age With Human's*. Int J Prev Med, 2013. **4**(6): p. 624-30.
324. Plomp, R., et al., *Comparative Glycomics of Immunoglobulin A and G From Saliva and Plasma Reveals Biomarker Potential*. Front Immunol, 2018. **9**: p. 2436.
325. Pfaffe, T., et al., *Diagnostic potential of saliva: current state and future applications*. Clin Chem, 2011. **57**(5): p. 675-87.
326. Hu, S., et al., *Salivary proteomics for oral cancer biomarker discovery*. Clin Cancer Res, 2008. **14**(19): p. 6246-52.

327. Horsfall, A.C., L.M. Rose, and R.N. Maini, *Autoantibody synthesis in salivary glands of Sjogren's syndrome patients*. J Autoimmun, 1989. **2**(4): p. 559-68.
328. Khan, R.S., Z. Khurshid, and F. Yahya Ibrahim Asiri, *Advancing Point-of-Care (PoC) Testing Using Human Saliva as Liquid Biopsy*. Diagnostics (Basel), 2017. **7**(3).
329. Liu, X., et al., *Salivary Glycopatterns as Potential Biomarkers for Screening of Early-Stage Breast Cancer*. EBioMedicine, 2018. **28**: p. 70-79.
330. Hall, S.C., et al., *Alterations in the Salivary Proteome and N-Glycome of Sjögren's Syndrome Patients*. Journal of proteome research, 2017. **16**(4): p. 1693-1705.
331. Albrecht, S., et al., *Glycosylation as a marker for inflammatory arthritis*. Cancer Biomark, 2014. **14**(1): p. 17-28.
332. Xue, J., L.P. Zhu, and Q. Wei, *IgG-Fc N-glycosylation at Asn297 and IgA O-glycosylation in the hinge region in health and disease*. Glycoconj J, 2013. **30**(8): p. 735-45.
333. Akmacic, I.T., et al., *Inflammatory bowel disease associates with proinflammatory potential of the immunoglobulin G glycome*. Inflamm Bowel Dis, 2015. **21**(6): p. 1237-47.
334. Rochereau, N., et al., *Dectin-1 is essential for reverse transcytosis of glycosylated SIgA-antigen complexes by intestinal M cells*. PLoS Biol, 2013. **11**(9): p. e1001658.
335. Novak, J., et al., *Glycosylation of IgA1 and pathogenesis of IgA nephropathy*. Semin Immunopathol, 2012. **34**(3): p. 365-82.
336. Mattu, T.S., et al., *The glycosylation and structure of human serum IgA1, Fab, and Fc regions and the role of N-glycosylation on Fcα receptor interactions*. J Biol Chem, 1998. **273**(4): p. 2260-72.
337. Wuhrer, M., et al., *Pro-inflammatory pattern of IgG1 Fc glycosylation in multiple sclerosis cerebrospinal fluid*. J Neuroinflammation, 2015. **12**: p. 235.
338. Scherer, H.U., et al., *Glycan profiling of anti-citrullinated protein antibodies isolated from human serum and synovial fluid*. Arthritis Rheum, 2010. **62**(6): p. 1620-9.
339. Huang, J., et al., *Site-specific glycosylation of secretory immunoglobulin A from human colostrum*. J Proteome Res, 2015. **14**(3): p. 1335-49.
340. Deshpande, N., et al., *GlycoSpectrumScan: fishing glycopeptides from MS spectra of protease digests of human colostrum sIgA*. J Proteome Res, 2010. **9**(2): p. 1063-75.
341. Stefanovic, G., et al., *Hypogalactosylation of salivary and gingival fluid immunoglobulin G in patients with advanced periodontitis*. J Periodontol, 2006. **77**(11): p. 1887-93.
342. Carpenter, G.H., G.B. Proctor, and D.K. Shori, *O-glycosylation of salivary IgA as determined by lectin analysis*. Biochem Soc Trans, 1997. **25**(4): p. S659.
343. Brandtzaeg, P., *Secretory immunity with special reference to the oral cavity*. J Oral Microbiol, 2013. **5**: p. 10.3402/jom.v5i0.20401.
344. Mortimer, P.P. and J.V. Parry, *The use of saliva for viral diagnosis and screening*. Epidemiol Infect, 1988. **101**(2): p. 197-201.
345. Horton, R. and G. Vidarsson, *Antibodies and their receptors: different potential roles in mucosal defense*. Frontiers in immunology, 2013. **4**: p. 200.
346. Brandtzaeg, P., *Presence of J chain in human immunocytes containing various immunoglobulin classes*. Nature, 1974. **252**(5482): p. 418-20.
347. Delacroix, D.L., et al., *IgA subclasses in various secretions and in serum*. Immunol, 1982. **47**(2): p. 383-385.
348. Zauner, G., et al., *Glycoproteomic analysis of antibodies*. Mol Cell Proteomics, 2013. **12**(4): p. 856-65.
349. Ruhaak, L.R., et al., *Mass Spectrometry Approaches to Glycomic and Glycoproteomic Analyses*. Chem Rev, 2018.
350. Alocci, D., et al., *Understanding the glycome: an interactive view of glycosylation from glycompositions to glycoepitopes*. Glycobiology, 2018.

351. Bondt, A., et al., *Longitudinal monitoring of immunoglobulin A glycosylation during pregnancy by simultaneous MALDI-FTICR-MS analysis of N- and O-glycopeptides*. Sci Rep, 2016. **6**: p. 27955.
352. Gomes, M.M., et al., *Analysis of IgA1 N-glycosylation and its contribution to FcαRI binding*. Biochemistry, 2008. **47**(43): p. 11285-99.
353. Tarelli, E., et al., *Human serum IgA1 is substituted with up to six O-glycans as shown by matrix assisted laser desorption ionisation time-of-flight mass spectrometry*. Carbohydr Res, 2004. **339**(13): p. 2329-35.
354. R Core Team, *R: A language and environment for statistical computing*. 2013, R Foundation for Statistical Computing: Vienna, Austria.
355. Flanagan, J.G., M.P. Lefranc, and T.H. Rabbitts, *Mechanisms of divergence and convergence of the human immunoglobulin alpha 1 and alpha 2 constant region gene sequences*. Cell, 1984. **36**(3): p. 681-8.
356. Torano, A. and F.W. Putnam, *Complete amino acid sequence of the alpha 2 heavy chain of a human IgA2 immunoglobulin of the A2m (2) allotype*. Proc Natl Acad Sci U S A, 1978. **75**(2): p. 966-9.
357. Tsuzukida, Y., C.C. Wang, and F.W. Putnam, *Structure of the A2m(1) allotype of human IgA-a recombinant molecule*. Proc Natl Acad Sci U S A, 1979. **76**(3): p. 1104-8.
358. Van Loghem, E., A.C. Wang, and J. Shuster, *A new genetic marker of human immunoglobulins determined by an allele at the 2 locus*. Vox Sang, 1973. **24**(6): p. 481-8.
359. Picariello, G., et al., *Identification of N-linked glycoproteins in human milk by hydrophilic interaction liquid chromatography and mass spectrometry*. Proteomics, 2008. **8**(18): p. 3833-47.
360. Klapoetke, S.C., J. Zhang, and S. Becht, *Glycosylation characterization of Human IgA1 with differential deglycosylation by UPLC-ESI TOF MS*. J Pharm Biomed Anal, 2011. **56**(3): p. 513-20.
361. Bondt, A., et al., *IgA N- and O-glycosylation profiling reveals no association with the pregnancy-related improvement in rheumatoid arthritis*. Arthritis Res Ther, 2017. **19**(1): p. 160.
362. Maverakis, E., et al., *Glycans in the immune system and The Altered Glycan Theory of Autoimmunity: a critical review*. J Autoimmun, 2015. **57**: p. 1-13.
363. Luton, F., et al., *Identification of a cytoplasmic signal for apical transcytosis*. Traffic (Copenhagen, Denmark), 2009. **10**(8): p. 1128-1142.
364. Stockert, R.J., *The asialoglycoprotein receptor: relationships between structure, function, and expression*. Physiol Rev, 1995. **75**(3): p. 591-609.
365. Falk, P., et al., *An in vitro adherence assay reveals that Helicobacter pylori exhibits cell lineage-specific tropism in the human gastric epithelium*. Proc Natl Acad Sci U S A, 1993. **90**(5): p. 2035-9.
366. Schroten, H., et al., *Fab-independent antiadhesion effects of secretory immunoglobulin A on S-fimbriated Escherichia coli are mediated by sialyloligosaccharides*. Infect Immun, 1998. **66**(8): p. 3971-3.
367. Royle, L., et al., *Secretory IgA N- and O-glycans provide a link between the innate and adaptive immune systems*. J Biol Chem, 2003. **278**(22): p. 20140-53.
368. Maurer, M.A., et al., *Glycosylation of Human IgA Directly Inhibits Influenza A and Other Sialic-Acid-Binding Viruses*. Cell Rep, 2018. **23**(1): p. 90-99.
369. Takahashi, K., et al., *Enzymatic sialylation of IgA1 O-glycans: implications for studies of IgA nephropathy*. PLoS One, 2014. **9**(2): p. e99026.
370. Basset, C., et al., *Enhanced sialyltransferase activity in B lymphocytes from patients with primary Sjogren's syndrome*. Scand J Immunol, 2000. **51**(3): p. 307-11.
371. Dueymes, M., et al., *IgA glycosylation abnormalities in the serum of patients with primary Sjogren's syndrome*. Clin Exp Rheumatol, 1995. **13**(2): p. 247-50.

372. Perrier, C., N. Sprenger, and B. Cortesy, *Glycans on secretory component participate in innate protection against mucosal pathogens*. J Biol Chem, 2006. **281**(20): p. 14280-7.
373. Phalipon, A., et al., *Secretory component: a new role in secretory IgA-mediated immune exclusion in vivo*. Immunity, 2002. **17**(1): p. 107-15.
374. de Haan, N., K.R. Reiding, and M. Wuhrer, *Sialic Acid Derivatization for the Rapid Subclass- and Sialic Acid Linkage-Specific MALDI-TOF-MS Analysis of IgG Fc-Glycopeptides*. Methods Mol Biol, 2017. **1503**: p. 49-62.
375. Bladergroen, M.R., et al., *Automation of High-Throughput Mass Spectrometry-Based Plasma N-Glycome Analysis with Linkage-Specific Sialic Acid Esterification*. J Proteome Res, 2015. **14**(9): p. 4080-6.
376. French, D., *Advances in Clinical Mass Spectrometry*. Adv Clin Chem, 2017. **79**: p. 153-198.
377. Wood, P.L., *Mass spectrometry strategies for clinical metabolomics and lipidomics in psychiatry, neurology, and neuro-oncology*. Neuropsychopharmacology, 2014. **39**(1): p. 24-33.
378. Hoofnagle, A.N. and M.H. Wener, *The fundamental flaws of immunoassays and potential solutions using tandem mass spectrometry*. J Immunol Methods, 2009. **347**(1-2): p. 3-11.
379. Echeverria, B., et al., *Chemo-Enzymatic Synthesis of (13)C Labeled Complex N-Glycans As Internal Standards for the Absolute Glycan Quantification by Mass Spectrometry*. Anal Chem, 2015. **87**(22): p. 11460-7.
380. Hong, Q., et al., *Absolute quantitation of immunoglobulin G and its glycoforms using multiple reaction monitoring*. Anal Chem, 2013. **85**(18): p. 8585-93.
381. Yuan, W., et al., *Quantitative analysis of immunoglobulin subclasses and subclass specific glycosylation by LC-MS-MRM in liver disease*. J Proteomics, 2015. **116**: p. 24-33.
382. Li, W., et al., *LC-MS/MS determination of a human mAb drug candidate in rat serum using an isotopically labeled universal mAb internal standard*. J Chromatogr B Analyt Technol Biomed Life Sci, 2017. **1044-1045**: p. 166-176.
383. Sigma Aldrich. [cited 2018 17-07-2018]; Available from: <https://www.sigmaaldrich.com/life-science/proteomics/mass-spectrometry/silumab-and-sigmamab-antibody-standards-for-mass-spectrometry.html>.
384. Wang, Z., et al., *A general strategy for the chemoenzymatic synthesis of asymmetrically branched N-glycans*. Science, 2013. **341**(6144): p. 379-83.
385. Overkleeft, H.S. and P.H. Seeberger, *Chemoenzymatic Synthesis of Glycans and Glycoconjugates*, in *Essentials of Glycobiology*, rd, et al., Editors. 2015: Cold Spring Harbor (NY). p. 691-700.
386. Orlando, R., et al., *IDAWG: Metabolic incorporation of stable isotope labels for quantitative glycomics of cultured cells*. J Proteome Res, 2009. **8**(8): p. 3816-23.
387. Prien, J.M., et al., *Mass spectrometric-based stable isotopic 2-aminobenzoic acid glycan mapping for rapid glycan screening of biotherapeutics*. Anal Chem, 2010. **82**(4): p. 1498-508.
388. Walker, S.H., et al., *Stable-isotope labeled hydrophobic hydrazide reagents for the relative quantification of N-linked glycans by electrospray ionization mass spectrometry*. Anal Chem, 2011. **83**(17): p. 6738-45.
389. Zhang, P., et al., *Relative quantitation of glycans using stable isotopic labels 1-(d0/d5) phenyl-3-methyl-5-pyrazolone by mass spectrometry*. Anal Biochem, 2011. **418**(1): p. 1-9.
390. Alvarez-Manilla, G., et al., *Tools for glycomics: relative quantitation of glycans by isotopic permethylation using 13CH3I*. Glycobiology, 2007. **17**(7): p. 677-87.
391. Shah, P., et al., *Mass spectrometric analysis of sialylated glycans with use of solid-phase labeling of sialic acids*. Anal Chem, 2013. **85**(7): p. 3606-13.
392. Kuroguchi, M. and J. Amano, *Relative quantitation of glycopeptides based on stable isotope labeling using MALDI-TOF MS*. Molecules, 2014. **19**(7): p. 9944-61.

393. Pabst, M., et al., *Differential Isotope Labeling of Glycopeptides for Accurate Determination of Differences in Site-Specific Glycosylation*. J Proteome Res, 2016. **15**(1): p. 326-31.
394. Ye, H., et al., *Direct approach for qualitative and quantitative characterization of glycoproteins using tandem mass tags and an LTQ Orbitrap XL electron transfer dissociation hybrid mass spectrometer*. Anal Chem, 2013. **85**(3): p. 1531-9.
395. Gardinassi, L.G., et al., *Clinical severity of visceral leishmaniasis is associated with changes in immunoglobulin g fc N-glycosylation*. MBio, 2014. **5**(6): p. e01844.
396. Franceschi, C., et al., *Inflamm-aging. An evolutionary perspective on immunosenescence*. Ann N Y Acad Sci, 2000. **908**: p. 244-54.
397. Peschke, B., et al., *Fc-Galactosylation of Human Immunoglobulin Gamma Isotypes Improves C1q Binding and Enhances Complement-Dependent Cytotoxicity*. Front Immunol, 2017. **8**: p. 646.
398. Dekkers, G., T. Rispens, and G. Vidarsson, *Novel Concepts of Altered Immunoglobulin G Galactosylation in Autoimmune Diseases*. Front Immunol, 2018. **9**: p. 553.
399. Iskandar, H.N. and M.A. Ciorba, *Biomarkers in inflammatory bowel disease: current practices and recent advances*. Transl Res, 2012. **159**(4): p. 313-25.
400. Wang, T.T., et al., *IgG antibodies to dengue enhanced for FcγRIIIA binding determine disease severity*. Science, 2017. **355**(6323): p. 395-398.
401. Oefner, C.M., et al., *Tolerance induction with T cell-dependent protein antigens induces regulatory sialylated IgGs*. J Allergy Clin Immunol, 2012. **129**(6): p. 1647-55 e13.
402. Kao, D., et al., *IgG subclass and vaccination stimulus determine changes in antigen specific antibody glycosylation in mice*. Eur J Immunol, 2017. **47**(12): p. 2070-2079.
403. Selman, M.H., et al., *Changes in antigen-specific IgG1 Fc N-glycosylation upon influenza and tetanus vaccination*. Mol Cell Proteomics, 2012. **11**(4): p. M111 014563.
404. Mahan, A.E., et al., *Antigen-Specific Antibody Glycosylation Is Regulated via Vaccination*. PLoS Pathog, 2016. **12**(3): p. e1005456.
405. Sonneveld, M.E., *IgG-Fc-glycosylation in immune-mediated cytopenias*, in *Faculteit der Geneeskunde*. 2017, University of Amsterdam: Amsterdam.

Nederlandse samenvatting

De eiwitten die in het menselijk bloed circuleren hebben een scala aan verschillende functies en eigenschappen. Onder deze functies vallen, bijvoorbeeld, het coördineren van biologische processen, het synthetiseren of bewerken van andere moleculen en de bescherming van het lichaam. Bepaalde eiwitmodificaties zijn van groot belang voor het goed kunnen functioneren van de eiwitten. Een belangrijk voorbeeld hiervan is de verscheidenheid aan suikerketens (glycanen) die op specifieke plaatsen aan een eiwit vast kunnen zitten. Deze suikergroepen zijn erg divers, zowel als het gaat om de compositie (de monosacchariden waar het glycaan uit is opgebouwd), als de structuur (de manier waarop de monosacchariden aan elkaar gebonden zijn). Veranderingen in de glycaan compositie en/of structuur worden waargenomen tijdens (patho)fysiologische processen, zoals veroudering, zwangerschap, menopauze en ziekten. Het is dus aannemelijk dat het bestuderen van deze glycanen inzicht zou kunnen geven in de biologische processen die in het lichaam plaatsvinden. Deze kennis kan mogelijk een rol spelen in de ontwikkeling van nieuwe farmaceutische en klinische producten, bijvoorbeeld door het blootleggen van nieuwe therapeutische doelwitten of ziekte-specifieke signaalstoffen.

Antilichamen, oftewel immunoglobulinen, zijn eiwitten die een belangrijke rol spelen in de bescherming van het lichaam tegen ziekteverwekkers. De functionaliteit van deze eiwitten is vaak voor een groot deel afhankelijk van de glycosylering op het *fragment crystallizable* (Fc) gedeelte van het antilichaam. Het is daarom van belang dat er betrouwbare methoden beschikbaar zijn die de antilichaamglycosylering in kaart kunnen brengen. Dit is echter niet eenvoudig, omdat antilichamen meerdere glycosyleringslocaties kunnen hebben, deze locaties niet altijd een glycaan bevatten en de glycanen vele, vaak isomere, structuren aan kunnen nemen. Het onderzoek, dat in dit proefschrift beschreven wordt, focust zich enerzijds op de ontwikkeling van massa spectrometrische methoden om antilichaamglycosylering te bekijken en anderzijds op de toepassing van deze methoden voor de karakterisering van antilichaamglycosylering van specifieke organismen, lichaamsvloeistoffen en/of medische condities.

In **Hoofdstuk 1** wordt eiwitglycosylering geïntroduceerd. In het bijzonder worden de glycaaneigenschappen en -functies voor immunoglobuline G (IgG) beschreven. Verder worden ook de massaspectrometrische methoden behandeld waarmee eiwitglycosylering in kaart kan worden gebracht. Hierbij wordt de nadruk gelegd op de methoden die in het onderzoek van dit proefschrift worden gebruikt. Deze zijn gebaseerd op het analyseren van glycopeptiden met behulp van *matrix assisted laser desorption/ionization* (MALDI)-*time-of-flight* (TOF)-massaspectrometrie (MS) en *electrospray ionization* (ESI)-TOF-MS. ESI-TOF-MS werd gebruikt in combinatie met vloeistofchromatografie (LC) om complexe mengsels te scheiden voordat deze de MS bereiken.

De twee, bovengenoemde massaspectrometrische methoden verschillen onderling in snelheid, resolutie en informatiedichtheid van de verkregen data. De MALDI-TOF-MS methode is relatief gemakkelijk en snel in gebruik. Echter, als een glycopeptiden monster wordt gemeten zonder verdere monstervoorbewerkingsstappen, kan dit resulteren in een vertekend beeld van de gesialyleerde glycoconjugaten. Dit komt doordat de siaalzuren instabiel zijn tijdens het ionisatieproces en doordat hun negatieve lading zorgt voor ongelijke ionisatie tussen gesialyleerde en ongesialyleerde glycaanstructuren en de formatie van zouten met alkalimetalen. In **Hoofdstuk 2** wordt een methode beschreven voor de derivatisering van IgG glycopeptiden. Deze methode zorgt voor de stabilisatie van de gesialyleerde glycoconjugaten. Bovendien zorgt de beschreven derivatisering ook voor twee verschillende producten voor siaalzuren die respectievelijk $\alpha 2,3$ - of $\alpha 2,6$ -gelinkt zijn aan de voorgaande galactoses. Hierdoor kunnen siaalzuurisomeren van elkaar onderscheiden worden op basis van de MS metingen en zonder voorgaande chromatografische scheiding.

Er is een groot repertoire aan voorgaande studies waarin IgG Fc glycosylering wordt beschreven onder verschillende klinische omstandigheden. Echter worden de functie en regulatie van IgG Fc glycosylering nog steeds niet volledig begrepen. Daarnaast zijn de meeste van deze studies uitgevoerd met monsters van volwassenen, terwijl er over IgG glycosylering in kinderen nog maar weinig bekend is. In **Hoofdstuk 3** wordt de methode die in **Hoofdstuk 2** is ontwikkeld, toegepast voor de analyse van IgG Fc glycopeptiden die zijn verkregen uit het plasma van gezonde kinderen en pasgeborenen. In deze studie werden verbanden aangetoond tussen IgG glycaaneigenschappen en de leeftijd van de kinderen. Deze resultaten dienden als uitgangspunt om ziekte gerelateerde glycaanveranderingen in kinderen verder te bestuderen.

Om meer inzicht te krijgen in hoe IgG Fc glycosylering gereguleerd wordt, wordt er in **Hoofdstuk 4** gekeken naar de IgG glycosylering van kinderen die behandeld zijn met een hematopoietische stamceltransplantatie. Hierbij worden patiëntmonsters van voor en na de transplantatie met elkaar vergeleken. Verder worden de patiëntmonsters vergeleken met de monsters van de donoren van voor transplantatie. Deze studie liet zien dat het micromilieu van de B cellen, de cellen die verantwoordelijk zijn voor de antilichaam productie, een grote invloed heeft op de glycaanstructuren die op de IgGs worden gevonden.

Eén aspect van het gebruik van antilichaamglycosylering in een klinische toepassing is de mogelijkheid om zieke individuen te onderscheiden van gezonde. Echter is het ook zeer relevant om iets te kunnen zeggen over zekere sub-varianten van bepaalde ziektebeelden of de ernst van een aandoening. Dit biedt namelijk de mogelijkheid om een ziekte en/of behandeling van een patiënt te volgen en de behandeling op individuele wijze aan te

passen. In **Hoofdstuk 5** wordt IgG Fc glycosylering bestudeerd van kinderen die lijden aan meningokokken sepsis. Naast glycaaneigenschappen die geassocieerd konden worden met de ziekte, werden er glycaanprofielen gevonden die specifiek waren voor de ernst van de ziekte. IgG glycaaneigenschappen lijken, wanneer deze gemeten worden kort nadat een patiënt is opgenomen in het ziekenhuis, een voorspellende waarde te hebben voor de uitkomst van de ziekte.

In **Hoofdstuk 6** wordt IgG Fc glycosylering bekeken in de context van inflammatoire darmziekten (IBD). Ook hier konden glycaanprofielen worden gevonden die correleerden met ziekte eigenschappen, zoals het IBD subtype (ziekte van Crohn en colitis ulcerosa) en de progressie. Verder werd ook het effect van een behandeling (met medicatie of operatie) teruggevonden in het IgG glycaanprofiel van de patiënten.

Het overgrote deel van de functionele studies naar IgG Fc glycosylering is uitgevoerd in muizen. Hoewel het gebruik van de muis als modelorganisme voor de mens een aantal grote voordelen heeft, zoals de mogelijkheid om de muizen genetisch te manipuleren, moet er rekening mee gehouden worden dat de glycosylering die in muizen gevonden wordt niet precies hetzelfde is als die van de mens. In **Hoofdstuk 7** wordt een systematische studie gepresenteerd waarin de IgG Fc glycosylering van verschillende muizenstammen met elkaar vergeleken wordt. Dit wordt gedaan op een glycaanlocatie- en eiwit-specifieke manier, via glycopeptide analyse met LC-ESI-TOF-MS.

In **Hoofdstuk 8** komt, naast IgG, ook een ander antilichaam aan bod: immunoglobuline A (IgA). Dit antilichaam wordt, samen met IgG, geïsoleerd uit humaan speeksel en bloedplasma, waarna er een LC-ESI-TOF-MS platform gebruikt wordt om de glycosylering van deze eiwitten te bestuderen. Hiermee werd aangetoond dat de IgA glycosylering in plasma en speeksel van elkaar verschilt, wat er op duidt dat de regulatie van de antilichaamglycosylering afhangt van de locatie waar deze worden geproduceerd.

Concluderend, en zoals verder bediscussieerd in **Hoofdstuk 9**, bied dit proefschrift nieuwe massaspectrometrische methoden die gebruikt kunnen worden voor het bestuderen van antilichaamglycosylering. Deze methoden werden toegepast op klinische monsters om het toekomstig gebruik van antilichaamglycosylering in de kliniek vooruit te brengen. Er is verder onderzoek nodig naar de mechanismen die er voor zorgen dat antilichaamglycosylering veranderd tijdens bepaalde fysiologische condities en naar het effect van deze veranderingen op een immuunrespons. Ook zullen er nog stappen gezet moeten worden op technologisch gebied. Het is voor de klinische toepassing van de bevindingen namelijk essentieel dat er een relevante deelverzameling van glycaanstructuren op een robuuste manier gemeten kan worden, over een lange tijdsperiode en met variërende monstereigenschappen (zoals eiwit concentratie en

monster matrix). Hiervoor zou de implementatie van interne standaarden in de massaspectrometrische werkprocessen weleens essentieel kunnen zijn.

Acknowledgments

Dear reader, thank you for ending up reading my thesis. Even if you went straight to the acknowledgments, I am very happy you are here! Because this is the place where I can truthfully thank all people that were important during the past four years. The ones who taught me, supported me, motivated me and made these years an amazing experience.

This brings me to my promotor, Manfred, who provided me with the opportunity and freedom to explore my own research. I do not think I could have wished for a better supervisor. Thank you for your confidence in my work and your valuable input and support.

I would also like to thank my co-promotor, David, who contributed with a lot of support and good scientific discussions, thereby shaping my thoughts. Also, thank you for the great lunch discussions, the board game nights and for letting me babysit your extremely cute kids.

Though not named as an official supervisor (except for my Master internship), but at least as important is Karli. Karli, the amount of stuff you taught me is incredible, both in terms of science, as well as in handling general PhD-related matters. I'm more than happy you will be on my side as paranymph during the defense of this thesis. And I'm so grateful that on my other side (to keep me in balance) will be Vika. Vika, I really value your deliberate input on science and non-science related matters and the fact that you always make me laugh.

When I started my work in the glycogroup I was quite insecure. However, there were amazing people who immediately accepted me as part of their group and made me feel at home sooner than I ever could have imagined. Stephi, Rosina, Karli, Manu, Albert, Yoann, David, Guinevere, Bas, Florent, Carolien and Agnes, thank you all so much for getting me started in the field, the lab and the office. I am grateful that our personal and/or scientific lives keep on crossing! Lise, I am so happy I met you swirling through our labs, thanks for being my PhD-, train-, car-, Haarlem- and hockey-buddy over the last couple of years.

In the years after I started, numerous people joined our dynamic group, always resulting in a new composition of fun and inspiring scientists. Thank you all a lot for the "gezelligheid" in the office, the good discussions and your help with my research.

I would also like to thank all my collaborators, both within the Netherlands and abroad. You made my research exciting, and I learned a lot from you! Furthermore, I had great times working together with my students Mike, Pablo, Shivani, Shane and Maria-Elena, thank you for all the work you have done. Wei, Sander, Steffen and Tamás, I enjoy working together with you a lot. I learned so much from interacting with you during the last year

and I am happy that I was given the opportunity to, as your PhD supervisor, disseminate what I learned from my mentors.

Lieve beste vrienden en familie die er bestaan, onze gezamenlijke etentjes, koffietjes, verjaardagen, feestdagen, en zo veel meer, zijn ongelooflijk belangrijk voor mij. Jullie leren mij vaak op een andere manier naar bepaalde situaties te kijken en ik kan altijd mijn ei bij jullie kwijt. Lieve oma Bep, met z'n allen bij jou eten en spelletjes spelen is onbeschrijfelijk waardevol. Lieve opa Niko, het is echt fijn dat je zo veel in Nederland bent en enorm bedankt voor jouw grote hulp bij het ontwerpen van mijn boekje. Lieve opa Cor, dank je voor jouw onuitputtelijke liefde en vertrouwen, op 14 februari had je je pak weer aan gemogen. Ik mis je. Lieve papa en mama (en Rubia), ik heb de afgelopen jaren weer zo veel nieuws van jullie geleerd, dat houdt gewoon nooit op. Jullie onvoorwaardelijke steun in alles wat ik doe, welke keuzes ik ook maak, en de adviezen die ik daarbij krijg, hebben een grote bijdrage geleverd in waar ik nu sta. Liefste Jordy, liefde van mijn leven, ik kan nog zo veel van jou leren. Dank je voor je geduld, je adviezen, je vertrouwen. Je leeft mee met mijn pieken en vult mijn dalen op, zonder jou waren de afgelopen vier jaar een heel stuk moeilijker geweest. Ik geniet van alle avonturen die wij samen meemaken!

Curriculum Vitae

Noortje de Haan was born on the 27th of January, 1991 in Amsterdam, The Netherlands. Both at primary and secondary school she received Montessori-based education and in 2009 she graduated from the Montessori Lyceum Amsterdam. She followed the interdisciplinary Bachelor's study of Pharmaceutical Sciences at the Vrije Universiteit Amsterdam. In addition, she enrolled in the VU Honours Programme to extend the interdisciplinary nature of her studies. She graduated *cum laude* for her Bachelor's degree in 2012 and started the Master's studies in Drug Discovery and Safety, also at the Vrije Universiteit Amsterdam. At this time, it became clear that Noortje had a strong fascination for the processes going on in the human body and specifically for how these could be studied with analytical chemical technologies. During her Master's studies, she specialized in Biomarkers and Clinical Chemical Analysis. Furthermore, she enrolled in the COAST MSc+ program, part of the "Topsector Chemie" talent program. Her literature thesis described the use of analytical technologies for the analysis of substance adsorption to medical implants and was performed in collaboration with DSM, under the supervision of Dr. Maarten Honing. Furthermore, she performed her internship at the Leiden University Medical Center, Center for Proteomics and Metabolomics (CPM), under the supervision of Dr. Karli Reiding and Prof. Dr. Manfred Wuhrer. This was the time Noortje first encountered the world of glycosylation and its application in medicine, something she did not let go of for the years to come. Following her *cum laude* graduation in 2014, she started a PhD program at the CPM, under the supervision of Dr. David Falck and Prof. Dr. Manfred Wuhrer. During her four years of PhD project she worked on the development and application of various mass spectrometry-based methods for the analysis of (antibody) glycosylation, which resulted in her learning a lot, twelve (co-authored) publications and this thesis. After the completion of her thesis, Noortje continued her postdoctoral research at the CPM.

List of publications

First author papers

- 1) **Linkage-Specific Sialic Acid Derivatization for MALDI-TOF-MS Profiling of IgG Glycopeptides**
N de Haan, KR Reiding, M Habberger, D Reusch, D Falck, M Wuhler
Analytical Chemistry 87 (16), 8284-8291, 2015
- 2) **Changes in Healthy Human IgG Fc-Glycosylation After Birth and During Early Childhood**
N de Haan, KR Reiding, G Driessen, M van der Burg, M Wuhler
Journal of Proteome Research 15 (6), 1853-1861, 2016
- 3) **The N-glycosylation of Mouse Immunoglobulin G (IgG)-Fragment Crystallizable Differs Between IgG Subclasses and Strains**
N de Haan, KR Reiding, J Krištić, AL Hipgrave Ederveen, G Lauc, M Wuhler
Frontiers in immunology 8, 608, 2017
- 4) **Glycosylation of Immunoglobulin G Associates With Clinical Features of Inflammatory Bowel Diseases**
M Šimurina*, N de Haan*, F Vučković*, NA Kennedy, J Štambuk, D Falck, I Trbojević-Akmačić, F Clerc, Ge Razdorov, A Khon, A Latiano, R D'Incà, S Danese, S Targan, C Landers, M Dubinsky, DPB McGovern, V Annese, M Wuhler, G Lauc
*contributed equally
Gastroenterology 154, 1320-1333, 2018
- 5) **IgG Fc Glycosylation After Hematopoietic Stem Cell Transplantation is Dissimilar to Donor Profiles**
N de Haan, MJD van Tol, GJ Driessen, M Wuhler, AC Lankester
Frontiers in Immunology 9, 1238, 2018
- 6) **Differences in IgG Fc Glycosylation Are Associated with Outcome of Pediatric Meningococcal Sepsis**
N de Haan, NP Boeddha, E Ekinci, KR Reiding, M Emonts, JA Hazelzet, M Wuhler, GJ Driessen
mBio 9 (3), 2018

7) **Comparative Glycomics of Immunoglobulin A and G from Saliva and Plasma Reveals Biomarker Potential**

R Plomp*, N de Haan*, A Bondt, J Murli, V Dotz, M Wuhrer

*contributed equally

Frontiers in Immunology 9, 2436, 2018

8) **Highly Sensitive CE-ESI-MS Analysis of N-glycans from Complex Biological Samples**

GSM Kammeijer*, N de Haan*, P Mohaupt, S Wagt, M Filius, J Nouta, D Falck, M Wuhrer

*contributed equally

Manuscript submitted

Co-authorships

9) **Linkage-Specific in situ Sialic Acid Derivatization for N-glycan Mass Spectrometry Imaging of Formalin-Fixed Paraffin-Embedded Tissues**

S Holst*, B Heijs*, N de Haan, RJM van Zeijl, IH Briare-de Bruijn, GW van Pelt, AS Mehta, PM Angel, WE Mesker, RA Tollenaar, RR Drake, JVMG Bovée, LA McDonnell, M Wuhrer

*contributed equally

Analytical Chemistry 88 (11), 5904-5913, 2016

10) **LaCyTools: A Targeted Liquid Chromatography–Mass Spectrometry Data Processing Package for Relative Quantitation of Glycopeptides**

BC Jansen, D Falck, N de Haan, AL Hipgrave Ederveen, G Razdorov, G Lauc, M Wuhrer

Journal of Proteome Research 15 (7), 2198-2210, 2016

11) **Recent Advances in Clinical Glycoproteomics of Immunoglobulins (Igs)**

R Plomp, A Bondt, N de Haan, Y Rombouts, M Wuhrer

Molecular & Cellular Proteomics 15 (7), 2217-2228, 2016

12) **Patients with IgG1-Anti-Red Blood Cell Autoantibodies Show Aberrant Fc-Glycosylation**

ME Sonneveld, M Haas, C Koeleman, N de Haan, SS Zeerleder, PC Ligthart, M Wuhrer, CE Schoot, G Vidarsson

Scientific Reports 7 (1), 8187, 2017

13) Plasma N-Glycan Signatures Associate With Features of Inflammatory Bowel Diseases

F Clerc*, M Novokmet*, V Dotz*, KR Reiding, N de Haan, GSM Kammeijer, H Dalebout, MR Bladergroen, F Vukovic, E Rapp, SR Targan, G Barron, N Manetti, A Latiano, DPB McGovern, V Annese, G Lauc, M Wuhrer

*contributed equally

Gastroenterology 155, 829-843, 2018

14) Age-dependent Functional Variation of IgG Fc Glycans in Childhood

HD Cheng, I Tirosh, N de Haan, H Stöckmann, B Adamczyk, CA McManus, R O'Flaherty, G Greville, R Saldova, F Bonilla, LD Notarangelo, GJ Driessen, IA Holm, PM Rudd, M Wuhrer, ME Ackerman and PA Nigrovic

Manuscript submitted

15) Distinct Inflammatory Germinal Center B Cell Responses Determine the Type of IgG Antibody Glycosylation

Y Bartsch*, S Eschweiler*, A Leliavski*, S Wagt*, C Schwab, J Rahmöller, N de Haan, E Raghu, A Lilian, A Giannou, A Winkler, D Braumann, A Epp, J Hobusch, G Lilienthal, J Petry, K Kuhnigk, M Steinhaus, R Thurman, A El Beidaq, W Lieb, J Behrends, T Scholzen, V Blanchard, T Gemoll, J Habermann, M Collin, G Salinas, M Kanariou, D Wolff, C Härtel, RA Manz, H Fukuyama, H Busch, S Huber, T Korn, A Waisman, N Yogev, B Rabe, S Rose-John, F Berberich-Siebelt, B Grimbacher, M Wuhrer and M Ehlers

*contributed equally

Manuscript submitted

16) NIST Interlaboratory Study on Glycosylation Analysis of Monoclonal Antibodies: Comparison of Analytical Methods

MLA De Leoz, DL Duewer, A Fung, L Liu, HK Yau, O Potter, G Staples, K Furuki, R Frenkel, Y Hu, Z Sosic, CHague, C Wong, Z Peiqing, F Altmann, C Grünwald-Gruber, C Shao, J Zaia, W Evers, S Pangelley, A Resemann, DSuckau, A Wiechmann, W Jabs, A Beck, JW Froehlich, C Huang, Y Li, Y Liu, D Bu, S Suo, Y Wang, Y Seo, HJ An, NC Reichardt, J Echevarria Ruiz, S Archer-Hartmann, P Azadi, L Bell, Z Lakos, Y An, JF Cipollo, M Pucic-Bakovic, J Štambuk, G Lauc, XM Li, P George Wang, A Bock, R Hennig, E Rapp, M Creskey, TD Cyr, M Nakano, T Sugiyama, PKA Leung, P Link-Lenczowski, S Yang, HZhang, R Cao, T Kelly, S Klapoetke, J Young Kim, HK Lee, JY Lee, JS Yoo, JH Eom, SR Kim, SK Suh, N de Haan, D Falck, GSM Kammeijer, M Wuhrer, RJ Emery, RP Kozak, LP Liew, L Royle, PA Urbanowicz, A Dass, N Packer, X Song, E Lattová, S Cajic, K Alagesan, D Kolarich, T Kasali, Vi Lindo, Y Chen, K Goswami, B Gau, R Amunugama, RJones, CJM Stroop, K Kato, S Kondo, H Yagi, CT

Yuen, A Harazono, X Shi, PE Magnelli, BT Kasper, L Mahal, DJ Harveyz, R O'Flaherty, PM Rudd, R Saldova, ES Hecht, DC Muddiman, J Kang, P Bhoskar, D Menard, A Saati, C Merle, S Mast, S Tep, J Truong, T Nishikaze, S Sekiya, A Shafer, S Funaoka, M Toyoda, P de Vreugd, CM Caron, P Pradhan, NC Tan, Y Mechref, S Patil, JS Rohrer, R Chakrabarti, D Dadke, M Lahori, C Zou, B Reiz, RM Whittal, C Cairo, CB Lebrilla, L Wu, A Guttman, M Szigeti, BG Kremkow, KH Lee, C Sihlbom, B Adamczyk, C Jin, NG Karlsson, J Örnros, G Larson, J Nilsson, B Meyer, A Wiegandt, ED Bodnar, H Perreault, V Reinhold, TT Tran, N Said, YN Francois, E Leize-Wagner, S Maier, A Zeck, AJR Heck, Y Yang, R Haselberg, W Alley, YQ Yu, JW Leone, H Yuan, SE Stein
Manuscript submitted

Book chapters

- 17) **High-Throughput Analysis of IgG Fc Glycopeptides by LC-MS**
D Falck, BC Jansen, N de Haan, M Wuhrer
High-Throughput Glycomics and Glycoproteomics, 31-47, 2017
Methods in Molecular Biology book series

- 18) **Sialic Acid Derivatization for the Rapid Subclass-and Sialic Acid Linkage-Specific MALDI-TOF-MS Analysis of IgG Fc-Glycopeptides**
N de Haan, KR Reiding, M Wuhrer
High-Throughput Glycomics and Glycoproteomics, 49-62, 2017
Methods in Molecular Biology book series